AD_____

Award Number: DAMD17-03-1-0203

TITLE: Clinical and Molecular Consequences of NF1 Microdeletion

PRINCIPAL INVESTIGATOR: Karen Stephens, Ph.D.

CONTRACTING ORGANIZATION: University of Washington
Seattle, WA 98195

REPORT DATE: August 2009

TYPE OF REPORT: Final

PREPARED FOR: U.S. Army Medical Research and Materiel Command
Fort Detrick, Maryland 21702-5012

REPORT DOCUMENTATION PAGE

Form Approved
OMB No. 0704-0188

1. REPORT DATE *(DD-MM-YYYY)*	**2. REPORT TYPE**	**3. DATES COVERED** *(From - To)*
01-08-2009	Final	7 APR 2003 - 6 JUL 2009

4. TITLE AND SUBTITLE
Clinical and Molecular Consequences of NF1 Microdeletion

5a. CONTRACT NUMBER

5b. GRANT NUMBER
DAMD17-03-1-0203

5c. PROGRAM ELEMENT NUMBER

6. AUTHOR(S)
Karen Stephens, Ph.D.

E-Mail: millie@u.washington.edu

5d. PROJECT NUMBER

5e. TASK NUMBER

5f. WORK UNIT NUMBER

7. PERFORMING ORGANIZATION NAME(S) AND ADDRESS(ES)
University of Washington
Seattle, WA 98195

8. PERFORMING ORGANIZATION REPORT NUMBER

9. SPONSORING / MONITORING AGENCY NAME(S) AND ADDRESS(ES)
U.S. Army Medical Research and Materiel Command
Fort Detrick, Maryland 21702-5012

10. SPONSOR/MONITOR'S ACRONYM(S)

11. SPONSOR/MONITOR'S REPORT NUMBER(S)

12. DISTRIBUTION / AVAILABILITY STATEMENT
Approved for Public Release; Distribution Unlimited

13. SUPPLEMENTARY NOTES

14. ABSTRACT

Previous work included development of sensitive assays for the detection and mapping of both the common 1.4 Mb NF1 microdeletion and novel microdeletions. Collaborations involving this work led to several key publications in prior years. Work subcontracted to Dr. Wallace at the University of Florida included screening for mutations in putative modifiers RAB11FIP4 and JJAZ1 (SUZ12) (in the microdeletion region), which found some novel JJAZ1 variants but nothing obviously functionally abnormal, in microdeletion patients and in non-deletion patients with heavy tumor loads. Thus, we have no evidence that these flanking genes modify the NF1 phenotype. No microsatellite instability was found in tumors from microdeletion patients (or some others from non-deletion patients). Several 2nd hits were found in tumors of microdeletion patients, with none being a large deletion (two nonsense, and one in-frame 3 bp deletion). The new specific aim, immortalization of Schwann cell cultures from neurofibromas, was successful, establishing the world's first immortalized normal human Schwann cell line and three Schwann cell lines from neurofibromas.

15. SUBJECT TERMS
Microdeletion, modifying gene, genotype/phenotype, neurofibroma, Schwann cell

16. SECURITY CLASSIFICATION OF:			**17. LIMITATION OF ABSTRACT**	**18. NUMBER OF PAGES**	**19a. NAME OF RESPONSIBLE PERSON**
a. REPORT	**b. ABSTRACT**	**c. THIS PAGE**			USAMRMC
U	U	U	UU	125	**19b. TELEPHONE NUMBER** *(include area code)*

Standard Form 298 (Rev. 8-98)
Prescribed by ANSI Std. Z39.18

Table of Contents

Introduction update

About 5-10% of patients with neurofibromatosis type 1 (NF1) are heterozygous for a contiguous gene deletion that includes the entire *NF1* gene. Although limited in scope, previous studies provide compelling evidence that microdeletion patients show early onset and large numbers of cutaneous neurofibromas, and a higher frequency of plexiform neurofibromas, malignant peripheral nerve sheath tumors, and other solid tissue malignancies. We propose to perform systematic, comprehensive clinical and molecular studies of subjects with *NF1* microdeletion to examine the gene(s) responsible for the severe tumor phenotype of microdeletion patients. The specific aims of this research are 1) To determine the clinical spectrum, genotype/phenotype correlations associated with heterozygosity for an *NF1* microdeletion. Genomic DNA of NF1 subjects will be examined by a multi-step screening protocol to identify germline microdeletion carriers, to map the extent of each deletion. We will correlate molecular data with the results of a comprehensive clinical evaluation of deletion and nondeletional NF1 control subjects. 2) To determine if cutaneous neurofibromas of germline *NF1* microdeletion patients show evidence of genomic instability or homozygous *NF1* microdeletion that may contribute to the early onset of neurofibromagenesis. Primary neurofibroma tissue from microdeletion patients will be analyzed to determine the presence and nature of 2nd hit mutations and whether these cells exhibit characteristics of genomic instability. 3) To screen candidate modifier genes in the *NF1* microdeletion region for mutations in subjects with early onset cutaneous neurofibromas whom are not carriers of an *NF1* microdeletion. 4) To employ the newly developed FLASH technology to interrogate the *NF1* microdeletion region and construct a physical map that will determine, the sequence of all of the genes, unique noncoding regions, and paralogs (including the putative *NF1* duplicated gene) of the *NF1* microdeletion region. New aims were approved for the no-cost extension and subcontract of work to the laboratory of Dr. Margaret Wallace (University of Flordia), these are 1) Similar to the original Aim 2, we will examine DNA from cutaneous neurofibromas for evidence of genomic instability (including those from individuals with NF1 microdeletions). 2) Similar to original Aim 3, we will sequence the JJAZ1 gene in NF1 patients who have early onset cutaneous neurofibromas with and without germline microdeletion. 3) A new aim was to immortalize Schwann cells from neurofibromas, to provide a resource for drug discovery experiments, since neurofibromas contain a mutant, clonally-expanded Schwann cell component.

Body

Preface: The accomplishments of this research grant comprise those addressing the initial, approved Statement of Work and those for the modified, approved Statement of Work when a portion of the grant/research was subcontracted to Dr. Margaret Wallace after Dr. Stephens accepted a new position at the same institution that precluded her from completing the research.

Year 1, Months 1-8: Statement of Work (underlined) in original grant application:

- Develop a clinical database, train personnel to use.
  - Completed, see details in Progress Reports, years 1 and 2.
    We developed 2 databases using the FileMaker Pro database software package. One contains confidential patient history information, while the second one employs only coded patient identifiers, clinical, and molecular data. Both databases comply with the new requirements of HIPAA regarding password and firewall protection and training of personnel.

- Design and test clinic evaluation forms for patient assessment.
  - Completed, see details in Progress Reports years 1 and 2.

The forms to record patient manifestations and history during clinic visits were approved by the Army IRB in February, 2003. Forms are in Progress report, year 1, appendix.

- Design STS primers for interrogation of fosmid library.
  - Completed, see details in Progress Report for year 3.
    In summary, our analyses of 4 different data sources of genomic sequences did not support the presence of tandem *NF1* duplications at 17q11.2. Therefore, there is no valid scientific basis for further work on aim #4 (a project that was to be supported by the University of Washington Genome Center and performed at no cost to this grant).

Years 1-2 Statement of Work (underlined) in original grant application:

- Enroll new patients in the study.
  - Completed, see details in Progress Reports from previous years.
- Screen for NF1 microdeletion patients, map extent of deletions, develop new deletion junction assays as needed.
  - Completed, see Progress Report year 4, which detailed final assays that were developed and validated.

Assay Type #1) Deletion-specific PCR-based assays to detect the recurrent 1.4 Mb deletions at PRS1 and PRS2 recombination hotspots. The majority (~70%) of *NF1*-REP-mediated microdeletions were detectable with these assays which were used for rapid detection and diagnosis of individuals with common *NF1* microdeletions.

In collaboration with Drs. Margaret Wallace and David Muir (University of Florida), assay type #1 facilitated development of a model for the study of plexiform neurofibroma tumorigenesis. In this research an NF1 tumor-derived Schwann cell line was chosen for xenografts into the peripheral nerve of scid mice. Our deletion specific assays were instrumental in screening NF1 tumor-derived cell lines in order to make a judicious choice on the one chosen for xenograft studies. The model facilitates testing of potential therapeutic interventions in a relevant cellular environment.

- Completed, research was detailed in Progress Reports, years 1-4 and in publications in the Appendix.
  - De Raedt T, Stephens M, Heyns I, Brems H, Thijs D, Messiaen L, Stephens K, Lazaro C, Wimmer K, Kehrer-Sawatzki H, Vidaud D, Kluwe L, Marynen P, Legius E. Conservation of hotspots for recombination in low-copy repeats associated with the NF1 microdeletion. Nature Genet 38:1419-1423, 2006.
  - Perrin GQ, Fishbein L, Thomson SA, Thomas SL, Stephens K, Garbern JY, Deries GH, Yachnis AT, Wallace MR, Muir D. Plexiform-like neurofibromas develop in the mouse by intraneural xenograft of an NF1 tumor-derived Schwann cell line. J Neurosci Res 85:1347-1357, 2007.

Assay type #2. Assays to detect microdeletions at unique regions, not at the recombination hotspots.

- Completed, research detailed in Progress Reports of years 1 through 3.

In summary, a series of quantitative PCR (qPCR) assays at 5 loci that we developed to detect *NF1* regional deletions. Assays were validated and exhibited reproducibility, low intra- and inter-assay

variation on bona fide disomic and monsomic NF1 patients, and ~ 95% confidence limits (± 2 S.D.) for the range of normal and deleted values which did not overlap. However, when we screened >250 patients for novel deletions in/near NF1, the 10 positives identified could not be confirmed by an independent method (FISH and polymorphic marker analysis). Extensive trouble-shooting led to the conclusion that for reasons that cannot be determined, these assays are not reproducible nor reliable when applied on a large scale to unknown patient samples.

- Ascertain NF1 subjects that show early onset cutaneous neurofibromas that do not carry microdeletions.
  - Completed. We identified 5 such patients, including one family that appears to have early onset cutaneous neurofibromas. No further analysis was pursued due to Dr. Stephens' job duty changes.

- Determine conditions for centrosome immunohistochemistry, test and choose optimal antibodies.
  This work relates to Aim #2 - To determine if cutaneous neurofibromas of germline NF1 microdeletion patients show evidence of genomic instability.
  - Completed; Results detailed in Progress Reports years 3 and 4.
  - There can be several types of genomic instability in cells, and one important type is centrosome abnormality, which can leads to abnormal mitoses and consequent aneuploidy. We proposed that this might be a mechanism in NF1-related tumorigenesis because, as detailed in previous progress reports, we found that neurofibromin localizes to the centrosome in human primary keratinocytes, several simple epithelial cell lines, and mouse 3T3 fibroblasts. We also documented neurofibromin co-localization to the abnormally structured and clumped multi-centrosomes in squamous cell carcinoma cell lines. We also found abnormally structured and clumped multi-centrosomes in one dermal neurofibroma from an NF1 patient with a ~1 kb microdeletion. To examine more pathologically-relevant cells, we obtained normal cultured Schwann cells (complements of Dr. David Muir, University of Florida) and found no nuclear localization of neurofibromin. A few months ago, we extended this study to examine primary cultured Schwann cells from a nonlesional, nontumor sciatic nerve site obtained at autopsy of a subject with neurofibromatosis, who was heterozygous for the 1.4 Mb NF1 microdeletion and died of an MPNST. These cultured cells also did not have centrosomal-neurofibromin, indicating that neurofibromin does not localize to the nucleus in Schwann cells. Because of this finding, we did not pursue the original plan to extend this analysis to NF1-related MPNST cell lines. We concluded that centrosome abnormalities are, at best, only occasionally involved in NF1 tumorigenesis.

- Genomic instability during leukemogenesis in children with NF1.
  - Completed. Results detailed in Stephens K, et al, 2006.
    In summary, these data suggest that the cases with interstitial uniparental isodisomy arose in a leukemia-initiating cell by double homologous recombination events at intervals of preferred mitotic recombination. Homozygous inactivation of *NF1* favored outgrowth of the leukemia-initiating cell. Our studies demonstrate that LOH analyses of loci distributed along the chromosomal length along with copy-number analysis can reveal novel mechanisms of LOH that may potentially identify regions harboring "cryptic" tumor suppressor or modifier genes whose inactivation contribute to tumorigenesis.

Year 2 Statement of Work (underlined) in original grant application:

- Screen subjects with early onset cutaneous neurofibromas that are heterozygous at *NF1* for somatic mosaicism for an *NF1* microdeletion.
    - Experiments related to this were not performed primarily because of Dr. Stephens' new job responsibilities.

- Construct STS-content maps, sequence fosmids, and construct haplotypes.
    - No longer applicable. This is part of Aim #4, which is not reasonable to pursue as we determined from our work in year 1 described above.

- Obtain cutaneous neurofibromas from *NF1* microdeletion adults.
    - Completed. We obtained neurofibromas from two microdeletion patients, including multiple neurofibromas from one of the patients. In addition, we obtained MPNST from one of these patients, which was sent to Dr. Wallace.

- Perform immunohistochemistry and nucleic acid extraction of neurofibromas.
    - Completed DNA purification from neurofibromas.
    - Results of immunohistochemistry are described above; this direction was abandoned based on early data.

- Assemble data on clinical spectrum of *NF1* microdeletion patients.
    - Completed.

    We were disappointed that we identified insufficient new deletion patients on whom we could obtain detailed clinical information. Our collaborator, Dr. Mautner in Germany, has a large patient population and many NF1 deletion patients. Our phenotypic and deletion data of our newly-identified patients with Dr. Mautner (anonymously as approved by the IRB) were to be combined with his data set.

Year 3 Statement of Work in original grant application (underlined):

- Screen JJAZ1 gene for inactivating mutations in subjects with early onset cutaneous neurofibromas who are heterozygous at *NF1*
    - Completed in years 4-5 by Dr. Wallace's lab, summarized here:

    Dr. Stephens developed PCR and sequencing primers, and Dr. Wallace's lab sequenced 7/16 JJAZ1 gene exons (note official gene name is now SUZ12) in 12 patients with early onset cutaneous neurofibromas who are heterozygous for the *NF1* gene. We also sequenced these exons in 27 microdeletion patients to test whether the remaining allele had any mutations or polymorphisms that might affect phenotype. PCR of the other exons was not worked out before the expiration of the grant. No inactivating mutations were found. However, there was a 5 bp deletion in one microdeletion patient (UW119-1) in intron 4, 1331 bp into IVS4 and 18 kb upstream of exon 5. This has not been previously reported. It is unclear whether this would have any effect on splicing or other gene function; it may be a novel rare neutral variant. No other patients showed this alteration. Another novel, unreported variant was found in one non-deletion case; a T>A substitution 10 bp into intron 4 on one allele. The effect on splicing, if any, is not known (RNA not available), but if by chance it caused skipping of exon 4 then it would cause an

in-frame loss of 23 amino acids. This could be deleterious but might not be a fully-inactivating mutation.

The known SNP rs530209 (A/G) in IVS7 was observed in the samples. Interestingly, the G allele was at a frequency of 0.238 in the microdeletion patients, but only 0.071 in the heterozygous patients. Both were different than the allele frequency reported in dbSNP for Caucasians of European descent (0.167-0.181), which is the genetic background of our cases. The G allele is significantly under-represented in the patients with heavy neurofibroma burdens (ten-fold less frequent), and is somewhat overrepresented in the microdeletion patients (but not dramatically). Although this SNP is not known to be functional, it could have an effect and/or be linked to a functional allele which could be influencing phenotype. It might bear examining in more cases, with and without heavy tumor burden, and at the RNA level.

- Continue to obtain cutaneous neurofibromas from *NF1* microdeletion adults.
  - Completed. All patient recruitment and specimen collection has been terminated at the University of Washington.

- Continue to perform immunohistochemistry of neurofibromas, MPNST, and tumor cells.
  Not completed, as indicated above due to lack of positive findings in Schwann cells.

- Perform microsatellite instability (MSI) studies on neurofibroma tissue.
  Completed (see Year 5 Statement of Work, modified during the subcontract to Dr. Wallace).

- Identify 2nd hit *NF1* mutations in neurofibromas.
  Not completed. Dr. Wallace's lab attempted to continue this although it was not on the subcontract. One MPNST cell line with a germline microdeletion was intensively studied. The entire open reading frame, 5' UTR and 3'UTR were sequenced in DNA and RNA, with no abnormalities found (no splice aberrations) and no RNA editing present. However, the RNA isoform that contains alternatively spliced exon 23a (type II) was the only isoform present; this form was experimentally shown to reduce RAS-GAP activity. Thus, the 2nd hit in this tumor is either something very subtle (e.g. promoter mutation or something that affects translation efficiency) or is the presence of only type II isoform, suggesting that there is a threshold effect for neurofibromin, below which is associated with tumors. This was published in the paper indicated below. Further analyses found L494X 2nd hit (exon 10b) in plexiform neurofibroma of patient UF303 (germline microdeletion), and two cutaneous neurofibromas of another microdeletion patient had 2nd hits identified (R1748X in exon 29, and a 3-bp in-frame deletion causing loss of arginine at position 1176 (exon 21)). These latter data were reported in a poster at the 2008 American Society of Human Genetics meeting (Wallace et al). This is consistent with 2nd hits in germline microdeletion tumors not consisting of large deletions, a paradigm gaining support in the field.
    - Wallace M, Loda R, Rasmussen S, Stephens K, Riccardi V. Maternal Germline Mosaicism and Somatic Mosaicism in NF1. American Society of Human Genetics, November, 2008.

    - Perrin GQ, Fishbein L, Thomson SA, Thomas SL, Stephens K, Garbern JY, Deries GH, Yachnis AT, Wallace MR, Muir D. Plexiform-like neurofibromas develop in the

mouse by intraneural xenograft of an NF1 tumor-derived Schwann cell line. J Neurosci Res 85:1347-1357, 2007.

- Continue fosmid analysis of *NF1* region; construct new libraries if needed.
  - Unnecessary. This is part of Aim #4, which our data described above indicate is not necessary to pursue.

Year 4 Statement of Work (underlined) in original grant application:

- Submit clinical information on *NF1* microdeletion patients to the National Neurofibromatosis Foundation International Database.
  - Unnecessary.

  Dr. Stephens has published clinical information on >90% of the NF1 microdeletion patients, so this information is now in the public domain and will not be submitted specifically to the National Neurofibromatosis Foundation International Database.

- Analyze data for phenotype/genotype correlations and prognostic utility.
  - Completed, but number of subjects ascertained was disappointing.

  Phenotype/genotype data from our patients will be shared with Dr. Mautner to contribute to his continuation of these studies as described above.

- Analyze the complete sequence of the *NF1* microdeletion region for new genes and paralogs.
  - Unnecessary. This is part of Aim #4, which our data above indicate is not necessary to pursue.

- Perform comparative mapping of final human sequence with that of the mouse.
  - Unnecessary. This is part of Aim #4, which our data described above indicate is not necessary to pursue. Furthermore this work has been completed and published by us and our collaborators (Jenne et al, 2003).

Year 5 Statement of Work, modified and approved as subcontract and no-cost extension to Dr. Wallace

This work was subcontracted to and performed by Dr. Margaret Wallace, University of Florida, with negligible input from Dr. Stephens.

Aim 1 Tasks 1-2: Microsatellite Instability (MSI) analysis.

- Completed. The following DNA samples were studied, and found to lack microsatellite instability at two of the standard MSI markers: DNA from 6 dermal neurofibromas and their tumor-derived Schwann cell cultures (patient with germline *NF1* microdeletion), DNA from 3 plexiform neurofibromas, and DNA from two MPNST cell lines (one with normal karyotype, *NF1* microdeletion germline mutation but no LOH; the other with a frameshift germline *NF1* mutation and LOH for the 2^{nd} hit, with aneuploidy). We conclude that MSI is not involved, or at least not common, in NF1 tumorigenesis regardless of presence of microdeletion, which is consistent with other reports that came out in the literature during the span of this project. Further analysis was deemed un-necessary in light of agreement of our results with other labs.

Aim 1 Task 3: Continue centrosome studies initiated by Dr. Stephens.

- Completed. As indicated above on pages 6 and 7, this line of work was deemed unworthy of continuing when the negative results were found in Schwann cells.

Aim 2 Task 1: Sequence *JJAZ1* and *RAB11FIP4* exons from DNA from 12 NF1 patients with early onset neurofibromas but no germline large deletion, and in 3-4 large deletion patients.

- Completed for *JJAZ1* as described above under Year 3 original aim/task (total 39 patients).
- Completed for *RAB11FIP4* (14/15 exons) by heteroduplex analysis and sequencing of DNA from the same 39 patients. No changes from consensus sequence were discovered. The exons and immediate flanking introns are highly invariant, which suggests that any other variants potentially elsewhere in the gene (e.g. deeper introns, UTRs, promoter) could have a substantial effect on gene function.

Aim 3 Task 1: This new aim's goal was to immortalize Schwann cells from one non-NF1 subject, and two neurofibromas, to provide a resource for drug discovery experiments.

- Completed. Various combinations of retro- or lenti-virus vector carrying human telomerase gene or *CDK4* gene were used to transfect Schwann cells toward immortalization. A normal Schwann cell culture, pn02.3, was immortalized, as well as three neurofibroma tumor Schwann cells: pNF95.11b, pNF95.6, and cNF04.9a. Some single-cell-derived cell lines have been established, and one culture grows without needing laminin substrate, while another has become growth factor independent. This has produced very useful cells for cell biology studies. Another culture (pNF05.5) senesced at passage 31, providing a more limited resource for studies (but much better than the original mixed culture which senesced at passage 7). This work is being prepared for publication.

Key Research Accomplishments

- Screened over 200 unselected individuals affected with NF1and 34 DNAs from known NF1 deletion patients with deletion-specific assays for the 1.4 Mb deletion and competitive PCR assays for novel deletions. We identified 56 subjects with the recurrent 1.4 Mb deletion and 16 subjects with novel deletions. Published in Raedt TD et al, 2003 and Forbes SH et al, 2004.
- Consistent with our hypothesis of genomic instability during NF1-related tumorigenesis, we have shown that loss of *NF1* heterozygosity in NF1-related leukemias occurs primarily by a novel mechanism of interstitial uniparental disomy with clustered breakpoints. The clustered breakpoints suggest chromosomal regions where mitotic recombination is favored along with selection for outgrowth of recombinants. Published in Stephens K, Weaver M, et al., 2006.
- We developed deletion-specific PCR assay for rapid and reliable detection of the 1/4Mb *NF1* microdeletions that occur at the common recombination hotspots, PRS1 and PRS2. These assays demonstrated that about 70% of germline deletions occur at these sites.
- Produced immortalized normal human Schwann cells (first and only such culture) and three immortalized neurofibroma tumor Schwann cell lines, novel reagents for cell biology and preclinical therapeutic testing. These cells were reported in a poster at the annual NF Conference in 2009 and have been shared with 6 labs since then (another pending).

Reportable Outcomes

Publications (in chronological order)

Stephens K. Genetics of neurofibromatosis 1- associated peripheral nerve sheath tumors. Cancer Investigation 21:897-914, 2003.

Forbes SH, Dorschner MO, Le R, Stephens K. Genomic context of paralogous recombination hotspots mediating the recurrent NF1 region microdeletion. Genes Chromosomes Cancer. 41:12-25, 2004.

Kelsell DP, Norgett EE, Unsworth H, Teh MT, Cullup T, Mein CA, Dopping-Hepenstal PJ, Dale BA, Tadini G, Fleckman P, Stephens KG, Sybert VP, Mallory SB, North BV, Witt DR, Sprecher E, E M Taylor A, Ilchyshyn A, Kennedy CT, Goodyear H, Moss C, Paige D, Harper JI, Young BD, Leigh IM, Eady RA, O'toole EA. Mutations in ABCA12 Underlie the Severe Congenital Skin Disease Harlequin Ichthyosis. Am J Hum Genet Mar 8;76, 2005.

Lombillo VA, Sybert VP. Mosaicism in cutaneous pigmentation. Curr Opin Pediatr.17:494-500, 2005.

De Raedt T, Stephens M, Heyns I, Brems H, Thijs D, Messiaen L, Stephens K, Lazaro C, Wimmer K, Kehrer-Sawatzki H, Vidaud D, Kluwe L, Marynen P, Legius E. Conservation of hotspots for recombination in low-copy repeats associated with the NF1 microdeletion. Nat Genet 38:1419-23, 2006.

Siegel DH, Sybert VP. Mosaicism in genetic skin disorders. Pediatr Dermatol. 23:87-92, 2006

Stephens K. Neurofibromatosis 1. *In Genomic Disorders*: *The Genomic Basis of Disease*, Eds.. JR Lupski, PT Stankiewicz. New Jersey: Humana Press, pp. 207-219, 2006

Stephens K. Clinical Molecular Genetics of the Neurofibromatoses. *In* Neurocutaneous syndromes in Children, Eds., P Curatolo, D Riva. Mariani Foundation Paediatric Neurology Series, n.15. Montrouge: John Libbey Eurotext, 2006.

Stephens K, Weaver M, Leppig KA, Maruyama K, Emanuel PD, Le Beau MM, Shannon KM. Interstitial uniparental isodisomy at clustered breakpoint intervals is a frequent mechanism of NF1 inactivation in myeloid malignancies. Blood 108:1684-9, 2006.

Perrin GQ, Fishbein L, Thomson SA, Thomas SL, Stephens K, Garbern JY, DeVries GH, Yachnis AT, Wallace MR, Muir D. Plexiform-like neurofibromas develop in the mouse by intraneural xenograft of an NF1 tumor-derived Schwann cell line. J Neurosci Res. 1;85:1347-1357, 2007.

Stephens K. Neurofibromatosis. In *Molecular Pathology in Clinical Practice*. D.G.B. Leonard, Ed. New York: Springer –Verlag, pp 243-250, 2007.

Li H et al. Immortalization of normal and NF1 neurofibroma-derived Schwann cells. In preparation.

Abstracts (listed chronologically)

Stephens K. About 70% of Nf1 microdeletions are recurrent and occur at discrete recombination sites within the flanking NF1REP paralogs, which are comple modular assemblies of low-copy repeats of different sequence families. National Neurofibromatosis Foundation International Consortium for the Molecular Biology of NF1 and NF2, Aspen, CO, June 1-4, 2003.

Stephens K. Neurocutaneous Syndromes in the Developmental Age, "Molecular Genetics of NF1 and NF12", Fondazione Mariani, Lucca, Italy, March 3-5, 2004.

Wang B, Vong S, Le R, Stephens K. Identification and mapping of NF1 contiguous gene deletions using real-time competitive PCR. National Neurofibromatosis Foundation International Consortium for the Molecular Biology of NF1 and NF2, Aspen, CO, June, 2004.

Kehrer-Sawatzki H, Tinschert S, Petek **E, Stephens K, Jenne** DE. The complete physical map of the NF1 gene region rultes out the duplication of the NF1 gene at 17q11.2 and reverals two new

types of NF1 microdeletions mediated by a pseudogene fragment of the JJAZF1 (KIAA0160) gene and a third medial copy of the WI-12393 gene, respectively. European Neurofibromatosis Meeting, Turku, Finland, 2004.

Shinohara MM, Kuechle MK, Graves J, Stephens K. Neurofibromin is a caspase target. The CTF International Consortium for the Molecular and Cell Biology of NF1, NF2 and Schwannomatosis, Aspen, June, 2005.

De Raedt, Heyns I, Brems H, Stephens K, Marynen P, Legius E. On the origin of NF1 microdeletions. The CTF International Consortium for the Molecular and Cell Biology of NF1, NF2 and Schwannomatosis, Aspen, June, 2005

Shinohara MM, Kuechle MK, Graves J, Stephens K. Caspase mediated proteolysis of neurofibromin. Society of Investigative Dermatology, St. Louis, May, 2005.

Wallace M, Loda R, Rasmussen S, Stephens K, Riccardi V. Maternal Germline Mosaicism and Somatic Mosaicism in NF1. American Society of Human Genetics, November, 2008(poster).

Loda-Hutchinson R, Li H, Wallace MR. NF1 exon 23a alternative splicing in neurofibromas and MPNSTs. Am Soc Hum Genet annual meeting, Philadelphia PA, November 2008, (poster).

Li H, Chang L-J, Muir D, Wallace MR. Immortalization of NF1 neurofibroma-derived Schwann cell cultures. NF Conference (formerly International Consortium on the Molecular Biology of NF1, NF2, and Schwannomatosis), June 2009 (poster).

Seminars (listed chronologically; *invited speaker)

*Stephens K. "Megabase Deletions" Aspen, CO, June, 2003 at conference of National Neurofibromatosis Foundation International Consortium on Gene Cloning and Gene Function of NF1 and NF2.

*Stephens K. "Molecular Genetics of NF1 and NF12", Fondazione Mariani, Lucca, Italy, March 3-5, 2004 at conference Neurocutaneous Syndromes in the Developmental Age.

Stephens K. "Large Scale Intra-Chromosomal Rearrangements & Contiguous Gene Disorders", April 9, 2004 in PATH516 Molecular Basis of Human Genetic Disease, University of Washington.

Stephens K. "Mechanisms of large scale intra-chromosomal rearrangements", April 12, 2004 in PATH516 Molecular Basis of Human Genetic Disease, University of Washington.

Stephens K. "Trinucleotide repeat disorders and Genetic Instability – Fragile X", April 16, 2004 in PATH516 Molecular Basis of Human Genetic Disease, University of Washington.

Stephens K. "Genetic Testing", May 7, 2004 in PATH516 Molecular Basis of Human Genetic Disease, University of Washington.

Stephens K. "Neurofibromatosis & Genomic Disorders", May 18, 2004 in GENOME531 Genetics of Human Disease, University of Washington.

*Stephens K. "Neurofibromatosis 1: Different paralogous recombination sites for meiotic versus mitotic NF1 microdeletion". Medical Genetics Seminar, University of Washington, Jan 21, 2005.

Stephens K. "NF1, Genomic Disorders and their Mechanisms", April 6, 2005 in PATH 516 Molecular Basis of Human Genetic Disease, University of Washington.

Stephens K. "Fragile X Mental Retardation Syndrome", April 11, 2005 in PATH 516 Molecular Basis of Human Genetic Disease, University of Washington.

Stephens K. "Genetic Testing", April 25, 2005 in PATH 516 Molecular Basis of Human Genetic Disease, University of Washington.

Stephens K. "Molecular Diagnostics" February 25, 2005, in Introduction to Medical Genetics, University of Washington.

*Sybert VP. "Molecular Genetics for Dermatologists" Massachusetts Academy of Dermatology, Woodstock, VT, September 2005.

*Stephens, K "How can new NF1 research help patients now and in the future?" Neurofibromatosis Symposium, Washington State Neurofibromatosis Families, Children's Hospital and Regional Medical Center, Seattle, WA, October 8, 2005.

*Sybert VP. "Genetic Disorders of Pigmentation" and "Molecular Genetics for Dermatologists, Mayo Clinic Visiting Professor, Genome Series Talks, Rochester, MN, January 2006.

*Sybert VP. "Molecular Genetics for Dermatologists", Grand Rounds, Div Derm, University of Washington, Seattle, WA, February 2006.

*Sybert VP. "Genetic disorders of Pigmentation", Teaching Conference, U. of Minnesota Dept Dermatology, March, 2006.

Stephens K. "Genomic Disorders and their Mechanisms", graduate class PATH 516 Molecular Basis of Human Genetic Disease, University of Washington, Seattle, WA, April 5, 2006.

Stephens K. "Nucleotide Expansion Disorders", graduate class PATH 516 Molecular Basis of Human Genetic Disease, University of Washington, Seattle, WA, April 12, 2006.

*Sybert VP. "Dermatologic Markers of Genetic Disease", CME for Pediatricians, Group Health Cooperative, Seattle, WA, May, 2006.

*M. Wallace "Molecular and Cellular Anecdotes from Analysis of NF1 Samples: Clues about Mechanism" International Consortium on the Molecular Biology of NF1 and NF2, Aspen, CO, June 2006.

Stephens Karen. "Genome duplications/deletions/ impact on disease", graduate class PATH530 Human Cytogenetics, University of Washington, Seattle, WA, May 16, 2006.

*Sybert VP. "Developmental Embryology of the Skin" September, 2006 at David W. Smith Dysmorphology Meeting, Lake Arrowhead CA.

*Sybert VP. "Developmental Embryology of the Skin" March 16-19, 2007 at Baylor University, Departments of Dermatology and Medical Genetics.

Sybert VP. "Molecular Mechanisms of Skin Development", April 27, 2007 at University of Washington, Department of Medicine, Division of Medical Genetics.

*M. Wallace "Tumorigenesis in NF1: New Models and Mechanisms". UF Shands Cancer Center, Topics in Cancer Biology Seminar series, University of Florida, Gainesville, Nov. 2007.

*M. Wallace "Mysteries of, and Research Insights into, Neurofibromatosis 1" Invited seminar, Jacksonville University Div. of Science and Mathematics, Jacksonville, FL, January 2007.

M. Wallace "Challenges and Frustrations in NF1 Research." Invited seminar, China Medical University, Shenyang, China. June 2007.

M. Wallace "Update from the International NF Conference" UF Pediatric Genetics Clinical Grand Rounds, University of Florida, Gainesville, July 2007.

R. Loda (M.Wallace graduate student) "Genetic Studies in NF1." Molecular Genetics Research Conference, University of Florida College of Medicine, Sept. 23, 2008.

H. Li "Immortalization of NF1 Schwann cells by hTERT and mCDK4". UF Epigenetics supergroup meeting, Gainesville FL, April 2008.

*M. Wallace "New Directions in Neurofibromatosis Research" UF Dept. of Neuroscience seminar series, University of Florida, Gainesville, April 2009.

Trainees

- The following individuals received postgraduate training from Dr. Karen Stephens in the field of neurofibromatosis:
    - Paula Zook, MD, dermatologist
    - Bingbing Wang, MD, molecular biologist
    - Melanie Kuechle, MD, PhD, dermatologist, cell biologist

  The following individual received predoctoral training from Dr. Wallace:
    - Rebecca Loda Hutchinson (Ph.D. 2009)

  The following individuals received postdoctoral training from Dr. Wallace:
    - Hua Li, Ph.D.
    - George Perrin, Ph.D.

Conclusions: This project identified a number of microdeletion cases, characterized the breakpoints of the deletions, and made the genetic and phenotype data available to the research community. There is no highly consistent phenotype in these patients, but they do tend to have a higher frequency of some features. The genomic tools were extended to NF1-related leukemia, revealing isodisomy on 17q in the leukemic cells. Mutation screening failed to find any evidence that the flanking genes RAB11FIP4 or JJAZ1 have variants that influence tumor phenotype, in patients with or without microdeletion. The tumors screened from microdeletion patients showed *NF1* mRNA with small mutations (or undetectable mutations), supporting the hypothesis that 2nd hits in such patients are not large deletions. But no microsatellite instability was found in any tumors. In cell biology experiments, the centrosome theory did not pan out (also consistent with lack of MSI), and we were able to establish immortalized Schwann cell lines from normal human Schwann cells and neurofibroma-derived Schwann cells. This resource is also being shared with the NF research community. Thus, important discoveries were made in the duration of this grant.

References:

Fukasawa, K. (2005) Centrosome amplification, chromosome instability and cancer development. *Cancer Lett,* **230,** 6-19.

Jefford, C.E. and Irminger-Finger, I. (2006) Mechanisms of chromosome instability in cancers. *Crit Rev Oncol Hematol*.

Jenne DE, Tinschert S, Dorschner MO, Hameister H, **Stephens K**, Kehrer-Sawatzki H. Complete physical map and gene content of the human NF1 tumor suppressor region in human and mouse. Genes Chromo Cancer 37:111-20, 2003.

Appendices

A. List of Personnel receiving pay from the research effort (don't list salaries)

- Karen Stephens, PhD
- Virginia P. Sybert, MD
- Margaret Wallace, PhD
- Mike Dorschner, PhD
- Steve Forbes, PhD
- Lynda Le, BS
- Shinny Vong, BS
- Bingbing Wang, PhD
- Molly Weaver, BS
- Paula Zook, MD
- Rebecca Loda Hutchinson, BA
- Hua Li, PhD
- George Perrin, PhD

B. Attached manuscripts

Stephens K. Genetics of neurofibromatosis 1- associated peripheral nerve sheath tumors. Cancer Investigation 21:897-914, 2003.

Forbes SH, Dorschner MO, Le R, Stephens K. Genomic context of paralogous recombination hotspots mediating the recurrent NF1 region microdeletion. Genes Chromosomes Cancer. 41:12-25, 2004.

Kelsell DP, Norgett EE, Unsworth H, Teh MT, Cullup T, Mein CA, Dopping-Hepenstal PJ, Dale BA, Tadini G, Fleckman P, Stephens KG, Sybert VP, Mallory SB, North BV, Witt DR, Sprecher E, E M Taylor A, Ilchyshyn A, Kennedy CT, Goodyear H, Moss C, Paige D, Harper JI, Young BD, Leigh IM, Eady RA, O'toole EA. Mutations in ABCA12 Underlie the Severe Congenital Skin Disease Harlequin Ichthyosis. Am J Hum Genet Mar 8;76, 2005.

Lombillo VA, Sybert VP. Mosaicism in cutaneous pigmentation. Curr Opin Pediatr.17:494-500, 2005.

De Raedt T, Stephens M, Heyns I, Brems H, Thijs D, Messiaen L, Stephens K, Lazaro C, Wimmer K, Kehrer-Sawatzki H, Vidaud D, Kluwe L, Marynen P, Legius E. Conservation of hotspots for recombination in low-copy repeats associated with the NF1 microdeletion. Nat Genet 38:1419-23, 2006.

Siegel DH, Sybert VP. Mosaicism in genetic skin disorders. Pediatr Dermatol. 23:87-92, 2006

Stephens K. Neurofibromatosis 1. *In Genomic Disorders*: *The Genomic Basis of Disease,* Eds.. JR Lupski, PT Stankiewicz. New Jersey: Humana Press, pp. 207-219, 2006

Stephens K. Clinical Molecular Genetics of the Neurofibromatoses. *In* Neurocutaneous syndromes in Children, Eds., P Curatolo, D Riva. Mariani Foundation Paediatric Neurology Series, n.15. Montrouge: John Libbey Eurotext, 2006.

Stephens K, Weaver M, Leppig KA, Maruyama K, Emanuel PD, Le Beau MM, Shannon KM. Interstitial uniparental isodisomy at clustered breakpoint intervals is a frequent mechanism of NF1 inactivation in myeloid malignancies. Blood 108:1684-9, 2006.

Perrin GQ, Fishbein L, Thomson SA, Thomas SL, Stephens K, Garbern JY, DeVries GH, Yachnis AT, Wallace MR, Muir D. Plexiform-like neurofibromas develop in the mouse by intraneural xenograft of an NF1 tumor-derived Schwann cell line. J Neurosci Res. 1;85:1347-1357, 2007.

Stephens K. Neurofibromatosis. In *Molecular Pathology in Clinical Practice*. D.G.B. Leonard, Ed. New York: Springer –Verlag, pp 243-250, 2007.

CANCER INVESTIGATION
Vol. 21, No. 6, pp. 897–914, 2003

MOLECULAR BIOLOGY AND GENETICS OF CANCER

Genetics of Neurofibromatosis 1-Associated Peripheral Nerve Sheath Tumors

Karen Stephens, Ph.D.*

Departments of Medicine and Laboratory Medicine, University of Washington, Seattle, Washington, USA

ABSTRACT

Neurofibromatosis 1, an inherited disorder that affects 1/3500 individuals worldwide, predisposes to the development of benign and malignant peripheral nerve sheath tumors. The disorder results from inactivation of one of the *NFI* genes. The second *NFI* gene is typically inactivated in Schwann cells during tumor formation. This article reviews the different types of genetic alterations in *NFI* in both constitutional and tumor tissues and genetic alterations of other genes that may affect tumorigenesis. These studies have provided insight into the genetic basis of both the variable expression of the disorder and of benign and malignant peripheral nerve sheath tumorigenesis.

Key Words: Neurofibromatosis; Neurofibroma; Genetic abnormalities; Nerve sheath tumors; Schwann cells; Tumorgenesis.

INTRODUCTION

Much of our current understanding of tumorigenesis is founded on genetic studies of relatively rare individuals with inherited disorders that predispose to certain cancers, e.g., retinoblastoma[1] and colorectal tumors.[2,3] Such genetic studies are consistent with a model whereby normal tissues become highly malignant due to successive mutation of multiple genes that dysregulate cellular proliferation and homeostasis. Important classes of mutated genes include oncogenes (positive growth regulators), tumor suppressors (negative growth regulators), and those encoding cell cycle regulators, antiapototic signals, and components of the DNA replication and repair machinery. Mutation during tumorigenesis can occur at the nucleotide level as inactivation of a single gene or at the chromosomal level as losses of large segments or entire chromosomes, as a fusion of two different chromosomal segments, or as a high level amplification of a segment.[4] Screening normal and tumor tissues of patients for common genetic alterations has been a productive strategy for identifying

*Correspondence: Karen Stephens, Ph.D., University of Washington, 1959 NE Pacific St., Rm I-204, Box 357720, Seattle, WA 98195-7720, USA; Fax: 206-685-4829; E-mail: millie@u.washington.edu.

DOI: 10.1081/CNV-120025093
0735-7907 (Print); 1532-4192 (Online)
www.dekker.com

MARCEL DEKKER, INC.
270 Madison Avenue, New York, New York 10016

genes that contribute to tumor formation. This article focuses on genetic changes commonly associated with peripheral nerve sheath tumors in individuals with the autosomal dominant tumor-prone disorder neurofibromatosis 1 (NF1).

Virtually all individuals affected with NF1 develop multiple peripheral nerve sheath tumors. The most common are neurofibromas, which are benign tumors that can occur anywhere along the length of epidermal, dermal, deep peripheral (including dorsal nerve roots in the paraspinal area), or cranial nerves. They do not occur in the brain or the spinal cord proper.[5] Although benign, neurofibromas can cause considerable morbidity by, e.g., infiltrating and functionally impairing normal tissues, causing limb hypertrophy, or masking an emerging malignancy. Some types of neurofibromas can transform into malignant peripheral nerve sheath tumors (MPNST), previously termed neurofibrosarcoma or malignant schwannoma. An estimated 20%–50% of MPNSTs are associated with NF1 disease,[6] and they are a significant cause of the decreased life expectancy in the NF1 patient population.[7,8] Recent population-based longitudinal studies detected an annual incidence of 1.6/1000 and a lifetime risk of 8%–13% for NF1-associated MPNST,[9] which is much higher than detected in previous cross-sectional studies[10] and over three orders of magnitude greater than that of the general population ($\sim$0.001%).[11] Furthermore, NF1-associated MPNST were diagnosed at an earlier age than sporadic tumors (26 vs. 62 years, $p < 0.001$) and associated with a poorer prognosis than sporadic MPNST (5-year survival of 21 vs. 42%, $p = 0.09$).[9]

This article reviews the genetic abnormalities that have been identified at the level of the gene, chromosome, and genome in NF1-associated neurofibromas and MPNST. Identifying commonly associated genetic alterations and the mechanisms by which they arise may potentially lead to markers for tumor staging, to new research approaches to pathogenesis, and to the identification of gene targets, which in conjunction with NF1, will be useful for mouse models.

THE MOLECULAR BASIS OF NF1

The NF1 is a common autosomal dominant disorder that affects about 1 in 3500 individuals worldwide. About 30%–50% of cases are sporadic, caused by de novo mutation in the *NF1* gene of an individual without a family history of the disorder. In addition to predisposing to tumorigenesis, NF1 is associated with characteristic changes in pigmentation and can be associated with a wide range of other manifestations such as learning disabilities and bony abnormalities (reviewed by Refs. [12–16]). All cases are caused by mutation of the *NF1* gene at chromosome 17 band q11.2, which contains 60 exons that encode the 2818 amino acid protein called neurofibromin.[17–21] Neurofibromin is widely expressed, predominantly in the central nervous system and sensory neurons and Schwann cells of the peripheral nervous system.[22,23] One functional domain of neurofibromin has been defined, the GAP-related domain (GRD), so called because of its structural and functional homology to mammalian p120-GAP (*G*TPase *a*ctivating *p*rotein) and yeast genes known to regulate the Ras pathway.[24,25] The Ras-GAP proteins function as negative regulators of Ras by catalyzing the conversion of active GTP-bound Ras to the inactive GDP-bound Ras form.[26] In NF1-associated peripheral nerve sheath tumors, it is hypothesized that neurofibromin deficiency leads to increased activated Ras, resulting in aberrant mitogenic signaling and the consequent growth of a tumor. The identification of an NF1 patient with a missense mutation in the GRD that specifically abolished the Ras-GAP activity of neurofibromin demonstrated the importance of neurofibromin GAP function in NF1 pathogenesis.[27] In at least some tissues, there is evidence that it is the Ras-GAP activity that accounts for the tumor suppressor function of neurofibromin. The most complete evidence comes from genetic and biochemical analyses of NF1-associated malignant myeloid disorders.[28,29] The tumor suppressor function of *NF1* has been reviewed recently[30–32] along with its potential as a therapeutic target.[33]

The NF1 disease is caused by haploinsufficiency for neurofibromin. The vast majority of *NF1* mutations are not in the GRD but are distributed throughout the gene. Over 80% of mutations inactivate or predict inactivation of neurofibromin; splicing defects and sequence alterations that create a premature translation termination codon are the most common.[34,35] About 10% of *NF1* mutations are missense,[35,36] which are typically clustered in the GRD or an upstream cysteine/serine-rich domain that may play a role in ATP binding.[36] Definitive evidence that neurofibromin haploinsufficiency underlies NF1 came with the identification of *NF1* whole gene deletions in an estimated 5%–10% of affected individuals.[37,38] Mutational analyses of patients with specific features, such as plexiform neurofibroma,[39] spinal neurofibroma,[40] or malignant myeloid disorders,[41] failed to detect any correlation between genotype and phenotype. A notable exception is the subset of patients heterozygous for a microdeletion spanning the entire *NF1* gene, who consistently show an early age at onset of cutaneous neurofibromas (see below).

Marcel Dekker, Inc.
270 Madison Avenue, New York, New York 10016

Virtually all NF1 patients develop neurofibromas. Neurofibromas are comprised of an admixture of largely Schwann cells and fibroblasts, along with mast cells, endothelial cells, and pericytes.[42,43] Although classification schemes vary, Friedman and Riccardi[13] define four types of neurofibromas. Discrete cutaneous neurofibromas of the epidermis or dermis are the most common, typically appearing near or at puberty and increasing in number to over 100 by the fourth decade of life.[44] They are a localized tumor of small nerves in the skin that feels fleshy and soft; they are more prevalent on the trunk but also occur frequently on the face and extremities. Discrete subcutaneous neurofibromas have a spherical or ovoid shape, feel firm or rubbery, and may be painful or tender. Deep nodular neurofibromas, also called nodular plexiform neurofibromas, involve major or minor nerves in tissues beneath the dermis. On gross pathology, they appear to grow inside the peripheral nerve, causing a fusiform enlargement, and may extend the entire length of a nerve.[43] Diffuse plexiform neurofibromas have a cellular composition similar to that of cutaneous neurofibromas, but in contrast, they have a tendency to become locally invasive.[5,43] Histologically, this tumor is a tangled network involving multiple nerve fascicles or branches of major nerves with poorly defined margins that makes complete surgical resection virtually impossible. Plexiform neurofibromas can be superficial with extensive involvement of underlying tissues, or they may involve deep tissues, particularly in the craniofacial region, paraspinal structures, retroperitoneum, and gastrointestinal tract.[13] They can infiltrate soft tissues resulting in localized hypertrophy and significant functional impairment. In contrast to other types of neurofibromas, diffuse plexiform tumors are considered congenital because they typically become evident in infancy or childhood and rarely, if ever, in late adulthood.[45,46] In a population-based study, 32% of individuals with NF1 had a plexiform neurofibroma(s) on physical examination.[47] Korf[5] recently reviewed plexiform neurofibromas.

Plexiform neurofibromas, both diffuse and nodular, are at a greater risk of transforming to an MPNST than other types of neurofibromas (reviewed in Refs. [5,43,48]). Pathological examination of MPNST from individuals, both with and without NF1, most often shows an association with a neurofibroma.[11,49–51] These data suggest that an early step in MPNST development may be preneoplastic process in the nerve sheath. Multiple pathological and molecular criteria are used to evaluate a neurofibroma for malignant transformation.[48] Several lines of evidence are consistent with cutaneous and plexiform neurofibromas and MPNSTs being clonal tumors that arise from an ancestral Schwann cell (see below).

GENETICS OF NEUROFIBROMAGENESIS

Homozygous Inactivation of *NF1*

Homozygous inactivation of a tumor suppressor gene(s) is a fundamental mechanism of tumorigenesis. It occurs by either sequential somatic inactivation of both alleles or by a somatic mutation in the single normal homolog in individuals who inherit a germline mutation in one allele. Somatic inactivation is frequently associated with loss of heterozygosity (LOH) at the tumor suppressor locus and at multiple flanking loci (reviewed in Refs. [52,53]). Evidence for such ''2nd hit'' somatic *NF1* mutations in neurofibromas has been sought in support of the hypothesis that neurofibromin functions as a tumor suppressor in Schwann cells. Initial reports of LOH at *NF1*[54] have been confirmed and extended by analyses of both primary tumor tissue and neurofibroma-derived Schwann cells. At least 25% of neurofibromas undergo LOH at *NF1*.[55,56] The cellular admixture in neurofibromas can mask allelic loss,[55,56] which is the likely explanation for reports that detected few, if any, tumors with LOH.[57–62] Compelling evidence that the somatic inactivation of the *NF1* gene itself is important was provided by the identification of a 4 bp deletion in exon 4b in a cutaneous neurofibroma of a patient with a germline *NF1* microdeletion.[63] Subsequent analyses of cDNA from neurofibromin-derived Schwann cells showed that 19% of neurofibromas carried somatic intragenic mutations, which were typically mRNA splicing defects.[34] Mutation frequency may be underrepresented due to the difficulty of recovering high-quality tumor RNA and the underrepresentation of mutant transcripts observed in some tumors. The latter could be attributed to mutations that induce nonsense-mediated decay or other mechanisms that affect mRNA content (reviewed in Ref. [64]) or to reduced expression for other reasons,[34] and/or a low proportion of mutant to normal Schwann cells in some tumors.[65,66] Homozygous inactivation of *NF1* also occurs in plexiform neurofibromas, where an estimated 40% (n = 10) showed LOH,[67] a result confirmed by subsequent reports.[57,58,68,69]

A predominant mechanism of somatic *NF1* inactivation in neurofibromas that underwent LOH was mitotic recombination.[56] A 17q proximal single mitotic recombination event near the centromere of the q arm between the normal chromosome 17 and the

homolog carrying the germline *NF1* mutation can generate a cell in which both *NF1* genes carry the germline mutation and all loci distal to the recombination site are identical. Less common were double recombination events that result in chromosome 17 interstitial loci showing LOH. The *NF1* mRNA in some neurofibromas is edited such that an arginine codon is changed to a nonsense codon.[70] Although only one-third of neurofibromas examined showed a low level (<2.5%) of edited *NF1* transcripts,[71] such modulation of neurofibromin expression may be important if, e.g., editing occurred at high frequency in transcripts from a specific minor cellular component of the tumor. In other neurofibromas, somatic mutations appear to destabilize *NF1* mRNA.[66] Transcriptional silencing via hypermethylation of promoter regions, a prominent mechanism of inactivating other tumor suppressor genes,[72] has not been detected in neurofibroma tissue.[73,74] As expected from the mutational and LOH analyses, some neurofibromas had no detectable *NF1* transcripts or neurofibromin.[75,76] A quantitative Ras activity assay demonstrated that activated Ras-GTP levels were about fourfold higher in neurofibromas than levels in non-NF1-associated schwannomas.[75,77]

Neurofibromas are most likely clonal tumors derived from a Schwann cell progenitor. The detection of LOH in a tumor operationally defines it as being clonal in origin, and these data are consistent with direct marker analyses in neurofibromas.[57,61] The LOH or other somatic mechanisms that inactivate *NF1* in a Schwann cell progenitor may be an early or initiating genetic event in neurofibromagenesis. Klewe and colleagues showed LOH in primary neurofibroma tissue and in tumor-derived Schwann cells but not fibroblasts.[78] Other investigators confirmed this observation.[66,68] Two genetically distinct Schwann cell populations, $NF1^{+/-}$ and $NF1^{-/-}$, were successfully cultured from 10 mutation-characterized neurofibromas, whereas tumor-derived fibroblasts carried only the germline $NF1^{+/-}$ genotype.[65] Sherman et al.[79] used an elegant single cell Ras-GTP assay to show elevated levels in neurofibroma-derived Schwann cells but not fibroblasts. Consistent with two Schwann cell populations, only a fraction (12%–62%) of neurofibroma-derived Schwann cells had elevated Ras-GTP levels. The basis of the Schwann cell heterogeneity is not known, but the authors speculate that the cells with high Ras-GTP (presumably neurofibromin-deficient) may recruit Schwann cells with lower Ras-GTP levels (presumably the constitutional neurofibromin-haploinsufficient cells) via the synthesis of growth factors. Whether this admixture of Schwann cells is important in tumorigenesis remains to be determined; however, its observation in primary neurofibroma tissues makes it more likely. Fluorescence in situ hybridization and immunohistochemistry demonstrated that S-100 protein (Schwann cell marker) immunopositive cells in sections of four of seven primary plexiform neurofibromas were monosomic for *NF1*.[80] Because other cells types were disomic at *NF1*, these results strongly implicate the Schwann cell as the target of the *NF1* 2nd hit mutation and verify that the results from neurofibroma-derived Schwann cells were not biased by cell culture. These data also support Schwann cell genetic heterogeneity, because the fraction of S-100 protein positive cells showing *NF1* deletion ranged from 50%–93%. Further evidence for the importance of Schwann cells in neurofibromagenesis comes from the tumorigenic properties exhibited by neurofibroma-derived cells.[81–84] In the most comprehensive studies, Muir and colleagues[83,84] showed that neurofibromin-deficient Schwann cells, derived from either dermal or plexiform neurofibromas, had high invasive potential and produce neurofibroma-like tumors when engrafted into peripheral nerves of *scid* mice.

Germline Alterations That May Modify Neurofibromagenesis

The considerable variable expressivity of NF1 disease among family members with presumably the same *NF1* mutation and results of a statistical trait analysis led to the contention that variation in an individual's genetic background modified the NF1 phenotype.[46,85] To date, no such germline modifying genes have been identified. However, the study of patients carrying *NF1* microdeletions has provided compelling evidence for a gene that modifies neurofibromagenesis. We first recognized that *NF1* microdeletion patients typically showed an early age at onset of localized cutaneous neurofibromas or, in cases in which age at onset could not be documented, they had significantly greater numbers of cutaneous neurofibromas relative to their age.[38,86] It is common to observe multiple cutaneous neurofibromas during physical examination of children under age 10 that are heterozygous for an *NF1* microdeletion,[38,87,88] whereas only about 10% in the general NF1 population have a tumor(s) by that age.[47] In our most severe case, a 5 year old with an *NF1* microdeletion had 51–100 tumors.[38] The *NF1* microdeletions can be inherited from an affected parent, and in these cases, the microdeletion cosegregated with the early age at onset of neurofibromas.[88,89] Other investigators have confirmed the early onset and heavy burden of cutaneous neurofibromas in *NF1* microdeletion patients, and over 50 such patients have been identified.[90–98]

Marcel Dekker, Inc.
270 Madison Avenue, New York, New York 10016

Most *NF1* microdeletions span 1.5 MB of DNA,[87] which harbors the entire 350 kb *NF1* gene and at least 11 additional genes, most of unknown function.[87,99] The microdeletions are preferentially maternal in origin[87,91,93,100,101] and arise by homologous recombination between 60 kb misaligned paralogs (termed NF1REP) that flank the *NF1* gene.[87] Paralogs are nonallelic DNA sequences with a high degree of identity that arose via duplication, e.g., the two functional $\propto$ globin genes. Over 25 human disorders are known to be caused by gene or chromosomal rearrangements mediated by homologous recombination between paralogs, a process correctly referred to as nonallelic homologous recombination in the review by Stankiewicz and Lupski.[102] Here, I propose that this process be called by the less awkward term of paralogous recombination and that disorders arising by this mechanism be called paralogous recombination disorders, rather than the currently used genomic disorders. Although the NF1REPs share >95% sequence identity over 60 kb of sequence, about 80% of the *NF1* deletion alleles are virtually identical because their breakpoints map to one of either two recombination hotspots of several kb in size located within the NF1REP[103] (M. Dorschner et al., submitted). Although the molecular basis for these hotspots is not yet known, their existence means that the majority of microdeletion patients will be deleted for the same set of genes. The early age at onset of cutaneous neurofibromas observed in several patients with larger deletions and/or different breakpoints indicates that generation of a deletion-specific fusion gene product is unlikely.[87]

We hypothesized that the codeletion of *NF1* and an unknown linked gene potentiates cutaneous neurofibromagenesis.[38,87] What might be the function of the putative neurofibromagenesis-potentiating locus (*NPL*)? Here I propose two models for the early age at onset of cutaneous neurofibromas in microdeletion patients. Haploinsufficiency for *NPL* could increase the frequency of somatic 2nd hit mutations in the *NF1* gene. This could result from a genomic instability in microdeletion patients, which is intriguing in view of reports detecting cytogenetic abnormalities and microsatellite instability in some neurofibromas (see below). It would be interesting to determine if somatic *NF1* mutations in cutaneous neurofibromas of microdeletion patients occur by a predominant mechanism. Only a single tumor from each of two deletion patients have been analyzed; one had a 4 bp intragenic deletion[63] and the other a splice site.[65] A second model for early onset of cutaneous neurofibromas proposes that *NPL* haploinsufficiency increases the probability that a neurofibromin-deficient progenitor cell proliferates and manifests as a neurofibroma. Multiple mechanisms could be proposed. For example, *NPL* could encode (or regulate) a cytokine, cell cycle regulator, tumor suppressor, or oncogene, which exerts a positive proliferative advantage on the progenitor cell. Because of the cellular heterogeneity of neurofibromas, this model does not necessarily require that the abnormal expression of *NPL* or its putative downstream targets occur in the neurofibromin-deficient Schwann clone.

Preliminary, but intriguing evidence suggests that genetic background, other than *NF1* microdeletion, may influence the somatic inactivation of *NF1*. In patients with multiple neurofibromas, it was determined that each of the tumors showed the same type of somatic mutation event (e.g., LOH of the entire q arm or interstitial LOH).[56] Depending on the extent of LOH and the particular genes involved, this could explain differences in the age at onset and/or numbers of neurofibromas that develop in an individual.

Somatic Alterations That May Modify Neurofibromagesis

The NF1-associated neurofibromas have been analyzed for genetic abnormalities at the chromosomal level by comparative genome hybridization (CGH) and cytogenetic analyses. Comparative genome hybridization is a powerful technique to detect and map chromosomal regions with copy number imbalances in tumor specimens (reviewed in Ref. [104]). Only two of eight neurofibromas (type not specified) examined showed chromosomal imbalances; one tumor showed three gains; the other only a single gain.[105,106] This observation is consistent with cytogenetic studies. Although Schwann cell cultures from dermal neurofibromas had normal karyotypes, cells derived from plexiform neurofibromas had abnormalities, which in some tumors consisted of unrelated non-clonal abnormalities.[107] One plexiform had structural abnormalities predominantly involving telomeres, which are typically associated with genomic instability in other syndromes/tumors.[107] Wallace et al. proposed that chromosomal abnormalities might be important in the development of plexiform neurofibromas. Chromosomal abnormalities in plexiform neurofibromas may account, at least in part, for their increased risk of malignant transformation. Whether other cellular components of neurofibromas show cytogenetic abnormalities is unclear. Some neurofibroma fibroblast-like derived cultures were reported to show an increased frequency of chromosomal aberrations,[108] whereas others were typically negative.[109]

Conflicting data have been reported regarding the presence of microsatellite instability in NF1-associated

neurofibromas. Some human tumors, most notably those of patients with hereditary nonpolyposis colon cancer HNPCC, show microsatellite instability, which is detected by random changes in the length of microsatellite (simple nucleotide repeats) loci. Length mutations at multiple microsatellite loci in a tumor reflect a genome-wide instability, which in the case of HNPCC is due to a defect in any of several mismatch repair genes (reviewed in Ref. [2]). Ottini et al.[110] reported that 50% (n = 16) of neurofibromas showed altered allele lengths compared with matched normal tissue, and instability at chromosome 9 loci has also been reported.[111] Birindelli et al.[112] observed instability in a primary MPNST and a metastasis in one of 25 cases. However, no evidence of instability was detected in two subsequent studies of 80 neurofibromas, of which 5% appear to be of the plexiform type.[55,73] This disparity may be due to technical differences, the number and type of microsatellite loci examined, and/or the stage of the neurofibromas. The LOH at *NF1* was not a factor, because all three studies analyzed neurofibromas that were both positive and negative. Of the eight neurofibromas with microsatellite instability, seven were unstable at only one of the five loci tested.[110] Due to the important implications that microsatellite instability would have for neurofibromagenesis, additional loci should be examined in these tumors, including those analyzed by the other investigators. In addition, it would be interesting to know if the neurofibromas that showed microsatellite instability were of the larger, central plexiform type, in which case they may have been transforming to malignancy. The proportion of loci that display instability is known to increase with tumor progression in HNPCC.[113]

GENETICS OF MPNST DEVELOPMENT

Homozygous Inactivation at *NF1*

The homozygous inactivation of *NF1* in NF1-associated MPNST, first reported by Skuse et al.,[60] has been confirmed in about 50% of tumors (n = 22) by LOH.[67,109,112,114,115] Mutations in both *NF1* alleles have been identified in a single MPNST.[114] Although the mechanism of LOH is not known, it does not generally involve cytogenetically detectable losses at 17q1.[116] Furthermore, NF1-associated MPNST-derived cell lines showed decreased or absent neurofibromin and high levels of active Ras-GTP,[117,118] and a quantitative Ras activity assay demonstrated that activated Ras-GTP levels in tumors were about 15-fold higher than levels in non-NF1-associated schwannomas.[77] Because homozygous inactivation of *NF1* occurs in benign neurofibromas, it is considered an early or initiating event that is necessary and sufficient for neurofibromagenesis but not MPNST development. Malignant transformation is presumably driven by predisposing genetic factors in the germline and/or by additional somatic mutations and positive growth selection in a malignant precursor cell. The role of *NF1* in the development of sporadic MPNST is not clear; only about 10% of these tumors show LOH at *NF1*.[112]

Germline Alterations That May Modify MPNST Development

Little is known about germline genetic modifiers that predispose to MPNST. Early speculation that patients with *NF1* microdeletion may be at increased risk for malignancy[38] is now supported by indirect evidence. Mutational analysis of germline DNA from seven patients who developed MPNST determined that three (42%) were heterozygous for an *NF1* microdeletion.[119] In another study, 2 of 17 (11%) unrelated *NF1* microdeletion patients developed MPNST, and affected first-degree relatives of two microdeletion patients had other malignancies.[87] Although additional cases are needed, these data suggest that the lifetime risk of MPNST in microdeletion patients may exceed the already high 10% in the general NF1 population.[9] If so, the underlying mechanism may be essentially the same as that proposed above for early onset neurofibromagenesis. Deletion of the putative *NPL* gene could result in genomic instability or exert positive growth selection for the malignant clone. If microdeletions do predispose to both cutaneous neurofibromas and MPNST, it seems reasonable to speculate that in at least this subset of patients, either the discrete cutaneous type of neurofibroma is at increased risk of malignant transformation or the frequency of nodular or diffuse plexiform neurofibromas is high.

Evidence from two families suggests the intriguing possibility that MLH1 deficiency predisposes to NF1 and early onset extracolonic tumors.[120,121] Germline heterozygous inactivating mutations in *MLH1* cause inefficient DNA mismatch repair, with the consequent increase in mutation frequency and susceptibility to hereditary nonpolyposis colorectal cancer (reviewed in Ref. [122]). Two rare and independent cases of consanguineous marriages between *MLH1* heterozygous first cousins each produced two children with NF1 disease and hematological malignancies.[120,121] The parents had no signs of NF1 and there was no family

Marcel Dekker, Inc.
270 Madison Avenue, New York, New York 10016

Table 1. Chromosomal gains and losses in MPNST detected by CGH.

	NF1-associated MPNST			Sporadic MPNST		
	Loethe[a]	Mechtersheimer[b]	Schmidt[c]	Loethe[a]	Mechtersheimer[b]	Schmidt[c]
No. tumors/No. patients	7/7	6/6	14/6	3/3	13/13	22/20
Imbalances	52	77	188	14	176	200
Per tumor	7.4	11.7	13.4	4.6	13.5	9.1
Range	1–17	6–30	7–29	1–7	0–34	0–25
Chromosome gains	14	48	139	4	125	179
Per tumor	2	8.0	10.0	1.3	9.6	8.1
Range	0–3	4–18	5–20	0–2	0–23	0–21
Chromosome losses	38	29	49	10	51	33
Per tumor	5.4	4.8	3.5	3.3	3.9	1.5
Range	0–14	1–12	0–11	1–4	0–11	0–9

[a]Ref. [123].
[b]Ref. [105].
[c]Ref. [106].

history of the disease. The MLH1 mutations were identified, confirming homozygosity in three of the four deceased children, who presented with mutiple café au lait spots (4/4), dermal neurofibromas (2/4), tibial pseudoarthrosis (1/4), non-Hodgkin's lymphoma (2/4), myeloid leukemia (2/4), and medulloblastoma (1/4). The authors suggest that these patients had a de novo postzygotic *NF1* mutation and that the *NF1* gene may be preferentially susceptible to mismatch repair deficiency. Unfortunately, the *NF1* gene was not analyzed for mutations, due in part to lack of patient tissue,[120] which could have confirmed mutation of *NF1* and differentiated between postzygotic mutation and germline mosaicism in a parent.

Somatic Alterations in NF1-Associated MPNST

All NF1-associated MPNST showed significant chromosomal imbalances by CGH.[105,106,123,124] Analysis of 27 total tumors from 19 NF1 patients showed an average of >7 imbalances per MPNST (Table 1). One tumor had only a single imbalance, a gain of

Table 2. Frequency of chromosomal gains in NF1-associated MPNST.

	% MPNST			
	Loethe[a]	Mechtersheimer[b]	Schmidt[c]	Total
No. MPNST/No. patients	7/7	6/6	14/6	27/19
Chromosome				
1q33	0	50	50	37
5p15	28	50	35	37
7p14	28	83	71	63
7p21	28	50	64	52
7q31	28	33	64	48
8q22	28	33	64	48
8q23-q24	14	33	85	55
15q24-q25	0	17	71	41
17q22-q24	42	83	85	74
17q25	71	83	78	78

[a]Refs. [105,123].
[b]Ref. [105].
[c]Ref. [106].

chromosome 8.[123] The studies led by Mechtersheimer and Schmidt,[105,106] which include 74% of tumors examined, detected chromosomal gains more frequently than losses (Table 1). Each of the 20 tumors in these studies had ≥ 4 chromosomal gains. Although the results of these two studies were comparable, they differed from a third study that found chromosomal losses more prevalent than gains.[123] The reason for the disparity is unclear; however it was also evident in the analyses of sporadic MPNST in each study (Table 1). Table 2 summarizes the chromosomal segments that most frequently showed gains in NF1-associated MPNST. The most common segments were on 17q22-q24, 17q25, 7p14, 7p21, 8q22, 8q23-q24, and 7q31. Chromosomal loss of these segments was rarely, if ever, observed.[105,106,123] A combined analysis of sporadic and NF1-associated MPNST revealed a significantly decreased survival rate of patients with MPNST with gains at both 7p15-21 and 17q22-qter.[124]

In addition to chromosomal gains, CGH analyses also revealed large-scale chromosomal amplifications.[105,106,124] One-third of MPNST of both NF1 and non-NF1 patients had at least one amplified chromosomal segment (Table 3). Although the number of tumors is small, there are differences in amplification patterns. In NF1-associated MPNST 7p and 17q22-qter, the same regions that commonly showed chromosomal gains (Table 1) were amplified frequently. The frequency of 7p amplifications may be overestimated because these four MPNST (considered as different primary tumors) were from a single patient.[106,124] In contrast, amplifications of 5p, 8q, and 12q were the most prevalent in sporadic MPNST. There was a significant difference in the frequency of tumors with more than one chromosomal segment amplified. Only 10% of NF1-associated MPNST had more than one amplified segment, whereas the frequency was 72% in sporadic tumors (Table 3). Differences in the location and number of chromosomal segments amplified were unlikely to be due to tumor grade, because the majority of MPNST, 14 of 20 (70%) of NF1-associated and 22 of 34 (64%) of sporadic, were grade 3 (poorly differentiated). Although amplifications were more frequent in NF1-associated than sporadic MPNST (50% vs. 32%), the number of NF1-associated tumors may be overestimated because it includes multiple tumors from the same patient. Adjustment for one tumor/patient gives a frequency of 25% (5 of 20) for NF1-associated MPNST. Similarly, there was no correlation between chromosomal amplification and progression to metastasis. Analysis of tissue from a primary tumor, recurrence, and metastasis from a single patient showed a single amplification (8q12-qter) in the recurrent tumor.[124]

Comparison of the chromosomal losses detected in the three CGH studies revealed the following five most frequent losses in 27 NF1-associated MPNST: 13q21-22 (12/27), 11q23-25 (10/27), 1p22-31 (9/27), 3q11-21 (8/27), and 17p12-pter (7/27).[105,106,123] It is of interest that the loss of 17p12-pter was detected in 50% (7 of 14) tumors in one study[106] and in none of the tumors of the other studies. The relatively low detection rate of chromosomal losses may be due to the decreased sensitivity of CGH in polyploid MPNST.[125]

The CGH analysis of multiple, presumably synchronous or metachronus, primary MPNST at different sites in three NF1 patients revealed a remarkable similarity in chromosomal gains and losses.[106,124] For example, five grade 3 (poorly differentiated) tumors of one patient each showed imbalances of $+7p$, $-13q21$, and $+17q22$-qter. These data showed that in the specific genetic background of each patient, a relatively limited, and defined, number of rearrangements were shared among the tumors. Similarly, nearly identical aberrations were found in different MPNST from the same patient.[125] Although limited, these data suggest that each individual's constitutional genotype sets a certain ''baseline'' on which a minimal and limited number of genetic alterations are necessary and sufficient for MPNST development.

Consistent with CGH analysis, the karyotype of NF1-associated MPNST-derived cells are complex with chromosomal numbers ranging from 34 to 270 indicative of hypodiploidy, hypotriploidy, hypotetraploidy, hypertriploidy, and hypertetraploidy (Refs. [109,116,125] and references therein). Although breakpoints were frequent, a common specific breakpoint was not detected. A comparison of CGH and karyotying in six MPNST revealed significant overlap in the most frequent gains and detected losses at 19q (3 of 6 tumors), a region not analyzed in the CGH studies.[106,125] Plaat et al.[116] performed a computer-assisted cytogenetic analysis of 46 MPNST reported in the literature and 7 new cases of both NF1-associated and sporadic tumors (Ref. [116] and references therein). These studies confirmed the CGH observation of high-frequency gains at chromosomes 7p and 7q and losses at 1p and 17p. However, their reported cytogenetic differences between NF1-associated and sporadic MPNST[116] were not confirmed in later studies.[125,126] In one study, near triploid or near tetraploid clones were associated with grade 3 tumors and a poor prognosis.[126] The detection of a t(X;18) translocation in MPNST[127] was not confirmed in either sporadic[128] or NF1-associated neurofibroma or MPNST.[129]

Inactivating mutations in several tumor suppressor genes have been identified in NF1-associated MPNST.

Marcel Dekker, Inc.
270 Madison Avenue, New York, New York 10016

Table 3. Large-scale chromosomal amplifications in MPNST.[a]

Chromosome segment amplified	No. NF1-associated MPNST[b] (N = 20)	No. sporadic MPNST[c] (N = 34)
4q12-q13		1
5p11-p15		1
5p14		1
5p15		2
5p13-pter		2
7p14-pter	2[d]	1
7p13-pter	1[d]	
7p12-pter	1[d]	
7p11-p12		1
8q12-qter		2
8q13		1
8q21-q22		1
8q22-q23		1
8q24		1
8q23-qter	1	
9p21-p23	1[e]	
9q31-q33		1
12p12	1[e]	
12p13		1
12q13-q14		1
12q14-q21		3
12q24		3
13q13-q33		1
13q32-q33		1
17p11-p12		1
17q24-qter	2	
17q22-q24	1	
20q12-qter		1
Xp11		1
Xp21-p22		1
Summary		
% tumors with an amplification	50 (10/20)	32 (11/34)
% tumors with >1 amplified segment	0.1 (1/10)	72 (8/11)
% patients with ≥ 1 tumor with an amplification	30 (4/12)	32 (11/34)

[a]Centromeric regions, chromosomes 19 and Y, and 1p32-p36 were not scored for technical reasons. (From Ref. [105].)
[b]Refs. [105,106,124].
[c]Refs. [105,124].
[d]Includes four of five primary MPNST from one patient. (From Ref. [106].)
[e]Includes two of four primary MPNST from one patient. (From Ref. [106].)

Both LOH and intragenic missense mutations of *TP53*[50,62,112,130] have been detected. Like many sarcomas, NF1-associated MPNST often showed overexpression of p53 (the protein product of the *TP53* gene) as assayed by immunoreactive positivity in the nucleus.[50,112,131,132] In keeping with findings in other tumors, this most likely is mutant p53 protein, which accumulates due to its increased stability. Mutant protein is thought to promote cancer by either complexing with and sequestering functional p53 or by complexing with p63 and p73 and blocking their normal transcription factor activities (reviewed in Ref. [133]). Immunohistochemical detection of p53 was more common in NF1-associated vs. sporadic MPNST, and it was associated with poor prognosis in NF1 children.[132] About 50% of NF1-associated MPNST showed homozygous deletion for exon 2 of the *INK4A* gene, and over 90% were immunonegative for its protein product p16.[112,134,135] Homozygous deletion of exon 2 results in deficiency for both p16 and $p14^{ARF}$, two proteins encoded by alternative splicing of *INK4A* (also known as *CDKN2A*). Both of these proteins are tumor suppressors that

modulate activities of the RB and p53 pathways, which are critical for cell cycle control and tumor surveillance (reviewed in Ref. [136]). *MXI1* mutations in regions that encode known functional domains have been detected in the two NF1-associated MPNST analyzed.[137] Mxi1 is an agonist of the oncoprotein Myc and is thought to limit cell proliferation and help maintain the differentiated state (reviewed in Ref. [138]). *Mxi1*-deficient mice develop tumors, and *Mxi1* deficiency decreases the latency of tumors that arise in Ink4a-deficient mice.[139] If additional studies show that somatic inactivation of *MXI1* is common, it would suggest a link between the pathways of Ink4a, Myc, and Ras in NF1-associated MPNST.[140,141]

Several differences observed in NF1-associated MPNST are likely involved in the malignant transformation of a preexisting neurofibroma. *TP53* or *INK4A* mutations/altered expression were not detected in neurofibromas.[50,51,54,62,67,69,112,132,134,135] Furthermore, p53-positive nuclei, typically associated with MPNST, were observed in a few cells at the transitional zone between an existing plexiform neurofibroma and an arising MPNST.[51] One plexiform neurofibroma proximal to an MPNST did show p16 immunonegativity.[112] Microdissection of a preexisting neurofibroma from its MPNST focal malignant process revealed 5 chromosomal imbalances in the neurofibroma, all of which were novel compared to the 10 imbalances in the MPNST component.[106] These data are consistent with a restructuring of the genome during transformation. An additional distinguishing feature of MPNST is the high labeling index of the nuclear proliferating antigen Ki67, which was correlated with reduced survival in a study that combined NF1-associated and sporadic MPNST.[51,132,142]

OTHER NF1-ASSOCIATED NEOPLASMS AND MOUSE MODELS

In addition to peripheral nerve sheath tumors, individuals affected with NF1 are at increased risk for an array of other tumors. Epidemiologically associated neoplasms include medulloblastoma, pheochromocytoma, astrocytoma, and adenocarcinoma of the ampulla of Vater (Ref. [143] and references therein).[144] Primarily children affected with NF1 are at increased risk for optic pathway gliomas and brainstem gliomas, rhabdomyosarcomas, and malignant myeloid leukemias.[41,145–149] The NF1 patients are also at increased risk for a second malignancy, some of which may be treatment-related.[146,150,151] In different studies, 8%–21% of NF1 patients with a first malignancy developed a second cancer, compared to a frequency of 4% in the general population.[143] Malignancy in NF1 has been reviewed recently.[152]

Although heterozygous mutant mice ($Nf1^{+/-}$) develop tumors, they are not the characteristic peripheral nerve sheath tumors characteristic of the human disease.[153–155] The *Nf1*-deficient mice ($Nf1^{-/-}$) die in utero from cardiac defects. Mice chimeric for ($Nf1^{-/-}$) and ($Nf1^{+/+}$) cells were able to develop many microscopic plexiform neurofibromas, but dermal tumors did not develop.[156] In addition, mice doubly heterozygous for mutations in *Nf1* and *p53* developed MPNST that showed LOH at both tumor suppressor loci.[156,157] Recently, mice were constructed such that only their Schwann cells were *Nf1* deficient.[158] Different tumor phenotypes were observed, depending on whether the *Nf1*–deficient Schwann cells were in an animal with an $Nf1^{+/-}$ or an $Nf1^{+/+}$ constitutional genotype. In the $Nf1^{+/-}$ genetic background, plexiform neurofibromas composed of *Nf1*–deficient Schwann cells, and the fibroblasts and mast cells that normally occur in human neurofibromas, developed on peripheral nerves. In the $Nf1^{+/+}$ genetic background, *Nf1*–deficient Schwann cells did not participate in neurofibromagenesis but did form relatively small hyperplastic lesions of the cranial nerves containing minimal mast cells. This mouse model demonstrates that neurofibromin deficiency in Schwann cells is sufficient for generating nascent tumor lesions, but frank plexiform neurofibroma development requires neurofibromin haploinsufficiency in cells of the surrounding tissues.

With the development of mouse models, understanding the genetics, pathology, and natural history of human benign and malignant peripheral nerve sheath tumors takes on new importance. It is only by accurate modeling of the human disease that progress can be made toward therapies that can slow or halt neurofibromagenesis and reduce the high risk of malignancy associated with NF1 disease.

ACKNOWLEDGMENTS

This work was supported by grants DAMD17-00-1-0542 and DAMD 17-01-1-0721 awarded to K. S. The U.S. Army Medical Research Acquisition Activity, 820 Chandler Street, Fort Detrick, Md 21702-5014 is the awarding and administering acquisition office. The content of the information does not necessarily reflect the position or the policy of the government, and no official endorsement should be inferred. Manuscript submitted 5/31/02, Accepted for publication 8/12/02.

REFERENCES

1. Newsham, I.; Hadjistilianou, T.; Cavenee, W.K.. Retinoblastoma. In *The Metabolic & Molecular Bases of Inherited Disease,* 8th Ed.; Scriver, C.R., Beaudet, A.L., Sly, W.S., Valle, D., Eds.; McGraw-Hill: New York, 2001; Vol. 1, 819–848.
2. Muller, A.; Fishel, R. Mismatch repair and the hereditary non-polyposis colorectal cancer syndrome (HNPCC). Cancer Investig. **2002**, *20*, 102–109.
3. Bodmer, W. Familial adenomatous polyposis (FAP) and its gene, APC. Cytogenet. Cell Genet. **1999**, *86*, 99–104.
4. Lengauer, C.; Kinzler, K.W.; Vogelstein, B. Genetic instabilities in human cancers. Nature **1998**, *396*, 643–649.
5. Korf, B.R. Plexiform neurofibromas. Am. J. Med. Genet. **1999**, *89*, 31–37.
6. Sorensen, S.A.; Mulvihill, J.J.; Nielsen, A. Long-term follow-up of von Recklinghausen neurofibromatosis. Survival and malignant neoplasms. N. Engl. J. Med. **1986**, *314*, 1010–1015.
7. Poyhonen, M.; Niemela, S.; Herva, R. Risk of malignancy and death in neurofibromatosis. Arch. Pathol. Lab. Med. **1997**, *121*, 139–143.
8. Rasmussen, S.A.; Yang, Q.; Friedman, J.M. Mortality in neurofibromatosis 1: an analysis using U.S. death certificates. Am. J. Hum. Genet. **2001**, *68*, 1110–1118.
9. Evans, D.G.; Baser, M.E.; McGaughran, J.; Sharif, S.; Howard, E.; Moran, A. Malignant peripheral nerve sheath tumours in neurofibromatosis 1. J. Med. Genet. **2002**, *39*, 311–314.
10. Huson, S.M.; Compston, D.A.; Clark, P.; Harper, P.S. A genetic study of von Recklinghausen neurofibromatosis in south east Wales. I. Prevalence, fitness, mutation rate, and effect of parental transmission on severity. J. Med. Genet. **1989**, *26*, 704–711.
11. Ducatman, B.S.; Scheithauer, B.W.; Piepgras, D.G.; Reiman, H.M.; Ilstrup, D.M. Malignant peripheral nerve sheath tumors. A clinicopathologic study of 120 cases. Cancer **1986**, *57*, 2006–2021.
12. Korf, B.R. Diagnosis and management of neurofibromatosis type 1. Curr. Neurol. Neurosci. Rep. **2001**, *1*, 162–167.
13. Friedman, J.M.; Riccardi, V.M.. Clinical and epidemiological features. In *Neurofibromatosis. Phenotype, Natural History, and Pathogenesis,* 3rd Ed.; Friedman, J.M., Gutmann, D.H., MacCollin, M., Riccardi, V.M., Eds.; The Johns Hopkins University Press: Baltimore, 1999; Vol. 1, 29–86.
14. North, K. Neurofibromatosis type 1. Am. J. Med. Genet. **2000**, *97*, 119–127.
15. Gutmann, D.H.; Aylsworth, A.; Carey, J.C.; Korf, B.; Marks, J.; Pyeritz, R.E.; Rubenstein, A.; Viskochil, D. The diagnostic evaluation and multidisciplinary management of neurofibromatosis 1 and neurofibromatosis 2. Jama **1997**, *278*, 51–57.
16. Lakkis, M.M.; Tennekoon, G.I. Neurofibromatosis type 1. I. General overview. J. Neurosci. Res. **2000**, *62*, 755–763.
17. Li, Y.; O'Connell, P.; Breidenbach, H.H.; Cawthon, R.; Stevens, J.; Xu, G.; Neil, S.; Robertson, M.; White, R.; Viskochil, D. Genomic organization of the neurofibromatosis 1 gene (NF1). Genomics **1995**, *25*, 9–18.
18. Marchuk, D.A.; Saulino, A.M.; Tavakkol, R.; Swaroop, M.; Wallace, M.R.; Andersen, L.B.; Mitchell, A.L.; Gutmann, D.H.; Boguski, M.; Collins, F.S. cDna cloning of the type 1 neurofibromatosis gene: complete sequence of the NF1 gene product. Genomics **1991**, *11*, 931–940.
19. Wallace, M.R.; Marchuk, D.A.; Andersen, L.B.; Letcher, R.; Odeh, H.M.; Saulino, A.M.; Fountain, J.W.; Brereton, A.; Nicholson, J.; Mitchell, A.L.; Brownstein, B.H.; Collins, F.S. Type 1 neurofibromatosis gene: identification of a large transcript disrupted in three NF1 patients 1749]. Science **1990**, *249*, 181–186.
20. Viskochil, D.; Buchberg, A.M.; Xu, G.; Cawthon, R.M.; Stevens, J.; Wolff, R.K.; Culver, M.; Carey, J.C.; Copeland, N.G.; Jenkins, N.A.; White, R.; O'Connell, P. Deletions and a translocation interrupt a cloned gene at the neurofibromatosis type 1 locus. Cell **1990**, *62*, 187–192.
21. Cawthon, R.M.; Weiss, R.; Xu, G.F.; Viskochil, D.; Culver, M.; Stevens, J.; Robertson, M.; Dunn, D.; Gesteland, R.; O'Connell, P.; White, R. A major segment of the neurofibromatosis type 1 gene: cDNA sequence, genomic structure, and point mutations. Cell **1990**, *62*, 193–201.
22. Daston, M.M.; Scrable, H.; Nordlund, M.; Sturbaum, A.K.; Nissen, L.M.; Ratner, N. The protein product of the neurofibromatosis type 1 gene is expressed at highest abundance in neurons, Schwann cells, and oligodendrocytes. Neuron **1992**, *8*, 415–428.
23. Huynh, D.P.; Lin, C.T.; Pulst, S.M. Expression of neurofibromin, the neurofibromatosis 1 gene product: studies in human neuroblastoma cells

MARCEL DEKKER, INC.
270 Madison Avenue, New York, New York 10016

and rat brain. Neurosci. Lett. **1992**, *143*, 233–236.
24. Buchberg, A.M.; Cleveland, L.S.; Jenkins, N.A.; Copeland, N.G. Sequence homology shared by neurofibromatosis type-1 gene and IRA-1 and IRA-2 negative regulators of the RAS cyclic AMP pathway. Nature **1990**, *347*, 291–294.
25. Xu, G.F.; O'Connell, P.; Viskochil, D.; Cawthon, R.; Robertson, M.; Culver, M.; Dunn, D.; Stevens, J.; Gesteland, R.; White, R.; Weiss, R. The neurofibromatosis type 1 gene encodes a protein related to GAP. Cell **1990**, *62*, 599–608.
26. McCormick, F. ras GTPase activating protein: signal transmitter and signal terminator. Cell **1989**, *56*, 5–8.
27. Klose, A.; Ahmadian, M.R.; Schuelke, M.; Scheffzek, K.; Hoffmeyer, S.; Gewies, A.; Schmitz, F.; Kaufmann, D.; Peters, H.; Wittinghofer, A.; Nurnberg, P. Selective disactivation of neurofibromin GAP activity in neurofibromatosis type 1. Hum. Mol. Genet. **1998**, *7*, 1261–1268.
28. Zhang, Y.Y.; Vik, T.A.; Ryder, J.W.; Srour, E.F.; Jacks, T.; Shannon, K.; Clapp, D.W. Nf1 regulates hematopoietic progenitor cell growth and ras signaling in response to multiple cytokines. J. Exp. Med. **1998**, *187*, 1893–1902.
29. The NF1 gene as a tumor suppressor in neurofibromatosis type 1. Side, L.D., Shannon, K.M., Eds.; Bios Scientific Publishers: Oxford, 1998.
30. Cichowski, K.; Jacks, T. NF1 tumor suppressor gene function: narrowing the GAP. Cell **2001**, *104*, 593–604.
31. Zhu, Y.; Parada, L.F. Neurofibromin, a tumor suppressor in the nervous system. Exp. Cell Res. **2001**, *264*, 19–28.
32. Gutmann, D.H. The neurofibromatoses: when less is more. Hum. Mol. Genet. **2001**, *10*, 747–755.
33. Weiss, B.; Bollag, G.; Shannon, K. Hyperactive Ras as a therapeutic target in neurofibromatosis type 1. Am. J. Med. Genet. **1999**, *89*, 14–22.
34. Serra, E.; Ars, E.; Ravella, A.; Sanchez, A.; Puig, S.; Rosenbaum, T.; Estivill, X.; Lazaro, C. Somatic NF1 mutational spectrum in benign neurofibromas: mRNA splice defects are common among point mutations. Hum. Genet. **2001**, *108*, 416–429.
35. Messiaen, L.M.; Callens, T.; Mortier, G.; Beysen, D.; Vandenbroucke, I.; Van Roy, N.; Speleman, F.; Paepe, A.D. Exhaustive mutation analysis of the NF1 gene allows identification of 95% of mutations and reveals a high frequency of unusual splicing defects. Human Mutat. **2000**, *15*, 541–555.
36. Fahsold, R.; Hoffmeyer, S.; Mischung, C.; Gille, C.; Ehlers, C.; Kucukceylan, N.; Abdel-Nour, M.; Gewies, A.; Peters, H.; Kaufmann, D.; Buske, A.; Tinschert, S.; Nurnberg, P. Minor lesion mutational spectrum of the entire NF1 gene does not explain its high mutability but points to a functional domain upstream of the GAP-related domain. Am. J. Hum. Genet. **2000**, *66*, 790–818.
37. Kayes, L.M.; Riccardi, V.M.; Burke, W.; Bennett, R.L.; Stephens, K. Large de novo DNA deletion in a patient with sporadic neurofibromatosis 1, mental retardation, and dysmorphism. J. Med. Genet. **1992**, *29*, 686–690.
38. Kayes, L.M.; Burke, W.; Riccardi, V.M.; Bennett, R.; Ehrlich, P.; Rubenstein, A.; Stephens, K. Deletions spanning the neurofibromatosis 1 gene: identification and phenotype of five patients. Am. J. Hum. Genet. **1994**, *54*, 424–436.
39. Kluwe, L.; Friedrich, R.E.; Korf, B.; Fahsold, R.; Mautner, V.F. NF1 mutations in neurofibromatosis 1 patients with plexiform neurofibromas. Human Mutat. **2002**, *19*, 309.
40. Kaufmann, D.; Muller, R.; Bartelt, B.; Wolf, M.; Kunzi-Rapp, K.; Hanemann, C.O.; Fahsold, R.; Hein, C.; Vogel, W.; Assum, G. Spinal neurofibromatosis without cafe-au-lait macules in two families with null mutations of the NF1 gene. Am. J. Hum. Genet. **2001**, *69*, 1395–1400.
41. Side, L.; Taylor, B.; Cayouette, M.; Conner, E.; Thompson, P.; Luce, M.; Shannon, K. Homozygous inactivation of the NF1 gene in bone marrow cells from children with neurofibromatosis type 1 and malignant myeloid disorders. N. Engl. J. Med. **1997**, *336*, 1713–1720.
42. Lott, I.T.; Richardson, E.P., Jr. Neuropathological findings and the biology of neurofibromatosis. Adv. Neurol. **1981**, *29*, 23–32.
43. Woodruff, J.M. Pathology of tumors of the peripheral nerve sheath in type 1 neurofibromatosis. Am. J. Med. Genet. **1999**, *89*, 23–30.
44. Huson, S.M.. Neurofibromatosis 1: a clinical and genetic overview. In *The Neurofibromatoses: A Pathogenetic and Clinical Overview,* 1st Ed.; Huson, S.M., Hughes, R.A.C., Eds.; Chapman and Hall Medical: London, 1994; 160–203.
45. Waggoner, D.J.; Towbin, J.; Gottesman, G.; Gutmann, D.H. Clinic-based study of plexiform neurofibromas in neurofibromatosis 1. Am. J. Med. Genet. **2000**, *92*, 132–135.
46. Riccardi, V.M. *Neurofibromatosis, Phenotype, Natural History, Pathogenesis;* The Johns Hopkins University Press: Batimore, 1992.
47. Huson, S.M.; Harper, P.S.; Compston, D.A. Von

Marcel Dekker, Inc.
270 Madison Avenue, New York, New York 10016

Recklinghausen neurofibromatosis. A clinical and population study in south-east Wales. Brain **1988**, *111* (Pt 6), 1355–1381.
48. Ferner, R.E.; Gutmann, D.H. International consensus statement on malignant peripheral nerve sheath tumors in neurofibromatosis. Cancer Res. **2002**, *62*, 1573–1577.
49. Molenaar, W.M.; Dijkhuizen, T.; van Echten, J.; Hoekstra, H.J.; van den Berg, E. Cytogenetic support for early malignant change in a diffuse neurofibroma not associated with neurofibromatosis. Cancer Genet. Cytogenet. **1997**, *97*, 70–72.
50. Leroy, K.; Dumas, V.; Martin-Garcia, N.; Falzone, M.C.; Voisin, M.C.; Wechsler, J.; Revuz, J.; Creange, A.; Levy, E.; Lantieri, L.; Zeller, J.; Wolkenstein, P. Malignant peripheral nerve sheath tumors associated with neurofibromatosis type 1: a clinicopathologic and molecular study of 17 patients. Arch. Dermatol. **2001**, *137*, 908–913.
51. Watanabe, T.; Oda, Y.; Tamiya, S.; Masuda, K.; Tsuneyoshi, M. Malignant peripheral nerve sheath tumour arising within neurofibroma. An immunohistochemical analysis in the comparison between benign and malignant components. J. Clin. Pathol. **2001**, *54*, 631–636.
52. Tischfield, J.A. Loss of heterozygosity or: how I learned to stop worrying and love mitotic recombination. Am. J. Hum. Genet. **1997**, *61*, 995.
53. Fearon, E.R. Human cancer syndromes: clues to the origin and nature of cancer. Science **1997**, *278*, 1043–1050.
54. Colman, S.D.; Williams, C.A.; Wallace, M.R. Benign neurofibromas in type 1 neurofibromatosis (NF1) show somatic deletions of the NF1 gene. Nat. Genet. **1995**, *11*, 90–92.
55. Serra, E.; Puig, S.; Otero, D.; Gaona, A.; Kruyer, H.; Ars, E.; Estivill, X.; Lazaro, C. Confirmation of a double-hit model for the NF1 gene in benign neurofibromas. Am. J. Hum. Genet. **1997**, *61*, 512–519.
56. Serra, E.; Rosenbaum, T.; Nadal, M.; Winner, U.; Ars, E.; Estivill, X.; Lazaro, C. Mitotic recombination effects homozygosity for NF1 germline mutations in neurofibromas. Nat. Genet. **2001**, *28*, 294–296.
57. Daschner, K.; Assum, G.; Eisenbarth, I.; Krone, W.; Hoffmeyer, S.; Wortmann, S.; Heymer, B.; Kehrer-Sawatzki, H. Clonal origin of tumor cells in a plexiform neurofibroma with LOH in NF1 intron 38 and in dermal neurofibromas without LOH of the NF1 gene. Biochem. Biophys. Res. Commun. **1997**, *234*, 346–350.
58. John, A.M.; Ruggieri, M.; Ferner, R.; Upadhyaya, M. A search for evidence of somatic mutations in the NF1 gene. J. Med. Genet. **2000**, *37*, 44–49.
59. Stark, M.; Assum, G.; Krone, W. Single-cell PCR performed with neurofibroma Schwann cells reveals the presence of both alleles of the neurofibromatosis type 1 (NF1) gene. Hum. Genet. **1995**, *96*, 619–623.
60. Skuse, G.R.; Kosciolek, B.A.; Rowley, P.T. Molecular genetic analysis of tumors in von Recklinghausen neurofibromatosis: loss of heterozygosity for chromosome 17. Genes Chromosomes Cancer **1989**, *1*, 36–41.
61. Skuse, G.R.; Kosciolek, B.A.; Rowley, P.T. The neurofibroma in von Recklinghausen neurofibromatosis has a unicellular origin. Am. J. Hum. Genet. **1991**, *49*, 600–607.
62. Menon, A.G.; Anderson, K.M.; Riccardi, V.M.; Chung, R.Y.; Whaley, J.M.; Yandell, D.W.; Farmer, G.E.; Freiman, R.N.; Lee, J.K.; Li, F.P.; Barker, D.F.; Ledbetter, D.H.; Kleider, A.; Martuza, R.L.; Gusella, J.F.; Seizinger, B.R. Chromosome 17p deletions and p53 gene mutations associated with the formation of malignant neurofibrosarcomas in von Recklinghausen neurofibromatosis. Proc. Natl. Acad. Sci. U. S. A. **1990**, *87*, 5435–5439.
63. Sawada, S.; Florell, S.; Purandare, S.M.; Ota, M.; Stephens, K.; Viskochil, D. Identification of NF1 mutations in both alleles of a dermal neurofibroma. Nat. Genet. **1996**, *14*, 110–112.
64. Mendell, J.T.; Dietz, H.C. When the message goes awry. Disease-producing mutations that influence mRNA content and performance. Cell **2001**, *107*, 411–414.
65. Serra, E.; Rosenbaum, T.; Winner, U.; Aledo, R.; Ars, E.; Estivill, X.; Lenard, H.G.; Lazaro, C. Schwann cells harbor the somatic NF1 mutation in neurofibromas: evidence of two different Schwann cell subpopulations. Hum. Mol. Genet. **2000**, *9*, 3055–3064.
66. Rutkowski, J.L.; Wu, K.; Gutmann, D.H.; Boyer, P.J.; Legius, E. Genetic and cellular defects contributing to benign tumor formation in neurofibromatosis type 1. Hum. Mol. Genet. **2000**, *9*, 1059–1066.
67. Rasmussen, S.A.; Overman, J.; Thomson, S.A.; Colman, S.D.; Abernathy, C.R.; Trimpert, R.E.; Moose, R.; Virdi, G.; Roux, K.; Bauer, M.; Rojiani, A.M.; Maria, B.L.; Muir, D.; Wallace, M.R. Chromosome 17 loss-of-heterozygosity studies in benign and malignant tumors in neurofibromatosis type 1. Genes Chromosomes Cancer **2000**, *28*, 425–431.

MARCEL DEKKER, INC.
270 Madison Avenue, New York, New York 10016

68. Eisenbarth, I.; Beyer, K.; Krone, W.; Assum, G. Toward a survey of somatic mutation of the NF1 gene in benign neurofibromas of patients with neurofibromatosis type 1. Am. J. Hum. Genet. **2000**, *66*, 393–401.
69. Kluwe, L.; Friedrich, R.E.; Mautner, V.F. Allelic loss of the NF1 gene in NF1-associated plexiform neurofibromas. Cancer Genet. Cytogenet. **1999**, *113*, 65–69.
70. Skuse, G.R.; Cappione, A.J.; Sowden, M.; Metheny, L.J.; Smith, H.C. The neurofibromatosis type I messenger RNA undergoes base-modification RNA editing. Nucleic Acids Res. **1996**, *24*, 478–485.
71. Mukhopadhyay, D.; Anant, S.; Lee, R.M.; Kennedy, S.; Viskochil, D.; Davidson, N.O. C→U editing of neurofibromatosis 1 mRNA occurs in tumors that express both the type II transcript and apobec-1, the catalytic subunit of the apolipoprotein B mRNA-editing enzyme. Am. J. Hum. Genet. **2002**, *70*, 38–50.
72. Jones, P.A. DNA methylation errors and cancer. Cancer Res. **1996**, *56*, 2463–2467.
73. Luijten, M.; Redeker, S.; van Noesel, M.M.; Troost, D.; Westerveld, A.; Hulsebos, T.J. Microsatellite instability and promoter methylation as possible causes of NF1 gene inactivation in neurofibromas. Eur. J. Hum. Genet. **2000**, *8*, 939–945.
74. Horan, M.P.; Cooper, D.N.; Upadhyaya, M. Hypermethylation of the neurofibromatosis type 1 (NF1) gene promoter is not a common event in the inactivation of the NF1 gene in NF1-specific tumours. Hum. Genet. **2000**, *107*, 33–39.
75. Guha, A. Ras activation in astrocytomas and neurofibromas. Can. J. Neurol. Sci. **1998**, *25*, 267–281.
76. Peters, N.; Waha, A.; Wellenreuther, R.; Friedrich, R.E.; Mautner, V.F.; Hoffmeyer, S.; Lenartz, D.; Schramm, J.; Wiestler, O.D.; von Deimling, A. Quantitative analysis of NF1 and OMGP gene transcripts in sporadic gliomas, sporadic meningiomas and neurofibromatosis type 1-associated plexiform neurofibromas. Acta Neuropathol. (Berl) **1999**, *97*, 547–551.
77. Guha, A.; Lau, N.; Huvar, I.; Gutmann, D.; Provias, J.; Pawson, T.; Boss, G. Ras-GTP levels are elevated in human NF1 peripheral nerve tumors. Oncogene **1996**, *12*, 507–513.
78. Kluwe, L.; Friedrich, R.; Mautner, V.F. Loss of NF1 allele in Schwann cells but not in fibroblasts derived from an NF1-associated neurofibroma. Genes Chromosomes Cancer **1999**, *24*, 283–285.
79. Sherman, L.S.; Atit, R.; Rosenbaum, T.; Cox, A.D.; Ratner, N. Single cell Ras-GTP analysis reveals altered Ras activity in a subpopulation of neurofibroma Schwann cells but not fibroblasts. J. Biol. Chem. **2000**, *275*, 30740–30745.
80. Perry, A.; Roth, K.A.; Banerjee, R.; Fuller, C.E.; Gutmann, D.H. NF1 deletions in S-100 protein-positive and negative cells of sporadic and neurofibromatosis 1 (NF1)-associated plexiform neurofibromas and malignant peripheral nerve sheath tumors. Am. J. Pathol. **2001**, *159*, 57–61.
81. Sheela, S.; Riccardi, V.M.; Ratner, N. Angiogenic and invasive properties of neurofibroma Schwann cells. J. Cell Biol. **1990**, *111*, 645–653.
82. Rosenbaum, T.; Rosenbaum, C.; Winner, U.; Muller, H.W.; Lenard, H.G.; Hanemann, C.O. Long-term culture and characterization of human neurofibroma-derived Schwann cells. J. Neurosci. Res. **2000**, *61*, 524–532.
83. Muir, D.; Neubauer, D.; Lim, I.T.; Yachnis, A.T.; Wallace, M.R. Tumorigenic properties of neurofibromin-deficient neurofibroma Schwann cells. Am. J. Pathol. **2001**, *158*, 501–513.
84. Muir, D. Differences in proliferation and invasion by normal, transformed and NF1 Schwann cell cultures are influenced by matrix metalloproteinase expression. Clin. Exp. Metastasis **1995**, *13*, 303–314.
85. Easton, D.F.; Ponder, M.A.; Huson, S.M.; Ponder, B.A. An analysis of variation in expression of neurofibromatosis (NF) type 1 (NF1): evidence for modifying genes. Am. J. Hum. Genet. **1993**, *53*, 305–313.
86. Kayes, L.M.; Schroeder, W.T.; Marchuk, D.A.; Collins, F.S.; Riccardi, V.M.; Duvic, M.; Stephens, K. The gene for a novel epidermal antigen maps near the neurofibromatosis 1 gene. Genomics **1992**, *14*, 369–376.
87. Dorschner, M.O.; Sybert, V.P.; Weaver, M.; Pletcher, B.A.; Stephens, K. NF1 microdeletion breakpoints are clustered at flanking repetitive sequences. Hum. Mol. Genet. **2000**, *9*, 35–46.
88. Leppig, K.A.; Kaplan, P.; Viskochil, D.; Weaver, M.; Ortenberg, J.; Stephens, K. Familial neurofibromatosis 1 microdeletions: cosegregation with distinct facial phenotype and early onset of cutaneous neurofibromata. Am. J. Med. Genet. **1997**, *73*, 197–204.
89. Wu, B.L.; Schneider, G.H.; Korf, B.R. Deletion of the entire NF1 gene causing distinct manifesta-

tions in a family. Am. J. Med. Genet. **1997**, *69*, 98–101.
90. Wu, B.L.; Austin, M.A.; Schneider, G.H.; Boles, R.G.; Korf, B.R. Deletion of the entire NF1 gene detected by the FISH: four deletion patients associated with severe manifestations. Am. J. Med. Genet. **1995**, *59*, 528–535.
91. Upadhyaya, M.; Ruggieri, M.; Maynard, J.; Osborn, M.; Hartog, C.; Mudd, S.; Penttinen, M.; Cordeiro, I.; Ponder, M.; Ponder, B.A.; Krawczak, M.; Cooper, D.N. Gross deletions of the neurofibromatosis type 1 (NF1) gene are predominantly of maternal origin and commonly associated with a learning disability, dysmorphic features and developmental delay. Hum. Genet. **1998**, *102*, 591–597.
92. Tonsgard, J.H.; Yelavarthi, K.K.; Cushner, S.; Short, M.P.; Lindgren, V. Do NF1 gene deletions result in a characteristic phenotype? Am. J. Med. Genet. **1997**, *73*, 80–86.
93. Lazaro, C.; Gaona, A.; Ainsworth, P.; Tenconi, R.; Vidaud, D.; Kruyer, H.; Ars, E.; Volpini, V.; Estivill, X. Sex differences in mutational rate and mutational mechanism in the NF1 gene in neurofibromatosis type 1 patients. Hum. Genet. **1996**, *98*, 696–699.
94. Fang, L.J.; Vidaud, D.; Vidaud, M.; Thirion, J.P. Identification and characterization of four novel large deletions in the human neurofibromatosis type 1 (NF1) gene. Human Mutat. **2001**, *18*, 549–550.
95. Lopez Correa, C.; Brems, H.; Lazaro, C.; Estivill, X.; Clementi, M.; Mason, S.; Rutkowski, J.L.; Marynen, P.; Legius, E. Molecular studies in 20 submicroscopic neurofibromatosis type 1 gene deletions. Human Mutat. **1999**, *14*, 387–393.
96. Ainsworth, P.J.; Chakraborty, P.K.; Weksberg, R. Example of somatic mosaicism in a series of de novo neurofibromatosis type 1 cases due to a maternally derived deletion. Human Mutat. **1997**, *9*, 452–457.
97. Cnossen, M.H.; van der Est, M.N.; Breuning, H.; van Asperen, C.J.; Breslau-Siderius, E.J.; van der Ploeg, A.T.; de Goede-Bolder, A.; van den Ouweland, A.M.W.; Halley, D.J.J.; Niermeijer, M.F. Deletions spanning the neurofibromatosis type 1 gene: implications for genotype-phenotype correlations in neurofibromatosis type 1? Human Mutat. **1997**, *9*, 458–464.
98. Jenne, D.E.; Tinschert, S.; Stegmann, E.; Reimann, H.; Nurnberg, P.; Horn, D.; Naumann, I.; Buske, A.; Thiel, G. A common set of at least 11 functional genes is lost in the majority of NF1 patients with gross deletions [in process citation]. Genomics **2000**, *66*, 93–97.
99. Jenne, D.E.; Tinschert, S.; Stegmann, E.; Reimann, H.; Nurnberg, P.; Horn, D.; Naumann, I.; Buske, A.; Thiel, G. A common set of at least 11 functional genes is lost in the majority of NF1 patients with gross deletions. Genomics **2000**, *66*, 93–97.
100. Valero, M.C.; Pascual-Castroviejo, I.; Velasco, E.; Moreno, F.; Hernandez-Chico, C. Identification of de novo deletions at the NF1 gene: no preferential paternal origin and phenotypic analysis of patients. Hum. Genet. **1997**, *99*, 720–726.
101. Correa, C.L.; Brems, H.; Lazaro, C.; Marynen, P.; Legius, E. Unequal meiotic crossover: a frequent cause of NF1 microdeletions. Am. J. Hum. Genet. **2000**, *66*, 1969–1974.
102. Stankiewicz, P.; Lupski, J.R. Genome architecture, rearrangements and genomic disorders. Trends Genet. **2002**, *18*, 74–82.
103. Lopez-Correa, C.; Dorschner, M.; Brems, H.; Lazaro, C.; Clementi, M.; Upadhyaya, M.; Dooijes, D.; Moog, U.; Kehrer-Sawatzki, H.; Rutkowski, J.L.; Fryns, J.P.; Marynen, P.; Stephens, K.; Legius, E. Recombination hotspot in NF1 microdeletion patients. Hum. Mol. Genet. **2001**, *10*, 1387–1392.
104. Tachdjian, G.; Aboura, A.; Lapierre, J.M.; Viguie, F. Cytogenetic analysis from DNA by comparative genomic hybridization. Ann. Genet. **2000**, *43*, 147–154.
105. Mechtersheimer, G.; Otano-Joos, M.; Ohl, S.; Benner, A.; Lehnert, T.; Willeke, F.; Moller, P.; Otto, H.F.; Lichter, P.; Joos, S. Analysis of chromosomal imbalances in sporadic and NF1-associated peripheral nerve sheath tumors by comparative genomic hybridization. Genes Chromosomes Cancer **1999**, *25*, 362–369.
106. Schmidt, H.; Taubert, H.; Meye, A.; Wurl, P.; Bache, M.; Bartel, F.; Holzhausen, H.J.; Hinze, R. Gains in chromosomes 7, 8q, 15q and 17q are characteristic changes in malignant but not in benign peripheral nerve sheath tumors from patients with Recklinghausen's disease. Cancer Lett. **2000**, *155*, 181–190.
107. Wallace, M.R.; Rasmussen, S.A.; Lim, I.T.; Gray, B.A.; Zori, R.T.; Muir, D. Culture of cytogenetically abnormal schwann cells from benign and malignant NF1 tumors. Genes Chromosomes Cancer **2000**, *27*, 117–123.
108. Kehrer, H.; Krone, W. Spontaneous chromosomal

MARCEL DEKKER, INC.
270 Madison Avenue, New York, New York 10016

aberrations in cell cultures from patients with neurofibromatosis 1. Mutat. Res. **1994**, *306*, 61–70.
109. Glover, T.W.; Stein, C.K.; Legius, E.; Andersen, L.B.; Brereton, A.; Johnson, S. Molecular and cytogenetic analysis of tumors in von Recklinghausen neurofibromatosis. Genes Chromosomes Cancer **1991**, *3*, 62–70.
110. Ottini, L.; Esposito, D.L.; Richetta, A.; Carlesimo, M.; Palmirotta, R.; Veri, M.C.; Battista, P.; Frati, L.; Caramia, F.G.; Calvieri, S. Alterations of microsatellites in neurofibromas of von Recklinghausen's disease. Cancer Res. **1995**, *55*, 5677–5680.
111. Fargnoli, M.C.; Chimenti, S.; Peris, K. Multiple microsatellite alterations on chromosome 9 in neurofibromas of NF-1 patients. J. Invest. Dermatol. **1997**, *108*, 812–813.
112. Birindelli, S.; Perrone, F.; Oggionni, M.; Lavarino, C.; Pasini, B.; Vergani, B.; Ranzani, G.N.; Pierotti, M.A.; Pilotti, S. Rb and TP53 pathway alterations in sporadic and NF1-related malignant peripheral nerve sheath tumors. Lab. Invest. **2001**, *81*, 833–844.
113. Shibata, D.; Navidi, W.; Salovaara, R.; Li, Z.H.; Aaltonen, L.A. Somatic microsatellite mutations as molecular tumor clocks. Nat. Med. **1996**, *2*, 676–681.
114. Legius, E.; Marchuk, D.A.; Collins, F.S.; Glover, T.W. Somatic deletion of the neurofibromatosis type 1 gene in a neurofibrosarcoma supports a tumour suppressor gene hypothesis. Nat. Genet. **1993**, *3*, 122–126.
115. Lothe, R.A.; Slettan, A.; Saeter, G.; Brogger, A.; Borresen, A.L.; Nesland, J.M. Alterations at chromosome 17 loci in peripheral nerve sheath tumors. J. Neuropathol. Exp. Neurol. **1995**, *54*, 65–73.
116. Plaat, B.E.; Molenaar, W.M.; Mastik, M.F.; Hoekstra, H.J.; te Meerman, G.J.; van den Berg, E. Computer-assisted cytogenetic analysis of 51 malignant peripheral-nerve-sheath tumors: sporadic vs. neurofibromatosis-type-1-associated malignant schwannomas. Int. J. Cancer **1999**, *83*, 171–178.
117. DeClue, J.E.; Papageorge, A.G.; Fletcher, J.A.; Diehl, S.R.; Ratner, N.; Vass, W.C.; Lowy, D.R. Abnormal regulation of mammalian p21ras contributes to malignant tumor growth in von Recklinghausen (type 1) neurofibromatosis. Cell **1992**, *69*, 265–273.
118. Basu, T.N.; Gutmann, D.H.; Fletcher, J.A.; Glover, T.W.; Collins, F.S.; Downward, J. Aberrant regulation of ras proteins in malignant tumour cells from type 1 neurofibromatosis patients. Nature **1992**, *356*, 713–715.
119. Wu, R.; Lopez-Correa, C.; Rutkowski, J.L.; Baumbach, L.L.; Glover, T.W.; Legius, E. Germline mutations in NF1 patients with malignancies. Genes Chromosomes Cancer **1999**, *26*, 376–380.
120. Wang, Q.; Lasset, C.; Desseigne, F.; Frappaz, D.; Bergeron, C.; Navarro, C.; Ruano, E.; Puisieux, A. Neurofibromatosis and early onset of cancers in hMLH1-deficient children. Cancer Res. **1999**, *59*, 294–297.
121. Ricciardone, M.D.; Ozcelik, T.; Cevher, B.; Ozdag, H.; Tuncer, M.; Gurgey, A.; Uzunalimoglu, O.; Cetinkaya, H.; Tanyeli, A.; Erken, E.; Ozturk, M. Human MLH1 deficiency predisposes to hematological malignancy and neurofibromatosis type 1. Cancer Res. **1999**, *59*, 290–293.
122. Boland, C.R.
123. Lothe, R.A.; Karhu, R.; Mandahl, N.; Mertens, F.; Saeter, G.; Heim, S.; Borresen-Dale, A.L.; Kallioniemi, O.P. Gain of 17q24-qter detected by comparative genomic hybridization in malignant tumors from patients with von Recklinghausen's neurofibromatosis. Cancer Res. **1996**, *56*, 4778–4781.
124. Schmidt, H.; Wurl, P.; Taubert, H.; Meye, A.; Bache, M.; Holzhausen, H.J.; Hinze, R. Genomic imbalances of 7p and 17q in malignant peripheral nerve sheath tumors are clinically relevant. Genes Chromosomes Cancer **1999**, *25*, 205–211.
125. Schmidt, H.; Taubert, H.; Wurl, P.; Bache, M.; Bartel, F.; Holzhausen, H.J.; Hinze, R. Cytogenetic characterization of six malignant peripheral nerve sheath tumors: comparison of karyotyping and comparative genomic hybridization. Cancer Genet. Cytogenet. **2001**, *128*, 14–23.
126. Mertens, F.; Dal Cin, P.; De Wever, I.; Fletcher, C.D.; Mandahl, N.; Mitelman, F.; Rosai, J.; Rydholm, A.; Sciot, R.; Tallini, G.; van Den Berghe, H.; Vanni, R.; Willen, H. Cytogenetic characterization of peripheral nerve sheath tumours: A report of the CHAMP study group. J. Pathol. **2000**, *190*, 31–38.
127. O'Sullivan, M.J.; Kyriakos, M.; Zhu, X.; Wick, M.R.; Swanson, P.E.; Dehner, L.P.; Humphrey, P.A.; Pfeifer, J.D. Malignant peripheral nerve sheath tumors with t(X;18). A pathologic and molecular genetic study. Mod. Path. **2000**, *13*, 1336–1346.
128. Ladanyi, M.; Woodruff, J.M.; Scheithauer, B.W.; Bridge, J.A.; Barr, F.G.; Goldblum, J.R.; Fisher, C.; Perez-Atayde, A.; Dal Cin, P.; Fletcher, C.D.;

Marcel Dekker, Inc.
270 Madison Avenue, New York, New York 10016

Fletcher, J.A. Re: O'Sullivan MJ, Kyriakos M, Zhu X, Wick MR, Swanson PE, Dehner LP, Humphrey PA, Pfeifer JD: malignant peripheral nerve sheath tumors with t(X;18). A pathologic and molecular genetic study. Mod pathol 2000;13:1336–46. Mod. Path. **2001**, *14*, 733–737.

129. Liew, M.A.; Coffin, C.M.; Fletcher, J.A.; Hang, M.T.; Tanito, K.; Niimura, M.; Viskochil, D. Peripheral nerve sheath tumors from patients with neurofibromatosis type 1 do not have the chromosomal translocation t(X;18). Pediatr. Dev. Pathol. **2002**, *5*, 165–169.
130. Legius, E.; Dierick, H.; Wu, R.; Hall, B.K.; Marynen, P.; Cassiman, J.J.; Glover, T.W. TP53 mutations are frequent in malignant NF1 tumors. Genes Chromosomes Cancer **1994**, *10*, 250–255.
131. Halling, K.C.; Scheithauer, B.W.; Halling, A.C.; Nascimento, A.G.; Ziesmer, S.C.; Roche, P.C.; Wollan, P.C. p53 expression in neurofibroma and malignant peripheral nerve sheath tumor. An immunohistochemical study of sporadic and NF1-associated tumors. Am. J. Clin. Pathol. **1996**, *106*, 282–288.
132. Liapis, H.; Marley, E.F.; Lin, Y.; Dehner, L.P. p53 and Ki-67 proliferating cell nuclear antigen in benign and malignant peripheral nerve sheath tumors in children. Pediatr. Dev. Pathol. **1999**, *2*, 377–384.
133. Guimaraes, D.P.; Hainaut, P. TP53: a key gene in human cancer. Biochimie **2002**, *84*, 83–93.
134. Kourea, H.P.; Orlow, I.; Scheithauer, B.W.; Cordon-Cardo, C.; Woodruff, J.M. Deletions of the INK4A gene occur in malignant peripheral nerve sheath tumors but not in neurofibromas. Am. J. Pathol. **1999**, *155*, 1855–1860.
135. Nielsen, G.P.; Stemmer-Rachamimov, A.O.; Ino, Y.; Moller, M.B.; Rosenberg, A.E.; Louis, D.N. Malignant transformation of neurofibromas in neurofibromatosis 1 is associated with CDKN2A/p16 inactivation. Am. J. Pathol. **1999**, *155*, 1879–1884.
136. Sherr, C.J. The INK4a/ARF network in tumour suppression. Nat. Rev., Mol. Cell Biol. **2001**, *2*, 731–737.
137. Li, X.J.; Wang, D.Y.; Zhu, Y.; Guo, R.J.; Wang, X.D.; Lubomir, K.; Mukai, K.; Sasaki, H.; Yoshida, H.; Oka, T.; Machinami, R.; Shinmura, K.; Tanaka, M.; Sugimura, H. Mxi1 mutations in human neurofibrosarcomas. Jpn. J. Cancer Res. **1999**, *90*, 740–746.
138. Foley, K.P.; Eisenman, R.N. Two MAD tails: what the recent knockouts of Mad1 and Mxi1 tell us about the MYC/MAX/MAD network. Biochim. Biophys. Acta **1999**, *1423*, M37–M47.
139. Schreiber-Agus, N.; Meng, Y.; Hoang, T.; Hou, H., Jr.; Chen, K.; Greenberg, R.; Cordon-Cardo, C.; Lee, H.W.; DePinho, R.A. Role of Mxi1 in ageing organ systems and the regulation of normal and neoplastic growth. Nature **1998**, *393*, 483–487.
140. Serrano, M.; Gomez-Lahoz, E.; DePinho, R.A.; Beach, D.; Bar-Sagi, D. Inhibition of ras-induced proliferation and cellular transformation by p16INK4. Science **1995**, *267*, 249–252.
141. Pomerantz, J.; Schreiber-Agus, N.; Liegeois, N.J.; Silverman, A.; Alland, L.; Chin, L.; Potes, J.; Chen, K.; Orlow, I.; Lee, H.W.; Cordon-Cardo, C.; DePinho, R.A. The Ink4a tumor suppressor gene product, p19Arf, interacts with MDM2 and neutralizes MDM2's inhibition of p53. Cell **1998**, *92*, 713–723.
142. Kindblom, L.G.; Ahlden, M.; Meis-Kindblom, J.M.; Stenman, G. Immunohistochemical and molecular analysis of p53, MDM2, proliferating cell nuclear antigen and Ki67 in benign and malignant peripheral nerve sheath tumours. Virchows Arch. **1995**, *427*, 19–26.
143. Mulvihill, J.J.. Malignancy: epidemiologically associated cancers. In *The Neurofibromatoses: A pathogenetic and Clinical Overview,* 1st Ed., Huson, S.M., Hughes, R.A.C., Eds.; Chapman & Hall Medical: London, 1994; 487.
144. Koch, C.A.; Vortmeyer, A.O.; Huang, S.C.; Alesci, S.; Zhuang, Z.; Pacak, K. Genetic aspects of pheochromocytoma. Endocr. Regul. **2001**, *35*, 43–52.
145. Listernick, R.; Charrow, J.; Gutmann, D.H. Intracranial gliomas in neurofibromatosis type 1. Am. J. Med. Genet. **1999**, *89*, 38–44.
146. Gutmann, D.H.; Gurney, J.G. Other malignancies. In *Neurofibromatosis. Phenotype, Natural History, and Pathogenesis;* Friedman, J.M., Butmann, D.H., MacCollin, M., Riccardi, V.M., Eds.; The Johns Hopkins University Press: Baltimore, 1999; 231–249.
147. Kluwe, L.; Hagel, C.; Tatagiba, M.; Thomas, S.; Stavrou, D.; Ostertag, H.; von Deimling, A.; Mautner, V.F. Loss of NF1 alleles distinguish sporadic from NF1-associated pilocytic astrocytomas. J. Neuropathol. Exp. Neurol. **2001**, *60*, 917–920.
148. Shannon, K.M.; O'Connell, P.; Martin, G.A.; Paderanga, D.; Olson, K.; Dinndorf, P.; McCormick, F. Loss of the normal NF1 allele from the bone marrow of children with type 1

MARCEL DEKKER, INC.
270 Madison Avenue, New York, New York 10016

neurofibromatosis and malignant myeloid disorders. N. Engl. J. Med. **1994**, *330*, 597–601.
149. Matsui, I.; Tanimura, M.; Kobayashi, N.; Sawada, T.; Nagahara, N.; Akatsuka, J. Neurofibromatosis type 1 and childhood cancer. Cancer **1993**, *72*, 2746–2754.
150. Maris, J.M.; Wiersma, S.R.; Mahgoub, N.; Thompson, P.; Geyer, R.J.; Hurwitz, C.G.H.; Lange, B.J.; Shannon, K.M. Monosomy 7 myelodysplastic syndrome and other second malignant neoplasms in children with neurofibromatosis type 1. Cancer **1997**, *79*, 1438–1446.
151. Mahgoub, N.; Taylor, B.R.; Le Beau, M.M.; Gratiot, M.; Carlson, K.M.; Atwater, S.K.; Jacks, T.; Shannon, K.M. Myeloid malignancies induced by alkylating agents in Nf1 mice. Blood **1999**, *93*, 3617–3623.
152. Korf, B.R. Malignancy in neurofibromatosis type 1. Oncologist **2000**, *5*, 477–485.
153. Jacks, T.; Shih, T.S.; Schmitt, E.M.; Bronson, R.T.; Bernards, A.; Weinberg, R.A. Tumour predisposition in mice heterozygous for a targeted mutation in Nf1. Nat. Genet. **1994**, *7*, 353–361.
154. Brannan, C.I.; Perkins, A.S.; Vogel, K.S.; Ratner, N.; Nordlund, M.L.; Reid, S.W.; Buchberg, A.M.; Jenkins, N.A.; Parada, L.F.; Copeland, N.G. Targeted disruption of the neurofibromatosis type-1 gene leads to developmental abnormalities in heart and various neural crest-derived tissues. Genes Dev. **1994**, *8*, 1019–1029.
155. Tischler, A.S.; Shih, T.S.; Williams, B.O.; Jacks, T. Characterization of pheochromocytomas in a mouse strain with a targeted disruptive mutation of the neurofibromatosis gene Nf1. Endocr. Pathol. **1995**, *6*, 323–335.
156. Cichowski, K.; Shih, T.S.; Schmitt, E.; Santiago, S.; Reilly, K.; McLaughlin, M.E.; Bronson, R.T.; Jacks, T. Mouse models of tumor development in neurofibromatosis type 1. Science **1999**, *286*, 2172–2176.
157. Vogel, K.S.; Klesse, L.J.; Velasco-Miguel, S.; Meyers, K.; Rushing, E.J.; Parada, L.F. Mouse tumor model for neurofibromatosis type 1. Science **1999**, *286*, 2176–2179.
158. Zhu, Y.; Ghosh, P.; Charnay, P.; Burns, D.K.; Parada, L.F. Neurofibromas in NF1: Schwann cell origin and role of tumor environment. Science **2002**, *296*, 920–922.

Marcel Dekker, Inc.
270 Madison Avenue, New York, New York 10016

Genomic Context of Paralogous Recombination Hotspots Mediating Recurrent *NF1* Region Microdeletion

Stephen H. Forbes,[1] Michael O. Dorschner,[1]† Rosalynda Le,[1] and Karen Stephens[1,2]*

[1]Department of Medicine, University of Washington, Seattle, Washington
[2]Department of Laboratory Medicine, University of Washington, Seattle, Washington

Recombination between paralogs that flank the *NF1* gene at 17q11.2 typically results in a 1.5-Mb microdeletion that includes *NF1* and at least 13 other genes. We show that the principal sequences responsible are two 51-kb blocks with 97.5% sequence identity (NF1REP-P1-51 and NF1REP-M-51). These blocks belong to a complex group of paralogs with three components on 17q11.2 and another on 19p13.13. Breakpoint sequencing of deleted chromosomes from multiple patients revealed two paralogous recombination hot spots within the 51-kb blocks. Lack of sequence similarity between these sites failed to suggest or corroborate any putative *cis*-acting recombinogenic motifs. However, the NF1REPs showed relatively high alignment mismatch between recombining paralogs, and we note that the NF1REP hot spots were regions of good alignment bordered by relatively large alignment gaps. Statistical tests for gene conversion detected a single significant tract of perfect match between the NF1REPs that was 700 bp long and coincided with PRS2, the predominant recombination hot spot. Tracts of perfect match occurring by chance may contribute to breakpoint localization, but our result suggests that perfect tracts at recombination hot spots may be a result of gene conversion at sites at which preferential pairing occurs for other, as-yet-unknown reasons.

INTRODUCTION

In the past 5 years, it has become apparent that recombination between pairs of nonallelic, high-identity, low-copy-number DNA repeat sequences is an important mechanism for chromosomal rearrangements that cause human genetic disease (reviewed by Emanuel and Shaikh, 2001; Stankiewicz and Lupski, 2002). These repeated DNA elements have been referred to as REPs (repeats; Lupski et al., 1991), LCRs (low-copy repeats; Shaikh et al., 2000), duplicons, or paralogs. Recombination between misaligned paralogs (unequal crossing over) on sister or nonsister chromatids, between paralogs on the same chromatid (loop-out excision), or between paralogs on different chromosomes can result in deletion, duplication, inversion, or translocation (reviewed by Inoue and Lupski, 2002). Recombination between paralogs has been referred to as "nonallelic homologous recombination" (Stankiewicz and Lupski, 2002), "ectopic recombination," (Kuroda-Kawaguchi et al., 2001), and "paralogous recombination" (Stephens, 2003) to distinguish it from classical allelic-homologous recombination.

Paralogous recombination is the dominant mechanism for submicroscopic contiguous gene deletions that encompass the *NF1* gene at chromosome segment 17q11.2. The consequent haploinsufficiency for the NF1 protein product causes neurofibromatosis 1 (NF1), an autosomal dominant multisystemic disorder that affects about 1 in 3,500 individuals worldwide. NF1 is primarily characterized by multiple benign nerve-sheath tumors or neurofibromas and pigmentary changes (reviewed by Korf, 2002). An estimated 5% of cases are a result of submicroscopic *NF1* microdeletion (Kluwe et al., 2004), whereas most of the remaining cases result from mutations that predict premature translation termination or splicing abnormalities (Messiaen et al., 2000). *NF1* microdeletion carriers are of great interest because they are predisposed to early onset and to excessive numbers of neurofibromas (Kayes et al., 1994; Leppig et al., 1997; Dorschner et al., 2000) and cardiovascular malformations (Venturin et al., 2004), and they are at increased risk of developing malignant peripheral

Supported by: Grant number: DAMD17-00-1-0542 (to K.S.); Grant numbers: DAMD17-00-1-0542 and T32 GM07454-27 (to S.H.F.); Grant nmber: DAMD17-00-1-0542 (to M.O.D.).

*Correspondence to: Karen Stephens, PhD, University of Washington, 1959 NE Pacific St., Room I-204, Seattle, WA 98195-7720. E-mail: millie@u.washington.edu

†Present address: Regulome Corporation, Seattle, WA 98103

Received 13 January 2004; Accepted 19 March 2004

DOI 10.1002/gcc.20065

Published online 2 June 2004 in Wiley InterScience (www.interscience.wiley.com).

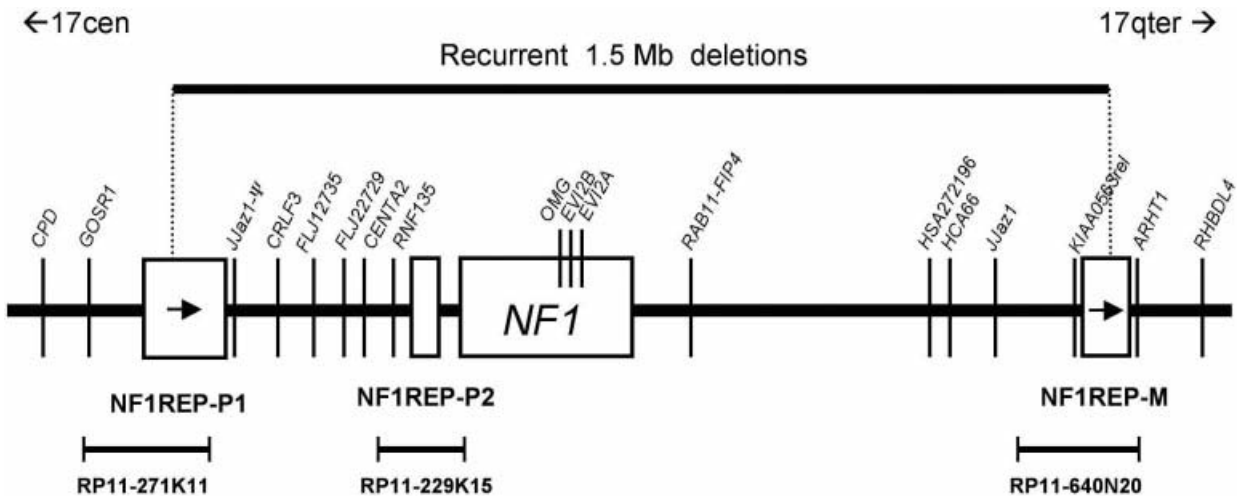

Figure 1. Arrangement and structure of the NF1REP paralogs flanking the *NF1* gene at chromosome segment 17q11.2. The 350-kb *NF1* gene (transcribed left to right) is flanked by the paralogs NF1REP-P1, -P2, and -M. NF1REP-P1 and NF1REP-M are in direct orientation (boxes with arrows). The extent of the recurrent 1.5-Mb constitutional microdeletion is shown above the map (Dorschner et al., 2000). Genes labeled with vertical bars are presumed functional genes from the RefSeq database, with the exception of *JJAZ1-Ψ*, a pseudogene of *JJAZ1* (Jenne et al., 2003), which was previously known as KIAA0160 (Dorschner et al., 2000). The reference BACs for NF1REP-P1, -P2, and -M are indicated. Drawing is to scale.

nerve-sheath tumors (De Raedt et al., 2003; Kluwe et al., 2003). Whether they are at increased risk for other manifestations, related or unrelated to NF1, awaits a comprehensive clinical evaluation of a cohort of *NF1* microdeletion subjects ascertained in an unbiased manner.

Sequence-tagged site (STS) mapping of 17 independent *NF1* microdeletions revealed that 82% had proximal and distal breakpoints clustered in two low-copy-repeat elements, designated NF1REPs, that flanked the *NF1* gene (Dorschner et al., 2000) (Fig. 1). The direct orientation of the NF1REPs suggests a mechanism whereby the proximal copy (designated NF1REP-P1) and a medial copy (designated NF1REP-M) misalign during meiosis with subsequent unequal crossing over between chromatids, or loop-out excision between the repeats on a single chromatid, resulting in a recurrent 1.5-Mb *NF1* microdeletion (Dorschner et al., 2000) (Fig. 1). About 80% of de novo *NF1* microdeletions occurred on maternally derived chromosomes (Upadhyaya et al., 1998; Lopez-Correa et al., 2001; Dorschner et al., submitted). This is consistent with haplotype analyses of healthy ancestors of de novo *NF1* microdeletion subjects, which suggested that paralogous recombination occurred during maternal meiosis II (Lopez-Correa et al., 2000).

NF1 microdeletion breakpoints were mapped to intervals defined by paralogous sequence variants (PSVs; Estivill et al., 2002), also referred to as "*cis*-morphisms" (Lupski, 2003), that were specific to an individual NF1REP paralog. The pattern of PSVs from amplicons of the deleted chromosomes 17 were expected to match that of either NF1REP-P1 or NF1REP-M or to show a transition from NF1REP-P1 to NF1REP-M if the amplicon contained the breakpoint of the recombinant NF1REP. This procedure identified a 2-kb recombination hot spot that accounted for 46% ($N = 54$) of cases with *NF1* region contiguous gene deletions (Lopez-Correa et al., 1999). Our recent breakpoint mapping of additional cases has extended this breakpoint cluster region, here designated as PRS2 (paralogous recombination site 2) to a 4,155-bp interval and identified an additional, independent breakpoint cluster region (designated PRS1) of 6,323 bp (Dorschner et al., submitted). Together, breakpoints at PRS1 and PRS2 accounted for 69% of *NF1* whole-gene deletions (Lopez-Correa et al., 2001; Dorschner et al., submitted). In all cases, the sequence of the breakpoint intervals was consistent with a perfect homologous exchange; there was no evidence of the small deletions that are commonly associated with nonhomologous end joining (Valerie and Povirk, 2003). Three of these cases (one at PRS1 and two at PRS2) showed evidence of gene conversion, with alternate NF1REP-P1 and NF1REP-M PSVs in the exchange region (Lopez-Correa et al., 2001; Dorschner et al., submitted). Apparent gene conversion tracts are consistent with a mechanism similar to the double-strand break

(DSB) repair model in yeast (Haber, 2000; Johnson and Jasin, 2001). In this model, the breakpoint hot spots at PRS1 and PRS2 imply the presence of a sequence motif, functional domain, or higher-order chromosomal feature that predisposes to DSB. The primary sequences of the short PRS1 and PRS2 recombination substrates revealed no apparent basis for regional DSBs (Dorschner et al., 2000; Lopez-Correa et al., 2001). However, knowledge about the number, orientation, and structure of NF1REPs in the genome in which PRS1 and PRS2 were embedded was lacking. Here we detail the primary structure of four NF1REPs, including the larger sequence context of PRS1 and PRS2. We searched for sequence features at breakpoint clusters that might explain their location, and we discuss evidence for gene conversion between the NF1REP paralogs.

MATERIALS AND METHODS

Patients

NF1 patients carrying microdeletions have been described previously (Dorschner et al., 2000; Lopez-Correa et al., 2001; Dorschner et al., submitted; and in references therein). Patient UWA160-1 is described in Leppig et al. (1997).

Identification of a Novel Breakpoint

The breakpoints of UWA160-1 were mapped previously to NF1REP-P1 and NF1REP-M by STS analyses of somatic-cell hybrid lines carrying only the deleted chromosome 17 (Dorschner et al., 2000). Here we mapped the breakpoint to a region about 10 kb centromeric of PRS1 by comparing sequences of the deleted chromosome 17 to paralogous sequences from bacterial artificial chromosome (BAC) clones and normal chromosomes 17, as described previously (Lopez-Correa et al., 2001). An approximately 5-kb amplicon containing the breakpoint was amplified from genomic DNA of the hybrid line carrying the deleted chromosome with primers 160P1-F (5′-GGCTCATGTGTAATGATCTTTAACGCG-3′) and MD1-R(v2) (5′-CAAAGATTATCACTGATGGAGTTGG-3′). This amplicon was sequenced with several internal primers for identification of the breakpoint interval. Note that the above primers are not necessarily NF1REP-specific and may amplify nonrecombinant NF1REP from normal individuals.

Defining REP-Specific Nucleotide Site Variants

PSVs were initially defined by differences between the reference BACs (see below) for each paralog. The pattern of PSVs from amplicons of the deleted chromosomes 17 were expected to match that of either NF1REP-P1 or NF1REP-M or to transition from NF1REP-P1 to NF1REP-M if the amplicon contained the breakpoint of the recombinant NF1REP. This strategy narrowed the recombination interval, which was subsequently identified by repetition of the process with closely spaced primers from the interval of interest.

To help differentiate PSVs from common polymorphisms at allelic sites (SNPs), we also amplified, cloned, and partially sequenced nonrecombinant PRS1 and PRS2 regions from both NF1REP-P1 and NF1REP-M of six normal chromosomes and of the NF1REP-M carried in BAC 951F11, using the Expand LT PCR system (Roche Molecular Biochemicals, Mannheim, Germany). Amplicons were column-purified and cloned into the TOPO XL PCR cloning kit (Invitrogen Corporation, Carlsbad, CA). Plasmid preparations of clones were purified and sequenced directly by use of internal primers as described previously (Lopez-Correa et al., 2001; Dorschner et al., submitted).

Genomic Contigs and Reference Sequences

The region spanning between and including NF1REP-P1 and NF1REP-M is a complete tiling path of finished BACs in NCBI build 32 (April 2003). Finished BACs for NF1REP-P1 (RP11-271K11 and CTD-2349P21) and NF1REP-M (RP11-640N20) were used as primary reference sequences (Figs. 1 and 2). Two additional BACs closely matching NF1REP-P1 are in the draft state (RP13-715K7; RP11-1403G4), and one additional BAC matching NF1REP-M is finished (CTD-2646J6). Finished chromosome 19 BACs representing NF1REP-E19 are indicated in Figure 3. For the proximal and distal CMT1A-REPs, our primary references were Genbank U71217 and U71218, respectively. Additional, finished copies of the CMT1A-REPs were taken from AC005838 (proximal) and assembled by use of AC005389 and AC005838 (distal).

Sequence Composition and Motif Searches

We searched for short sequence motifs with the EMBOSS program Fuzznuc (http://bioweb.pasteur.fr/seqanal/interfaces/fuzznuc.html). Putative recombination motifs were chosen from lists in previous publications (Lopes et al., 1998; Badge et al., 2000; Lopez-Correa et al., 2001; and references therein): *E. coli Chi* sequence (5′-GCTGGTGG-3′), yeast Ade6-M26 heptamer (5′-ATGACGT-3′), XY32 homopurine/homopyrimidine (5′-AAGG-

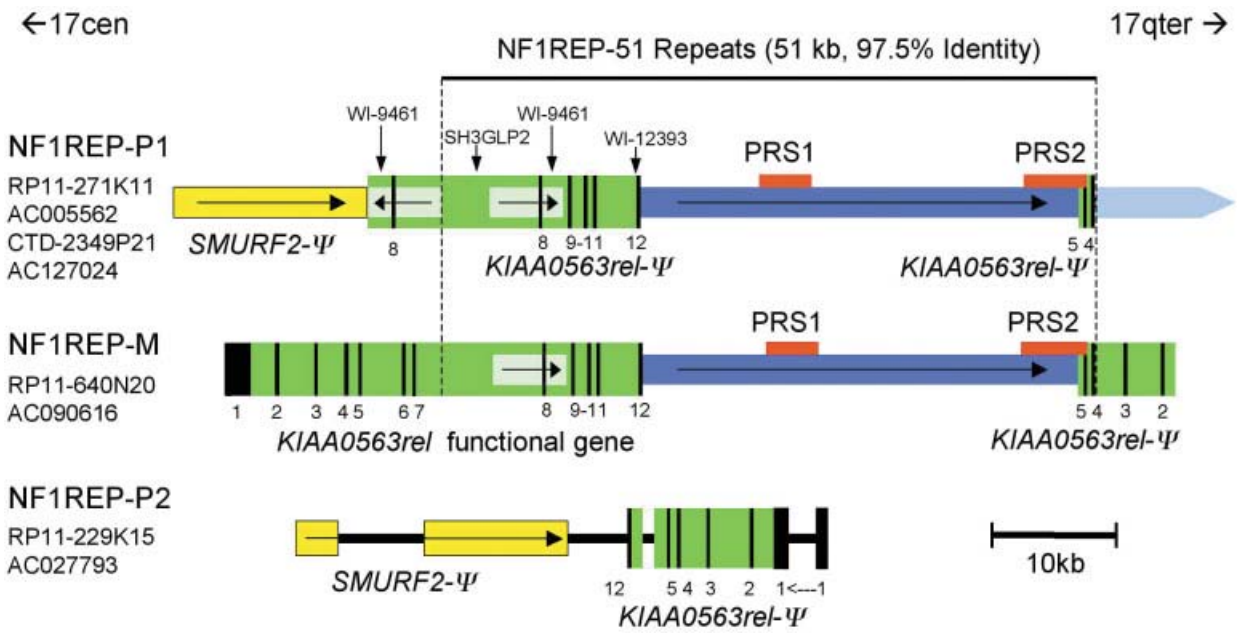

Figure 2. Detailed structures of the three paralogous sequence blocks flanking the *NF1* gene, oriented from centromere to telomere. BAC identities and accession numbers are shown. Green blocks indicate the *KIAA0563rel* functional gene and related pseudogene fragments (Ψ), with numbered black bars designating exons or exon-derived sequences. Light green boxes within *KIAA0563rel* copies indicate the orientation of a 5.8-kb inverted repeat with two copies in NF1REP-P1 and one copy in NF1REP-M. Landmark STSs in the *KIAA0563rel* gene and pseudogenes cited previously and present in both NF1REP-P1 and NF1REP-M (Dorschner et al., 2000) are indicated above NF1REP-P1. Yellow blocks depict *SMURF2*-derived pseudogene fragments, and red boxes denote the PRSs. NF1REP-P1 extends farther toward the telomere, as indicated by the pointed light-blue box; see Figure 3 for complete structure. Precise lengths and BAC coordinates for each NF1REP are given in the Results section.

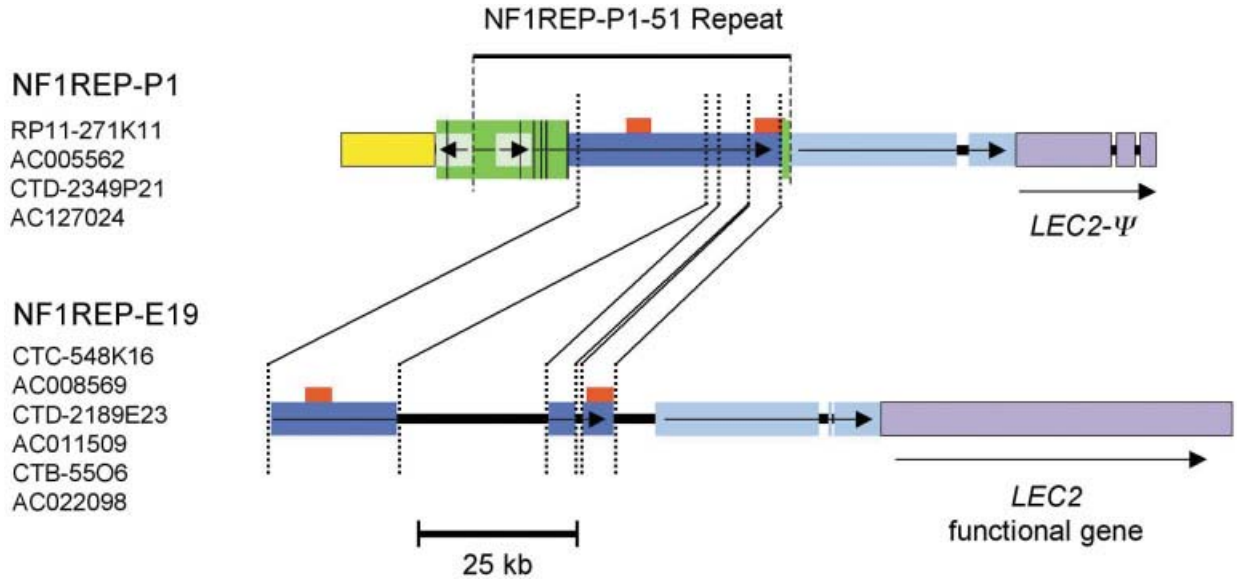

Figure 3. Comparison of NF1REP-P1 to NF1REP-E19, at chromosome segment 19p13.13. Colored boxes match those described for Figure 2. PRS1 and PRS2 in NF1REP-E19 are not known to serve as recombination substrates. NF1REP-E19 contains the *LEC2* functional gene, and NF1REP-P1 contains pseudogene fragments of *LEC2* (purple).

GAGAARGGGTAAAGGGRAAGAGGGAA-3′), retroposon LTR (5′-TCATACACCACGCAGGGG-TAGAGGACT-3′), the long terminal repeat element LTR-IS (5′-TGGAAATCCCC-3′), protein-binding site *pur* (5′-GGNNGAGGGAGARRRR-3′), translin consensus 1 (5′-GCNCWSSW-

$N_{(0-2)}$GCCCWSSW-3′), translin consensus 2 (5′-MTGCAG$N_{(0-4)}$GCCCWSSW-3′), *Saccharomyces cerevisiae* ARS (5′-WTTTATRTTTW-3′), *Schizosaccharomyces pombe* ARS (5′-WRTTTATTTAW-3′), human replication origin consensus (5′-WAWTTDDWWWDHWGWHMA-WTT-3′), and human minisatellite core sequences (5′-GGGCAGGAG-3′; 5′-GGAGGTGGGCAGGARG-3′; 5′-AGAGGTGGGCAGGTGG-3′). Minisatellite core sequences were searched by use of a 9-bp core sequence allowing one mismatch and 16-bp core sequences allowing up to 4 mismatches.

Known genes and annotated features were assessed with the NCBI (Genbank) and UCSC Human Genome Working Draft databases and browsers. We searched the NF1REP for internal repeats by pairwise BLAST (NCBI), Tandem Repeats Finder (Benson, 1999), PatternHunter (Ma et al., 2002), and the EMBOSS program Palindrome (http://bioweb.pasteur.fr/intro-uk.html). We tested for matrix attachment regions (MARs) using MarWiz (Singh et al., 1997). High-copy repeats, simple repeats, and other simple sequences were detected with RepeatMasker (http://ftp.genome.washington.edu/cgi-bin/RepeatMasker), and graphic results for repeats and percentage G+C base composition were obtained with Gestalt Workbench (Glusman and Lancet, 2000). Candidate promoters and first exons were detected with First Exon Finder (FirstEF; Davuluri et al., 2001).

Polymorphic Sites and Gene Conversion Tests

Sliding window sequence polymorphism and divergence plots were created with DnaSP (Rozas and Rozas, 1999), which tabulates differences within and between populations, reports shared variants, and outputs alignments listing polymorphic sites only (with alignment gaps included or excluded). The gene conversion test "GeneConv" (Sawyer, 1989, 1999) tabulates all differences between sequences, tests the distribution of perfect fragment sizes against random simulations of the dataset, and reports *P* values for the probability of obtaining a particular perfect match by chance. This can be done with or without inclusion of insertions and deletions (indels, or alignment gaps) as polymorphic sites. When included, contiguous indel sites are treated as single variants. Significance values are Bonferroni-corrected for the number of tests, and results are listed by decreasing fragment size and *P* value.

RESULTS

NF1REPs Are Complex Assemblies of Paralogs from Different Sequence Families

The paralogs NF1REP-P1, NF1REP-P2, and NF1REP-M flanking the *NF1* gene at 17q11.2 (Fig. 1) are represented by finished BACs in the April 2003 assembly of the public Human Genome Project (NCBI build 32). This is the first NCBI assembly in which NF1REP ordering and orientation are consistent with previously reported evidence, including public Human Genome Project BAC sequences, STS mapping, sequencing of breakpoint regions in *NF1* de novo microdeletion patients and normal controls, and *NF1* microdeletion–specific assays (Dorschner et al., 2000; Jenne et al., 2001; Lopez-Correa et al., 2001; Dorschner et al., submitted). This public assembly and the BAC contig of Jenne et al. (2003) are based largely on different BACs, but both nevertheless show a finished tiling path across 1.5 Mb from NF1REP-P1 through NFREP-M.

Sequence and structural analyses showed that NF1REP-P1, NF1REP-P2, and NF1REP-M vary in length and composition, but are generally comprised of gene and gene-derived fragments and larger sequence blocks apparently lacking genes (Fig. 2). NF1REP-P1 is 131 kb in length, is contained largely on BAC RP11-271K11 (nt 75477–199182), and extends 6,944 bp into the overlapping BAC CTD-2349P21. NF1REP-M is 75 kb in length and is fully contained in BAC RP11-640N20 (nt 102147–177525). NF1REP-P2 is 43 kb and fully contained in BAC RP11-229K15 (nt 43619–86245).

The apparently functional copy of the gene *KIAA0563rel* is contained in NF1REP-M (see Fig. 2; Jenne et al., 2003). It is supported by a full-length mRNA (KIAA0563-related gene; Genbank NM_052888) and a substantial Unigene cluster (Hs.367593). This gene is also known by an STS marker (WI-12393) contained within it (Dorschner et al., 2000; Jenne et al., 2000, 2001). Fragments derived from this gene are present in NF1REP-P1, in the distal region of NF1REP-M, and in NF1REP-P2 (green blocks, Fig. 2). NF1REP-M carries the 12 exons and introns of the functional *KIAA0563rel*, whereas NF1REP-P1 has an inverted segment containing exon 8, followed by a segment matching NF1REP-M and containing exons 8–12. Additional *KIAA0563rel* fragments are scattered throughout distal 17q and on several other chromosomes. A 33,692-bp paralogous sequence block (BAC RP11-271K11; nt 112506–146198) is shared

by NF1REP-P1 and NF1REP-M and apparently lacks genes or pseudogene sequences (Fig. 2, dark blue).

The largest sequence blocks shared by NF1REP-P1 and NF1REP-M are 51 kb in length and show 97.5% sequence identity (analysis of manually aligned sequences using the DnaSP program; Rozas and Rozas, 1999). Here we refer to these blocks (represented by BAC RP11-271K11; nt 96901–147876) as NF1REP-P1-51 and NF1REP-M-51, or collectively as NF1REP-51. These repeats are of particular interest because they contain PRS1 and PRS2, the sites where an estimated 69% of *NF1* microdeletion breakpoints occur (Fig. 2, red blocks; Lopez-Correa et al., 2001; Dorschner et al., submitted).

Two additional pseudogenes comprise the flanking regions of NF1REP-P1. *SMURF2* pseudogene fragments matching at 96% sequence identity (Fig. 2, yellow blocks) were present on NF1REP-P1 (RP11-271K11; nt 75477–91072) and on NF1REP-P2 (RP11-229K15; nt 43619–64829). The functional copy of the *SMURF2* gene encodes E3 ubiquitin ligase (NM_022739), located at 17q24 and not associated with any other NF1REP-related elements. Distal to NF1REP-P1-51 is a segment with no apparent genes (RP11-271K11, nt 147872–184526), and a *LEC2* pseudogene fragment beginning at RP11-271K11 nt 184527 and extending into CTD-2349P21 (Fig. 3, light blue and purple, respectively). Parts of NF1REP-P1-51 and these distal blocks have paralogs at chromosome band 19p13, which we designated NF1REP-E19 (Fig. 3). This REP contains the functional *LEC2* gene and resides on the three BACs indicated. It spans 151 kb, includes 33 kb of dispersed blocks matching NF1REP-P1-51 and NF1REP-M-51 (Fig. 2, dark blue blocks) and contains the PRS1 and PRS2 breakpoint clusters (Fig. 2, red blocks). NF1REP-E19 matches both NF1REP-P1-51 and NF1REP -M-51 at only 94–95% sequence identity. It contains no sequences matching *KIAA0563rel*, and *KIAA0563rel* copies are not associated with any *SMURF2* or *LEC2* copies elsewhere. No chromosomal translocation has been noted that is attributable to the sites occupied by these REPs (17q11.2 and 19p13.13), either in cancer cytogenetics (Mitelman, 2003) or in constitutional chromosome rearrangement databases (Borgaonkar, 1997).

Sequence Composition of Breakpoint Clusters and Hotspots

The positions of breakpoint intervals with respect to sequence features of the NF1REPs are detailed in Figure 2. The breakpoint intervals that define PRS1 and PRS2 were reported previously (Lopez-Correa et al., 2001; Dorschner et al., submitted). Within each PRS, a majority of breakpoints were concentrated in a smaller hot spot. Within PRS1, an interval of 551 bp accounted for 60% (9 of 15) of the breakpoints, and within PRS2, an interval of 2,292 bp accounts for 93% (27 of 29) of the breakpoints (Fig. 4; Dorschner et al., submitted).

Here, we report an additional, unique *NF1* microdeletion case with breakpoints mapping within the NF1REP-51 repeats but outside either PRS. The breakpoint interval of patient UWA160-1 mapped to an interval about 20 kb proximal to PRS1 (nt 102102–102186 in BAC RP11-271K11; Fig. 4). Sequencing of the breakpoint region of the deleted chromosome 17 of this patient, which had been segregated into a human–rodent somatic cell hybrid line, showed a single transition from an NF1REP-P1-specific PSV to an NF1REP-M-specific PSV. This case demonstrates that paralogous recombination can occur between the NF1REP-51 repeats at sites other than PRS1 and PRS2, albeit at a significantly reduced frequency. This breakpoint occurred in intron 7 of *KIAA0563rel*, and it is the only NF1REP-51 breakpoint found to date that is in a coding region.

If recombination hot spots occur because of obligate local sequence features, we might expect the PRS clusters to show some similarity in sequence composition, but sequence and structural analyses of PRS1 and PRS2 revealed no common features. BLAST comparison of PRS1 and PRS2 showed no significant sequence identity, with the exception of Alu elements, LINES, SINES, and other high-copy repeats, which typically shared <80% identity and lengths of <500 bp. Furthermore, PRS1 and PRS2 showed entirely different patterns of high-copy repeats and G+C content (Fig. 4). PRS1 had high-copy repeats spread throughout, and overall 67% was repeats, whereas only 44% of PRS2 was repeats, and the PRS2 hot spot was devoid of high-copy repeats. The entire NF1REP-51 repeat is 55% high-copy repeats, and the entire BAC 271K11 is 51% high-copy repeats. Thus, one PRS region had more repeats than average for the region, and the other had fewer. The PRS1 and PRS2 clusters both had higher-than-average G+C for their contexts (53.0% and 55.7%, respectively, versus 48.4% for the entire 51-kb high-identity repeat). However, the PRS2 hot spot was especially G+C-rich (63.7%), whereas the PRS1 hot spot was not (52.7%). These sequence composition values

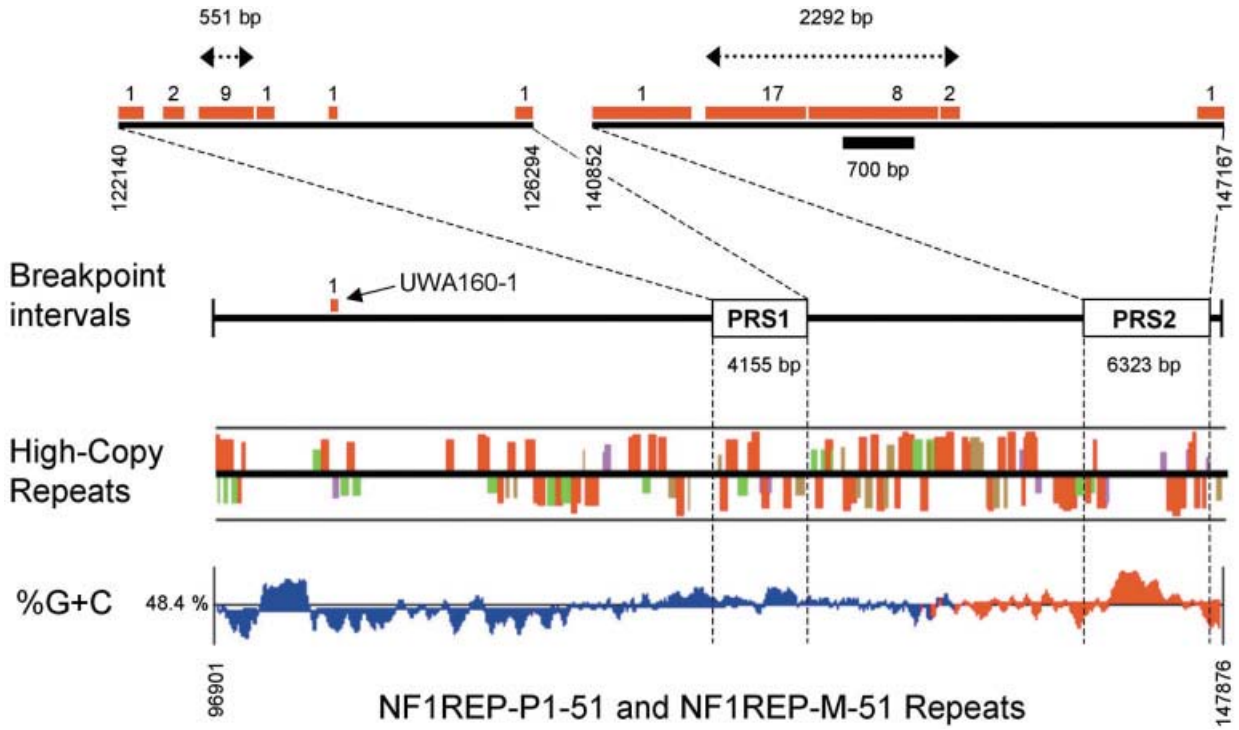

Figure 4. Paralogous recombination sites and sequence composition of the NF1REP 51-kb paralogous segments. Nucleotide coordinates and sequence features refer to the NF1REP-P1 reference BAC RP11-271K11. In the top panel, breakpoint intervals are shown as red bars, with the number of *NF1* microdeletion cases mapped to each interval indicated. Dotted arrows indicate the 551-bp PRS1 and the 2,292-bp PRS2 recombination hot spots. The black bar below PRS2 indicates the 700-bp putative gene conversion tract between the NF1REP 51-kb repeats (see text and Fig. 6). Patient UWA160-1 is a new microdeletion case that maps within the 51-kb segments but outside the PRS (see text). High-copy repeats in NF1REP-P-51 (forward strand on top, reverse strand on bottom) and percentage of G+C are displayed using graphic output from the Gestalt Workbench (Glusman and Lancet, 2000). Bar size indicates the relative repeat age, and colors indicate repeat class [LINE elements in green, Alus in red, MIRs in purple, tRNAs in blue (none found here), and all others in brown]. Overall, G+C content is 48.4%, and the blue-to-red transition indicates an isochore transition from H1-2 (43–50% G+C) to H3 (>50% G+C).

were calculated for the NF1REP-P1-51, but because of the 97.5% identity, these values did not differ markedly from those for the paralogous NF1REP-M-51 repeat.

NF1REP Sequence Alignment, Sequence Identity, and Breakpoint Localizations

The NF1REP-51 paralogs that harbored the breakpoints in 69% of the *NF1* whole-gene deletions differed more than do typical allelic recombination substrates. The mean sequence similarity was 97.5% taking into consideration both alignment gaps (insertions and deletions, or indels) and PSVs. Of the 2.5% overall divergence, 1.4% was represented by PSVs and 1.1% by indels (analysis of manually aligned sequences using the DnaSP program; Rozas and Rozas, 1999).

Segments of the aligned NF1REP-51 paralogs differed in alignment quality. The top panel of Figure 5 shows the size of all indels between the NF1REP-P1-51 and NF1REP-M-51 repeats. PRS1 and PRS2 contain sparse misalignments of 1–4 bp. Both PRSs are devoid of large gaps, although both are flanked proximally by markedly larger gaps. The 36-bp alignment gap at the front of PRS1 is a result of a $(GA)_n$ microsatellite that in NF1REP-P1 sequences from normal individuals is fixed at nine repeat units ($N = 24$) and in NF1REP-M sequences from normal individuals ranges from 15 to 31 units ($N = 26$). PRS2 is bordered by a unique 24-bp indel that is a fixed difference among the three NF1REP-P1 and two NF1REP-M sequences currently available in Genbank (accession numbers in Materials and Methods; our own PRS2 sequences from patients and from normal controls did not extend proximally to this site). These relatively large alignment gaps flanking the PRS apparently do not prevent pairing for recombination, as exchange can occur within distances of less than 1 kb from the gaps. However, the principal hot spots were 1–2 kb distal to these alignment gaps (Fig. 2). Within the hot spots, paralogous misalignments are limited to 1–4 bp both in available Genbank entries and in our hot-

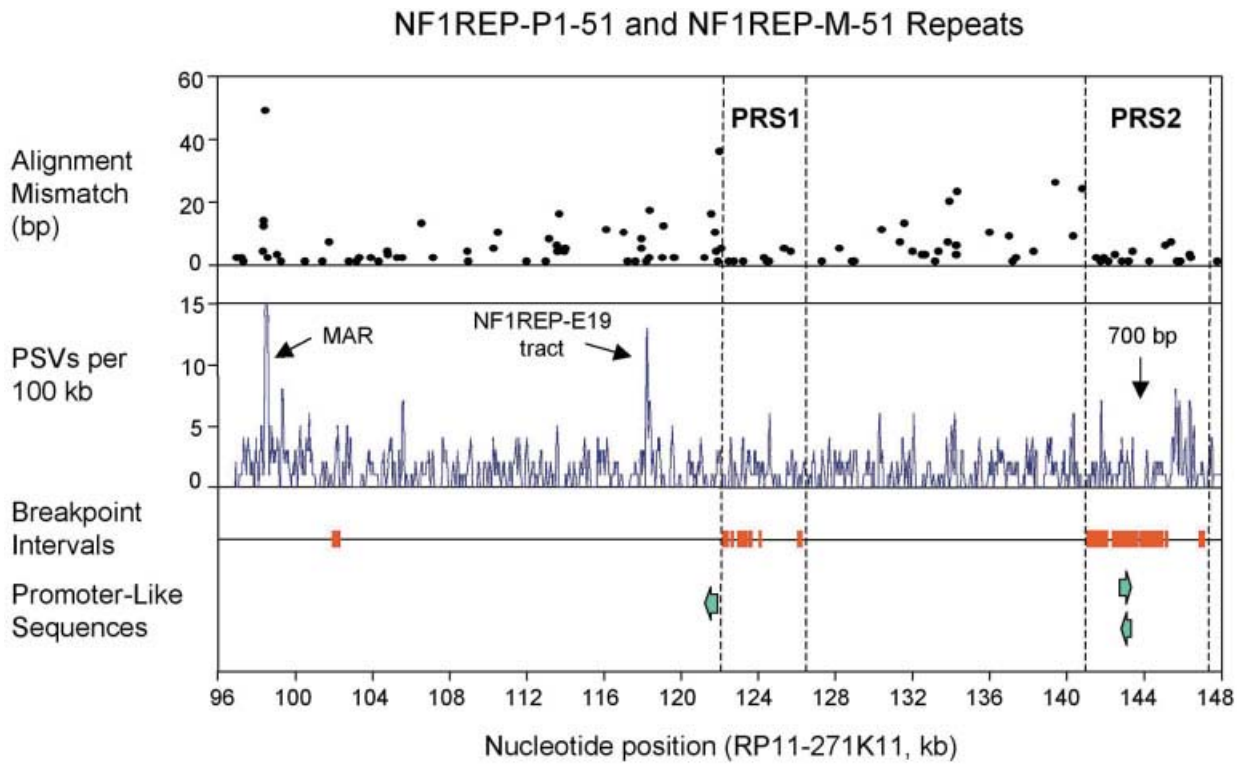

Figure 5. Alignment, sequence identity, and sequence features of the 51-kb high-identity paralogs NF1REP-P1-51 and NF1REP-M-51. Nucleotide coordinates refer to the NF1REP-P1 reference BAC RP11-271K11. The top panel shows the size of alignment gaps using reference BACs 271K11 (NF1REP-P1-51) and 640N20 (NF1REP-M-51). The middle panel shows nucleotide site differences between REPs (paralogous sequence variants, or PSVs), indels excluded, tabulated with a sliding 100-bp window stepped by 25 bp. Noted are two sites of greater-than-average sequence difference, including a single high-scoring matrix attachment region (MAR) and an apparent gene conversion tract with variants matching NF1REP-E19 (see Results section). The 700-bp fragment of perfect match with statistical evidence of gene conversion is indicated. The promoterlike sequences (green arrows; see Materials and Methods section) are not associated with known genes.

spot sequences from patients and from normal controls (see Materials and Methods section).

On a kilobase scale, PRS1 and PRS2 are not regions of greater or lesser paralogous sequence identity, as shown by the spatial distribution of PSVs in the middle panel of Figure 5. The overall percentage of divergence for NF1REP-P1-51 and NF1REP-M-51 was 1.36% (indels excluded), and the corresponding values for PRS1 (1.17%) and PRS2 (1.45%) were not significantly different from the overall mean (2×2 contingency chi-square tests; $P > 0.1$). Nucleotide site differences (PSVs) appeared to be uniformly distributed across the entire NF1REP-51, with two notable exceptions. One high-divergence tract, at 98.4 kb, contained a matrix attachment region (MAR; see below). The other high-divergence tract, at 118 kb, was a short (95 bp) segment with 15 variable sites (13 PSVs and 2 indels of 1 bp each) in which NF1REP-P1-51 matched a segment of NF1REP-E19. These variable sites are fixed in the three sequenced alleles of NF1REP-P1-51 available in Genbank (accession numbers in Materials and Methods), and they are likely to represent an early gene conversion event that followed duplication of the NF1REP-51 paralogs. The NF1REP-E19 blocks matching the NF1REP-P1-51 (Fig. 3) showed only 94–95% identity between these interchromosomal paralogs. Gene conversion tests and searches for other NF1REP-specific variants shared between NF1REP-E19 and its paralogs on chromosome 17 found no other evidence of historical gene conversion or recombination (data not shown).

Recombinogenic Structures and Domains

We searched the NF1REP breakpoint cluster regions for structures reported to be associated with recombination in other settings (see below and Materials and Methods section). In addition, we looked for commonalities between the breakpoint clusters of NF1REPs and the REPs involved in Charcot-Marie-Tooth disease type 1A (CMT1A), another paralogous recombination disorder in

which breakpoints have been mapped in similar detail.

Several genomic rearrangements have been associated with palindromes (Nag and Kurst, 1997; Nasar et al., 2000; Kurahashi and Emanuel, 2001; Repping et al., 2002; Kurahashi et al., 2003). The NF1REP-51 repeats contain no palindromes larger than 18 bp and separated by 63 bp when the arms are allowed to be 100 bp and separated by up to 100 bp. Yet these default settings of the *Palindrome* program readily detected the 195-bp AT-rich palindrome in *NF1* intron 31 (Kurahashi et al., 2003). More permissive pattern searches for large inverted repeats performed on the entire NF1REP-P1 and NF1REP-M revealed a single significant pair of sequences that straddle the proximal boundary of the NF1REP-P1-51 repeat (Fig. 2; light green blocks). These nontandem inverted repeats are 5,778 bp long, are separated by 3,708 bp of unrelated sequence, show 98.6% sequence identity, and contain copies of *KIAA0563rel* exon 8. The "inverted" segment of the pair is present only on NF1REP-P1 (Fig. 2). Pairing between these repeats of NF1REP-P1 is unlikely to account for preferential DSBs that initiate paralogous recombination at PRS1 and PRS2, which are 15 and 36 kb telomeric to the distal copy of the repeat.

A role for specific sequence signals in mammalian recombination is not established, but tests for the presence of motifs with demonstrated or suspected roles in recombination, transcription, or replication are still warranted. In *E. coli*, recombination is stimulated by the 8-bp *Chi* sequence (5′-GCTGGTGG-3′; Tracy et al., 1997). BAC 271K11 contains 20 *Chi* elements in a span of 200 kb. Within this span, the NF1REP-P1-51 block (51 kb) contains five *Chi* elements [at RP11-271K11 nt 142004 (+strand) and nt 101334, 119727, 128422, and 137390 (−strand)]. The +-strand *Chi* element falls within the PRS2 hot spot (Lopez-Correa et al., 2001), but the other four are evenly spaced without apparent association with breakpoints. NF1REP-M-51 has *Chi* element sequences at the same five sites. Because of their association with recombination in yeast (Gale et al., 1992; Badge et al., 2000), we also searched for autonomously replicating sequences (ARSs). BAC 271K11 contains 13 *S. cerevisiae* ARS sites. The NF1REP-51 both contain the same five *S. cerevisiae* ARS sites, one of which is within PRS1 but 2 kb distal to the PRS1 hot spot. This does not indicate a marked excess of ARS sites in the 51-kb repeat or in the PRS, and the proximity of one ARS site to the PRS1 hot spot could be purely due to chance. The other putative recombinogenic motifs (see Materials and Methods) also were not found to be preferentially associated with PRS1 or PRS2 in this or in previous studies (Dorschner et al., 2000; Lopez-Correa et al., 2001; Dorschner et al., submitted).

A search for functional chromatin based on promoter sequences (First Exon Finder; see Materials and Methods section) found two overlapping promoter/first exons on opposite strands within the PRS2 hot spot and one proximal to PRS1 (Figs. 4 and 5). However, PRS1 and PRS2 are not associated with any known genes. About half the reported paralogous recombination disorders involve recombination either between related expressed genes or between an expressed gene and its pseudogene (Stankiewicz and Lupski, 2002), and the relative accessibility of promoterlike chromatin may persist even as the transcription unit becomes nonfunctional.

A search for functional chromatin based on MARs (Singh et al., 1997) detected a single 800-bp high-scoring MAR centered 1,500 bp into the NF1REP-51 repeats (Fig. 5), and the NF1REP-P1-51 and NF1REP-M-51 paralogs of this tract were each the highest-scoring MAR in the context of their respective BACs. Any role that a strong MAR may play in the likelihood that paralogs will pair is unclear. Also, none of the *NF1* microdeletion breakpoints occurred at or near the MAR site, arguing against matrix/scaffold attachment as a primary breakpoint-localizing feature in this disorder.

Gene Conversion Tests in the NF1REPs

In the absence of gene conversion or recombination, paralogous sequences should have evolved independently, and sequence differences should be distributed at random. Larger stretches of perfect match than expected at random are evidence of gene conversion. The longest fragment of perfect match between the finished BAC sequences for NF1REP-P1-51 and NF1REP-M-51 was a 700-bp tract located in the PRS2 hot spot (nt 143268–143967; Figs. 4–6). A statistical test called "GeneConv" (see Materials and Methods), performed using the NF1REP-51 repeats from the reference BACs 271K11 and 640N20, revealed this to be the single significant fragment ($P = 0.008$; indels included as polymorphisms). Among the five Genbank NF1REP sequences (three proximal and two medial; accession numbers in Materials and Methods section), a perfect tract at this location was the largest in each of the six paralogous comparisons, ranging in size from 627 to 700 bp because of polymorphisms. In each case, when the

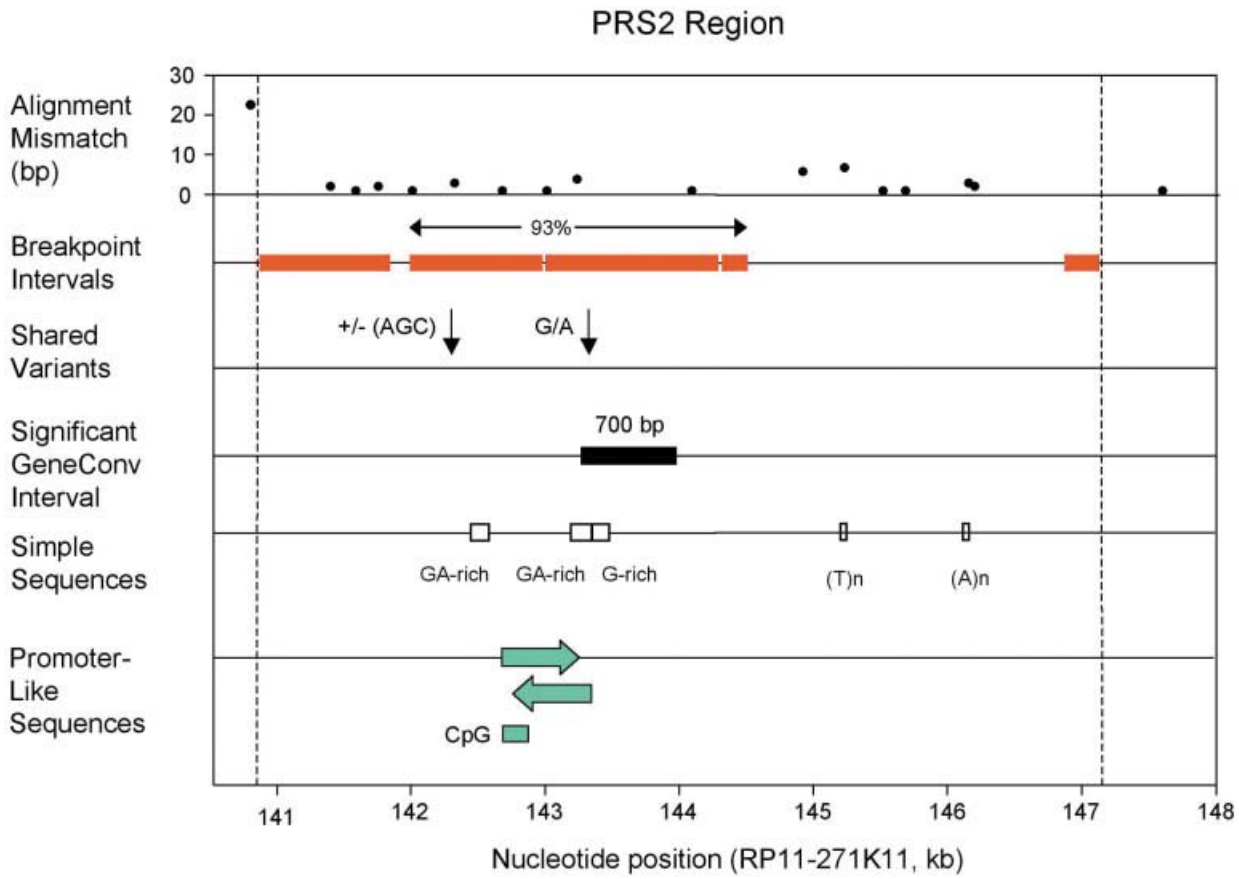

Figure 6. Detailed structure of the PRS2 region. Alignment gaps (indels) in the top panel match those in the PRS2 region shown in Figure 5 and are based on the two reference BACs with finished sequences (RP11-271K11 and RP11-640N20). Breakpoint intervals (red bars) are defined by sites found to be invariant within each paralog (PSVs) in sequences from normal individuals and Genbank entries (see Materials and Methods section; Dorschner et al., 2000; Dorschner et al., submitted). Hence, breakpoint intervals contain some small alignment gaps (shown) and site variants (not shown) that were polymorphic within either or both paralogs and were not used for breakpoint mapping. The shared variants (third panel) are sites found to be polymorphic in both paralogs, based on three proximal and two medial Genbank sequences and on our sequences from hot-spot regions for normal individuals (see Materials and Methods). By definition, these are not PSVs and were not used for interval mapping. Ninety-three percent of all PRS2 exchanges occurred in the indicated 2.3-kb hot-spot interval. Simple sequences were detected by the UCSB Genome Browser, and candidate promoters were detected with First Exon Finder (Davuluri et al., 2001).

tract was shorter (e.g., 627 bp using NF1REP-P1 BAC 271K11 and NF1REP-M BAC 2646J6), the *P* value increased but remained significant ($P = 0.019$; indels included as polymorphisms).

We also searched the alignment of the five copies of NF1REPs for shared polymorphisms. Two sites, both on the proximal border of the 700-bp putative gene conversion tract, showed the same two variants in both paralogs (a 3-bp, +/−[AGC] indel, and a G/A SNP; nt 142308 and 143314, respectively; Fig. 6). Such polymorphisms in both paralogs, especially the identical 3-bp indel, suggest a gene conversion event subsequent to duplication of the region.

DISCUSSION

Disease-causing genome rearrangements from recombination between paralogs range in size from less than 10 kb to as large as 4 Mb, and the REPs involved range in size from a few kilobases to more than 500 kb (reviewed by Inoue and Lupski, 2002; Stankiewicz and Lupski, 2002). The NF1REPs that mediate *NF1* microdeletion have a modular sequence structure, scattered pseudogene fragments, expression of a single functional gene, and a related set of paralogs on a different chromosome. NF1REPs are more complex than CMT1A-REPs (Reiter et al., 1996; Lopes et al., 1999), which are simple related sequence blocks in direct orientation. However, they are not as complex as several other examples such as the REPs that mediate deletion in Smith–Magenis and Williams–Beuren syndromes (Park et al., 2002; Bayes et al., 2003; Bi et al., 2003), which contain multiple clusters of larger blocks in different combinations and different orientations. In all these examples, the

REPs contain, or are contained in, transcription units, and the derived paralog often contains a pseudogene or pseudogene fragments of the original gene.

Hotspots and Sequence Motifs

The predominant mechanism of *NF1* microdeletion is paralogous pairing and recombination between NF1REPs. From 17 *NF1* whole-gene-deletion cases previously ascertained by apparent hemizygosity for *NF1* markers, Dorschner et al. (2000) found that 14 were a result of paralogous recombination between NF1REP-P1-51 and NF1REP-M-51. Sequence analysis of the deleted chromosome in these 14 cases showed that 13 occurred within PRS1 or PRS2 (Lopez-Correa et al., 2001; Dorschner et al., submitted) and only one (UWA160-1, reported here; Fig. 4) mapped within the REPs but outside the PRSs. The PRS clusters represent only 19% of the 51 kb of sequence apparently available for pairing and exchange in NF1REP-P1-51 and NF1REP-M-51, indicating a strong positional bias for strand exchange.

Breakpoint mapping in the CMT1A/HNPP duplication/deletion disorders also identified two recombination hot spots (Lopes et al., 1998; Reiter et al., 1998), and additional comparisons to the NF1REPs are instructive. In neither NF1REPs nor CMT1A-REPs were there common sequence-level features that would suggest an explanation for why the breakpoint clusters occur where they do. We found no sequence identity between paralogous recombination hot spots either within or between these two disorders and no similarity in sequence features or composition. In the NF1REPs, PRS2 contains a *Chi* sequence and promoterlike elements, but PRS1 contains neither. Likewise, the two CMT1A paralogous recombination hot spots are entirely different. The major hot spot (75% of cases) is flanked by a Mariner-like transposon element, a *Chi*-like site, and a minisatellite, but the secondary hot spot (20% of cases) is associated with no such motifs (Reiter et al., 1998). At only 24 kb (Reiter et al., 1996), CMT1A-REPs are smaller than NF1REP-51 and their modular structure simpler (Inoue et al., 2001). CMT1A-REPs also have a lower percentage of G+C (41% vs. 48% for NF1REP-51), fewer high-copy repeats (31% vs. 55% for NF1REP-51), no strong MAR sites, and tighter breakpoint clustering. From the evidence of these two paralogous recombination disorders and from similar analysis of a primary hot spot involved in Smith–Magenis syndrome microdeletion (Bi et al., 2003), there is no support for the presence of *cis*-acting motifs or features localizing paralogous exchange breakpoints.

There are to date many more examples of breakpoints mapped at the sequence level for allelic recombination events (reviewed by de Massy, 2003) than for paralogous recombination events. In both homologous and paralogous recombination, however, multiple examples suggest that putative recombinogenic motifs may be influential, but they are not obligatory. Several examples in yeast (Nag and Kurst, 1997; Nasar et al., 2000) suggest that large palindromes enhance recombination by inducing DSBs, and a variety of local sequence features ranging from simple repeats to promoters and transposons can enhance recombination at specific sites. For example, a hot spot of 1.0–1.6 kb in the mouse major histocompatibility complex (MHC) was found to be centered on an MT element (Yauk et al., 2003). In humans, specific sequences such as microsatellites (Benet et al., 2000) and minisatellites (Wahls et al., 1990; Boan et al., 1998; Jeffreys et al., 1998) are strongly associated with recombination hot spots. However, it is unclear what features serve to localize breakpoints when such recombinogenic motifs are apparently lacking, as in the *NF1* microdeletion.

Breakpoint Clustering and Alignment Mismatch

NF1REPs and CMT1A-REPs differ markedly in the degree and nature of sequence differences between paralogs. This may be related to differences between the two systems in causes of breakpoint localization. The NF1REP-51 repeats show 97.5% sequence identity, lower than for the CMT1A-REPs, which is 98.3%. The proportions of PSVs are approximately the same (1.4% and 1.2%, respectively). However, the NF1REP-51 repeats have nearly three times the proportion of bases in alignment gaps that the CMT1A-REPs have (1.1% and 0.4%, respectively). Despite the greater proportion of gaps in the NF1REPs, within them, the PRSs are regions of relatively good alignment, with indels of only 1–4 bp (Figs. 5 and 6). Larger gaps of approximately 10–40 bp are contiguous to but not contained within the two PRSs. The lack of such large alignment gaps in the CMT1A-REPs means that study of these REPs does not so directly address the effect of gaps on breakpoint clustering. The simplest explanation for the location of the *NF1* PRS clusters is that gaps of 1–4 bp do not prevent effective pairing and subsequent genetic exchange, but larger gaps (here approximately 10

to 40 bp) do not allow effective pairing and exchange in their immediate vicinity.

Gene Conversion Between Paralogs

The finding of significantly long identical sequences and shared polymorphisms suggests that gene conversion occurred in the *NF1* PRS2 hot spot. In addition, in the three cases cited above, sufficient sequence detail from the parental chromosomes demonstrated gene conversion in the process of strand exchange (Lopez-Correa et al., 2001; Dorschner et al., submitted). Gene conversion accompanying crossover also was described for the primary CMT1A/HNPP recombination hot spot (Reiter et al., 1998; Lopes et al., 1999). If gene conversion accompanies crossover events ascertained by pathology, it is also possible—even likely—that gene conversion between the same paralogs occurs in the absence of crossover. Such events would not be pathologic, but they should be detectable by sequencing of a large number of normal alleles. Analysis of the two diseases cited here has provided promising early evidence that recombination hot spots coincide with and are mechanistically related to gene conversion hot spots.

It has been suggested that gene conversion acts to homogenize paralogous sequence, which, in turn, makes them more likely to pair (Hurles, 2001; Stankiewicz and Lupski, 2002). However, we cannot say with certainty which is cause and which is effect. That is, either (1) a hot-spot region is prone to effective pairing for reasons external to the tract, and gene conversion events within the tract serve to homogenize the paralogs at this site; or (2) a hot-spot region preferentially pairs because it happens to be a larger perfect tract than the neighboring sequence, and the resulting gene conversion helps to maintain this high sequence identity.

Some care is warranted in using single copies of paralogous sequences to test for paralogous gene conversion because the size of perfect fragments depends strongly on population variation for defining PSVs. Among the five copies of the NF1REPs available in Genbank (including two of NF1REP-P1 and two of NF1REP-M; see Materials and Methods section), a fragment at the site of the 700-bp matching fragment reported above varies in size but is always the largest and always a statistically significant matching fragment (all $P < 0.05$). We also applied the same test we used on the NF1REPs (Sawyer's GeneConv; see Materials and Methods section) to the original Genbank copies of the CMT1A-REPs (Reiter et al., 1996; accession numbers in Materials and Methods section) and found a significant fragment of 950 bp ($P = 0.0004$; indels included as variants). This tract coincides with the secondary (20% of cases) CMT1A recombination hot spot (nt 24879–25830 in Genbank #U71218; Reiter et al., 1998). Using alternate CMT1A-REP sequences (accession numbers in Materials and Methods section) shortened the significant 950-bp fragment to 658 bp, but even at this length it was still significant ($P = 0.020$). Hurles et al. (2001) reported statistical evidence of gene conversion in these sequences, but they did not identify particular significant fragments.

Analysis of normal sequences for conversion tracts detects where paralogous pairing apparently has occurred, but crossover has not. Sampling of more alleles at these sites in normal genomes would help to characterize these events. If borne out by subsequent studies, the coincidence of the hot spots for both crossover and gene conversion would strongly support a dual-pathway recombination model in humans similar to that proposed for yeast, in which the initial steps include a DSB and pairing, but the outcome may be either gene conversion without crossover or recombination (with or without gene conversion; reviewed by de Massy, 2003).

Pairings between paralogs are "mistakes" where paired sequences may differ considerably more than do homologs (alleles), but still match sufficiently such that subsequent recombination steps proceed normally. The main contribution that paralogous pairing adds to our knowledge of recombination in general may be in those examples where the paralogs are especially small or (as in the NF1REPs) the paralogous alignment match displays substantial gaps. Accumulation of such examples will serve to illustrate the minimal length and quality of sequence pairing needed to effect recombination in humans.

REFERENCES

Badge RM, Yardley J, Jeffreys AJ, Armour JA. 2000. Crossover breakpoint mapping identifies a subtelomeric hotspot for male meiotic recombination. Hum Mol Genet 9:1239–1244.

Bayes M, Magano LF, Rivera N, Flores R, Perez Jurado LA. 2003. Mutational mechanisms of Williams–Beuren syndrome deletions. Am J Hum Genet 73:131–151.

Benet A, Molla G, Azorin F. 2000. d(GA × TC)(n) Microsatellite DNA sequences enhance homologous DNA recombination in SV40 minichromosomes. Nucleic Acids Res 28:4617–4622.

Benson G. 1999. Tandem repeats finder: a program to analyze DNA sequences. Nucleic Acids Res 27:573–580.

Bi W, Shaw CJ, Withers MA, Park SS, Pragnal PI, Lupski JR. 2003. Reciprocal crossovers and a positional preference for strand exchange in recombination events resulting in deletion/duplication. Am J Hum Genet 73:1302–1315.

Boan F, Rodriguez JM, Gomez-Marquez J. 1998. A non-hypervariable human minisatellite strongly stimulates in vitro intramolecular homologous recombination. J Mol Biol 278:499–505.

Borgaonkar DS, editor. 1997. Chromosomal variation in man: a catalog of chromosomal variants. 8th ed. New York: John Wiley & Sons.

Davuluri RV, Grosse I, Zhang MQ. 2001. Computational identification of promoters and first exons in the human genome. Nat Genet 29:412–417.

de Massy B. 2003. Distribution of meiotic recombination sites. Trends Genet 19:514–522.

De Raedt T, Brems H, Wolkenstein P, Vidaud D, Pilotti S, Perrone F, Mautner V, Frahm S, Sciot R, Legius E. 2003. Elevated risk for MPNST in NF1 microdeletion patients. Am J Hum Genet 72: 1288–1292.

Dorschner MO, Sybert VP, Weaver M, Pletcher BA, Stephens K. 2000. NF1 microdeletion breakpoints are clustered at flanking repetitive sequences. Hum Mol Genet 9:35–46.

Dorschner MO, Brems H, Le R, De Raedt T, Wallace MR, Curry CJ, Aylsworth AS, Haan EA, Zackai EH, Lazaro C, Messiaen L, Legius E, Stephens K. Two paralogous recombination hotspots mediate 69% of *NF1* microdeletions. Submitted.

Emanuel BS, Shaikh TH. 2001. Segmental duplications: an "expanding" role in genomic instability and disease. Nat Rev Genet 2:791–800.

Estivill X, Cheung J, Angel Pujana M, Nakabayashi K, Scherer SW, Tsui LC. 2002. Chromosomal regions containing high-density and ambiguously mapped putative single nucleotide polymorphisms (SNPs) correlate with segmental duplications in the human genome. Hum Mol Genet 11:1987–1995.

Gale JM, Tobey RA, D'Anna JA. 1992. Localization and DNA sequence of a replication origin in the rhodopsin gene locus of Chinese hamster cells. J Mol Biol 224:343–358.

Glusman G, Lancet DO. 2000. GESTALT: a workbench for automatic integration and visualization of large-scale genomic sequence analyses. Bioinformatics 16:482–483.

Haber JE. 2000. Partners and pathways—repairing a double-strand break. Trends Genet 16:259–264.

Hurles ME. 2001. Gene conversion homogenizes the CMT1A paralogous repeats. BMC Genomics 2:11–20.

Inoue K, Lupski JR. 2002. Molecular mechanisms for genomic disorders. Annu Rev Genomics Hum Genet 3:199–242.

Inoue K, Dewar K, Katsanis N, Reiter LT, Lander ES, Devon KL, Wyman DW, Lupski JR, Birren B. 2001. The 1.4-Mb CMT1A duplication/HNPP deletion genomic region reveals unique genome architectural features and provides insights into the recent evolution of new genes. Genome Res 11:1018–1033.

Jeffreys AJ, Murray J, Neumann R. 1998. High-resolution mapping of crossovers in human sperm defines a minisatellite-associated recombination hotspot. Mol Cell 2:267–273.

Jenne DE, Tinschert S, Stegmann E, Reimann H, Nurnberg P, Horn D, Naumann I, Buske A, Thiel G. 2000. A common set of at least 11 functional genes is lost in the majority of NF1 patients with gross deletions. Genomics 66:93–97.

Jenne DE, Tinschert S, Reimann H, Lasinger W, Thiel G, Hameister H, Kehrer-Sawatzki H. 2001. Molecular characterization and gene content of breakpoint boundaries in patients with neurofibromatosis type 1 with 17q11.2 microdeletions. Am J Hum Genet 69:516–527.

Jenne DE, Tinschert S, Dorschner MO, Hameister H, Stephens K, Kehrer-Sawatzki H. 2003. Complete physical map and gene content of the human NF1 tumor suppressor region in human and mouse. Genes Chromosomes Cancer 37:111–120.

Johnson RD, Jasin M. 2001. Double-strand-break-induced homologous recombination in mammalian cells. Biochem Soc Trans 29: 196–201.

Kayes LM, Burke W, Riccardi VM, Bennett R, Ehrlich P, Rubenstein A, Stephens K. 1994. Deletions spanning the neurofibromatosis 1 gene: identification and phenotype of five patients. Am J Hum Genet 54:424–436.

Kluwe L, Friedrich RE, Peiper M, Friedman J, Mautner VF. 2003. Constitutional NF1 mutations in neurofibromatosis 1 patients with malignant peripheral nerve sheath tumors. Hum Mutat 22: 420.

Kluwe L, Siebert R, Gesk S, Friedrich RE, Tinschert S, Kehrer-Sawatzki H, Mautner VF. 2004. Screening 500 unselected neurofibromatosis 1 patients for deletions of the NF1 gene. Human Mutation 23:111–116.

Korf BR. 2002. Clinical features and pathobiology of neurofibromatosis 1. J Child Neurol 17:573–577, discussion 602–604, 646–651.

Kurahashi H, Emanuel BS. 2001. Long AT-rich palindromes and the constitutional t(11;22) breakpoint. Hum Mol Genet 10:2605–2617.

Kurahashi H, Shaikh T, Takata M, Toda T, Emanuel BS. 2003. The constitutional t(17;22): another translocation mediated by palindromic AT-rich repeats. Am J Hum Genet 72:733–738.

Kuroda-Kawaguchi T, Skaletsky H, Brown LG, Minx PJ, Cordum HS, Waterston RH, Wilson RK, Silber S, Oates R, Rozen S, Page DC. 2001. The AZFc region of the Y chromosome features massive palindromes and uniform recurrent deletions in infertile men. Nat Genet 29:279–286.

Leppig KA, Kaplan P, Viskochil D, Weaver M, Ortenberg J, Stephens K. 1997. Familial neurofibromatosis 1 microdeletions: cosegregation with distinct facial phenotype and early onset of cutaneous neurofibromata. Am J Med Genet 73:197–204.

Lopes J, Ravise N, Vandenberghe A, Palau F, Ionasescu V, Mayer M, Levy N, Wood N, Tachi N, Bouche P, Latour P, Ruberg M, Brice A, LeGuern E. 1998. Fine mapping of de novo CMT1A and HNPP rearrangements within CMT1A-REPs evidences two distinct sex-dependent mechanisms and candidate sequences involved in recombination. Hum Mol Genet 7:141–148.

Lopes J, Tardieu S, Silander K, Blair I, Vandenberghe A, Palau F, Ruberg M, Brice A, LeGuern E. 1999. Homologous DNA exchanges in humans can be explained by the yeast double-strand break repair model: a study of 17p11.2 rearrangements associated with CMT1A and HNPP. Hum Mol Genet 8:2285–2292.

Lopez-Correa C, Brems H, Lazaro C, Estivill X, Clementi M, Mason S, Rutkowski JL, Marynen P, Legius E. 1999. Molecular studies in 20 submicroscopic neurofibromatosis type 1 gene deletions. Hum Mutat 14:387–393.

Lopez-Correa C, Brems H, Lazaro C, Marynen P, Legius E. 2000. Unequal meiotic crossover: a frequent cause of NF1 microdeletions. Am J Hum Genet 66:1969–1974.

Lopez-Correa C, Dorschner M, Brems H, Lazaro C, Clementi M, Upadhyaya M, Dooijes D, Moog U, Kehrer-Sawatzki H, Rutkowski JL, Fryns JP, Marynen P, Stephens K, Legius E. 2001. Recombination hotspot in NF1 microdeletion patients. Hum Mol Genet 10:1387–1392.

Lupski JR, Deocaluna RM, Slaugenhaupt S, Pentao L, Guzzetta V, Trask BJ, Saucedocardenas O, Barker DF, Killian JM, Garcia CA, Chakravarti A, Patel PI. 1991. DNA duplication associated with Charcot-Marie-Tooth disease type 1A. Cell 66:219–232.

Lupski JR. 2003. 2002 Curt Stern Award Address—Genomic disorders: Recombination-based disease resulting from genome architecture. Am J Hum Genet 72:246–252.

Ma B, Tromp J, Li M. 2002. PatternHunter: faster and more sensitive homology search. Bioinformatics 18:440–445.

Messiaen LM, Callens T, Mortier G, Beysen D, Vandenbroucke I, Van Roy N, Speleman F, Paepe AD. 2000. Exhaustive mutation analysis of the NF1 gene allows identification of 95% of mutations and reveals a high frequency of unusual splicing defects. Hum Mutat 15:541–555.

Mitelman F, Johansson B, Mertens F, editors. 2003. Catalog of chromosome aberrations in cancer. New York: John Wiley & Sons.

Nag DK, Kurst A. 1997. A 140-bp-long palindromic sequence induces double-strand breaks during meiosis in the yeast *Saccharomyces cerevisiae*. Genetics 146:835–847.

Nasar F, Jankowski C, Nag DK. 2000. Long palindromic sequences induce double-strand breaks during meiosis in yeast. Mol Cell Biol 20:3449–3458.

Park SS, Stankiewicz P, Bi W, Shaw C, Lehoczky J, Dewar K, Birren B, Lupski JR. 2002. Structure and evolution of the Smith–Magenis syndrome repeat gene clusters, SMS-REPs. Genome Res 12:729–738.

Reiter LT, Murakami T, Koeuth T, Pentao L, Muzny DM, Gibbs RA, Lupski JR. 1996. A recombination hotspot responsible for two inherited peripheral neuropathies is located near a mariner transposon–like element. Nat Genet 12:288–297.

Reiter LT, Hastings PJ, Nelis E, De Jonghe P, Van Broeckhoven C, Lupski JR. 1998. Human meiotic recombination products revealed by sequencing a hotspot for homologous strand exchange in multiple HNPP deletion patients. Am J Hum Genet 62:1023–1033.

Repping S, Skaletsky H, Lange J, Silber S, Van Der Veen F, Oates RD, Page DC, Rozen S. 2002. Recombination between palindromes P5 and P1 on the human Y chromosome causes massive deletions and spermatogenic failure. Am J Hum Genet 71:906–922.

Rozas J, Rozas R. 1999. DnaSP version 3: an integrated program for molecular population genetics and molecular evolution analysis. Bioinformatics 15:174–175.

Sawyer S. 1989. Statistical tests for detecting gene conversion. Mol Biol Evol 6:526–538.

Sawyer S. 1999. GENECONV: A computer package for the statistical detection of gene conversion. Distributed by the author, Department of Mathematics, Washington University in St. Louis. Available at http://www.math.wustl.edu/~sawyer

Shaikh TH, Kurahashi H, Saitta SC, O'Hare AM, Hu P, Roe BA, Driscoll DA, McDonald-McGinn DM, Zackai EH, Budarf ML, Emanuel BS. 2000. Chromosome 22-specific low copy repeats and the 22q11.2 deletion syndrome: genomic organization and deletion endpoint analysis. Hum Mol Genet 9:489–501.

Singh GB, Kramer JA, Krawetz SA. 1997. Mathematical model to predict regions of chromatin attachment to the nuclear matrix. Nucleic Acids Res 25:1419–1425.

Stankiewicz P, Lupski JR. 2002. Molecular-evolutionary mechanisms for genomic disorders. Curr Opin Genet Dev 12:312–319.

Stephens K. 2003. Genetics of neurofibromatosis 1- associated peripheral nerve sheath tumors. Cancer Invest 21:901–918.

Tracy RB, Chedin F, Kowalczykowski SC. 1997. The recombination hot spot chi is embedded within islands of preferred DNA pairing sequences in the E-coli genome. Cell 90:205–206.

Upadhyaya M, Ruggieri M, Maynard J, Osborn M, Hartog C, Mudd S, Penttinen M, Cordeiro I, Ponder M, Ponder BA, Krawczak M, Cooper DN. 1998. Gross deletions of the neurofibromatosis type 1 (NF1) gene are predominantly of maternal origin and commonly associated with a learning disability, dysmorphic features and developmental delay. Hum Genet 102:591–597.

Valerie K, Povirk LF. 2003. Regulation and mechanisms of mammalian double-strand break repair. Oncogene 22:5792–5812.

Venturin M, Guarnieri P, Natacci F, Stabile M, Tenconi R, Clementi M, Hernandez C, Thompson P, Upadhyaya M, Larizza L, Riva P. 2004. Mental retardation and cardiovascular malformations in NF1 microdeleted patients point to candidate genes in 17q11.2. J Med Genet 41:35–41.

Wahls WP, Wallace LJ, Moore PD. 1990. Hypervariable minisatellite DNA is a hotspot for homologous recombination in human cells. Cell 60:95–103.

Yauk CL, Bois PR, Jeffreys AJ. 2003. High-resolution sperm typing of meiotic recombination in the mouse MHC Ebeta gene. EMBO J 22:1389–1397.

Mutations in *ABCA12* Underlie the Severe Congenital Skin Disease Harlequin Ichthyosis

David P. Kelsell,[1] Elizabeth E. Norgett,[1] Harriet Unsworth,[1] Muy-Teck Teh,[1] Thomas Cullup,[2] Charles A. Mein,[2] Patricia J. Dopping-Hepenstal,[5] Beverly A. Dale,[8,9,10] Gianluca Tadini,[13] Philip Fleckman,[10] Karen G. Stephens,[11] Virginia P. Sybert,[10,12] Susan B. Mallory,[14] Bernard V. North,[3] David R. Witt,[15] Eli Sprecher,[16] Aileen E. M. Taylor,[17] Andrew Ilchyshyn,[18] Cameron T. Kennedy,[19] Helen Goodyear,[20] Celia Moss,[21] David Paige,[6] John I. Harper,[7] Bryan D. Young,[4] Irene M. Leigh,[1] Robin A. J. Eady,[5] and Edel A. O'Toole[1]

[1]Centre for Cutaneous Research, Institute of Cell and Molecular Science, [2]Genome Centre, William Harvey Research Institute, [3]Academic Department of Psychiatry, and [4]Molecular Oncology Unit, Institute of Cancer, Barts and the London School of Medicine and Dentistry, Queen Mary, University of London, [5]Genetic Skin Disease Group, Division of Skin Sciences, Guy's, King's, and St. Thomas' School of Medicine, St. Thomas' Hospital, [6]Department of Dermatology, Royal London Hospital, and [7]Department of Paediatric Dermatology, Great Ormond Street Hospital for Children, London; Departments of [8]Oral Biology, [9]Biochemistry, [10]Medicine/Dermatology, and [11]Laboratory Medicine, University of Washington, and [12]Department of Dermatology, Group Health Permanente, Seattle; [13]Institute of Dermatological Sciences, University of Milan, Milan; [14]Division of Dermatology, Department of Internal Medicine, Washington University School of Medicine, St. Louis; [15]Genetics Department, Kaiser Permanente, San Jose, CA; [16]Department of Dermatology and Laboratory of Molecular Dermatology, Rambam Medical Center, Haifa; [17]Department of Dermatology, Royal Victoria Infirmary, Newcastle upon Tyne, United Kingdom; [18]Department of Dermatology, Walsgrave Hospital, Coventry, United Kingdom; [19]Department of Dermatology, Southmead Hospital, Bristol, United Kingdom; and [20]Department of Paediatrics, Birmingham Heartlands Hospital, and [21]Department of Dermatology, Birmingham Children's Hospital, Birmingham, United Kingdom

Harlequin ichthyosis (HI) is the most severe and frequently lethal form of recessive congenital ichthyosis. Although defects in lipid transport, protein phosphatase activity, and differentiation have been described, the genetic basis underlying the clinical and cellular phenotypes of HI has yet to be determined. By use of single-nucleotide–polymorphism chip technology and homozygosity mapping, a common region of homozygosity was observed in five patients with HI in the chromosomal region 2q35. Sequencing of the *ABCA12* gene, which maps within the minimal region defined by homozygosity mapping, revealed disease-associated mutations, including large intragenic deletions and frameshift deletions in 11 of the 12 screened individuals with HI. Since HI epidermis displays abnormal lamellar granule formation, ABCA12 may play a critical role in the formation of lamellar granules and the discharge of lipids into the intercellular spaces, which would explain the epidermal barrier defect seen in this disorder. This finding paves the way for early prenatal diagnosis. In addition, functional studies of ABCA12 will lead to a better understanding of epidermal differentiation and barrier formation.

Introduction

Harlequin ichthyosis (HI [MIM 242500]) is a very severe and usually lethal skin disorder of unknown cause (Hsu et al. 1989; Moreau et al. 1999; Sarkar et al. 2000). HI is also known as "harlequin fetus" because of the tendency for affected babies to be born prematurely. The neonate is covered in a thick "coat of armor" that severely restricts movement (Hsu et al. 1989; Dahlstrom et al. 1995; Sarkar et al. 2000). The skin dries out to form hard diamond-shaped plaques separated by fissures, resembling "armor plating." The normal facial features are severely affected, with distortion of the lips (eclabion), eyelids (ectropion), ears, and nostrils. Historically, an HI-affected neonate would usually die within 2 d of birth because of feeding problems, bacterial infection, and/or respiratory distress. However, a number of patients have survived because of the wider availability of neonatal intensive care and likely benefits from oral retinoids (Hsu et al. 1989; Moreau et al. 1999; Elias et al. 2000; Sarkar et al. 2000). In survivors, the disease comes to resemble severe nonbullous congenital ichthyosiform erythroderma (NBCIE) (Haftek et al. 1996; Choate et al. 1998). The skin barrier remains severely compromised, which leads to increased transepidermal water loss, impaired thermal regulation, and increased risk of secondary infection (Moskowitz et al. 2004).

HI occurs in both sexes and in many ethnic groups. Autosomal recessive (AR) inheritance of HI has been

Received January 4, 2005; accepted for publication February 21, 2005; electronically published March 8, 2005.

Address for correspondence and reprints: Prof. David P. Kelsell, Centre for Cutaneous Research, Institute of Cell and Molecular Science, Barts and the London School of Medicine and Dentistry, 2 Newark Street, London E1 2AT, United Kingdom. E-mail: d.p.kelsell@qmul.ac.uk

0002-9297/2005/7605-00XX$15.00

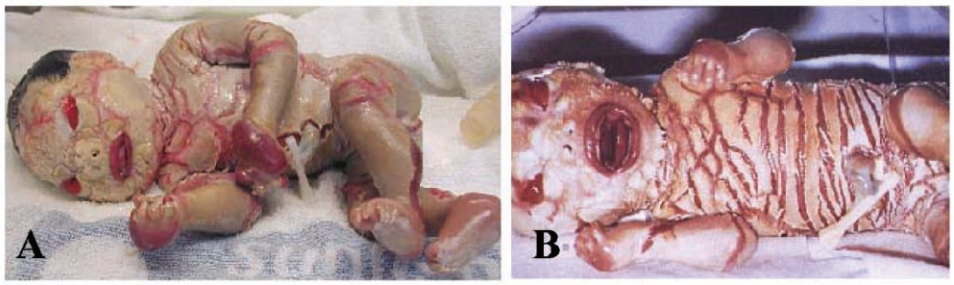

Figure 1 Typical clinical presentation of HI at birth

inferred, but, in a large number of cases, the inheritance pattern cannot be ascertained, and the disorder could be due to a new dominant mutation. It has been subdivided into three types based on the expression of keratin 16 and profilaggrin and the appearance of keratohyalin granules (Dale et al. 1990). Studies have also reported abnormalities in the localization of epidermal lipids and have highlighted the abnormal ultrastructure of epidermal lamellar granules in HI that are associated with the absence of extracellular lamellar structures in all three subtypes (Dale et al. 1990; Akiyama et al. 1996, 1997, 1998). The nuclei of the keratinocytes also show abnormalities, since they appear to become flattened early on in differentiation (in the lower cell layers), but some are retained even as the cornified layer is sloughed off. This parakeratosis along with hyperkeratosis and hypergranulosis (retention of keratohyalin granules in the stratum granulosum) is a characteristic phenotype of the epidermis of neonates with HI (Buxman et al. 1979; Hsu et al. 1989). This may suggest that the process of terminal differentiation is not completed in HI-affected skin. Alterations in calcium-mediated signaling and protein phosphatase activity have also been reported in HI keratinocytes (Kam et al. 1997; Michel et al. 1999). Plausible candidate genes underlying these diverse cellular phenotypes in HI have included *filaggrin, claudins, PP2A,* and *calpain 1* (Kam et al. 1997; Michel et al. 1999).

Mutations in the genes encoding transglutaminase-1 (*TGM1* [MIM 190195]), ichthyin, 4 lipoxygenase 3 (*ALOXE3* [MIM 607206]), and 12(R)-lipoxygenase (*ALOX12B* [MIM 603741]) have all been shown to underlie both NBCIE and lamellar ichthyosis (LI) (Huber et al. 1995; Jobard et al. 2002; Lefevre et al. 2004). Recently, missense mutations in the gene encoding the adenosine triphosphate (ATP)-binding cassette (ABC [GenBank accession number NM_173076]) transporter protein ABCA12 (MIM 607800) have also been shown to cause LI (Lefevre et al. 2003). Unlike the other AR forms of ichthyosis, the genetic basis of HI has not been elucidated.

In the present study, we have used SNP-array technology to localize the HI gene, on the basis of the principle of homozygosity mapping. This identified a major locus for HI on chromosome 2q35 and subsequent disruptive mutations in the *ABCA12* gene in 11 of the 12 analyzed patients with HI. Most of the mutations identified would result in a severely truncated protein. This genetic study immediately establishes the means for early prenatal DNA diagnosis of HI and provides a molecular clue toward understanding the numerous biological abnormalities of epidermal differentiation in HI-affected skin.

Material and Methods

Clinical

Twelve families, from diverse ethnic backgrounds, with individuals affected with HI were included in the present genetic study—three from the United States, seven from Great Britain, and two from Italy. Ethical approval was obtained from the local research ethics committees. The clinical phenotype was verified as HI by at least two clinicians; the typical clinical presentation at birth is shown in figure 1. A summary of the clinical details is shown in table 1. The control population was of mixed ethnicity and consisted of 60 unrelated individuals.

SNP-Array Analysis

A SNP GeneChip Mapping 10K (Affymetrix) array analysis was performed on affected individuals from six families. Two of these families were consanguineous, with AR inheritance of HI. Patient DNA samples were processed in accordance with the standard GeneChip Mapping 10K *Xba* Assay protocol. Briefly, 350 ng of DNA was digested with *Xba*I and ligation to the *Xba*I adaptor prior to PCR amplification by use of AmpliTaq Gold with Buffer II (Applied Biosystems). For each DNA sample, four 100-μl PCRs were set up to obtain sufficient purified PCR product (20 μg), by use of Ultrafree-MC filtration column (Millipore), for subsequent fragmenta-

Table 1

Clinical Details of Patients with HI

Patient	Ethnicity	Gestation (wk)	Birth Weight (g)	Treatment		Outcome	Other Problems
				Retinoid (Dose [mg/kg/d])	Begun at Age (d)		
49	British Bangladeshi	35	2,500	Acitretin (1)	2	SIE, now aged 2.5 years[a]	Pseudomonal SI, FTT, gastrostomy
6	British Pakistani	34	1,750	Etretinate (1.15)	2	SIE, now aged 20 years[b]	Anemia ectropion (surgery)
7	Bangladeshi	38	2,800	Acitretin	NA	SIE, now aged 14 years[c]	FTT, limb deformity
55	British Indian	36	2,600	Acitretin (.75)	4	SIE, now aged 8 years[b]	Neonatal sepsis (SA), hypernatremia, ectropion
40	Italian	40	3,200	Acitretin (1)	3	SIE, now aged 6 years[a]	Neonatal sepsis (CA), ectropion surgery, limb strictures
44	Italian	36	2,000	Acitretin (1)	7	SIE, now aged 6 years[a]	Nystagmus, PDA, neonatal sepsis
63	British Pakistani	36	2,600	Acitretin (.5)	4	SIE, now aged 2 years[b]	Nystagmus, MDD, cataracts, FTT
50	British white	36	2,300	Acitretin (1)	3	SIE, now aged 4 years[b]	Neonatal mild hypothermia
955-01	African-American	36	2,355	Isotretinoin (1)	7	Died at age 6 mo	Septicemia
915-06	Iranian	36	2,980	Isotretinoin (2)	19	Died at age 4 mo	Septicemia (SA)
928-01	Native American	40	NA	Not given		Died at age 1.5 d	Respiratory failure
69	British Pakistani	36	2,820	Not given		Died at age 3 d	Gram-negative sepsis

Note.—CA = *Candida albicans*; FTT = failure to thrive; MDD = motor developmental delay; NA = information not available; PDA = patent ductus arteriosus; SA = *Staphylococcus aureus*; SI = skin infection; SIE = severe ichthyosiform erythroderma.

[a] Remains on retinoids.

[b] Now off retinoids.

[c] Intermittent courses of retinoids.

tion with DNase I. Fragmentation was visualized by 4% agarose-gel electrophoresis to confirm the production of 50–100-bp PCR fragments prior to 3′ labeling with biotin and hybridization to the SNP array. Hybridized arrays were processed with an Affymetrix Fluidics Station 450, and fluorescence signals were detected using the Affymetrix GeneChip Scanner 3000. Raw SNP call data were exported to Microsoft Excel for analysis. The average call rate (expressed as a percentage) ± SEM for the six patients was 97.62% ± 0.41%.

Microsatellite and Linkage Analysis

Data from SNP chips revealed an overlapping region of homozygosity, in five of the six affected individuals, at a position on chromosome 2. Microsatellite markers mapping to this region were used to confirm and refine the minimal region of homozygosity. DNA from patient blood samples was first amplified with the microsatellite markers *D2S325* (chromosome 2q33.3) and *D2S126* (chromosome 2q36.1) from the Applied Biosystems Linkage Mapping Set. Sample DNA was amplified with these primers at 5 μM for 30 cycles at 55°C, by use of Amplitaq Gold PCR Mastermix (Applied Biosystems). *D2S128* (chromosome 2q34) and *D2S1345* (chromosome 2q34) were selected from the University of California–Santa Cruz (UCSC) Genome Bioinformatics database, and PCR was performed using Bioline Biotaq DNA Polymerase, Bioline PCR buffer, 60 nM $MgCl_2$, and 20 pM of each primer, with a final reaction volume of 20 μl. Fluorescent-tagged PCR products were analyzed using the ABI 3700 capillary sequencer. Haplotypes were constructed from the microsatellite data of affected individuals and unaffected siblings. Linkage analysis was performed using the Genehunter program (Kruglyak et al. 1996).

Sequence Analysis of ABCA12

Primer design and PCR conditions were the same as those described elsewhere (Lefevre et al. 2003), with the exception that a 15-μl reaction volume was used. The PCR products covering each of the 53 exons and respective intron boundaries were purified using ExoSAP-IT (Amersham Pharmacia Biotech) and were sequenced on either the forward or reverse strand, by use of ABI BigDye Terminator reagents (Applied Biosystems) and an ABI 3700 sequencer (sequencing reaction conditions: 5 μl of purified product, 1 μl of BigDye Terminator v.1.1, 3 μl of Better Buffer [Microzone], 1 μl water; annealing temperature of 60°C). Sequence analysis was performed using Phred, Phrap, and Consed, and variants were detected using reference sequences taken from the Ensembl Genome Browser (Ewing and Green 1998; Ewing et al. 1998; Gordon et al. 1998). Likely disease-associated mutations were screened in a total of 120 control chromosomes—either by direct sequencing or by RFLP analysis if the mutation altered a restriction site.

Results

Genetic Mapping

From the SNP-array analysis, only one region of the genome, 2q35, was found to have large blocks of homozygosity in common for five of the six affected individuals assessed by means of this methodology (fig. 2). This common interval was calculated to be a genetic distance of ~1.5 Mb. To support linkage of HI to 2q35, microsatellite markers that map to this region were identified using the UCSC Genome Browser. The microsatellite genotype data are consistent with a recessive mode of inheritance of HI and linkage of the disease gene to 2q35 in the largest consanguineous family with HI (fig. 3*A*). Linkage analysis was performed for this family, but the size of the family prohibited the calculation of a statistically significant LOD score (data not shown). This highlights the usefulness of the SNP array for homozygosity mapping in diseases not applicable to classic genetic linkage studies. Affected individuals from families in which the mode of inheritance is unknown were also genotyped with these microsatellite markers. Of the 12 affected individuals analyzed in the present study, 11 were homozygous for one or more of the markers analyzed in the 2q35 region (fig. 3*B*).

Candidate-Gene Analysis

Six genes were identifiable, from the UCSC Genome Browser, that map within the minimal region, including *BARD1,* which interacts with the breast-ovarian cancer–associated protein BRCA1; *ATIC,* in which mutations are the cause of a purine biosynthesis disorder (AICA-ribosuria [MIM 608688]); *Fibronectin 1,* which is involved in cell adhesion and migration; the *FLJ10116* gene, which encodes a protein of unknown biological function; and the *PECR* gene, which encodes a peroxisomal trans 2-enoyl CoA reductase. The gene *ABCA12,* which encodes the ABC transporter protein, also maps within the minimal homozygous region on chromosome 2q35. Missense mutations in this gene have recently been shown to underlie the less severe ichthyotic disorders LI and NBCIE (Lefevre et al. 2003). Since the transport of extracellular epidermal lipids is abnormal in HI (Dale et al. 1990) and a defect in epidermal lipid metabolism has been suggested in the pathogenesis of the disease (Buxman et al. 1979), *ABCA12* could be a plausible candidate gene on the basis of chromosome position and function. The 53 coding exons of the *ABCA12* gene were individually amplified by PCR and were sequenced for 12 patients. Mutations in *ABCA12* were detected in 11 of the 12 patients (fig. 4). This indicates that *ABCA12*

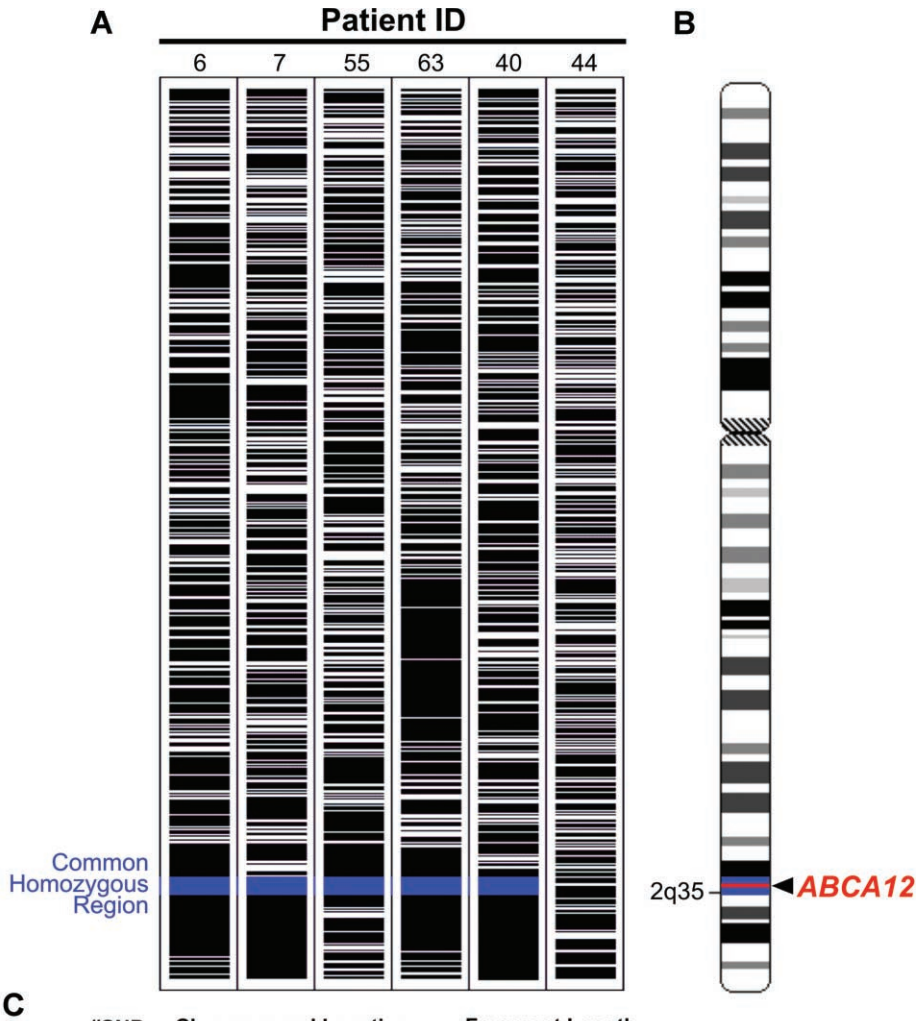

Figure 2 Localization of the HI gene to chromosome 2q35 by use of SNP-array mapping. *A*, Homozygous SNP profiles of chromosome 2 in six patients with HI. Black bars indicate homozygous SNP call data. Blue bars indicate the minimal common region of homozygous SNPs in patients 1–5, a genetic distance of ~1.5 Mb. *B*, Ideogram of chromosome 2 showing the position of *ABCA12* (*red bar*), located within the minimal common region of homozygous SNPs (*blue*) identified in panel A. *C*, The genetic interval of the homozygous SNP "blocks" in each patient with HI, with clear indication that the *ABCA12* gene maps within the common homozygous region for five of the six patients.

mutations are a major genetic cause of HI. The majority of the mutations were predicted to result in a truncated protein; indeed, in one patient (40), the last 25 exons were homozygously deleted. Four patients all harbored the same homozygous frameshift mutation and, on the basis of haplotype analysis (see fig. 3*B*) and their shared ethnicity, it is likely to be the same founder mutation in at least three of the four patients. In individual 955–01, a homozygous missense substitution (W198C) in exon 6 was identified in addition to the more disruptive homozygous nonsense substitution in exon 44. The latter sequence change is more likely to be associated with HI. Unlike the other individuals with HI in the mutation study who were homozygous for a specific *ABCA12* mutation, individual 44 was a compound heterozygote for two different *ABCA12* mutations. Both SNP and microsatellite genotypes were heterozygous in the chromosomal region harboring the *ABCA12* locus in this pa-

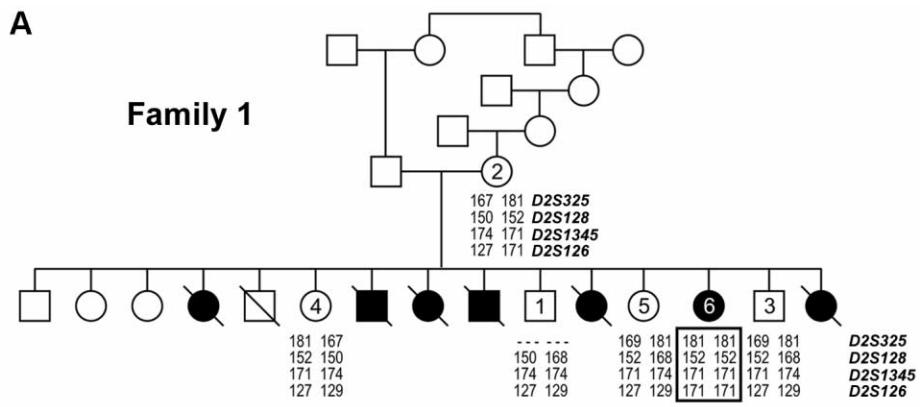

B

ABCA12
(chr 2q35)

Affected Patient ID	Marker (*chr location*)	*D2S325* (*chr 2q33.3*)		*D2S128* (*chr 2q34*)		*D2S1345* (*chr 2q34*)		*D2S126* (*chr 2q36.1*)	
	6	**181**	**181**	**152**	**152**	**171**	**171**	**171**	**171**
	69	---	---	**152**	**152**	**171**	**171**	---	---
	55	**159**	**159**	**152**	**152**	**171**	**171**	---	---
	63	---	---	150	152	171	168	**141**	**141**
	7	**169**	**169**	**160**	**160**	174	177	**141**	**141**
	40	169	173	148	150	---	---	**127**	**127**
	49	**161**	**161**	**160**	**160**	**174**	**174**	**139**	**139**
	50	---	---	154	158	**174**	**174**	---	---
	915-06	**177**	**177**	148	150	**168**	**168**	**126**	**126**
	955-01	**169**	**169**	**143**	**143**	**174**	**174**	**138**	**138**
	928-01	**169**	**169**	152	154	**177**	**177**	**138**	**138**
	44	183	179	156	158	174	177	139	141

Figure 3 Analysis of microsatellite markers flanking the *ABCA12* gene. *A,* Segregation of microsatellite markers flanking *ABCA12* at chromosome 2q35 in a family with HI. Only affected individual 6 is homozygous at this region of chromosome 2. Note that the majority of siblings with HI are deceased. *B,* Haplotype analysis of individuals with HI. Microsatellite markers map around the *ABCA12* gene locus (215, 621, 772–215, 828, 657) at chromosome 2q35. Several patients are homozygous for the markers *D2S325* (208, 096, 142–208, 096, 490), *D2S128* (214, 917, 811–214, 918, 065), *D2S1345* (214, 991, 103–214, 991, 425), and *D2S126* (221, 842, 419–221, 842, 782). The genome positions (Mb) for *ABCA12* and microsatellite markers on chromosome 2 are shown in parentheses.

tient. In only one patient (50) with HI was there no *ABCA12* mutation detected. None of the mutations were detected in the control population.

Discussion

The ABC superfamily is a large family of transmembrane proteins involved in transport of substrates across both the plasma membrane and intracellular membranes. Mutations in ABC genes cause diverse diseases, including cystic fibrosis, X-linked adrenoleukodystrophy, Tangier disease, pseudoxanthoma elasticum, and Dubin-Johnson syndrome (Stefkova et al. 2004). In the present article, we report, we believe for the first time, that mutations in the *ABCA12* gene, a member of the ABCA subfamily, cause HI. Genetic studies of this disorder have been hampered by the fact that families with more than one affected child are rare. Families with only one affected individual are unsuitable for genetic linkage studies because of (1) the difficulties in determining whether the

A

Patient	Mutation type	Resultant change	Exon	Mutation
49	Exon deletion	Truncated protein	23	Homozygous exon deletion
6	Frameshift	Truncated protein	49	7541delC/7541delC TACAGAACAAATGTTC[C]GTCATCCTCACATCTC
7	Frameshift	Truncated protein	42	6378delGC/6378delGC TCAATTGGTATCATT[GC]GATTTTCAAATTACC
55	Frameshift	Truncated protein	49	7541delC/7541delC TACAGAACAAATGTTC[C]GTCATCCTCACATCTC
40	Exon deletion	Truncated protein	28-53	Homozygous deletion from exon 28 to 53
44	Frameshift/amino acid change	Truncated protein/Reduced protein function	33/47	5229delA AAAGAGTCACAAAAAA[A]TAGTGCTATGAGTC D2363N ATTCCAGAAAAG[G]ATATTAAAGAAACTGTTC
63	Frameshift	Truncated protein	49	7541delC/7541delC TACAGAACAAATGTTC[C]GTCATCCTCACATCTC
50	None found			
955-01	Nonsense substitution	Truncated protein	44	R2203* CATGTTTTTTTCCTTG[C/T]GACTCTTAATCAACGA
915-06	Base change at splice junction	Unknown, possible splice variants	42	TGTATCTCTCCTACTTCTCCTGTTTGG[g/t]taagctgc (lower case are intronic)
928-01	Nonsense substitution	Truncated protein	34	W1742* CCACACCCGCAGGAACT[G/A]GAAAGGTCTCATT
69	Frameshift	Truncated protein	49	7541delC/7541delC TACAGAACAAATGTTC[C]GTCATCCTCACATCTC

B

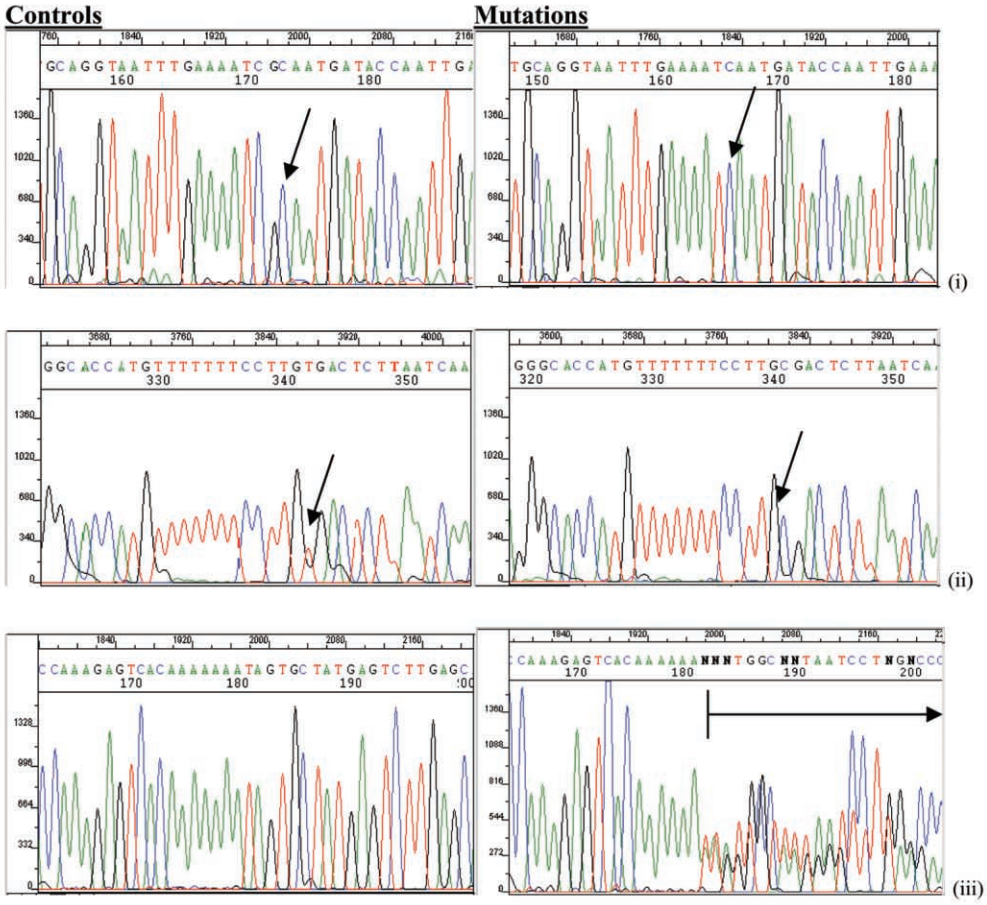

Figure 4 Mutation analysis of the *ABCA12* gene in patients with HI. *A*, Table summarizing mutation analysis. An asterisk (*) indicates a sequence change to a stop codon. *B, i,* Chromatogram showing homozygous GC deletion in exon 42 of patient 7. *ii*, Chromatogram showing homozygous T→C substitution in exon 44 in patient 955-01. *iii*, Chromatogram showing heterozygous A deletion in exon 33 of patient 44.

disease has been inherited in an AR mode or is due to a new dominant mutation and (2) the low statistical power for linkage analysis. An additional complicating factor is the possibility of genetic heterogeneity.

The results of the Affymetrix 10K SNP-array genome scan of five unrelated patients with HI showed suggestive linkage to a region on chromosome 2q35 on the basis of having a large homozygous SNP haplotype "block" in common, a genetic distance of ~1.5 Mb. Microsatellite markers from this region were identified from the UCSC Genome Browser, and subsequent genotypes were consistent with a locus for HI on 2q35 on the basis of homozygosity at that locus in 11 of the 12 patients with HI described in this study. The *ABCA12* gene encoding an ABC transporter protein that is postulated to be involved in the transport of epidermal lipids is localized within the chromosomal region encompassed by these microsatellite markers. This was regarded as an excellent candidate gene to underlie the HI phenotype, since abnormal or absent epidermal lipids in HI skin have been described. Mutation analysis revealed that 11 of the 12 analyzed patients with HI had a disease-associated mutation in the *ABCA12* gene. The majority of the mutations were predicted to lead to a severely truncated protein, with the exception of a missense substitution and a splice-site mutation. In contrast, the *ABCA12* mutations in LI/NCBIE were all missense and were restricted to within the ATP-binding domain of the protein. Thus, the mutations in HI are likely to disrupt other aspects of *ABCA12* function and may provide the molecular reason behind the severity of HI compared with the milder skin conditions LI and NCBIE. Further mutation studies are in progress to identify the molecular spectra of mutations in a larger panel of patients with HI, including those subcategorized into the different types of HI (Dale et al. 1990). The data in the present article reveal that *ABCA12* mutations are the major cause of HI.

In normal epidermis, the cytoplasm of cells of the upper spinous and granular cell layers contain small granules, 100–300 nm in size, known as "Odland bodies" (Odland 1960); lamellar granules; lamellar bodies; or membrane-coating granules. These move toward the cell membrane as they enter the granular cell layer. They discharge their lipid components and proteases into the intercellular space and play important roles in barrier function, desquamation, and intercellular cohesion within the stratum corneum (Menon et al. 1992; Elias et al. 2000). Lipid delivery to lamellar bodies has also been shown to be required for subsequent delivery of protein to the organelle (Rassner et al. 1999). The defect in *ABCA12* in HI may explain the observed abnormalities in the lamellar granules, possibly associated with severely compromised skin-barrier function. This is analogous to the situation in lung in which surfactant is stored in lamellar bodies in alveolar type II cells. Mutations in *ABCA3* cause fatal surfactant deficiency in newborns, with markedly abnormal lamellar bodies observed ultrastructurally (Shulenin et al. 2004). The lamellar bodies in epidermis also contain beta-defensin, a microbicidal peptide that is also found in the intercellular space, which suggests that it might be discharged with lipid components of the lamellar body (Oren et al. 2003). The defect in epidermal barrier and the loss of beta-defensin may also result in increased susceptibility to infection. Additionally, mutations in two other genes of the ABCA family cause disorders of lipid transport. The *ABCA1* gene is mutated in Tangier disease and in the less severe, heterozygous, familial hypoalphalipoproteinemia as well as in premature atherosclerosis, the resultant disorder dependent on the site of the mutation (Brooks-Wilson et al. 1999; Rust et al. 1999; Clee et al. 2000). The *ABCA4* gene is mutated in patients with Stargardt disease, in some patients with AR retinitis pigmentosa, and in patients with AR cone-rod dystrophy (Stefkova et al. 2004). Our observation that mutations in the *ABCA12* gene cause HI is analogous to other systemic disorders of lipid transport. In addition, like *ABCA1* and *ABCA4*, the site and type of mutation in the *ABCA12* gene determine the severity of the condition, with the more disruptive genetic lesions, such as deletion or frameshift mutations, causing HI.

Prenatal screening tests for HI historically involved invasive procedures, such as fetoscopically and ultrasonographically guided fetal-skin biopsies that reveal key ultrastructural features, such as multivesicular lamellar granules in affected fetuses at 20–24 wk of gestation (Elias et al. 1980; Suzumori and Kanzaki 1991). Similar morphological changes have been described in amniotic fluid cells at 17 wk of gestation (Akiyama et al. 1994). Other methods that have been used in recent years for the prenatal diagnosis of HI are three-dimensional and four-dimensional real-time sonography (Vohra et al. 2003). A major translational benefit of our present findings is that DNA-based analysis should now be possible, which paves the way for earlier (i.e., first trimester) prenatal testing that is more reliable and conclusive than the other non-DNA–based prenatal screening techniques.

In summary, we have applied the rapid SNP-array genotyping technology to identify, by homozygosity mapping, *ABCA12* mutations as the major underlying genetic cause of the devastating skin disease HI. Previously, this disease had proved difficult to map by classic linkage analysis because of the limited size of pedigrees. The association of *ABCA12* mutations with HI will facilitate prenatal DNA diagnosis of this life-threatening disorder as well as the possibility of preimplantation genetic testing. In addition, results of the present study suggest a major role for ABCA12 in lipid transport, barrier formation, and keratinocyte differentia-

tion. The increased understanding of the biological role of ABCA12 in HI may lead to the development of targeted therapy to lessen the burden of this disease for both surviving children with HI and their parents.

Acknowledgments

The authors acknowledge the patients and their families who have contributed to the study. In addition, we acknowledge the contributions of Drs. Nick Lench and Sarah Hatsell during the early stages of our genetic studies of HI; Tracy Chaplin, who runs the SNP Array facility at Queen Mary; and Drs. Sandra Charles-Holmes (Coventry), Vinnie Biggs (Holyoke, MA), Michael Heffernan (St. Louis), and Richard Mupanemunda (Birmingham), for assistance with the clinical aspects of this study. We also acknowledge the major contribution of Dr. Karen Holbrook (Columbus, OH) to our understanding of the pathogenesis of HI. Funding was from the Wellcome Trust (to R.A.J.E.), a Wellcome Trust Prize Studentship (to E.E.N.), United States Public Health Service grant 2P01 AR 21557 (to P.F.), the Odland Endowed Research Fund (to P.F.), and the Barts and The London Charitable Foundation (to B.D.Y.).

Electronic-Database Information

The accession number and URLs for data presented herein are as follows:

Ensembl Genome Browser, http://www.ensembl.org/
GenBank, http://www.ncbi.nlm.nih.gov/Genbank/ (for ABC [accession number NM_173076])
Online Mendelian Inheritance in Man (OMIM), http://www.ncbi.nlm.nih.gov/Omim/ (for HI, *TGM1, ALOXE3, ALOX12B,* ABCA12, and AICA-ribosuria)
UCSC Genome Bioinformatics, http://www.genome.ucsc.edu/ (for the Human Genome working draft of chromosome 2)

References

Akiyama M, Dale BA, Smith LT, Shimizu H, Holbrook KA (1998) Regional difference in expression of characteristic abnormality of harlequin ichthyosis in affected fetuses. Prenat Diagn 18:425–436

Akiyama M, Kim DK, Main DM, Otto CE, Holbrook KA (1994) Characteristic morphologic abnormality of harlequin ichthyosis detected in amniotic fluid cells. J Invest Dermatol 102:210–213

Akiyama M, Shimizu H, Yoneda K, Nishikawa T (1997) Collodion baby: ultrastructure and distribution of cornified cell envelope proteins and keratins. Dermatology 195:164–168

Akiyama M, Yoneda K, Kim SY, Koyama H, Shimizu H (1996) Cornified cell envelope proteins and keratins are normally distributed in harlequin ichthyosis. J Cutan Pathol 23:571–575

Brooks-Wilson A, Marcil M, Clee SM, Zhang LH, Roomp K, van Dam M, Yu L, et al (1999) Mutations in ABC1 in Tangier disease and familial high-density lipoprotein deficiency. Nat Genet 22:336–345

Buxman MM, Goodkin PE, Fahreenback WH (1979) Harlequin icthyosis with epidermal lipid abnormality. Arch Dermatol 115:189–193

Choate KA, Williams ML, Elias PM, Khavari PA (1998) Transglutaminase 1 expression in a patient with features of harlequin ichthyosis: case report. J Am Acad Dermatol 38:325–329

Clee SM, Kastelein JJ, van Dam M, Marcil M, Roomp K, Zwarts KY, Collins JA, Roelants R, Tamasawa N, Stulc T, Suda T, Ceska R, Boucher B, Rondeau C, DeSouich C, Brooks-Wilson A, Molhuizen HO, Frohlich J, Genest J Jr, Hayden MR (2000) Age and residual cholesterol efflux affect HDL cholesterol levels and coronary artery disease in ABCA1 heterozygotes. J Clin Invest 106:1263–1270

Dahlstrom JE, McDonald T, Maxwell L, Jain S (1995) Harlequin ichthyosis—a case report. Pathology 27:289–292

Dale BA, Holbrook KA, Fleckman P, Kimball JR, Brumbaugh S, Sybert VP (1990) Heterogeneity in harlequin icthyosis, an inborn error of epidermal keratinisation: variable morphology and structural protein expression and a defect in lamellar granules. J Invest Dermatol 94:6–18

Elias PM, Fartasch M, Crumrine D, Behne M, Uchida Y, Holleran WM (2000) Origin of the corneocyte lipid envelope (CLE): observations in harlequin ichthyosis and cultured human keratinocytes. J Invest Dermatol 115:765–769

Elias S, Mazur M, Sabbagha R, Esterly NB, Simpson JL (1980) Prenatal diagnosis of harlequin ichthyosis. Clin Genet 17: 275–280

Ewing B, Green P (1998) Base-calling of automated sequencer traces using Phred. II. Error probabilities. Genome Res 8: 186–194

Ewing B, Hillier L, Wendl MC, Green P (1998) Base-calling of automated sequencer traces using Phred. I. Accuracy assessment. Genome Res 8:175–185

Gordon D, Abajian C, Green P (1998) Consed: a graphical tool for sequence finishing. Genome Res 8:195–202

Haftek M, Cambazard F, Dhouailly D, Reano A, Simon M, Lachaux A, Serre G, Claudy A, Schmitt D (1996) A longitudinal study of a harlequin infant presenting clinically as non-bullous congenital ichthyosiform erythroderma. Br J Dermatol 135:448–453

Hsu WY, Chen JY, Lin WL, Tsay CH (1989) [Harlequin fetus: a case report.] Zhonghua Yi Xue Za Zhi (Taipei) 43:63–66

Huber M, Rettler I, Bernasconi K, Frenk E, Lavrijsen SP, Ponec M, Bon A, Lautenschlager S, Schorderet DF, Hohl D (1995) Mutations of keratinocyte transglutaminase in lamellar ichthyosis. Science 267:525–528

Jobard F, Lefevre C, Karaduman A, Blanchet-Bardon C, Emre S, Weissenbach J, Ozguc M, Lathrop M, Prud'homme JF, Fischer J (2002) Lipoxygenase-3 (ALOXE3) and 12(R)-lipoxygenase (ALOX12B) are mutated in non-bullous congenital ichthyosiform erythroderma (NCIE) linked to chromosome 17p13.1. Hum Mol Genet 11:107–113

Kam E, Nirunsuksiri W, Hager B, Fleckman P, Dale BA (1997) Protein phosphatase activity in human keratinocytes cultured from normal epidermis and epidermis from patients with harlequin ichthyosis. Br J Dermatol 137:874–882

Kruglyak L, Daly MJ, Reeve-Daly MP, Lander ES (1996) Parametric and nonparametric linkage analysis: a unified multipoint approach. Am J Hum Genet 58:1347–1363

Lefevre C, Audebert S, Jobard F, Bouadjar B, Lakhdar H, Boughdene-Stambouli O, Blanchet-Bardon C, Heilig R, Foglio M, Weissenbach J, Lathrop M, Prud'homme JF, Fischer J (2003) Mutations in the transporter ABCA12 are associated with lamellar ichthyosis type 2. Hum Mol Genet 12: 2369–2378

Lefevre C, Bouadjar B, Karaduman A, Jobard F, Saker S, Ozguc M, Lathrop M, Prud'homme JF, Fischer J (2004) Mutations in ichthyin a new gene on chromosome 5q33 in a new form of autosomal recessive congenital ichthyosis. Hum Mol Genet 13:2473–2482

Menon GK, Ghadially R, Williams ML, Elias PM (1992) Lamellar bodies as delivery systems of hydrolytic enzymes: implications for normal and abnormal desquamation. Br J Dermatol 126:337–345

Michel M, Fleckman P, Smith LT, Dale BA (1999) The calcium-activated neutral protease calpain I is present in normal foetal skin and is decreased in neonatal harlequin ichthyosis. Br J Dermatol 141:1017–1026

Moreau S, Salame E, Goullet de Rugy M, Delmas P (1999) Harlequin fetus: a case report. Surg Radiol Anat 21:215–216

Moskowitz DG, Fowler AJ, Heyman MB, Cohen SP, Crumrine D, Elias PM, Williams ML (2004) Pathophysiologic basis for growth failure in children with ichthyosis: an evaluation of cutaneous ultrastructure, epidermal permeability barrier function, and energy expenditure. J Pediatr 145:82–92

Odland GF (1960) A submicroscopic granular component in human epidermis. J Invest Dermatol 34:11–15

Oren A, Ganz T, Liu L, Meerloo T (2003) In human epidermis, β-defensin 2 is packaged in lamellar bodies. Exp Mol Pathol 74:180–182

Rassner U, Feingold KR, Crumrine DA, Elias PM (1999) Coordinate assembly of lipids and enzyme proteins into epidermal lamellar bodies. Tissue Cell 31:489–498

Rust S, Rosier M, Funke H, Real J, Amoura Z, Piette JC, Deleuze JF, Brewer HB, Duverger N, Denefle P, Assmann G (1999) Tangier disease is caused by mutations in the gene encoding ATP-binding cassette transporter 1. Nat Genet 22: 352–355

Sarkar R, Sharma RC, Sethi S, Basu S, Das R, Mendiratta V, Sardana K, Kakar N (2000) Three unusual siblings with harlequin icthyosis in an Indian family. J Dermatol 27:609–611

Shulenin S, Nogee LM, Annilo T, Wert SE, Whitsett JA, Dean M (2004) ABCA3 gene mutations in newborns with fatal surfactant deficiency. N Engl J Med 350:1296–1303

Stefkova J, Poledne R, Hubacek JA (2004) ATP-binding cassette (ABC) transporters in human metabolism and diseases. Physiol Res 53:235–243

Suzumori K, Kanzaki T (1991) Prenatal diagnosis of harlequin ichthyosis by fetal skin biopsy: report of two cases. Prenat Diagn 11:451–457

Vohra N, Rochelson B, Smith-Levitin M (2003) Three-dimensional sonographic findings in congenital (harlequin) ichthyosis. J Ultrasound Med 22:737–739

Mosaicism in cutaneous pigmentation

Vivian A. Lombillo[a] and Virginia P. Sybert[b,c]

Purpose of review

This article reviews the disorders of patterned dyspigmentation and discusses the pathogenesis of the pigmentary changes.

Recent findings

A range of cytogenetic abnormalities has been detected in patterned pigmentary disease. This molecular heterogeneity correlates with the wide spectrum of clinical phenotypes observed. Many of the molecular defects overlap with genes known to play a role in pigmentation. Our understanding of the underlying genetic mechanisms for these mosaic conditions is evolving with advances in technology and dissection of the molecular pathways involved in melanocyte biology.

Summary

The causal heterogeneity of patterned dyspigmentation promises to reveal clues about the differentiation, function, and control of melanocytes in embryonic and postnatal development.

Keywords

hypomelanosis of Ito, lines of Blaschko, mosaicism, pigment disorders

Curr Opin Pediatr 17:494–500. © 2005 Lippincott Williams & Wilkins.

Divisions of [a]Dermatology and [b]Medical Genetics, Department of Medicine, University of Washington, and [c]Department of Dermatology, Group Health Permanente, Seattle, Washington, USA

Supported in part by a grant from the Department of Defense- DAMD 17-03-1-0203 (VPS)

Correspondence to Vivian A. Lombillo, MD, PhD, Division of Dermatology, Department of Medicine, Box 356524, University of Washington, Seattle, WA 98195-6524, USA
Tel: 206 543 5290; fax: 206 543 2489; e-mail: lombillo@u.washington.edu

Current Opinion in Pediatrics 2005, 17:494–500

Abbreviations

HI	hypomelanosis of Ito
IP	incontinentia pigmenti
LWNH	linear and whorled nevoid hypermelanosis
NFκB	nuclear factor kappa B

1040-8703

Introduction

Pigmentary mosaicism is a term that has been used to describe variegated patterns of pigmentation in the skin caused by genetic heterogeneity in the cells that make up the skin [1••]. It is a term we prefer not to use because it implies that the cause is two or more genetically or chromosomally abnormal cell populations within a single individual. This has not yet been proved to be the cause of all conditions in which one sees variegation of pigment; therefore, we prefer to use the more inclusive term 'patterned dyspigmentation,' reserving the use of 'mosaicism' to indicate genetic or chromosomal mosaicism. The molecular mechanisms that underlie these patterns are largely not understood, and there are likely to be many. In this review, we outline what is currently understood about the molecular and biochemical pathogenesis of patterned dyspigmentation.

Genetics of pigmentation

Although many components besides melanin contribute to skin color (e.g., bilirubin, hemoglobin), in this review the term 'pigment' will be used to refer to those changes caused by melanin. Abnormal pigmentation can result from perturbations in any gene that participates in melanocyte development or function. Melanocyte biology is complex; numerous (>100) loci are associated with pigmentary defects in mice. Nearly as many genes have been described in humans; however, the list of human pigmentary genes is by no means complete. Several excellent reviews of the genetics of pigmentation have recently been published [2,3,4•]. Genes associated with pigmentation are broadly classified according to their role in melanocyte biology: (1) genes involved in the embryologic development of melanocytes (e.g., KIT in piebaldism and PAX3 in Waardenburg's syndrome), (2) genes contributing to melanosome formation in the melanocytes (e.g., the HPS genes in Hermansky–Pudlak syndrome and CHS1 in Chediak–Higashi syndrome), (3) genes responsible for melanin synthesis in the melanosome (e.g., TYR in oculocutaneous albinism 1), and (4) genes preserving melanosome transfer to neighboring keratinocytes (e.g., RAB27A and MYO5A in Griscelli's syndrome). Defects anywhere within this pathway may result in dyspigmentation. A partial list of genes known to be involved in disorders of pigmentation is shown in Table 1. A more comprehensive catalogue of the pigmentary genes has recently been compiled [1••].

Mechanisms of mosaicism

A mosaic in the conventional sense is a composite of different materials. A mosaic organism is composed of

Table 1. Partial list of human skin disorders associated with dyspigmentation

Disorder	Gene	Inheritance
Piebaldism	KIT	AD
Waardenburg syndrome (WS)		
WS1	PAX3	AD
WS2	MITF, SLUG	AD
WS3	PAX3	AD, AR
WS4	EDN3, EDNRB, SOX10	AD, AR
Oculocutaneous albinism		
OCA1	TYR	AR
OCA2	P	AR
OCA3	TYRP1	AR
OCA4	MATP	AR
Hermansky–Pudlak Syndrome (HPS)		
HPS1	HPS1	AR
HPS2	AP3B1	AR
HPS3	HPS3	AR
HPS4	HPS4	AR
HPS5	HPS5	AR
HPS6	HPS6	AR
HP7	DTNBP1	AR
Chediak–Higashi syndrome (CHS)	CHS1	AR
Griscelli syndrome (GS)		
GS1	RAB27A	AR
GS2	MYO5A	AR
GS3	MLPH	AR
Incontinentia pigmenti	NEMO/IKBKG	XLD
Tuberous sclerosis	TSC1, TSC2	AD

AD, autosomal dominant; AR, autosomal recessive; XLD, X-linked dominant.

two or more genetically or chromosomally distinct populations of cells. A somatic or postzygotic mutation is a de-novo genetic change that occurs after fertilization, during embryogenesis, during fetal development, or during postnatal life. The stage of development in which the mutation or change occurs will determine which tissues and what proportion of cells within the tissue will contain the change. Only the tissue derived from the precursor cell in which the alteration has occurred is affected (Fig. 1a). Somatic mosaicism implies that two or more genetically or chromosomally distinct cell populations are present in the organism (Fig. 1b) and may or may not involve the gonad. If the gonad is not involved, there is no risk to offspring. Gonadal mosaicism implies that the tissue giving rise to the gametes is also mosaic and therefore carries with it the risk that gametes will contain genetic information from one or the other of the distinct populations and the risk that the mutation or chromosomal abnormality will be transmitted to offspring. Mosaicism always underlies the phenotypic variation of certain diseases, such McCune–Albright syndrome (which is lethal in the fully heterozygous state) and explains the phenomenon of segmental disease (localized involvement) in conditions such as neurofibromatosis type 1, Darier's disease, and Hailey–Hailey disease [5,6,7•]. Mosaicism has also been implicated to contribute to malignant transformation in cancer

Figure 1. The making of a mosaic organism

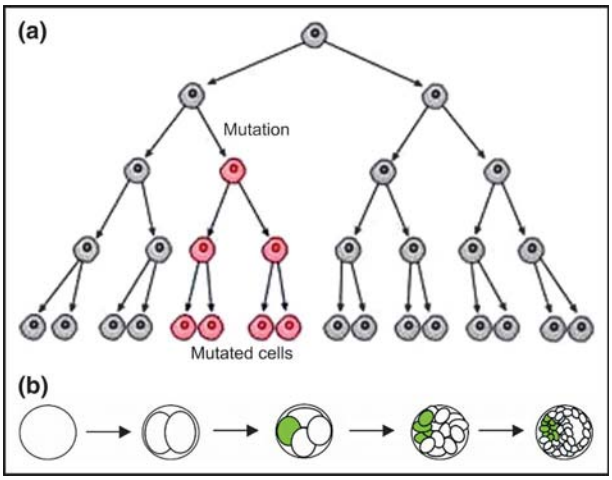

(a) Demonstration of how a de-novo mutation generates a mutant population of cells after subsequent mitotic divisions. (b) An early mutation (green) at the four-cell stage generates a mosaic organism. Reproduced with permission by Dr. Carol Guze, PhD.

[8]. The phenomenon of mosaicism may occur by way of several mechanisms.

Chromosome aneuploidy or polyploidy

Failure of chromosomes to separate properly during cell division can result in daughter cells with different or aberrant chromosome numbers or structures. Chromosomal mosaicism is common in Turner's syndrome; almost half of affected individuals have two or more chromosomally distinct cell populations. These may both be abnormal, as in 45,X/46,X,i(Xq), or one may be normal and the other not, as in 45,X/46,XX mosaicism. Some chromosomal aberrations are lethal when they are present in all tissues and are seen in live-born infants only in the mosaic state (e.g., tetrasomy $12p^{+}$ or Pallister–Killian syndrome).

Lyonization

In humans, to compensate for the presence of two X chromosomes (paternal and maternal) in females, one X chromosome in every cell of a developing female embryo is randomly but stably inactivated in the late blastocyst stage by way of alterations in chromatin structure and methylation states [9]. All females are therefore functionally mosaic with respect to most genes on their X chromosome. This process, also called lyonization, contributes to 'rescue' of otherwise lethal phenotypes in dominant X-linked conditions such as incontinentia pigmenti (IP) [10]. It is also responsible for the mosaic pattern of expression in carrier females of X-linked recessive conditions, such as hypohidrotic ectodermal dysplasia (Christ–Seimens–Touraine syndrome).

Epigenetic mosaicism

There may be environmental mechanisms that can alter the genetic information within a cell that then gives rise to genetically distinct cell populations. One example is that of retrotransposons, DNA sequences of viral origin that are incorporated in to the nuclear DNA and replicated. These may silence or activate gene expression [11]. These elements have been studied in relation to variegation of coat color in mice and dogs and have been shown to be heritable in mice [12–13]. Nothing is currently known about their role in human disorders of pigmentation.

Changes in chromatin structure due to chemical modification of histones (e.g., acetylation states) by encoded proteins also influence the phenotype of cells by altering gene expression [14•]. Our understanding of the effects of chromatin structure on phenotypic variation in human disease is in its infancy, but this will be an important mechanism to consider. Lyonization and imprinting are specialized forms of epigenetic regulation of gene expression that are inherent and not environmental.

Chimeric mosaicism

Although it is rare, some individuals with segmental or patterned dyspigmentation have been shown to be hematologically chimeric, composed of two genetically distinct cell populations [15]. This presumably results from an early fusion event of two zygotes or intra-uterine transfusion of cells between dizygotic twins. Chimeras may be 46,XX/46,XX or 46,XY/46,XY or 46,XX/46,XY. In the last, genital ambiguity and hermaphroditism is seen. The former situations presumably give rise to otherwise normal individuals. The distribution of pigment in these individuals is often in a geometric block pattern and not along the lines of Blaschko.

Revertant mosaicism

A revertant mutation is a mutation that occurs focally and restores local function to a previously defective (inherited) gene. Although rare, this has been described in types of epidermolysis bullosa and tyrosinemia type I [16,17]. Whether this phenomenon occurs in single-gene disorders of pigmentation in which patchy repigmentation may occur (e.g., piebaldism) is not known.

Patterns of dyspigmentation: lines of Blaschko and its variations

Dermatoses resulting from mosaicism may show a classic distribution on the skin along the lines of Blaschko [18–20]. On the basis of the distribution of different nevoid and non-nevoid skin disorders, Blaschko [21] described a unique pattern of sharply demarcated lines and swirls, which is distinct from any other linear pattern on the skin, such as dermatomes or Langer's lines (lines of cleavage). On the back there is a V-shaped or 'fountain spray' configuration, and on the abdomen the pattern is more S-shaped (Fig. 2). On the vertex of the scalp the lines are spiral. The extent and pattern of distribution in the skin is presumed to be dependent on the stage of development during which the event causing mosaicism took place. Very early events result in widespread variegation. Late events may cause changes to appear in only one sector, or even a small area within a sector. The patterns are seen in epidermal and sebaceous nevi, in the expression of X-linked conditions in carrier females, and in patterned dyspigmentation due to chromosomal mosaicism.

The lines of Blaschko are believed to map the route of embryonic ectodermal cell migration (Fig. 3) [19,22]. Both melanocytes and keratinocytes are derived from ectoderm. Whereas cytogenetic confirmation of tissue or cellular mosaicism for chromosomal abnormalities has been demonstrated in many patients with patterned dyspigmentation, failure to find it in all instances may be due to the fact that the mosaicism is not present in the cells that are usually studied, lymphocytes and fibroblasts, which are not of ectodermal origin. Somatic mutations have been demonstrated from keratinocytes isolated from

Figure 2. Lines of Blaschko

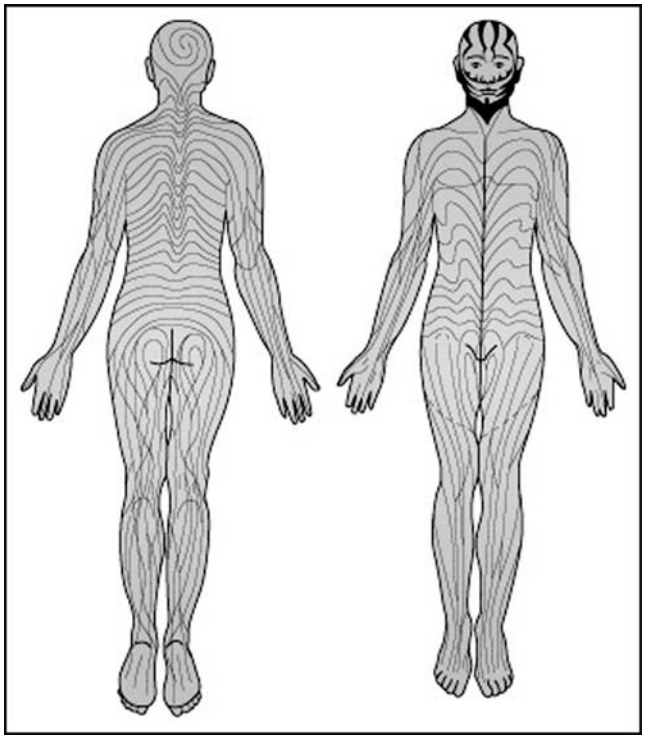

The developmental lines of Blaschko are distinct from any other linear pattern observed on the skin, such as dermatomes. Reproduced with permission from [20].

Figure 3. Ectodermal migration and theory for the development of lines of Blaschko

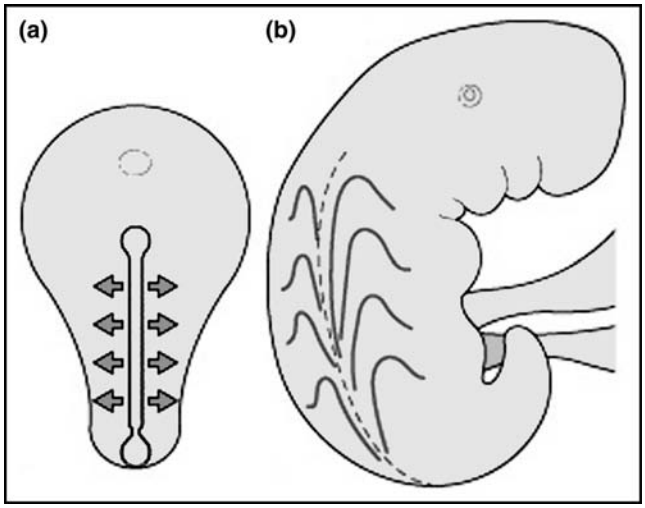

(a) Ectoderm-derived cells of the neural crest, including melanoblasts, migrate transversely along distinct dorsal-ventral pathways in the developing vertebrate embryo. (b) Happle has hypothesized that longitudinal growth and flexion of the embryo contributes to the fountain-like pattern known as Blaschko's lines. Reproduced with permission from [20].

epidermis in several cases of patterned skin disease [6,23,24].

Happle [25] describes several variations of the classic Blaschko pattern. A block-like or 'checkerboard' distribution has been described in speckled lentiginous nevus and Becker's nevi. The en-bloc or checkerboard pattern of pigment variegation is also typical of chimeras. A phylloid or 'leaflike' variant has been described for patients with mosaic hypopigmentation due to polyploidy or translocations involving chromosomes 13 or 5 [26–29].

Clinical presentation of patterned dyspigmentation

The most common manifestations of patterned dyspigmentation are discussed in the next section.

Hypomelanosis of Ito

Hypomelanosis of Ito (HI), also called incontinentia pigmenti achromians, is a term used to describe distinct hypopigmentation in whorls and streaks that lie in the lines of Blaschko (Fig. 4a–c). Whereas the original description by Ito [30] was of a patient with patterned depigmentation, subsequent reports described individuals with hypopigmentation in the same pattern. The term 'HI' has also been applied to individuals with hyperpigmentation along the same lines. In some cases, it is not clear whether the normal skin is the darker or the lighter (e.g., Fig. 4a and c). The hypomelanosis may be present at birth, or it may become more apparent during early childhood. HI affects both sexes equally and is considered sporadic. The distribution may be bilateral or unilateral and can involve any part of the body or face. The pigment variegation is most dramatic in individuals with darker skin and appears as a negative image of the hyperpigmented stage of IP. The textural skin changes of IP are not seen in HI. Chromosomal mosaicism has been reported in blood or skin fibroblasts of more than half of patients with fully evaluated HI [31]. Abnormalities have included chimerism; mosaicism for 2, $4p^+$, 7, 8, 9,10,13, 14, 15, and 17; ring X; tetrasomy $12p^+$ (Pallister–Killian syndrome); X-autosome translocations; and diploid/triploid mosaicism. The specific chromosomes involved seem to be less important than the state of mosaicism for the abnormality. Mosaics for presumably balanced translocations in otherwise normal individuals can also give rise to the pigment pattern of HI. Systemic manifestations are seen in 30 to 90% of patients (depending on the study cited) and may involve the neurologic, ocular, cardiac, and musculoskeletal systems [32–34]. This heterogeneity is not surprising because it reflects the very different effects of different cytogenetic deletions or duplications.

Children with pigmentary changes along the lines of Blaschko should be examined for structural malformations and for developmental problems. In the absence of any phenotypic abnormalities, the karyotype is likely to be normal. In the presence of other major or minor malformations or developmental abnormalities, both lymphocyte and fibroblast karyotyping should be considered.

Nevus depigmentosus

Nevus depigmentosus (or achromic nevus) is a well-defined area of hypopigmentation or depigmentation, which is typically present at birth, although it may not be evident until the first years of life [35]. A single irregular ovoid patch (like a splash of paint) is commonly seen on the trunk and proximal extremities (Fig. 4d). Multiple patches and segmental forms along dermatomes or Blaschko developmental lines have also been described. Nevus depigmentosus is usually sporadic, with no gender predominance. By skin examination alone it may be difficult to differentiate the ash-leaf macule of tuberous sclerosis complex from a nevus depigmentosus. Nevus anemicus may also have a similar appearance. One can differentiate the two by rubbing the skin; a nevus depigmentosus will become more erythematous; however, a nevus anemicus will remain hypopigmented as the surrounding skin reddens. The underlying cause of nevus depigmentosus has not been identified. A case series of 67 patients with nevus depigmentosus found no associated abnormalities, and this is generally considered to be an isolated cutaneous finding [35]. A small handful of case reports, however, have described neurologic defects in children with nevus depigmentosus [33]. Two patients in a series

Figure 4. Presentations of patterned dyspigmentation

(a–c) Hypomelanosis of Ito. (d) Nervus depigmentosus. (e) Linear and whorled nevoid hypermelanosis. (f) Hyperpigmented stage of incontinentia pigmenti. Reprinted with permission from [34] (a–c,e,f) and www.dermatlas.org (Mary Tonsager) (d).

of 20 patients with a segmental type of nevus depigmentosus had mental retardation and seizures [36].

If systemic manifestations are not present, no further management is necessary for nevus depigmentosus. There is no effective therapy for repigmentation.

Linear and whorled nevoid hypermelanosis

Linear and whorled nevoid hypermelanosis (LWNH) is a usually sporadic disorder of hyperpigmentation in swirls and streaks along the lines of Blaschko (Fig. 4e) [34]. This is also considered to be an isolated cutaneous condition. Both sexes are equally affected. The hyperpigmentation is seen in the first weeks of life and is not preceded by inflammatory stages, unlike IP. The pigmentation may expand for 1 or 2 years, but it stabilizes thereafter and may become less prominent in time. There have been reports of LWNH in association with central nervous sytem abnormalities and chromosomal mosaicism [33,37,38]. We prefer, however, to categorize these as HI, rather than

LWNH, and reserve the term LWNH for individuals who are otherwise normal.

Incontinentia pigmenti

Incontinentia pigmenti is an X-linked dominant disorder, lethal in males, in which lethality in females is rescued by lyonization. Survival in males has been attributed to the presence of an extra X chromosome (Klinefelter's syndrome) or mosaicism for the gene because of post-zygotic mutations [39]. Infants with IP initially have blisters in lines and swirls along the lines of Blaschko that become erythematous and verrucous. Hyperpigmentation along the lines of Blaschko ensues (Fig. 4f). The fourth stage of IP occurs later and consists of hypopigmentation and loss of sweat glands and hair follicles in a similar Blaschko pattern. The early stages may occur *in utero*, and not all stages may be present. The blistering may recrudesce with illness in later childhood. Mutations in NFκB essential modulator (NEMO/IKBKG located on Xq28), a subunit of a kinase that activates NFκB, cause IP [40]. Failure to activate NFκB renders the affected tissue susceptible to apoptosis. In addition to the skin changes, ectodermal defects (e.g., pegged teeth, alopecia, and nail dystrophy), neurologic, and skeletal and ocular involvement may also be present.

McCune-Albright syndrome

McCune-Albright syndrome (polyostotic fibrous dysplasia) is a disorder in which affected individuals are mosaic for mutations in GNAS1. Presumably, full heterozygosity for mutations in this gene is lethal, and mosaics survive because of the presence of a proportion of normal cells. It affects the skeleton, skin, and endocrine systems. Large 'coast of Maine' café-au-lait patches with midline demarcation characterize the pigmentary changes. Polyostotic fibrous dysplasia, hyperfunction of endocrine glands, and precocious puberty (almost exclusively in females) also occur. The café-au-lait patches are first noted in infancy. They are typically larger and have rougher edges than the café-au-lait macules of neurofibromatosis type 1; occasionally individuals with neurofibromatosis type 1 may have similar large café-au-lait patches. There may be distribution within Blaschko lines, although this is not always apparent [41]. The disorder is caused by missense mutations in GNAS1, a gene that encodes a G protein subunit (Gs-α) that activates adenylate cyclase. This results in the production of excess endogenous cAMP in mutant cells [42]. How this causes cutaneous hyperpigmentation is not known; however, cAMP is known to play a role in melanogenesis and in melanosome transport [43,44,45•].

Theories for patterned dyspigmentation

An insightful review of the literature by Taibjee and Moss [1••] revisits the pathomechanism for pigment variation in mosaic conditions. The authors raise the possibility of a nonspecific border effect between two distinct cell lines. In other words, both the dark and light areas may be normal in melanocyte distribution and function, but different in the amounts of pigment produced. The apposition of the two different clones makes them clinically apparent. However, the authors favor the hypothesis that normal pigment production is disrupted because of the loss or gain of function of specific genes controlling pigment production. They systematically compared the locations of karyotypic abnormalities of 98 cases of patterned dyspigmentation with known loci for 76 pigmentation genes. 88% of the chromosomal abnormalities overlapped with the location of at least one known pigmentary gene. Conversely, three quarters of all known pigmentary genes are in regions that overlap with the chromosomal abnormalities found in cases of patterned dyspigmentation. Although this is not evidence for a causal relation of the disruption of specific genes involved in pigmentary changes, it is suggestive.

Conclusion

We have not come much further in our understanding of the mechanisms leading to dyspigmentation in chromosomal mosaicism since the association of HI with chromosomal mosaicism was first recognized [46–48]. The role of cell–cell communication in the control of melanogenesis has not yet been investigated in HI. This may prove to be extremely interesting and may ultimately explain normal patterns of pigment distribution such as Futcher's lines. Why the single-gene disorders of Waardenburg's syndrome and piebaldism result in patterned dyspigmentation is also not understood. With the sequencing of the human genome and the rapid advances in genomic technologies, the next decade promises to greatly enhance our understanding of the molecular underpinnings of pigmentation.

Acknowledgement

VAL thanks Corey Nislow, PhD, for discussions and his thoughtful review of the manuscript.

References and recommended reading

Papers of particular interest, published within the annual period of review, have been highlighted as:

- • of special interest
- •• of outstanding interest

1 •• Taibjee SM, Moss C. Abnormal pigmentation in hypomelanosis of Ito and pigmentary mosaicism: the role of pigmentary genes. Br J Dermatol 2004; 151:269–282.

This is a comprehensive and thoughtful review of the pathogenesis of mosaic diseases of pigmentation, with particular attention to the association between pigmentary loci and chromosomal defects in patterned dyspigmentation.

2 Spritz RA, Pei-Wen C, Oiso N, Alkhateeb A. Human and mouse disorders of pigmentation. Curr Opin Genet Dev 2003; 13:284–289.

3 Tomita Y, Suzuki T. Genetics of pigmentary disorders. Am J Med Genet 2004;131C:75–81.

4 • Passeron T, Mantoux F, Ortonne JP. Genetic disorders of pigmentation. Clin Dermatol 2005; 23:56–67.

This is a concise review of inherited conditions in humans with hypopigmentation and hyperpigmentation.

5 Gottlieb B, Beitel L, Trifiro MA. Somatic mutation and variable expressivity. Trends Genet 2001; 17:79–82.

6 Youssoufian H, Pyeritz RE. Mechanism and consequences of somatic mosaicism in humans. Nat Rev Genet 2002; 3:748–758.

7 • Poblete-Gutierrez P, Wiederholt T, Konig A, *et al*. Allelic loss underlies type 2 segmental Hailey-Hailey disease, providing molecular confirmation of a novel genetic concept. J Clin Invest 2004; 114:1467–1474.
This is a molecular demonstration that a mosaic presentation of an erosive skin condition, Hailey–Hailey disease, is due to loss of a paternal allele in keratinocytes, presumably by way of mitotic recombination.

8 Rajagopalan H, Lengauer C. Aneuploidy and cancer. Nature 2004; 432:338–341.

9 Lyon MF. X-chromosome inactivation. Curr Biol 1999; 9:235–237.

10 Lyon MF. Gene action in the X chromosome of the mouse (*Mus musculus* L.). Naturwissenschaften 1961; 190:372–373.

11 Happle R. Transposable elements and the lines of Blaschko: a new perspective. Dermatology 2002; 204:4–7.

12 Whitelaw E, Martin DIK. Retrotransposons as epigenetic mediators of phenotypic variation in mammals. Nat Genet 2001; 27:361–364.

13 Blewitt ME, Chong S, Whitelaw E. How the mouse got its spots. Trends Genet 2004; 20:550–553.

14 • Jiang YH, Bressler J, Beaudet AL. Epigenetics and human disease. Annu Rev Genomics Hum Genet 2004; 5:479–510.
This excellent treatise summarizes the evidence for epigenetic contributions to gene expression in humans.

15 Findlay GH, Moores PP. Pigment anomalies of the skin in human chimaera: their relation to systematized naevi. Br J Dermatol 1980; 103:489–498.

16 Smith FJ, Morley SM, McLean WH. Novel mechanism of revertant mosaicism in Dowling-Meara epidermolysis bullosa simplex. J Invest Dermatol 2004; 122:73–77.

17 Hirschhorn R. In vivo reversion to normal of inherited mutations in humans. J Med Genet 2003; 40:721–728.

18 Blaschko A. Die Nervenverteilung in der Haut in ihrer Beziehung zu den Erkrankungen der Haut. Beilage zu den Verhandlungen der Deutschen Dermatologischen Gesellschaft VII Congress. Breslau. 1901; Braumuller, Wien.

19 Happle R. Mosaicism in human skin: understanding the pattern and mechanisms. Arch Dermatol 1993; 129:1460–1470.

20 Schachner LA, Hansen RD, editors. Pediatric dermatology. 3rd ed. New York: Mosby; 2003; CD rom.

21 Dupin E, Le Douarin NM. Development of melanocyte precursors from the vertebrate neural crest. Oncogene 2003; 22:3016–3023.

22 Moss C. Cytogenetic and molecular evidence for cutaneous mosaicism: the ectodermal origin of Blaschko lines. Am J Med Genet 1999; 85:330–333.

23 Paller AS, Syder AJ, Chan Y-M, *et al*. Genetic and clinical mosaicism in a type of epidermal nevus. N Engl J Med 1994; 331:1408–1415.

24 Moss C. Birthmark due to cutaneous mosaicism for keratin 10 mutation. Lancet 1995; 345:596.

25 Happle R. Pigmentary patterns associated with human mosaicism: a proposed classification. Eur J Dermatol 1993; 3:170–174.

26 Happle R. Phylloid hypomelanosis and mosaic trisomy 13: a new etiologically defined neurocutaneous syndrome. Hautarzt 2001; 52:3–5.

27 Rebiero Noce T, de Pina-Neto JM, Happle R. Phylloid pattern of pigmentary disturbance in a case of complex mosaicism. Am J Med Genet 2001; 98: 145–147.

28 Happle R. Phylloid hypomelanosis is closely related to mosaic trisomy 13. Eur J Dermatol 2000; 10:511–512.

29 Hansen LK, Brandrup F, Rasmussen K. Pigmentary mosaicism with mosaic chromosome 5p tetrasomy. Br J Dermatol 2003; 149:414–416.

30 Ito M. Studies on melanin XI. Incontinentia pigmenti achromians: a singular case of nevus depigmentosus systematicus bilateralis. Tohoku J Exp Med 1952; 55:57–59.

31 Sybert VP. Hypomelanosis of Ito: a description, not a diagnosis. J Invest Dermatol 1994; 103:141S–143S.

32 Ruiz-Maldonado R, Toussaint S, Tamayo L, *et al*. Hypomelanosis of Ito: diagnostic criteria and report of 41 cases. Pediatr Dermatol 1992; 9:1–10.

33 Nehal KS, Pebenito R, Orlow SJ. Analysis of 54 cases of hypopigmentation and hyperpigmentation along the lines of Blaschko. Arch Dermatol 1996; 132:1167–1170.

34 Sybert VP. Genetic skin disorders. New York: Oxford University Press; 1997. pp. 318–321.

35 Lee HS, Chun YS, Hann SK. Nevus depigmentosus: clinical features and histopathologic characteristics in 67 patients. J Am Acad Dermatol 1999; 40:21–26.

36 Di Lernia V. Segmental nevus depigmentosus: analysis of 20 patients. Pediatr Dermatol 1999; 16:349–353.

37 Alrobaee AA, Alsaif F. Linear and whorled nevoid hypermelanosis associated with developmental delay and generalized convulsions. Int J Dermatol 2004; 43:145–147.

38 Hartmann A, Hofmann UB, Hoehn H, *et al*. Postnatal confirmation of prenatally diagnosed trisomy 20 mosaicism in a patient with linear and whorled nevoid hypermelanosis. Pediatr Dermatol 2004; 21:636–641.

39 Kenwrick S, Woffendin H, Jakins T, *et al*. Survival of male patients with IP carrying a lethal mutation can be explained by somatic mosaicism or Klinefelter syndrome. Am J Hum Genet 2001; 69:1210–1217.

40 Berlin A, Paller AS, Chan LS. Incontinentia pigmenti: a review and update on the molecular basis of pathophysiology. J Am Acad Dermatol 2002; 47:169–187.

41 Rieger E, Kofler R, Borkensstein M, *et al*. Melanotic macules following Blaschko's lines in McCune-Albright syndrome. Br J Dermatol 1994; 130:215–220.

42 Ringel MD, Schwindinger WF, Levine MA. Clinical implications of genetic defects in G proteins: the molecular basis of McCune-Albright syndrome and Albright hereditary osteodystrophy. Medicine 1996; 75:171–184.

43 Passeron T, Bahadoran T, Bertolotto C. Cyclic AMP promotes a peripheral distribution of melanosomes and stimulates melanophilin/Slac2alpha and acting association. FASEB 2004; 18:989–991.

44 Busca R, Balotti R. Cyclic AMP a key messenger in the regulation of skin pigmentation. Pigment Cell Res 2000; 13:60–69.

45 • Van Raamsdonk CD, Fitch KR, Fuchs H, *et al*. Effects of G protein mutations on skin color. Nat Genet 2004; 36:961–968.
A large-scale mutagenic screen in mice uncovers new mutations in G proteins that contribute to pigment variegation of skin and hair, furthering our understanding of signal pathways that affect melanocytic development.

46 Donnai D, Read AP, McKeown C, Andrews T. Hypomelanosis of Ito: a manifestation of mosaicism or chimerism. J Med Genet 1988; 25:809–818.

47 Thomas IT, Frias JL, Cantu ES, *et al*. Association of pigmentary anomalies with chromosomal and genetic mosaicism and chimerism. Am J Hum Genet 1989; 45:193–205.

48 Sybert VP, Pagon RA, Donlan M, Bradley CM. Pigmentary abnormalities and mosaicism for chromosomal aberration: association with clinical features similar to hypomelanosis of Ito. J Pediatr 1990; 116:581–586.

nature genetics

Conservation of hotspots for recombination in low-copy repeats associated with the *NF1* microdeletion

Thomas De Raedt[1], Matthew Stephens[2], Ine Heyns[1], Hilde Brems[1], Daisy Thijs[1], Ludwine Messiaen[3], Karen Stephens[4], Conxi Lazaro[5], Katharina Wimmer[6], Hildegard Kehrer-Sawatzki[7], Dominique Vidaud[8], Lan Kluwe[9], Peter Marynen[1] & Eric Legius[1]

Several large-scale studies of human genetic variation have provided insights into processes such as recombination that have shaped human diversity. However, regions such as low-copy repeats (LCRs) have proven difficult to characterize, hindering efforts to understand the processes operating in these regions. We present a detailed study of genetic variation and underlying recombination processes in two copies of an LCR (NF1REPa and NF1REPc) on chromosome 17 involved in the generation of *NF1* microdeletions and in a third copy (REP19) on chromosome 19 from which the others originated over 6.7 million years ago. We find evidence for shared hotspots of recombination among the LCRs. REP19 seems to contain hotspots in the same place as the nonallelic recombination hotspots in NF1REPa and NF1REPc. This apparent conservation of patterns of recombination hotspots in moderately diverged paralogous regions contrasts with recent evidence that these patterns are not conserved in less-diverged orthologous regions of chimpanzees.

Recombination in LCRs is particularly interesting because crossovers that occur between two nearby copies of an LCR (generally referred to as nonallelic homologous recombination; NAHR) result in deletion or duplication of the region between the copies and are often associated with genomic disorders such as Charcot-Marie-Tooth type 1A, hereditary neuropathy with liability to pressure palsies, Williams-Beuren syndrome and neurofibromatosis type 1 (NF1). These NAHR events have sometimes been observed to cluster in relatively short hotspots[1–3], but otherwise, little is known about recombination in LCRs, including the extent to which patterns of recombination are shared across different copies of the same LCR and whether hotspots for NAHR also correspond to hotspots for nonallelic homologous gene conversion (NAHGC) and/or allelic homologous recombination (AHR). In principle, one can obtain considerable insight into these questions through studying patterns of genetic variation in LCRs. However, because of high sequence identity, accurate genotyping of SNPs in LCRs is not straightforward, and when such SNPs are typed in high-throughput genotyping projects, the obtained genotypes are often inaccurate and show nonmendelian inheritance or lack of Hardy-Weinberg equilibrium. As a result, virtually no reliable data are available on population genetic variation in LCRs.

We therefore undertook a detailed sequencing-based study of the patterns of genetic variation in three copies of an LCR, of which two are associated with the *NF1* microdeletion. **Supplementary Figure 1** online gives a schematic overview of the *NF1* microdeletion region and its LCRs, NF1REPa and NF1REPc (on chromosome 17) and REP19 (on chromosome 19). Two types of recurrent *NF1* microdeletions have been described. Type I *NF1* microdeletions are typically 1.4 Mb in length and of meiotic origin[4]. In individuals with type I *NF1* microdeletions, the deletion breakpoints tend to cluster in two regions called PRS1 (ref. 5) and PRS2 (ref. 1) (**Supplementary Fig. 1**). Regions paralogous to PRS1 and PRS2 are also present in REP19 (**Supplementary Fig. 1**) but with about 22 kb of extra sequence inserted between them compared with NF1REPa and NF1REPc. Type II *NF1* microdeletions are less frequent, have a length of 1.2 Mb and are mitotic in origin; their breakpoints tend to cluster in a different segment of the LCRs[6,7]. **Supplementary Figure 1** gives an overview of the repeat content of the different LCRs and the location of the typed SNPs.

To better characterize NAHR in NF1REPa and NF1REPc, we accurately mapped the location of the breakpoints in 60 individuals with type I *NF1* microdeletions ascertained in an unbiased manner. The results (**Fig. 1**) confirmed the presence of two clusters of breakpoints: a larger cluster in PRS2 (3.4 kb, containing 40/60 breakpoints) and a smaller cluster in PRS1 (1.8 kb, containing 13/60 breakpoints). This suggests the presence of hotspots for the initiation of NAHR in PRS1 and PRS2, in either one or both of NF1REPa and NF1REPc.

The effect of NAHGC will be to 'insert' a small segment of one LCR into another LCR. Thus, frequent NAHGC would tend to lead to

[1]Department of Human Genetics, Catholic University Leuven, Leuven, Belgium. [2]Department of Statistics, University of Washington, Seattle, Washington, USA. [3]Laboratory Medical Genetics, Department of Genetics, University of Alabama, Birmingham, Alabama, USA. [4]Department of Medicine, University of Washington, Seattle, Washington, USA. [5]Institut Catala d'Oncologia–Instituto de Investigación Biomédica de Bellvitge, L'Hospitalet de Llobregat, Barcelona, Spain. [6]Department of Human Genetics, Medical University of Vienna, Vienna, Austria. [7]Department of Human Genetics, University of Ulm, Ulm, Germany. [8]Laboratoire de Génétique Moléculaire, Institut National de la Santé et de la Recherche Médicale U745, Université Paris 5, Paris, France. [9]Laboratory for Tumor Biology and Development and Malformation, University Hospital Eppendorf, Hamburg, Germany. Correspondence should be addressed to E.L. (Eric.Legius@uz.kuleuven.ac.be).

Received 6 July; accepted 16 October; published online 19 November 2006; doi:10.1038/ng1920

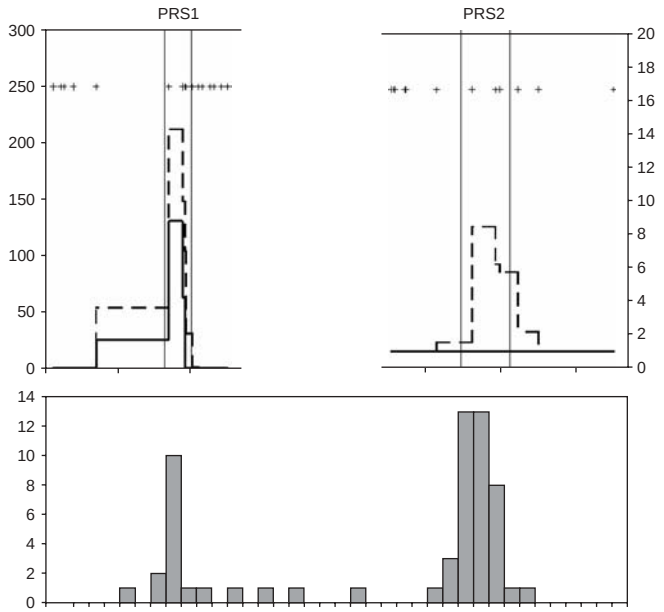

Figure 1 Comparison of hotspots of recombination inferred from haplotype and microdeletion data. Top: estimated rates of crossover across PRS1 and PRS2 in REP19 as calculated by PHASE. Lines show the posterior mean (dashed line) and median (full line) crossover rates from PHASE when both the location and intensity of any hotspot are estimated from the population haplotype data. The position of the SNPs (REP19) is represented by +. Vertical lines show locations of the NAHR breakpoint hotspots identified from the data in the bottom figure. Bottom: distribution of the NAHR breakpoints of 60 individuals with *NF1* microdeletions. The upper and lower panels are aligned: the estimated locations of AHR hotspots from the haplotype data on chromosome 19 agree closely with the locations of the NAHR breakpoint hotspots in the paralogous regions on chromosome 17. Note the very different scales of the *y* axes in the upper plot.

'shared' SNPs that are polymorphic in both LCRs. We therefore assessed relative rates of NAHGC in three regions (900 bp in PRS1, 1,500 bp in PRS2 and 800 bp in a region between PRS1 and PRS2) by sequencing these regions in both NF1REPa and NF1REPc (**Supplementary Table 1** online) and determining how many of the identified SNPs were 'shared' (that is, polymorphic in both NF1REPa and NF1REPc). In total, we identified 28 SNPs in NF1REPa and 26 in NF1REPc in the three specified regions. Of these, 12 were shared, providing strong evidence for NAHGC (the probability of 12 or more SNPs being shared if one draws 28 and 26 SNPs independently at random from 3,200 bp is $P = 2.2 \times 10^{-18}$). The region sequenced in PRS2 contained a higher proportion of shared SNPs (9/22) than the region sequenced in PRS1 (2/9), which contained a higher proportion than the intervening region (1/11; **Table 1**). Although only the difference between PRS2 and the intervening region approached statistical significance ($P = 0.066$), the results are consistent with the possibility that rates of NAHGC vary in a similar way to rates of NAHR; that is, the highest rate is found in PRS2, an intermediate rate in PRS1 and a lower rate in the intervening region, just as hotspots for allelic homologous gene conversion (AHGC) have been found to coincide with hotspots for AHR in the MHC and PAR1 regions[8]. This would be expected if NAHGC and NAHR were two alternative resolutions of a Holliday junction formed after a double-strand break, and if the hotspots for NAHR were due to an increased rate of double-strand break formation. Sequencing the same three regions in REP19, we did not find any SNPs shared with either NF1REPa or NF1REPc, and thus, as expected, there is no evidence for any ongoing genetic exchange between NF1REPa or NF1REPc and REP19.

In order to assess patterns of AHR, we first identified and typed SNPs in each of the three LCRs in 43 trios (parents plus child). We typed a total of 20 SNPs in the 33-kb region surrounding PRS1 and PRS2 in NF1REPa and NF1REPc. In REP19, where an additional 22 kb is found between PRS1 and PRS2, we typed 16 SNPs surrounding PRS1 and 12 SNPs surrounding PRS2 (**Supplementary Table 2** online; LD patterns are shown in **Supplementary Fig. 2** online). We then used a statistical approach[9–11] based on the observed haplotype data to assess the evidence for AHR hotspots at PRS1 and PRS2 in each of the LCRs. Specifically, as in ref. 11, we prespecified PRS1 and PRS2 as locations for potential hotspots and used the statistical method to estimate the background population-scaled recombination rate (ρ) and the relative intensity of recombination in the hotspot segments (λ). Thus, $\lambda = 1$ corresponds to no hotspot; we will refer to λ between 1 and 10 as a 'weak' hotspot and $\lambda > 10$ as a 'strong' hotspot. To summarize the strength of the evidence for either a strong or weak hotspot, we use the Bayes factor (BF), which is the probability of obtaining the data under the model that a weak or strong hotspot is present divided by the probability of obtaining the data under the model that no hotspot is present. Thus, a BF of >1 is evidence for a hotspot, and a BF of 10 means that the data are ten times more likely under a hotspot model than under a model without a hotspot, which might be considered strong evidence for a hotspot. The results are summarized in **Table 2**. One explanation for the different results for NF1REPa and NF1REPc (BFs ranging from 1.1–3.2) as compared with REP19 (BFs of 10.1 and 14,835) is that the polymorphism data for the former are comparatively uninformative about the presence or absence of a hotspot. This is suggested by results shown in **Supplementary Figure 3** online, which demonstrates little difference between the prior and posterior distribution of λ. In contrast, the polymorphism data in REP19 are substantially more informative and provide strong evidence for a hotspot of some kind in both PRS1 and PRS2 (BF $>$ 10,000 (strong hotspot) in PRS1, and BF $=$ 10.1 (weak hotspot) in PRS2). Further, when we repeated these analyses for the REP19 data without prespecifying the location of the hotspot and allowing the statistical method to estimate the location, the estimated hotspot locations corresponded very closely to the regions paralogous to PRS1 and PRS2 (**Fig. 1**). (The estimated positions of the AHR and NAHR hotspots are, respectively, 6973–9059 and 7682–9525 for PRS1 and 5567–7316 and 4394–7564 for PRS2.)

Table 1 Number of SNPs across the different regions of the LCRs

	PRS1 (900 bp)	PRS2 (1,500 bp)	Region between hotspots (800 bp)	Total (3,200 bp)
NF1REPa only	4	5	7	16
NF1REPc only	3	8	3	14
Shared NF1REPa/c	2	9	1	12
REP19 only	6	11	2	19
Shared 17/19	0	0	0	0

'NF1REPa only': total number of nucleotide positions polymorphic only in NF1REPa and not at the paralogous position in NF1REPc. 'NF1REPc only': total number of nucleotide positions polymorphic only in NF1REPc and not at the paralogous position in NF1REPa. 'Shared NF1REPa/c': number of nucleotide positions polymorphic in NF1REPa and at the paralogous position in NF1REPc. 'REP19 only': total number of nucleotide positions polymorphic only in REP19 and not at the paralogous position in NF1REPa and/or NF1REPc. 'Shared 17/19': total number of nucleotide positions polymorphic in REP19 and at the paralogous position in NF1REPa or NF1REPc.

Table 2 Background recombination rates and λ values in the PRS1 and PRS2 regions of the LCRs

		NF1REPa	NF1REPc	REP19
PRS1	P(λ > 1)[a]	0.707	0.564	1.00
	P(λ > 10)[a]	0.393	0.296	0.989
	BF(weak)[b]	3.2	1.8	327[d]
	BF(strong)[c]	2.0	1.0	14,835[d]
	Median λ	5.47	1.78	152
PRS2	P(λ > 1)	0.719	0.532	0.865
	P(λ > 10)	0.429	0.327	0.412
	BF(weak)[b]	3.1	1.3	10.1[d]
	BF(strong)[c]	2.2	1.1	4.6
	Median λ	7.23	1.66	7.99
Background recombination rate (90% confidence interval)		1.31×10^{-4} (2.3×10^{-5} to 3.3×10^{-4})	6.41×10^{-5} (1.0×10^{-5} to 1.7×10^{-4})	PRS1: 1.48×10^{-4} (3.8×10^{-5} to 5.9×10^{-4}) PRS2: 5.09×10^{-4} (1.9×10^{-4} to 1.1×10^{-3})

[a]Proportion of the 50,000 iterations with λ > 1 or λ > 10. [b]BF comparing the model 'weak hotspot' versus the model 'no hotspot'. [c]BF comparing the model 'strong hotspot' versus the model 'no hotspot'. [d]BF values >10: strong indication in favor of a hotspot.

The high informativeness of the population data in REP19 compared with NF1REPa and NF1REPc could be due to several factors, including the greater number of SNPs available (28 in REP19 versus 20 in NF1REPa and NF1REPc) and the higher average minor allele frequency (average minor allele frequency of 29.8% in REP19 compared with 18.0% in NF1REPa and 14.7% in NF1REPc)[12,13]. It is also possible that differences in the background recombination rates[14] in the different regions could contribute to different power to detect hotspots, as the estimated background recombination rate (ρ) differs in the three LCRs. The estimate of ρ is about two times higher in NF1REPa (1.31×10^{-4}) compared with NF1REPc (6.41×10^{-5}). The background recombination rate for REP19 PRS1 is 1.48×10^{-4} (comparable to NF1REPa), whereas the background in REP19 PRS2 is higher (5.09×10^{-4}). It is possible that, due to the formation of deleterious microdeletions, a selective pressure against recombination exists in the LCRs of chromosome 17, reducing the historical recombination signature in the region.

Although it is notable that hotspots for AHR in REP19 identified from population data seem to occur in the same locations as the PRS1 and PRS2 hotspots for NAHR identified from individuals with *NF1* microdeletions, it is also worth noting that the estimated relative intensities of the hotspots identified from the two approaches differ appreciably. Intensities of the NAHR hotspots, computed by comparing the frequency of deletion breakpoints occurring inside each hotspot versus outside the hotspots, are 28.7 for PRS1 and 46.7 for PRS2. (Note that these estimates are likely biased slightly upward because the locations of the breakpoint hotspots were based on the observed NAHR events.) In contrast, estimated intensities of these hotspots from the REP19 population data are 152 and 8, respectively. In addition, in REP19, the population data suggest a lower average rate of AHR in the region surrounding PRS2 than in the region surrounding PRS1 (**Supplementary Fig. 3**), whereas the microdeletion data suggest the reverse for NAHR in chromosome 17. Although some of these discrepancies could be due to imprecision of the estimated intensities and deviations from modeling assumptions, other factors could also have a role. For example, the NAHR data measure the current recombination rate (microdeletions being formed), whereas population genetic data reflect the average historical recombination rate, and differences can exist between current and historical recombination rates[15]. Other factors that could influence the relative intensity of the recombination hotspots include the fact that REP19 contains 22 kb of additional sequence inserted between PRS1 and PRS2, or that differences in methylation pattern could result in a different DNA folding in each LCR (epigenetic effects).

In summary, the mapping of *NF1* microdeletion breakpoints (**Fig. 1**) and the presence of NAHGC give a clear view that sites of NAHR in (at least one of) NF1REPa and NF1REPc are not randomly distributed and are located in two distinct hotspots. Population genetic data in both NF1REPa and NF1REPc are not very informative for a hotspot of AHR but do not argue strongly against the presence of hotspots in either NF1REPa or NF1REPc. Population genetic data in the paralogous regions of REP19 provide strong evidence for hotspots of AHR. The initial duplication of the LCR from chromosome 19 to the *NF1* region took place before the human-gorilla split, about 6.7 million years ago[16]. Conservation of AHR hotspots in REP19 with NAHR hotspots in NF1REPa and NF1REPc in sequences that have been evolving separately for such a long time is notable, as hotspots for recombination in humans do not seem to be highly conserved in chimpanzee[11,17]. Others[18] have investigated the fine-scale recombination rate of three 500-kb regions both in humans and chimpanzees. Eighteen hotspots for recombination were found in humans, and of these, only one may correspond to a site of historical recombination in chimpanzees. Although it could be that we have simply found hotspots that happen to be conserved by chance, it is also possible that patterns of recombination in orthologous regions between humans and chimpanzees are less evolutionarily stable than patterns of recombination in paralogous regions. This could be due, for example, to differences in the recombination machinery or in epigenetic factors in the two species[17,18]. This potential role in hotspot evolution for distal regulators of recombination or epigenetic factors has been suggested before when looking at the presence or absence polymorphism of a human recombination hotspot[19]. Examining whether the AHR hotspots in PRS1 and PRS2 are present in the chimpanzee orthologs could help distinguish among these competing explanations.

METHODS

Samples. We collected DNA samples extracted from blood leukocytes from 43 nuclear families (trios). In addition, genomic DNA from 70 individuals was available for full sequencing of three regions in each LCR investigated. All individuals were of Flemish origin and gave their informed consent, and all experiments were approved by the ethical commission of the medical faculty of the Catholic University of Leuven.

Specific PCR amplification of sequences from the three different copies of the LCRs. Using the Expand Long Template PCR system (Roche), we amplified each copy of the LCR in fragments of a maximum of 5 kb. Primers were chosen to end on paralogous sequence variants (PSVs) in such a way that only one copy of the LCR would be amplified. Genotypes from some SNPs showed problems with mendelian inheritance and Hardy-Weinberg equilibrium. Primer positions of the relevant PCR fragments were sequenced in all individuals, and the PSV sites used for the LCR-specific amplification proved to be polymorphic and hence not LCR specific. In these cases, new primers were designed using other PSVs in the vicinity that were not polymorphic in

our set of 43 families. With the new primer sets, there were no longer problems with mendelian inheritance or Hardy-Weinberg Equilibrium. A complete list of primers is available in **Supplementary Table 3** online.

Detection of type I *NF1* microdeletion breakpoints. We amplified, nonspecifically, fragments from both NF1REPa and NF1REPc simultaneously during the same PCR reaction and sequenced PSVs at several sites throughout the LCR. In an individual with a microdeletion, one typically amplifies three different fragments, one derived from the normal NF1REPa, one derived from the normal NF1REPc and one derived from the hybrid NF1REPa/NF1REPc on the chromosome 17 with the microdeletion. By simply scoring the relative copy number of both nucleotides of the PSV, one can determine if the breakpoint is located centromeric of the PSV investigated (NF1REPc-specific nucleotide has a higher relative intensity on sequencing readout) or telomeric of the PSV (NF1REPa-specific nucleotide has a higher relative intensity) (**Supplementary Fig. 4** online). In this way, the interval where the breakpoint is located can be narrowed to an interval between two PSVs.

SNP discovery. In NF1REPa and NF1REPc, 31 kb of the 33 kb region investigated in the three LCRs were fully sequenced, and about 22 kb were sequenced in REP19 (BigDye Terminator Sequencing Kit v3.1, Applied Biosystems) in ten random individuals for SNP discovery. Regions left unsequenced in NF1REPa and NF1REPc had a high repetitive content. All SNPs typed in the 43 families were submitted to the dbSNP database. **Supplementary Table 2** gives an overview of all the SNPs typed in the different LCRs together with the minor allele frequency. In addition, three smaller regions in the different LCRs were fully sequenced in 70 unrelated individuals (900 bp in PRS1, 1,500 bp in PRS2 and 800 bp in a region between PRS1 and PRS2). The number of SNPs shared between the different copies of the LCRs was counted. **Supplementary Table 1** gives an overview of the total number of SNPs and the number of SNPs shared between LCRs.

SNP typing. A total of 68 SNPs (20 in NF1REPa and NF1REPc, 16 in the PRS1 region of REP19 and 12 in the PRS2 region of REP19) were typed in the 43 nuclear families and were submitted to the dbSNP database (**Supplementary Table 2**). The SNPs were typed by direct sequencing (BigDye Terminator Sequencing Kit v3.1, Applied Biosystems) or by SNaPshot analysis (Applied Biosystems) on the LCR-specific amplified PCR products. Because of the high sequence identity between the different copies of the LCR and the inherent problems of specific amplification of the LCRs, extensive precautions were taken to avoid mistyping. None of the SNPs in this report showed problems with mendelian inheritance, and all genotypes are in Hardy-Weinberg equilibrium. SNPs with a frequency lower than 4% were not included in the data analysis.

Haplotype analysis. For each copy of the LCR, the 172 parental haplotypes were estimated from the genotype data of the 43 trios using PHASE v2.1.1 (refs. 9,10,20–22). These estimated haplotypes were assumed to be known without error for subsequent analyses. We then used PHASE to assess the evidence for the presence of AHR hotspots in the three LCRs (NF1REPa, NF1REPc and REP19) at the location of the NAHR hotspots (PRS1 and PRS2) in NF1REPa and NF1REPc. The boundaries of PRS1 and PRS2 were chosen in such a way that they encompassed 90% of the breakpoints located in the PRS1 and PRS2 area, respectively. Based on the haplotype data, PHASE estimates the overall background recombination rate (ρ) and the relative intensity of any hotspots (λ). For example, $\lambda = 1$ corresponds to no hotspot, whereas $\lambda = 10$ corresponds to a hotspot where recombination occurs at a rate 10 times higher than in the surrounding sequence. The program makes a number of iterations (for example 10,000), and each iteration produces a sampled value of ρ and λ. We assumed the following prior distribution on λ: with probability 0.5, $\lambda = 1$ (that is, no hotspot); otherwise a hotspot is present ($\lambda > 1$) and $\log10(\lambda)$ is uniform in the range 0–3. The number of iterations that provide a sampled value of $\lambda > 1$ indicates the strength of the evidence for a hotspot. For our analysis, we used five different seeds, each time making 10,000 iterations, to provide a total of 50,000 samples. The numbers shown in **Table 2** reflect the proportion of iterations where $\lambda > 1$ or $\lambda > 10$, with $1 < \lambda < 10$ being considered a weak hotspot, and $\lambda > 10$ being considered a strong hotspot. For the prior on λ we assumed (see above) the prior probability of no hotspot is 0.5, the prior probability of a weak hotspot λ is 1/6 and the prior probability of a strong hotspot is 1/3. The evidence for a weak or strong hotspot is measured using the Bayes factor (BF). The BF is the probability of obtaining the data under the model that a weak or strong hotspot is present divided by the probability of obtaining the data under the model that no hotspot is present. A BF of 10 indicates that the data are ten times more likely to be obtained if there is a hotspot than if there is no hotspot. The BF is calculated as follows: $BF(\text{weak}) = (Pr(\text{weak hotspot}) \times 0.5)/(Pr(\lambda = 1) \times 1/6)$, and $BF(\text{strong}) = (Pr(\text{strong hotspot}) \times 0.5)/(Pr(\lambda = 1) \times 1/3)$, where $Pr(x)$ is the percentage of iterations observed under condition x, and 0.5, 1/6 and 1/3 are the prior probabilities of finding 'no hotspot', a 'weak hotspot' or a 'strong hotspot', respectively.

For the REP19PRS1 and REP19PRS2 regions, a second analysis with PHASE was performed, assuming that one AHR hotspot was present in each region without specifying the exact location of the AHR hotspot.

Statistical analysis. The number of observed shared SNPs between the different copies of the LCR was compared with the expected number by the binomial distribution. The *a priori* probability was calculated as the number of SNPs per bp present in the copy of the LCR to which the other LCR was compared. The α-level was Bonferroni corrected.

Statistical analysis software and URLs. PHASE can be found at http://www.stat.washington.edu/stephens/software.html. All input files for PHASE and all derived haplotypes are available in **Supplementary Table 4** online.

Note: Supplementary information is available on the Nature Genetics website.

ACKNOWLEDGMENTS

The authors thank T. de Ravel for critically reading the manuscript. T.D. is supported by the Emmanuel Vanderschueren Fonds. M.S. is supported by US National Institutes of Health grant 1RO1HG/LM02585-01. E.L. is a part-time clinical researcher of the Fonds voor Wetenschappelijk Onderzoek Vlaanderen (FWO). This work is also supported by research grants from the Fonds voor Wetenschappelijk Onderzoek Vlaanderen (G.0096.02, E.L.; G.0507.04, P.M.); the Interuniversity Attraction Poles (IAP) granted by the Federal Office for Scientific, Technical and Cultural Affairs, Belgium (2002-2006; P5/25) (P.M. and E.L.); by a Concerted Action Grant from the Catholic University of Leuven and by the Belgian Federation against Cancer (SCIE2003-33 to E.L.).

AUTHOR CONTRIBUTIONS

This study was coordinated by T.D., P.M. and E.L.; the manuscript was written by T.D., M.S. and E.L.; breakpoint detection was performed by T.D., I.H., H.B., L.M., K.S., C.L., K.W., H.K., D.V. and L.K.; SNP detection and typing was performed by T.D., I.H., H.B. and D.T. and computational analysis was performed by T.D. and M.S.

COMPETING INTERESTS STATEMENT

The authors declare that they have no competing financial interests.

Published online at http://www.nature.com/naturegenetics
Reprints and permissions information is available online at http://npg.nature.com/reprintsandpermissions/

1. Lopez-Correa, C. *et al.* Recombination hotspot in NF1 microdeletion patients. *Hum. Mol. Genet.* **10**, 1387–1392 (2001).
2. Repping, S. *et al.* Recombination between palindromes P5 and P1 on the human Y chromosome causes massive deletions and spermatogenic failure. *Am. J. Hum. Genet.* **71**, 906–922 (2002).
3. Reiter, L.T. *et al.* Human meiotic recombination products revealed by sequencing a hotspot for homologous strand exchange in multiple HNPP deletion patients. *Am. J. Hum. Genet.* **62**, 1023–1033 (1998).
4. Lopez Correa, C., Brems, H., Lazaro, C., Marynen, P. & Legius, E. Unequal meiotic crossover: a frequent cause of NF1 microdeletions. *Am. J. Hum. Genet.* **66**, 1969–1974 (2000).
5. Forbes, S.H., Dorschner, M.O., Le, R. & Stephens, K. Genomic context of paralogous recombination hotspots mediating recurrent NF1 region microdeletion. *Genes Chromosom. Cancer* **41**, 12–25 (2004).
6. Petek, E. *et al.* Mitotic recombination mediated by the JJAZF1 (KIAA0160) gene causing somatic mosaicism and a new type of constitutional NF1 microdeletion in two children of a mosaic female with only few manifestations. *J. Med. Genet.* **40**, 520–525 (2003).
7. Kehrer-Sawatzki, H. *et al.* High frequency of mosaicism among patients with neurofibromatosis type 1 (NF1) with microdeletions caused by somatic recombination of the JJAZ1 gene. *Am. J. Hum. Genet.* **75**, 410–423 (2004).

8. Jeffreys, A.J. & May, C.A. Intense and highly localized gene conversion activity in human meiotic crossover hot spots. *Nat. Genet.* **36**, 151–156 (2004).
9. Li, N. & Stephens, M. Modeling linkage disequilibrium and identifying recombination hotspots using single-nucleotide polymorphism data. *Genetics* **165**, 2213–2233 (2003).
10. Crawford, D.C. *et al.* Evidence for substantial fine-scale variation in recombination rates across the human genome. *Nat. Genet.* **36**, 700–706 (2004).
11. Ptak, S.E. *et al.* Absence of the TAP2 human recombination hotspot in chimpanzees. *PLoS Biol.* **2**, e155 (2004).
12. Fearnhead, P., Harding, R.M., Schneider, J.A., Myers, S. & Donnelly, P. Application of coalescent methods to reveal fine-scale rate variation and recombination hotspots. *Genetics* **167**, 2067–2081 (2004).
13. Fearnhead, P. & Smith, N.G. A novel method with improved power to detect recombination hotspots from polymorphism data reveals multiple hotspots in human genes. *Am. J. Hum. Genet.* **77**, 781–794 (2005).
14. Hudson, R.R. Two-locus sampling distributions and their application. *Genetics* **159**, 1805–1817 (2001).
15. Jeffreys, A.J., Neumann, R., Panayi, M., Myers, S. & Donnelly, P. Human recombination hot spots hidden in regions of strong marker association. *Nat. Genet.* **37**, 601–606 (2005).
16. De Raedt, T. *et al.* Genomic organization and evolution of the NF1 microdeletion region. *Genomics* **84**, 346–360 (2004).
17. Ptak, S.E. *et al.* Fine-scale recombination patterns differ between chimpanzees and humans. *Nat. Genet.* **37**, 429–434 (2005).
18. Winckler, W. *et al.* Comparison of fine-scale recombination rates in humans and chimpanzees. *Science* **308**, 107–111 (2005).
19. Neumann, R. & Jeffreys, A.J. Polymorphism in the activity of human crossover hotspots independent of local DNA sequence variation. *Hum. Mol. Genet.* **15**, 1401–1411 (2006).
20. Stephens, M., Smith, N.J. & Donnelly, P. A new statistical method for haplotype reconstruction from population data. *Am. J. Hum. Genet.* **68**, 978–989 (2001).
21. Stephens, M. & Donnelly, P. A comparison of bayesian methods for haplotype reconstruction from population genotype data. *Am. J. Hum. Genet.* **73**, 1162–1169 (2003).
22. Marchini, J. *et al.* A comparison of phasing algorithms for trios and unrelated individuals. *Am. J. Hum. Genet.* **78**, 437–450 (2006).

Pediatric Dermatology Vol. 23 No. 1 87–92, 2006

Mosaicism in Genetic Skin Disorders

Dawn H. Siegel, M.D.* and Virginia P. Sybert, M.D.†

**Department of Dermatology, University of California San Francisco, San Francisco, California, †Department of Medicine, Division of Medical Genetics, Group Health Cooperative, Section of Dermatology and University of Washington, Seattle, Washington*

Mosaicism for genodermatoses often comes to the attention of pediatric dermatologists either because of patterned pigmentation or skin eruptions following the lines of Blaschko. For example, chromosomal mosaicism can result in linear and whorled pigmentary alteration. The same distribution pattern is seen in diseases resulting from the functional mosaicism in females for genes on the X chromosome including sweat patterns in carriers of X-linked hypohidrotic ectodermal dysplasia and females with incontinentia pigmenti. It is also found in the expression of X-linked disorders in males with Klinefelter syndrome, 47, XXY. Somatic mosaicism for single gene disorders explains the segmental distribution of many conditions (Table 1). In this column, we will review mechanisms and clinical examples of single gene, chromosomal, functional, and revertant mosaicism.

Mosaicism for single gene mutations results from events occurring after fertilization. This is referred to as somatic mosaicism. The earlier the mutational event occurs, the more likely it is that the individual will express the condition to a significant degree and the more likely it is that the gonadal tissue will be involved; thus conferring a risk of transmission to offspring. This is also called gonosomal mosaicism, meaning both the gonadal tissues and the somatic tissues are involved. If the mutation occurs after the cells that are committed to the gonad have formed, then the mosaicism will not involve the germline and reproductive risk is not an issue.

Gonosomal mosaicism is the mechanism for the occurrence of segmental neurofibromatosis (*NF*) in which affected individuals manifest the pigment changes and development of neurofibromas in a sector or quadrant or multiple, but noncontiguous areas, of the body, and subsequently have children with full-blown NF1. Another example is perinatal lethal osteogenesis imperfecta (OI type II), a biochemically heterogeneous disorder, usually caused by new mutations in the genes for type I collagen (1). Somatic mosaicism with germline mosaicism (gonosomal mosaicism) in a mildly manifesting parent has been implicated as the cause for the occurrence of lethal type II osteogenesis imperfecta in offspring.

Gonosomal mosaicism was also demonstrated in 1994 when Paller et al (2) evaluated cells from individuals with epidermal nevi of the epidermolytic hyperkeratosis type who had offspring with generalized epidermolytic hyperkeratosis (EHK) for mutations in the keratin 1 (K1) and keratin 10 (K10) genes. They studied peripheral blood lymphocytes, and did skin biopsies from affected and unaffected skin to create keratinocyte and fibroblast clones. They found K10 point mutations in 50% of the alleles from cultured keratinocytes from epidermal nevi, whereas no mutations were detected in normal skin or blood from these parents. Their fully affected offspring were found to be heterozygous for the causal mutation in all cells examined.

As opposed to gonosomal, which involves both gonads and somatic tissue as described previously, mosaicism may also occur exclusively in gonadal tissue; this is referred to as gonadal mosaicism. Gonadal mosaicism has been implicated in the recurrences among siblings of autosomal dominant disorders such as achondroplasia, tuberous sclerosis, and neurofibromatosis in families where neither parent is apparently affected. This mechanism has been proved by examination of sperm from the fathers in some of these families, in which two genetically distinct cell populations can be found.

Two mechanisms for segmental mosaicism of autosomal dominant disorders were proposed by Happle. Type

Address correspondence to Dawn H. Siegel, M.D., 1701 Divisadero Street, 3rd Floor, San Francisco, CA 94115, or e-mail: siegeld@derm.ucsf.edu.

TABLE 1. *Mosaicism in Selected Genetic Skin Disorders*

	Autosomal dominant/single gene		Functional		
Chromosomal	Lethal	Nonlethal	X-linked dominant	X-linked recessive	Revertant focal correction
• Hypomelanosis of Ito	• McCune–Albright • CHILD	• NF1 • Tuberous sclerosis • Epidermolytic hyperkeratosis • Darier • Hailey–Hailey	• Focal dermal hypoplasia • Incontinentia pigmenti • Conradi–Hunermann	• Hypohidrotic ectodermal dysplasia	• Dowling–Meara EB simplex • Recessive EB simplex • Non-Herlitz junctional EB

CHILD, *c*ongenital *h*emidysplasia with *i*chthyosiform erythoderma and *l*imb *d*efects.

1 presents with a segmental phenotype because of a somatic mutation, and the skin outside of the affected segment is normal, as is the genomic DNA (3). In type 2 segmental mosaicism, the affected individual has a heterozygous genomic mutation for an autosomal dominant condition but with exacerbation because of loss of heterozygosity within a segment or along the lines of Blaschko. This pattern has been described in individuals with several genodermatoses including superficial actinic porokeratosis with regions of overlying linear porokeratosis, Darier disease, tuberous sclerosis complex, and Hailey–Hailey disease. Hailey–Hailey disease is an autosomal dominant disorder caused by a mutation in the gene, *ATP2C1*, which encodes a calcium pump protein. Individuals with Hailey–Hailey present with red scaly plaques in the intertriginous areas of the body. Poblete-Gutierrez et al (4) described a patient with Hailey–Hailey disease who also had unilateral exacerbation with erythematous crusted plaques along the lines of Blaschko. Keratinocytes isolated from the classically affected areas were heterozygous for the mutation in *ATP2C1* as expected, whereas keratinocytes from the regions of linear exacerbation were homozygous for the mutation.

Segmental neurofibromatosis will now be reviewed in greater detail as a clinical example of nonlethal single-gene mosaicism. Segmental neurofibromatosis is a term that describes individuals who have cutaneous signs of neurofibromatosis limited to a defined area of the body. This may be either half of the body, a quadrant, or a smaller area defined by several lines of Blaschko. Skip or patchy involvement has also been described. Localized NF1 follows a similar natural history to generalized NF1 in the affected tissues. Café au lait patches and plexiform neurofibromas present early, whereas neurofibromas develop later in adolescence. Localized NF1 is unlikely to cause systemic complications (5).

Individuals with segmental NF1 are thought to develop their condition as the result of postzygotic mutations in the *NF1* gene. More extensive cutaneous involvement is likely to be the result of an earlier mutational event and therefore carries a greater likelihood for involvement of the gonads and risk of transmission to offspring. Mosaicism caused by very late postzygotic mutations may be a mechanism by which isolated café au lait spots develop. Tinschert et al (6) recently published a study using fluorescence in situ hybridization on cultured fibroblasts from skin with a café au lait patch, and compared it with fibroblasts from normal-appearing skin from the same patient. They detected only a single hybridization signal in the affected skin, compared with two signals from clinically normal skin and lymphocytes, thereby demonstrating mosaicism for a deletion of the *NF1* gene in the fibroblasts from the café au lait patch (6). Consoli et al (7) described a parent with segmental NF who gave birth to a child with generalized NF1. They were able to demonstrate heterozygosity for a nonsense mutation in exon 31 of the *NF1* gene at variable levels in the affected skin from the mother, but not present in her peripheral blood lymphocytes. The mutation was present in the heterozygous state in both the fibroblasts and the peripheral blood lymphocytes of her child. What remains unexplained are several reports of families in which segmental NF1 appears to be segregating as an autosomal dominant condition with segmental expression in parent and child.

Individuals with autosomal dominant lethal conditions can sometimes survive as mosaics. McCune–Albright syndrome, which is characterized by large, segmental, unilateral, dark café au lait patches, polyostotic fibrous dysplasia, and endocrine abnormalities, is likely an autosomal dominant lethal condition in the heterozygous state. Happle (8) suggested that the individual can only survive when there is mosaicism for the mutation. It is now proved that McCune–Albright syndrome is caused by sporadic postzygotic mutations in *GNAS1* gene on chromosome 20q13.2 and that affected individuals are mosaic for these alterations (9). The severity and distribution of expression is dependent on the tissue distribution of the cells with the mutation. Individuals with

McCune–Albright are not at risk to have affected children, even if the germline is involved, because fertilization by a gamete with the *GNAS1* mutation will result in lethality of the conceptus.

Chromosomal mosaicism results from nondisjunction events that also occur after fertilization. This failure of the chromosomes to divide normally may lead to mosaicism for abnormal and normal cell populations, such as 45, X/46, XX Turner syndrome, or to mosaicism for two abnormal cell populations, such as 45, X/46, X, +ring(X) Turner syndrome. In the former situation, the conceptus was presumably chromosomally normal, with the failure of normal mitotic cell division subsequently; in the latter, the conceptus was abnormal and the small ring chromosome was presumably lost at some stage in cell division, giving rise to the 45, X cells.

Nevoid hyper or hypopigmentation refers to a pattern of hypopigmentation or hyperpigmentation of the skin distributed along the lines of Blaschko. Among children with this finding, as many as a third will have other congenital anomalies. In this group, as many as 60% have been shown to be mosaic for chromosomal abnormalities, either in lymphocytes, in fibroblasts, or in both. This condition has been frequently referred to in the literature as "hypomelanosis of Ito," but this designation implies a single disease entity or cause, whereas mosaicism for many different chromosomal abnormalities has been reported. Mosaicism may involve both normal and abnormal cell populations, such as 46, XY/47, XY, +18, or two abnormal cell populations, such as 45, X/46, X, +ring X. Mosaicism for triploidy (46, XY/69, XXY) can also cause hypopigmentation along the lines of Blaschko. Mosaicism for ostensibly balanced (i.e., all the chromosomal material is present, it is just rearranged in an abnormal fashion) chromosomal translocations, where one of each member of two different chromosome pairs have exchanged pieces, has also been shown to cause nevoid hypo/hyperpigmentation. Taibjee and colleagues (10) have suggested that the genome has many genes responsible for pigment production and that the chromosomal abnormalities demonstrated in hypomelanosis of Ito all involve regions where pigment genes are disrupted, but this does not explain the patterns seen in chimeras, who presumably have two normal, albeit distinct, genomes.

Functional mosaicism for genes on the X chromosome occurs in human females because early in embryogenesis, perhaps at about the 32 cell stage of development, one or the other of the two X chromosomes inactivates or turns off. This is true for most of the regions on the X, although a few areas, including the region with the gene for sterol sulfatase, mutations in which cause X-linked ichthyosis, escape inactivation. This inactivation is random, the maternal and the paternal X have equal chances of being inactivated, and it is permanent. Thus, females who are carriers for X-linked recessive conditions may express the condition to varying degrees depending on the proportion and distribution of cells that are expressing the X chromosome with the mutation. In X-linked dominant disorders, affected females are spared the lethality seen in males because of the presence of some cells in which the X chromosome without the mutation is active and thus maintains normal function. Males with Klinefelter syndrome also undergo X-inactivation and thus they may survive in the presence of a lethal X-linked gene because some cells will have an active normal X chromosome.

Focal dermal hypoplasia (FDH: Goltz syndrome) is an X-linked dominant disorder characterized by asymmetric, atrophic, hyperpigmented, or hypopigmented, linear streaks and punctuate cribriform scarring and telangiectases along the lines of Blaschko. Fat herniations appear as linear arrays of yellow nodules. Osteopathia striata is the characteristic radiologic feature, and cutaneous or bony syndactyly is common. In addition, eye abnormalities and dental defects are typical. Focal dermal hypoplasia is generally lethal in hemizygous males. Females survive because of X inactivation, because not all cells in the body express the mutated gene. There have been a few males reported with FDH likely either caused by Klinefelter syndrome (47, XXY) or by a mutation during embryologic development, making the individual mosaic for the condition, thus escaping lethality (11).

Incontinentia pigmenti (IP) is another X-linked dominant condition with similar linear patterns of expression on the skin because of functional mosaicism. It is characterized in the neonatal period by blisters on an erythematous base along the lines of Blaschko (Fig. 1). This is followed by a verrucous phase, then a phase characterized by swirly hyperpigmentation, and ultimately by hypopigmentation and drop-out of follicles and sweat glands. Incontinentia pigmenti is caused by mutations in the *NEMO* gene (NF-kappa B essential modulator) located on the X chromosome (12). The mutation is usually lethal in utero in hemizygous males, resulting in spontaneous abortion. Occasionally, males survive, presumably by one of the same mechanisms – postzygotic mutations (mutations occurring after fertilization) and Klinefelter syndrome (47, XXY).

X-linked recessive hypohidrotic ectodermal dysplasia (HED/EDA1) is manifest in hemizygous males who have only one X chromosome, but are often not clinically apparent in carrier females. However, females can show subtle clinical features due to mosaicism caused by X inactivation, for example, having areas of affected skin in which the normal X is inactivated and only the X

Figure 1. Linear brown verrucous papules demonstrating the lines of Blaschko in a patient with incontinentia pigmenti. Photograph courtesy of Ilona J. Frieden, MD.

chromosome with the mutant gene is expressed. This has been shown in female carriers of X-linked recessive hypohidrotic ectodermal dysplasia (HED) (Christ–Siemens–Touraine syndrome), a severe disorder of the hair, sweat glands, and teeth. Using a starch iodine test, a mosaic distribution of functional sweat glands has been demonstrated along the lines of Blaschko in female carriers (13). Abnormalities of vellus hairs are seen in the same distribution. The authors suggest that testing to show the distribution of sweat glands in females with signs of hypohidrotic ectodermal dysplasia serves as a good tool to distinguish X-linked HED from autosomal recessive HED, because in the latter, homozygous females have a complete absence of sweat glands, and heterozygotes for the autosomal recessive form do not have partial manifestation.

What is shared in common by all these forms of somatic mosaicism: single gene, chromosomal, or X-linked, is that the cutaneous manifestations of mosaicism most often follow the lines of Blaschko.

The lines of Blaschko were first described by the German dermatologist, Alfred Blaschko, in 1901. He recognized lines and whorls of pigmentary and nevoid genetic skin conditions in a V shape on the back that he called the "fountain spray" and an S-shape on the abdomen. This distribution differs from dermatomes, and it has been hypothesized that this pattern may depict the destined and directed route of embryonic ectodermal cell migration, namely keratinocytes and melanocytes (14,15). The extent of skin involvement may depend on the stage of development during which the mutation or chromosomal nondisjunction took place, or on the proportion and distribution of cells that have the normal X inactivated. If the mutation occurs early in embryologic development, then widespread skin patterning may result. If the event takes place later in development, then the mosaicism may be limited to a more confined anatomic region.

Pigmentary mosaicism can also present in several other patterns, including phylloid (meaning leaflike), checkerboard, and patchy pigmentation without midline separation (16).

OTHER MECHANISMS OF MOSAICISM

Revertant mosaicism

Recently, several examples of revertant mosaicism have been described (17–21). Revertant refers to the reversal or correction of a mutation; in other words, a restoration of the wild-type amino acid sequence. When this occurs either during embryogenesis or when the onset is after birth, patches or localized areas of skin show the revertant phenotype on a molecular and clinical level. This mechanism was first described in 1997 for autosomal recessive (AR) non-Herlitz junctional epidermolysis bullosa (EB) when Jonkman et al (19) described a patient who was a compound heterozygote for nonsense and frame-shift mutations in type XVII collagen gene, *COL17A1*. In this case, expression of normal-type XVII collagen occurred in revertant patches of skin that were phenotypically normal and did not blister. The authors hypothesized that the rescue of the phenotype resulted from gene conversion, in which one allele converts the mutated sequence of the other allele to the wild-type sequence (possibly by nonreciprocal exchange).

Another mechanism for reversion is by mRNA rescue of a frame-shift mutation by a downstream second-site mutation. In this situation, the original mutation remains, but the second mutation restores the normal reading frame and allows for effective translation of the protein. If the expressed protein is normal, complete reversion or correction occurs. If the protein now being expressed is aberrant, partially impaired function results and is referred to as a partial revertant. This was demonstrated in another patient with AR non-Herlitz junctional EB. Keratinocytes obtained for culture by laser capture microdissection contained a second insertion downstream from the deletion that restored the reading frame (17). This change was only seen at the molecular level; the phenotype in the patient was not corrected. According to Jonkman (18), several factors are key in determining the revertant phenotype; these include cell lineage, the percentage of cells reverted, and the timing of the reversion, whether during embryogenesis or later in life. Revertant mosaicism is sometimes referred to as "natural gene therapy" and may have implications for future strategies for gene therapy.

Epigenetic mosaicism

Epigenetic mosaicism refers to environmental factors, such as retrotransposons, that cause alterations in the genetic material. Retrotransposons are viral DNA sequences that are incorporated into the nuclear DNA, are replicated, and regulate local genes often by silencing or activating a gene through methylation or demethylation (22). This has been shown to be important in coat color in mice and dogs, but has not been demonstrated in humans. Epigenetic events may play a role in the development of cancer.

Chimeras

A chimera is an organism created when two zygotes (usually both normal) are fused, resulting in an individual who is composed of two genetically distinct cell populations. Although, technically, chimeras are not mosaic because the presence of distinct cell populations is not the result of events arising in a single zygote, we include it here because it can also manifest with segmental pigment patterns on the skin.

CONSIDERATIONS ON SKIN BIOPSIES

Skin biopsy to obtain cell lines to test for mosaicism can be challenging. One must consider which cell lines are likely to be affected when establishing the cell culture and which molecular study will have the greatest sensitivity to detect the mutation. Gonosomal mutations can usually be detected from peripheral blood lymphocytes, whereas the blood is unlikely to show a mutation in somatic mosaicism that has occurred later in embryogenesis. Disorders that follow the lines of Blaschko are expressing in ectodermal derivatives and therefore keratinocyte or melanocyte culture will likely have the highest yield (15). In segmental neurofibromatosis, in which neurofibromas predominate in a dermatomal pattern, fibroblast culture is likely to reveal the mutation.

ACKNOWLEDGMENTS

We would like to thank Ilona J. Frieden, M.D., for her critical review of the manuscript.

REFERENCES

1. Byers PH, Tsipouras P, Bonadio JF et al. Perinatal lethal osteogenesis imperfecta (OI type II): a biochemically heterogeneous disorder usually due to new mutations in the genes for type I collagen. Am J Hum Genet 1988;42:237–248.
2. Paller AS, Syder AJ, Chan YM et al. Genetic and clinical mosaicism in a type of epidermal nevus. N Engl J Med 1994;331:1408–1415.
3. Happle R. Segmental forms of autosomal dominant skin disorders: different types of severity reflect different states of zygosity. Am J Med Genet 1996;66:241–242.
4. Poblete-Gutierrez P, Wiederholt T, Konig A et al. Allelic loss underlies type 2 segmental Hailey–Hailey disease, providing molecular confirmation of a novel genetic concept. J Clin Invest 2004;114:1467–1474.
5. Ruggieri M, Huson SM. The clinical and diagnostic implications of mosaicism in the neurofibromatoses. Neurology 2001;56:1433–1443.
6. Tinschert S, Naumann I, Stegmann E et al. Segmental neurofibromatosis is caused by somatic mutation of the neurofibromatosis type 1 (NF1) gene. Eur J Hum Genet 2000;8:455–459.
7. Consoli C, Moss C, Green S et al. Gonosomal mosaicism for a nonsense mutation (R1947X) in the NF1 gene in segmental neurofibromatosis type 1. J Invest Dermatol 2005;125:463–466.
8. Happle R. The McCune–Albright syndrome: a lethal gene surviving by mosaicism. Clin Genet 1986;29:321–324.
9. Weinstein LS, Yu S, Warner DR, Liu J. Endocrine manifestations of stimulatory G protein alpha-subunit mutations and the role of genomic imprinting. Endocr Rev 2001;22:675–705.
10. Taibjee SM, Bennett DC, Moss C. Abnormal pigmentation in hypomelanosis of Ito and pigmentary mosaicism: the role of pigmentary genes. Br J Dermatol 2004;151:269–282.
11. Happle R. Cutaneous manifestation of lethal genes. Hum Genet 1986;72:280.
12. Smahi A, Courtois G, Vabres P et al. Genomic rearrangement in NEMO impairs NF-kappaB activation and is a cause of incontinentia pigmenti. The International

Incontinentia Pigmenti (IP) Consortium. Nature 2000;405:466–472.
13. Cambiaghi S, Restano L, Paakkonen K et al. Clinical findings in mosaic carriers of hypohidrotic ectodermal dysplasia. Arch Dermatol 2000;136:217–224.
14. Dupin E, Le Douarin NM. Development of melanocyte precursors from the vertebrate neural crest. Oncogene 2003;22:3016–3023.
15. Moss C. Cytogenetic and molecular evidence for cutaneous mosaicism: the ectodermal origin of Blaschko lines. Am J Med Genet 1999;85:330–333.
16. Happle R. Mosaicism in human skin. Understanding the patterns and mechanisms. Arch Dermatol 1993;129:1460–1470.
17. Darling TN, Yee C, Bauer JW et al. Revertant mosaicism: partial correction of a germ-line mutation in COL17A1 by a frame-restoring mutation. J Clin Invest 1999;103:1371–1377.
18. Jonkman MF, Castellanos Nuijts M, van Essen AJ. Natural repair mechanisms in correcting pathogenic mutations in inherited skin disorders. Clin Exp Dermatol 2003;28:625–631.
19. Jonkman MF, Scheffer H, Stulp R et al. Revertant mosaicism in epidermolysis bullosa caused by mitotic gene conversion. Cell 1997;88:543–551.
20. Pasmooij AM, Pas HH, Deviaene FC et al. Multiple correcting COL17A1 mutations in patients with revertant mosaicism of epidermolysis bullosa. Am J Hum Genet 2005;77:727–740.
21. Smith FJ, Morley SM, McLean WH. Novel mechanism of revertant mosaicism in Dowling–Meara epidermolysis bullosa simplex. J Invest Dermatol 2004;122:73–77.
22. Druker R, Whitelaw E. Retrotransposon-derived elements in the mammalian genome: a potential source of disease. J Inherit Metab Dis 2004;27:319–330.

Chapter 20

The Neurofibromatoses

Karen Stephens

Neurofibromatosis type 1 and neurofibromatosis type 2 are two distinct genetic disorders that predispose to the development of tumors primarily of the nervous system (Table 20-1).[1] A recently recognized third form of neurofibromatosis, known as schannomatosis,[2] is not included in this review, as molecular genetic testing is unavailable for this disorder.

NEUROFIBROMATOSIS TYPE 1

Molecular Basis of Disease

Neurofibromatosis type 1 (NF1) is an autosomal dominant progressive disorder with high penetrance but extremely variable expressivity (reviewed in References 1, 3, and 4). The cardinal features are café au lait macules, intertrigenous freckling, Lisch nodules, and multiple neurofibromas, although numerous other features and complications are common. Criteria for a diagnosis of NF1 were established in 1987 by a consensus meeting of the National Institutes of Health diagnostic criteria and are widely used.[5] Neurofibromas are benign nerve sheath tumors that arise on peripheral nerves. Cutaneous neurofibromas develop in virtually all cases of NF1, typically appear in the second decade of life, grow slowly, increase in number with age, and are considered at low risk for transformation to a malignant peripheral nerve sheath tumor (MPNST; previously known as neurofibrosarcoma). In contrast, diffuse plexiform neurofibromas and deep nodular plexiform neurofibromas are considered at increased risk for transformation to MPNST. Individuals affected with NF1 have a lifetime risk for MPNST of 8% to 13%.[6] Other neoplasms epidemiologically associated with NF1 include medulloblastoma, pheochromocytoma, astrocytoma, and adenocarcinoma of the ampulla of Vater. Primarily children affected with NF1 are at increased risk for optic pathway and brainstem gliomas, rhabdomyosarcomas, and malignant myeloid leukemias. NF1 patients are also at increased risk for a second malignancy, some of which may be treatment related.

NF1 is caused by inactivating mutations of 1 copy of the *NF1* gene resulting in haploinsufficiency for the gene product neurofibromin (Table 20-1). About 85% to 90% of constitutional mutations are nonsense, splicing, and missense; they are distributed throughout the gene, although some exons appear to be mutation rich (Figure 20-1). An estimated 5% of mutations are large contiguous gene deletions typically of 1.4 megabases (Mb) that delete 1 entire *NF1* allele (reviewed in Reference 7). About one half of cases are familial (inherited from an affected parent) and one half are sporadic, resulting from a de novo *NF1* mutation. An unknown fraction of sporadic cases are due to postzygotic mutation of the *NF1* gene, which complicates mutation detection and counseling issues. Neurofibromin functions as a negative regulator of the *RAS* oncogene by stimulating the conversion of active guanosine 5′-triphosphate (GTP)-bound RAS to the inactive guanosine 5′-diphosphate (GDP)-bound form by hydrolyzing GTP. Biochemical, cell culture, and genetic studies in both NF1 patients and mouse models are consistent with a model whereby a somatic mutation inactivates the remaining functional *NF1* gene (leading to increased activated RAS) in a progenitor Schwann cell as an early, probably initiating, event in the development of neurofibromas (reviewed in Reference 8). Biallelic inactivation of *NF1* also occurs in other types of progenitor cells that give rise to NF1-associated tumors such as glioma and myeloid malignancies.

Clinical Utility of Testing

A diagnosis of NF1 can almost always be made based on clinical findings, particularly after 8 years of age. Clinical DNA-based testing is available from many licensed clinical laboratories (see GeneTests, http://www.genetests.org/). Testing is not typically used for diagnostic purposes, but can be useful for confirming a clinical diagnosis, reproductive counseling, and prenatal or preimplantation diagnosis. Blanket recommendations for diagnostic testing for NF1 cannot be made because the sensitivity of clinical

Table 20-1. Comparison of Features of the NF1 and NF2 Disorders

Feature	Neurofibromatosis 1	Neurofibromatosis 2
Alternate name	Peripheral neurofibromatosis; von Recklinghausen neurofibromatosis	Central neurofibromatosis; bilateral acoustic neuroma
OMIM accession number*	162200	101000
Mode of inheritance	Autosomal dominant	Autosomal dominant
Frequency of disorder	1/3000–1/4000	1/25,000
Fraction of sporadic cases	30–50%	~50%
Gene symbol	*NF1*	*NF2*
Chromosomal location	17q11.2	22q12.2
Gene size; transcript size	~350 kb; ~11–13 kb†	~110 kb; 2 kb†
GenBank accession no. (gene; cDNA)‡	NT_010799; NM_000267	Y18000; NM••000268
Number of exons	60	17
Tissue expression pattern	Widely expressed	Widely expressed
Protein product (size; no. of residues)	Neurofibromin (>220 kDa; 2818)	Merlin; also known as schwannomin (65 kDa; 595)
Normal functions of protein	Tumor suppressor; negative regulator of ras oncogene	Tumor suppressor; associates with proteins of the cytoskeleton
Commonly associated tumors	Neurofibroma, MPNST, optic pathway and brainstem gliomas	Bilateral vestibular schwannomas, schwannomas of other central and peripheral nerves, meningiomas
Animal models	Mouse, fruit fly	Mouse, fruit fly

* Online Mendelian Inheritance in Man [database online] (http://www.ncbi.nlm.nih.gov:80/entrez/query.fcgi?db=OMIM).
† Alternative splicing produces transcripts of varying lengths.
‡ See Gene Lynx Human (http://www.genelynx.org/) for a compilation of, and hyperlinks to, gene, protein structure, and genomic resources.

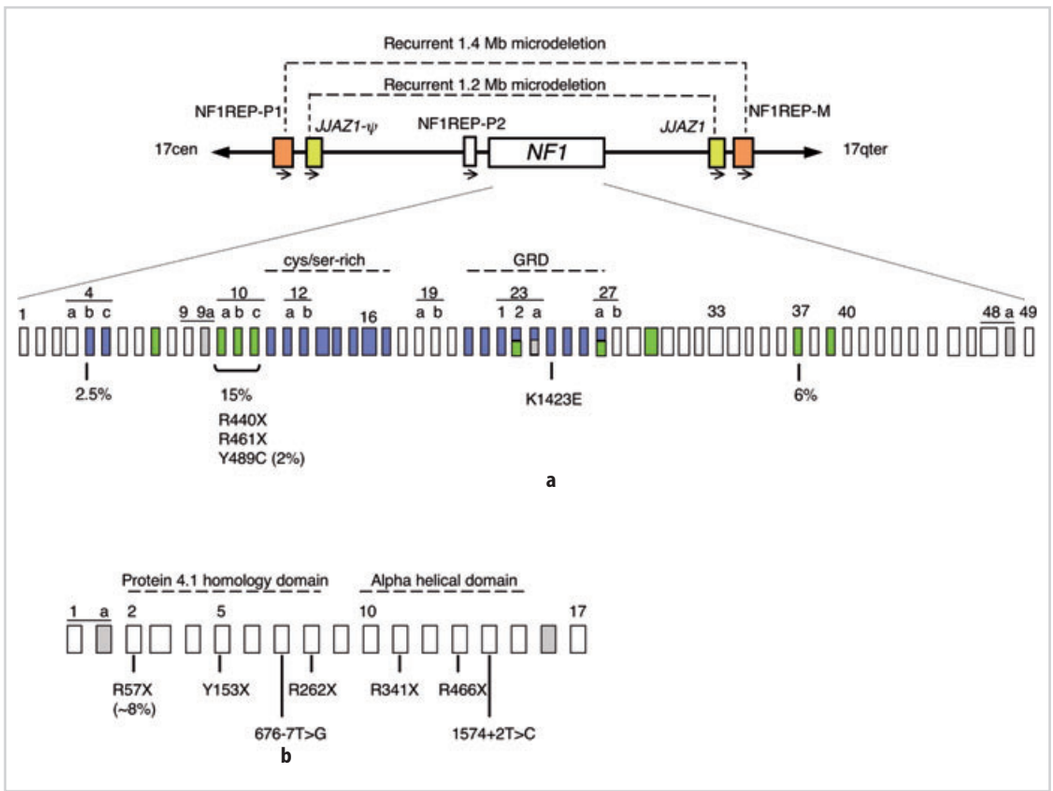

Figure 20-1. *NF1* and *NF2* genes: genomic structure and mutations. (a) At the top is a schematic of the *NF1* gene region at chromosome segment 17q11.2. The 350 kb *NF1* gene is flanked by 2 different sets of directly oriented paralogs. The 51 kb paralogs NF1REP-P1 (previously termed NF1REP-P) and NF1REP-M (orange boxes) and the 46 kb *JJAZ1* gene and pseudogene (−ψ) (yellow boxes) are shown. Homologous recombination between NF1REP elements results in a recurrent 1.4 megabase (Mb) microdeletion, while recombination between the *JJAZ1* paralogs results in a recurrent 1.2 Mb microdeletion.[11,16] NF1REP-P2 is a partial element with a limited role in mediating *NF1* microdeletions. The 60 exons of *NF1* are represented by boxes (not to scale), and exon numbering is sequential except as indicated. The GRD (exons 21-27a) and a cysteine/serine-rich domain with 3 cysteine pairs suggestive of ATP binding (exons 11-17) are indicated. Gray boxes indicate alternatively spliced exons that vary in abundance in different tissues. Mutations have been identified in virtually every exon. Exons where mutations are apparently in greater abundance than expected are indicated (green boxes).[21,22,25] In one study, exons 7, 10a, b, c, 23-2, 27a, 29, and 37 accounted for 30% of mutations, 15 of which were in exons 10a, b, and c, which harbor 3 recurrent mutations, including Y489C, which alone accounts for approximately 2% of mutations.[21] Blue boxes indicate exons that have clusters of missense or single base or codon deletion mutations, or both.[22] Some of the recurrent, although still infrequent, mutations are given below the exons. (b) The 17 exons of the *NF2* gene are represented by boxes (drawing not to scale), and the exon numbering is sequential. The protein 4.1-homology domain thought to mediate binding to cell surface glycoproteins (exons 2-8), the α-helical domain (exons 10-15), and the unique C-terminus (exons 16-17) are shown. Gray boxes indicate alternatively spliced exons; the inclusion of exon 16 creates an alternate termination codon resulting in a slightly truncated protein. Mutations have been identified involving each exon except for 16. Selected recurrent mutations found in a limited survey of references cited in the text are indicated. In several studies, R57X occurred in 8% of familial constitutional mutations.

diagnosis for NF1 is very high and the sensitivity of molecular testing is not 100%. Furthermore, benefits of diagnostic testing are subjective and may differ from family to family. Early planning is necessary for couples considering prenatal diagnosis using amniocytes or chorionic villus tissue or preimplantation diagnosis. These tests are available only when the pathogenic familial germline mutation (or the predisposing haplotype in the case of linkage testing) has been identified previously in an affected parent, a process that can require weeks or months.

The primary genetic counseling issue related to molecular testing of *NF1* is the inability to predict the severity or course of the disorder in a patient or fetus. Even among family members who carry the same *NF1* mutation, there can be considerable variation in clinical manifestations and complications. For the majority of cases, there is no correlation between genotype and phenotype. For the approximately 5% of individuals who carry a constitutional *NF1* deletion (most commonly 1.4 Mb), there is a 2-fold increased lifetime risk of MPNST,[9] a predisposition to childhood overgrowth,[10] an early age of onset with excessive numbers of cutaneous neurofibromas, numerous internal neurofibromas, learning disabilities, vascular anomalies, and astrocytomas (References 7 and 11 to 14 and references therein). A recommendation for routine testing for *NF1* microdeletion has been proposed, with follow-up for increased suspicion for MPNST.[9]

NF1 testing may be useful to confirm a diagnosis in a patient with equivocal findings, such as child who has a few café au lait macules and carries a presumptive diagnosis of NF1. In such cases, it is important to realize that the sensitivity and specificity of testing patients who do not fulfill the NIH diagnostic criteria for a diagnosis of *NF1* is unknown but is likely to be quite low.

For unaffected parents of a child with sporadic NF1, recurrence risk is a concern. Although thought to be rare, germline mosaicism has been reported in an asymptomatic parent of a child with sporadic NF1.[15] Therefore, there is a small, but unknown, increased risk of recurrence even if the child's pathogenic mutation is not detected in the genomic DNA from parental leukocytes. Although the frequency is unknown, sporadic NF1 cases with postzygotic mutations resulting in somatic mosaicism may not be as rare as once thought. One study suggests that among NF1 microdeletion cases, the frequency of somatic deletion may be very high (~40%).[16] Assuming that 10% of NF1 cases have microdeletions, a frequency of 4% mosaicism is expected in the general NF1 population. This is certainly an underestimate, as it does not consider mosaicism for intragenic *NF1* mutations. Mosaic individuals carry the *NF1* mutation in only a fraction of their cells, depending on the developmental interval and the cell type in which the mutation occurred. The phenotype of mosaic individuals ranges from localized (segmental) disease to mild or severe generalized disease.[16,17] The sensitivity of mutation detection may be lower due to an increased signal to noise ratio, that is, a low level of a mutant allele in a background of 2 normal *NF1* alleles. Offspring that inherit an NF1 mutation from a parent with mosaicism, however, will have a constitutional *NF1* mutation and may have more severe disease than their mosaic parent. Genetic counseling regarding the clinical and reproductive implications of NF1 mosaicism is highly recommended.[17]

Available Assays

Mutation of the *NF1* gene is the only known cause of the disorder. Molecular tests for diagnostic, prenatal, and preimplantation diagnosis are available. The choice of assay and testing laboratory depends upon the reason for referral and mutation types and detection rates of their assay(s).

Fluorescent in situ hybridization (FISH; see chapter 2) with *NF1* probes of either metaphase or interphase white blood cells is the optimal test to rule out or confirm the approximately 5% of cases due to a submicroscopic NF1 microdeletion (Figure 20-1).[18] In the future, a first-tier test may employ an *NF1* deletion junction-specific polymerase chain reaction (PCR) assay.[19] The recent availability of high-resolution genomic microarrays of the NF1 deletion region will facilitate clinical testing by array–comparative genomic hybridization (CGH),[20] which may become clinically important in the future if deletions involving a subset of genes predispose to certain manifestations. The sensitivity of deletion-specific PCR and array-CGH assays to detect low-level *NF1* deletion mosaicism will need to be determined. Routine cytogenetic analysis is of limited clinical utility, as the *NF1* microdeletions are submicroscopic, and translocation and rearrangement involving *NF1* are extremely rare.

Linkage analysis is an indirect test that tracks the inheritance of the mutant *NF1* allele in members of a family. This may be the quickest, most economical NF1 test for at-risk individuals and fetuses of families that fulfill the testing criteria. The primary requirement is the availability and cooperation of multiple family members whose NF1 status is known by detailed clinical evaluation. Multiple *NF1* intragenic polymorphic markers are available that facilitate identification and tracking of the predisposing haplotype in a family and provide the specificity for linkage testing.

Efficient detection of subtle intragenic *NF1* gene mutations, for purposes of diagnostic testing or mutation typing for prenatal or preimplantation diagnosis, is complicated by the large number of exons and large size of the gene (Table 20-1), variation in type and distribution of mutations, and large fraction of private mutations. About 70% to 80% of mutations result in a premature translation termination codon, with nonsense and splicing defects being

the most common.[21] These mutations can be detected by the protein truncation test (PTT; see chapter 2), which detects truncated neurofibromin polypeptides synthesized by in vitro translation of multiple overlapping *NF1* complementary DNA (cDNA) segments. A detection rate of about 80% can be attained with an optimized PTT testing protocol (see below). The majority of such mutations are private to each individual or family, although there are recurrent mutations that may account for, at most, a few percent of cases (Figure 20-1).

About 10% of *NF1* mutations are missense or in-frame insertions or deletions of a few nucleotides,[21,22] some of which show clustering (Figure 20-1). Their identification requires direct sequence analysis of *NF1* exons and splice junctions in genomic DNA or cDNA segments. Prospective testing of NF1 subjects by direct genomic sequence analysis revealed a detection rate of 89%, which is more streamlined than PTT testing and allows for automation.[23] Various mutation scanning techniques of *NF1* genomic or cDNA are also employed by clinical laboratories, including denaturing high-performance liquid chromatography (DHPLC), temperature gradient gel electrophoresis (TGGE), single-strand conformation polymorphism (SSCP), and heteroduplex analysis (HA; see chapter 2). Although high detection rates are reported in the literature using DHPLC (72–95%),[24,25] it is important to realize that the detection rates for mutation scanning protocols will be laboratory specific due to the degree of optimization of the specific technique. A survey of clinical laboratories is recommended prior to sample submission. DHLPC has the advantages of using genomic DNA and high-throughput capability compared to the cDNA/gel-based PTT; however, a recently reported high-throughput PTT may be available for clinical testing in the future.[26]

Interpretation of Test Results

The detection of a truncated neurofibromin polypeptide by PTT can result in false positives.[21] High specificity requires identifying the underlying mutation at the genomic DNA or cDNA level, or both, since false positives can arise during sample handling (see below). The interpretation of missense and subtle in-frame alterations as pathogenic mutations rather than neutral polymorphisms is complicated by the lack of a functional assay for neurofibromin. Apparent recurrence of a putative mutation requires careful study of the literature, since not all *NF1* mutational studies sequenced the entire gene. No comprehensive *NF1* mutation database is available; however, some mutations have been submitted to the Human Gene Mutation Database (http://archive.uwcm.ac.uk/uwcm/mg/hgmd0.html), and the largest NF1 database is actively managed and analyzed by Jan Friedman (http://www.medgen.ubc.ca/friedmanlab/). Although most likely rare, affected family members with different independent *NF1* inactivating mutations have been reported,[27] presumably a reflection of the high mutation rate of the gene (~10^5/gamete/generation). The interpretation of FISH with *NF1* probes can be complicated by mosaicism for an *NF1* microdeletion; therefore, an appropriate number of cells must be analyzed.[16] The frequency of mosaicism for an *NF1* mutation is not known; however, this is likely the underlying mechanism for patients with segmental or localized signs of the disorder.

Laboratory Issues

Optimal detection of mutations that predict a truncated neurofibromin polypeptide occurs when the nonsense-mediated decay pathway is at least partially inhibited, thereby increasing the ratio of mutant transcripts with a premature termination codon to normal transcripts. A protein synthesis inhibitor, such as puromycin, in the culture medium is effective for EBV-transformed lymphoblasts or phytohemaglutinin-stimulated primary lymphocytes.[21,28] Furthermore, blood handling and shipping protocols must be used to reduce false positives in PTT resulting from environmental effects such as cold shock[29] or delay in messenger RNA isolation.[21,28] There is no standardized proficiency program of interlaboratory comparison for *NF1* testing; performance assessment must be conducted by participation in ungraded proficiency survey programs, split sample analysis with other laboratories, or other suitable and documented proficiency-testing methods. No *NF1* testing kits, probes, or controls are approved or cleared by the Food and Drug Administration. Intronic primers for amplification of *NF1* exons and associated splice junctions that apparently do not coamplify the *NF1* pseudogene fragments have been reported.[23,30] Two other factors require consideration during test development and interpretation. Reports in support of,[31] and in opposition to,[32] an apparent tandem duplication of the *NF1* gene region have been published. In addition, transcriptional activity from *NF1* pseudogenes or pseudogene fragments has been reported.[33] Some issues related to *NF1* testing have been reviewed recently.[34]

NEUROFIBROMATOSIS TYPE 2

Molecular Basis of Disease

The development of bilateral vestibular schwannomas is a hallmark of neurofibromatosis type 2 (NF2). Other commonly associated tumors include schwannomas of other central, spinal, and peripheral nerves and meningiomas (reviewed in References 1 and 35 to 38). This is a life-threatening disorder due to the location of the tumors, along with the propensity for development of multiple

tumors. Most patients become completely deaf and can have poor balance and vision, and weakness. The mean age of onset is 18 to 24 years and the mean age of death is 36 years. The age at onset of symptoms and age at diagnosis are predictors of vestibular schwannoma growth rates and risk of death (Reference 39 and references therein). Ependymomas and astrocytomas occur less frequently and are usually indolent central nervous system tumors. Patients affected with NF2 are at minimal increased risk for malignancy. Juvenile posterior subcapsular cataract is a common nontumor manifestation. The disorder may be underdiagnosed in children who present with ocular and skin manifestations. Early diagnosis improves management, which is primarily surgical and radiological. Modifications to the criteria for a diagnosis of NF2, initially established by the 1987/1991 National Institute of Health Consensus Conference, have been proposed to increase the specificity.[40] A consensus statement on management of the NF2 patient and family was recently published.[41]

NF2 is caused by haploinsufficiency for the tumor suppressor merlin (also known as schwannomin), the protein product of the *NF2* gene (Table 20-1). About one half of patients are the first case of NF2 in the family. These sporadic cases result from de novo mutation of the *NF2* gene, a significant fraction of which are postzygotic mutations that result in mosaicism. The majority of constitutional mutations are private, predict the truncation of merlin, and are distributed throughout the gene (see below). In NF2 patients, a vestibular schwannoma develops from a progenitor Schwann cell that carries a somatic inactivating mutation in the single remaining *NF2* gene. Merlin is a protein of the cytoskeleton whose normal function remains to be determined, although it is known to associate with transmembrane proteins important in adhesion, proteins involved in signaling pathways, and cytoskeletal proteins (reviewed in Reference 42).

Clinical Utility of Testing

DNA-based clinical testing for NF2 is available (see GeneTests, http://www.genetests.org) and primarily is used for presymptomatic testing of at-risk individuals, typically young children of an affected parent. An early diagnosis of NF2 may improve outcome, and at-risk children who did not inherit the *NF2* mutation can be spared worry, costly brain imaging, and audiologic screening. Genetic counseling is recommended prior to testing presymptomatic at-risk children. Testing is also useful to confirm a clinical diagnosis, which may be most helpful in sporadic cases of NF2, particularly children who present with ocular or skin manifestations or adults with equivocal findings or mild disease. Some of these cases may be mosaic for an *NF2* mutation, as the estimated frequency of mosaicism is high (16.7–24.8% of sporadic cases).[43] Genetic counseling regarding the clinical and reproductive implications of *NF2* mosaicism is recommended.[17] Testing is also useful for reproductive counseling and prenatal or preimplantation diagnosis.[44] Prenatal diagnosis of NF2 using amniocytes or chorionic villus tissue is available only in cases where the pathogenic *NF2* germline familial mutation (or predisposing haplotype in the case of linkage testing) has been identified previously in an affected parent. For preimplantation genetic diagnosis, the specific parental *NF2* mutation must be known. Prepregnancy planning is important for couples considering prenatal diagnosis or preimplantation diagnosis. For sporadic NF2 patients undergoing surgery, it is advisable to freeze a portion of the tumor, which may be valuable at a later date for mutation identification if the patient is mosaic.

The primary genetic counseling issues regard predicting the course of the disorder and recurrence risks. There are genotype-phenotype correlations, but they cannot predict the age of onset or the course of disease for an individual patient. About 50% of *NF2* mutations are nonsense or frameshift, with about 24% splice site, 11% to 30% submicroscopic deletion, and 5% missense.[45] Typically, constitutional frameshift and nonsense mutations are associated with more severe NF2, defined by earlier age at onset and higher frequency and mean number of tumors.[46,47] Constitutional missense and small in-frame mutations are associated with mild disease,[47] and mutations in splice donor and acceptor sites result in variable clinical outcomes.[48] Interestingly, individuals with *NF2* splice-site mutations in exons 1 through 5 had an earlier age at onset and greater numbers of intracranial meningiomas compared to those with splice-site mutations in exons 11 through 15 (Figure 20-1b).[45] The type of constitutional *NF2* mutation is also correlated with the number of NF2-associated nonvestibular nervous system tumors including intracranial meningiomas, spinal tumors, and peripheral nerve tumors.[39] Individuals with constitutional nonsense or frameshift *NF2* mutations had significantly more of these tumors than individuals carrying missense, splice-site, or deletion mutations or somatic mosaicism.

Recurrence risks for asymptomatic parents of an affected child are unknown but are somewhat greater than the population risk, due to the possibility of germline mosaicism in a parent.[49] For mosaic patients, the risk of transmitting NF2 to offspring is ≤50%, depending on the proportion of gametes that carry the *NF2* mutation.[17] Offspring that do inherit the mutation, however, will have a constitutional *NF2* mutation and may have more severe disease than their mosaic parent. Testing asymptomatic parents of a child with NF2 has the potential to identify a mosaic mutation.

Available Assays

Mutation of the *NF2* gene is the only known cause of this disorder. Linkage analysis is clinically available for at-risk individuals and fetuses with multiple family members of

unambiguous clinical status regarding NF2 disease who are willing to participate in the testing process. The availability of highly informative intragenic *NF2* polymorphisms increases the specificity of this method. For certain families, linkage analysis will be the most cost- and time-effective test that gives a definitive diagnosis. It can sometimes be an option when mutation-scanning or sequencing test results are negative. See "Interpretation of Test Results," below, for cautions regarding linkage test interpretation.

Identifying an *NF2* mutation typically requires a multipronged testing protocol due to the high frequency of private constitutional mutations, the high frequency of postzygotic mutations, the different types of *NF2* mutations, and the distribution of mutations throughout the gene. Wallace et al.[50] (Figure 20-1b) describe a comprehensive testing service that includes 4 PCR reactions using a meta-PCR technique to link the amplicons into chimeric concatemers for direct sequencing, gene dosage PCR for deletions, loss of heterozygosity (LOH) studies, and subsequent sequencing of the gene in tumor tissue. In prospective studies, this approach yielded an 88% detection rate in familial NF2 cases and a 59% detection rate in sporadic NF2 cases. Direct sequencing or exon-scanning techniques (e.g., SSCP, TGGE, and HA; see chapter 2) of DNA from peripheral leukocytes, followed by direct sequencing to identify the underlying *NF2* mutation, generally have a lower detection rate.[46,47,51–53] The detection rate of either sequencing or exon scanning methods is significantly lower (34–51%) in sporadic cases in part due to the high frequency of postzygotic *NF2* mutations, which can be masked by the presence of normal alleles.[47,48,51,53] The mutation detection rate of mosaic cases can be increased 6 significantly by analysis of tumor tissue (see below).

Because schwannomas are clonal tumors with minimal cellular admixture, *NF2* mutations can be detected at high frequency in tumor tissue. Testing of tumor tissue is available clinically (see GeneTests, http://www.geneclinics.org/) and is most useful in cases where a mutation is not detected in primary lymphoblasts, where clinical manifestations are suggestive of somatic mosaicism, or where constitutional tissue is unavailable.[43,50,53] Moyhuddin et al.[53] nearly doubled the mutation detection rate among mosaic cases using vestibular schwannoma tissue rather than peripheral leukocytes. Mutations are likely to be germline (rather than somatic) if the identical mutation is detected in 2 or more pathologically or anatomically distinct tumors or if a tumor shows LOH for *NF2* intragenic or flanking loci, while constitutional tissue is heterozygous at these loci. Mutational analysis of tumor tissues is expected to have the greatest sensitivity for *NF2* somatic mosaic mutations[43] and sporadic cases with negative results from mutation scanning or sequencing tests.[54]

Efficient detection of the 11% to 30% of constitutional *NF2* deletions (typically multiexonic in nature) has been accomplished using numerous techniques, including FISH, various gene dosage PCR assays, multiplex ligation-dependent probe amplification (MPLA), and high-resolution genomic arrays.[53,55–57] 7

Note that for mutation scanning tests and deletion-detection assays, detection rates will be laboratory specific due to the varying degrees of optimization of the technique; therefore, a survey of testing laboratories is recommended prior to sample submission.

Interpretation of Test Results

Interpretation of the results of exon-scanning tests requires identifying the underlying *NF2* mutation at the genomic DNA or cDNA level, or both, to avoid false positives. Functional assays for merlin have been developed that can provide insight into the interpretation of missense and subtle in-frame alterations as pathogenic mutations rather than neutral polymorphisms;[58–60] however, such assays may not be part of a clinical testing protocol. An international *NF2* mutation database is available (Neurofibromatosis 2 (NF2) Mutation Databases, http://uwcmml1s.uwcm.ac.uk/uwcm/mg/nf2/), and this site also recognizes the United Kingdom population-based registry. Some mutations are also detailed in the Human Gene Mutation Database Cardiff (http://archive.uwcm.ac.uk/uwcm/mg/hgmd0.html). Somatic mosaicism or *NF2* gene deletions must be considered in patients who have a negative mutation test using DNA from peripheral leukocytes, regardless of the severity of their manifestations. The risk of recurrence from mosaic parent to offspring is considered very low if an *NF2* mutation cannot be identified in the parent.[53] NF2 linkage tests should consider excluding the first affected member in a family; if they are mosaic, the linkage results will be misleading in the next generation.[61] For similar reasons, linkage analysis for presymptomatic testing of subjects in this "next" generation should be performed with caution.

Laboratory Issues

There is no standardized proficiency program of interlaboratory comparison for *NF2* testing; performance assessment must be conducted by participation in ungraded proficiency survey programs, split sample analysis with other laboratories, or other suitable and documented proficiency-testing methods. No *NF2* testing kits, probes, or controls are approved or cleared by the Food and Drug Administration. Direct gene sequencing may not be the optimal test to detect *NF2* mosaic mutations in lymphoblasts, since reliable detection of a low-level point mutation will be difficult. Exon-scanning techniques that are semiquantitative, such as TGGE, will detect relative intensity differences between heteroduplexes and homoduplexes that suggest possible mosaicism.[51] Depending on age, fixation, and storage conditions, some tumors may not yield nucleic acid of sufficient quality for mutational analysis.

References

1. Friedman JM, Butmann DH, MacCollin M, Riccardi VM, eds. *Neurofibromatosis: Phenotype, Natural History, and Pathogenesis.* 3rd ed. Baltimore: Johns Hopkins University Press; 1999.
2. MacCollin M, Chiocca EA, Evans DG, et al. Diagnostic criteria for schwannomatosis. *Neurology.* 2005;64:1838–1845.
3. Friedman JM. Neurofibromatosis 1: clinical manifestations and diagnostic criteria. *J Child Neurol.* 2002;17:548–554.
4. Friedman JM. Neurofibromatosis 1. In: GeneReviews at GeneTests: Medical Genetics Information Resource [database online]. Seattle: University of Washington; 1997–2005. Available at: http://www.genetests.org. Accessed October 20, 2005. Updated October 5, 2004.
5. DeBella K, Szudek J, Friedman JM. Use of the national institutes of health criteria for diagnosis of neurofibromatosis 1 in children. *Pediatrics.* 2000;105(pt 1):608–614.
6. Evans DG, Baser ME, McGaughran J, Sharif S, Howard E, Moran A. Malignant peripheral nerve sheath tumours in neurofibromatosis 1. *J Med Genet.* 2002;39:311–314.
7. Stephens K. Neurofibromatosis 1. In: Lupski JR, Stankiewicz P, eds. *Genomic Disorders: The Genomic Basis of Genetic Disease.* Trenton, NJ: Humana Press; in press.
8. Dasgupta B, Gutmann DH. Neurofibromatosis 1: closing the GAP between mice and men. *Curr Opin Genet Dev.* 2003;13:20–27.
9. De Raedt T, Brems H, Wolkenstein P, et al. Elevated risk for MPNST in NF1 microdeletion patients. *Am J Hum Genet.* 2003;72:1288–1292.
10. Spiegel M, Oexle K, Horn D, et al. Childhood overgrowth in patients with common NF1 microdeletions. *Eur J Hum Genet.* 2005;13:883–888.
11. Dorschner MO, Sybert VP, Weaver M, Pletcher BA, Stephens K. NF1 microdeletion breakpoints are clustered at flanking repetitive sequences. *Hum Mol Genet.* 2000;9:35–46.
12. Gutmann DH, James CD, Poyhonen M, et al. Molecular analysis of astrocytomas presenting after age 10 in individuals with NF1. *Neurology.* 2003;61:1397–1400.
13. Venturin M, Guarnieri P, Natacci F, et al. Mental retardation and cardiovascular malformations in NF1 microdeleted patients point to candidate genes in 17q11.2. *J Med Genet.* 2004;41:35–41.
14. Kehrer-Sawatzki H, Kluwe L, Funsterer C, Mautner VF. Extensively high load of internal tumors determined by whole body MRI scanning in a patient with neurofibromatosis type 1 and a non-LCR-mediated 2-Mb deletion in 17q11.2. *Hum Genet.* 2005;116:466–475.
15. L'Azaro C, Gaona A, Lynch M, Kruyer H, Ravella A, Estivill X. Molecular characterization of the breakpoints of a 12-kb deletion in the NF1 gene in a family showing germ-line mosaicism. *Am J Hum Genet.* 1995;57:1044–1049.
16. Kehrer-Sawatzki H, Kluwe L, Sandig C, et al. High frequency of mosaicism among patients with neurofibromatosis type 1 (NF1) with microdeletions caused by somatic recombination of the JJAZ1 gene. *Am J Hum Genet.* 2004;75:410–423.
17. Ruggieri M, Huson SM. The clinical and diagnostic implications of mosaicism in the neurofibromatoses. *Neurology.* 2001;56:1433–1443.
18. Leppig KA, Viskochil D, Neil S, et al. The detection of contiguous gene deletions at the neurofibromatosis 1 locus with fluorescence in situ hybridization. *Cytogenet Cell Genet.* 1996;72:95–98.
19. Lopez-Correa C, Dorschner M, Brems H, et al. Recombination hotspot in NF1 microdeletion patients. *Hum Mol Genet.* 2001;10:1387–1392.
20. Mantripragada KK, Thuresson AC, Piotrowski A, et al. Identification of novel deletion breakpoints bordered by segmental duplications in the NF1 locus using high-resolution array-CGH. *J Med Genet.* 2005.
21. Messiaen LM, Callens T, Mortier G, et al. Exhaustive mutation analysis of the NF1 gene allows identification of 95% of mutations and reveals a high frequency of unusual splicing defects. *Hum Mutat.* 2000;15:541–555.
22. Fahsold R, Hoffmeyer S, Mischung C, et al. Minor lesion mutational spectrum of the entire NF1 gene does not explain its high mutability but points to a functional domain upstream of the GAP-related domain. *Am J Hum Genet.* 2000;66:790–818.
23. Mattocks C, Baralle D, Tarpey P, Ffrench-Constant C, Bobrow M, Whittaker J. Automated comparative sequence analysis identifies mutations in 89% of NF1 patients and confirms a mutation cluster in exons 11–17 distinct from the GAP related domain. *J Med Genet.* 2004;41:e48.
24. Han SS, Cooper DN, Upadhyaya MN. Evaluation of denaturing high performance liquid chromatography (DHPLC) for the mutational analysis of the neurofibromatosis type 1 (NF1) gene. *Hum Genet.* 2001;109:487–497.
25. De Luca A, Buccino A, Gianni D, et al. NF1 gene analysis based on DHPLC. *Hum Mutat.* 2003;21:171–172.
26. Gite S, Lim M, Carlson R, Olejnik J, Zehnbauer B, Rothschild K. A high-throughput nonisotopic protein truncation test. *Nat Biotechnol.* 2003;21:194–197.
27. Klose A, Peters H, Hoffmeyer S, et al. Two independent mutations in a family with neurofibromatosis type 1 (NF1). *Am J Med Genet.* 1999;83:6–12.
28. Wimmer K, Eckart M, Rehder H, Fonatsch C. Illegitimate splicing of the NF1 gene in healthy individuals mimics mutation-induced splicing alterations in NF1 patients. *Hum Genet.* 2000;106:311–313.
29. Ars E, Serra E, de la Luna S, Estivill X, Lazaro C. Cold shock induces the insertion of a cryptic exon in the neurofibromatosis type 1 (NF1) mRNA. *Nucleic Acids Res.* 2000;28:1307–1312.
30. Li Y, O'Connell P, Breidenbach HH, et al. Genomic organization of the neurofibromatosis 1 gene (NF1). *Genomics.* 1995;25:9–18.
31. Gervasini C, Bentivegna A, Venturin M, Corrado L, Larizza L, Riva P. Tandem duplication of the NF1 gene detected by high-resolution FISH in the 17q11.2 region. *Hum Genet.* 2002;110:314–321.
32. Kehrer-Sawatzki H, Messiaen L. Interphase FISH, the structure of reciprocal translocation chromosomes and physical mapping studies rule out the duplication of the NF1 gene at 17q11.2. A reply. *Hum Genet.* 2003;113:188–190.
33. Yu H, Zhao X, Su B, et al. Expression of NF1 pseudogenes. *Hum Mutat.* 2005;26:487–488.
34. Thomson SA, Fishbein L, Wallace MR. NF1 mutations and molecular testing. *J Child Neurol.* 2002;17:555–561; discussion 71–72, 646–651.
35. Ruggieri M, Iannetti P, Polizzi A, et al. Earliest clinical manifestations and natural history of neurofibromatosis type 2 (NF2) in childhood: a study of 24 patients. *Neuropediatrics.* 2005;36:21–34.
36. Baser ME, DG RE, Gutmann DH. Neurofibromatosis 2. *Curr Opin Neurol.* 2003;16:27–33.
37. Evans DG, Sainio M, Baser ME. Neurofibromatosis type 2. *J Med Genet.* 2000;37:897–904.
38. Evans DG. Neurofibromatosis 2. In: GeneReviews at GeneTests: Medical Genetics Information Resource [database online]. Seattle: University of Washington, 1997–2005. Available at: http://www.genetests.org. Accessed October 20, 2005. Updated April 6, 2004.
39. Baser ME, Kuramoto L, Joe H, et al. Genotype-phenotype correlations for nervous system tumors in neurofibromatosis 2: a population-based study. *Am J Hum Genet.* 2004;75:231–239.
40. Baser ME, Friedman JM, Wallace AJ, Ramsden RT, Joe H, Evans DG. Evaluation of clinical diagnostic criteria for neurofibromatosis 2. *Neurology.* 2002;59:1759–1765.
41. Evans DG, Baser ME, O'Reilly B, et al. Management of the patient and family with neurofibromatosis 2: a consensus conference statement. *Br J Neurosurg.* 2005;19:5–12.
42. McClatchey AI, Giovannini M. Membrane organization and tumorigenesis—the NF2 tumor suppressor, merlin. *Genes Dev.* 2005;19:2265–2277.
43. Kluwe L, Mautner V, Heinrich B, et al. Molecular study of frequency of mosaicism in neurofibromatosis 2 patients with bilateral vestibular schwannomas. *J Med Genet.* 2003;40:109–114.
44. Abou-Sleiman PM, Apessos A, Harper JC, Serhal P, Winston RM, Delhanty JD. First application of preimplantation genetic diagnosis to neurofibromatosis type 2 (NF2). *Prenat Diagn.* 2002;22:519–524.

45. Baser ME, Kuramoto L, Woods R, et al. The location of constitutional neurofibromatosis 2 (NF2) splice site mutations is associated with the severity of NF2. *J Med Genet.* 2005;42:540–546.
46. Parry DM, MacCollin MM, Kaiser-Kupfer MI, et al. Germ-line mutations in the neurofibromatosis 2 gene: correlations with disease severity and retinal abnormalities. *Am J Hum Genet.* 1996;59:529–539.
47. Evans DG, Trueman L, Wallace A, Collins S, Strachan T. Genotype/phenotype correlations in type 2 neurofibromatosis (NF2): evidence for more severe disease associated with truncating mutations. *J Med Genet.* 1998;35:450–455.
48. Kluwe L, MacCollin M, Tatagiba M, et al. Phenotypic variability associated with 14 splice-site mutations in the NF2 gene. *Am J Med Genet.* 1998;77:228–233.
49. Sestini R, Vivarelli R, Balestri P, Ammannati F, Montali E, Papi L. Neurofibromatosis type 2 attributable to gonosomal mosaicism in a clinically normal mother, and identification of seven novel mutations in the NF2 gene. *Hum Genet.* 2000;107:366–371.
50. Wallace AJ, Watson CJ, Oward E, Evans DG, Elles RG. Mutation scanning of the NF2 gene: an improved service based on meta-PCR/sequencing, dosage analysis, and loss of heterozygosity analysis. *Genet Test.* 2004;8:368–380.
51. Kluwe L, Mautner VF. Mosaicism in sporadic neurofibromatosis 2 patients. *Hum Mol Genet.* 1998;7:2051–2055.
52. Evans DG, Wallace AJ, Wu CL, Trueman L, Ramsden RT, Strachan T. Somatic mosaicism: a common cause of classic disease in tumor-prone syndromes? Lessons from type 2 neurofibromatosis. *Am J Hum Genet.* 1998;63:727–736.
53. Moyhuddin A, Baser ME, Watson C, et al. Somatic mosaicism in neurofibromatosis 2: prevalence and risk of disease transmission to offspring. *J Med Genet.* 2003;40:459–463.
54. Kluwe L, Friedrich RE, Tatagiba M, Mautner VF. Presymptomatic diagnosis for children of sporadic neurofibromatosis 2 patients: a method based on tumor analysis. *Genet Med.* 2002;4:27–30.
55. Kluwe L, Nygren AO, Errami A, et al. Screening for large mutations of the NF2 gene. *Genes Chromosomes Cancer.* 2005;42:384–391.
56. Diebold R, Bartelt-Kirbach B, Evans DG, Kaufmann D, Hanemann CO. Sensitive detection of deletions of one or more exons in the neurofibromatosis type 2 (NF2) gene by multiplexed gene dosage polymerase chain reaction. *J Mol Diagn.* 2005;7:97–104.
57. Buckley PG, Mantripragada KK, Benetkiewicz M, et al. A full-coverage, high-resolution human chromosome 22 genomic microarray for clinical and research applications. *Hum Mol Genet.* 2002;11:3221–3229.
58. Stokowski RP, Cox DR. Functional analysis of the neurofibromatosis type 2 protein by means of disease-causing point mutations. *Am J Hum Genet.* 2000;66:873–891.
59. Gutmann DH, Hirbe AC, Haipek CA. Functional analysis of neurofibromatosis 2 (NF2) missense mutations. *Hum Mol Genet.* 2001;10:1519–1529.
60. Ryu CH, Kim SW, Lee KH, et al. The merlin tumor suppressor interacts with Ral guanine nucleotide dissociation stimulator and inhibits its activity. *Oncogene.* 2005;24:5355–5364.
61. Bijlsma EK, Wallace AJ, Evans DG. Misleading linkage results in an NF2 presymptomatic test owing to mosaicism. *J Med Genet.* 1997;34:934–936.

QUERY FORM

During the preparation of your manuscript for publication, the questions listed below have arisen. Please attend to these matters and return this form with your proof.

Many thanks for your assistance.

Query References	Query	Remarks
1.	Au: I've spelled out CGH in the 3rd sentence, okay?	
2.	Au: In the penultimate sentence, can you reference a particular section rather than saying "below"?	
3.	Au: Can you point to a particular section rather than say "below" in the 2nd sentence?	
4.	Au: Please spell out EBV in the 2nd sentence.	
5.	Au: In the 4th sentence, refer to a section rather than "below"?	
6.	Au: In the last sentence, can you refer to a particular section instead of "below"?	
7.	Au: Can you confirm multiplex ligation-dependent probe amplification in the last sentence? In earlier chapters, MPLA is defined as multiplex ligation probe amplification.	
8.	Au: Can you update ref. 7?	
9.	Au: Please provide volume and page numbers for ref. 20.	
10.	Au: Please give full surname for 2nd author in ref. 36.	

Interstitial uniparental isodisomy at clustered breakpoint intervals is a frequent mechanism of *NF1* inactivation in myeloid malignancies

Karen Stephens, Molly Weaver, Kathleen A. Leppig, Kyoko Maruyama, Peter D. Emanuel, Michelle M. Le Beau, and Kevin M. Shannon

To identify the mechanism of loss of heterozygosity (LOH) and potential modifier gene(s), we investigated the molecular basis of somatic *NF1* inactivation in myeloid malignancies from 10 children with neurofibromatosis type 1. Loci across a minimal 50-Mb region of primarily the long arm of chromosome 17 showed LOH in 8 cases, whereas a less than 9-Mb region of loci flanking *NF1* had LOH in the remaining 2 cases. Two complementary techniques, quantitative polymerase chain reaction (PCR) and fluorescence in situ hybridization (FISH), were used to determine whether the copy number at loci that showed LOH was 1 or 2 (ie, deleted or isodisomic). The 2 cases with LOH limited to less than 9 Mb were intrachromosomal deletions. Among the 8 leukemias with 50-Mb LOH segments, 4 had partial uniparental isodisomy and 4 had interstitial uniparental isodisomy. These isodisomic cases showed clustering of the centromeric and telomeric LOH breakpoints. This suggests that the cases with interstitial uniparental isodisomy arose in a leukemia-initiating cell by double-homologous recombination events at intervals of preferred mitotic recombination. Homozygous inactivation of *NF1* favored outgrowth of the leukemia-initiating cell. Our studies demonstrate that LOH analyses of loci distributed along the chromosomal length along with copy-number analysis can reveal novel mechanisms of LOH that may potentially identify regions harboring "cryptic" tumor suppressor or modifier genes whose inactivation contributes to tumorigenesis. (Blood. 2006;108:1684-1689)

Introduction

Tumor suppressor gene (TSG) inactivation commonly occurs by sequential somatic inactivation of both alleles or, in individuals who inherit a germline mutation, by a somatic mutation in the single normal homolog. In both groups of patients, somatic inactivation is frequently associated with loss of heterozygosity (LOH) at the TSG locus and at flanking loci.[1,2] Defining the minimal chromosomal region with LOH in a collection of tumors has been a successful strategy for mapping and cloning TSGs. LOH can occur by multiple mechanisms as demonstrated by the extensive analyses of retinoblastomas, which identified *RB1* intragenic deletions, segmental chromosomal deletions, loss of the entire chromosome, or mitotic recombination.[2-4] While hundreds of TSGs have been identified, LOH studies typically focus on the TSG and/or closely flanking loci. For most TSGs, remarkably little is known about the extent and underlying mechanism(s) of LOH in tumor tissues.

In this study, we sought to examine the extent and mechanism of LOH in myeloid leukemias from children affected with neurofibromatosis 1 (NF1). The gene responsible for this disorder, *NF1* at chromosome band 17q11.2, encodes neurofibromin, a GTPase-activating protein that negatively regulates the biochemical activation of $p21^{ras}$ (Ras) family members (reviewed in Boguski and McCormick[5] and Donovan et al[6]). Germline *NF1* mutations cause NF1, a dominant familial cancer syndrome that affects about 1 in 4000 people. Clinical features of NF1 include neurocutaneous abnormalities, learning disabilities, and a predisposition to specific benign and malignant tumors (reviewed in Friedman and Riccardi[7]). Children with NF1 are at a markedly increased risk of developing myeloid malignancies, particularly juvenile myelomonocytic leukemia (JMML).[8] JMML is an aggressive myeloproliferative disease (MPD) characterized by monocytosis, thrombocytopenia, splenomegaly, and by malignant infiltration of the skin, lymph nodes, lungs, liver, and other organs (reviewed in Arico et al[9] and Emanuel et al[10]). Together, the biochemical activity of neurofibromin and the dominant cancer predisposition seen in affected persons suggests that *NF1* functions as a TSG. Indeed, LOH at the *NF1* locus occurs in JMML and in other NF1-associated cancers (reviewed in Side and Shannon[11]). Similarly, tumorigenesis in heterozygous *Nf1* mutant mice is associated with loss of the wild-type *Nf1* allele.[12,13] Consistent with the Knudson model of

From the Departments of Medicine, Laboratory Medicine, Pathology, and Pediatrics, University of Washington, Seattle; the Division of Hematology/Oncology, Department of Medicine and Comprehensive Cancer Center, University of Alabama at Birmingham; the Department of Medicine, Section of Hematology/Oncology, University of Chicago, IL; and the Department of Pediatrics and Comprehensive Cancer Center, University of California, San Francisco.

Submitted November 22, 2005; accepted April 24, 2006. Prepublished online as *Blood* First Edition Paper, May 11, 2006; DOI 10.1182/blood-2005-11-011486.

Supported by U.S. Army Medical Research and Materiel Command grants DAMD17-97-1-7344 and DAMD17-03-1-0203 (K.S.), and National Institutes of Health grants PO1 CA40046 (M.M.L., K.M.S.), R01 CA72614 (K.M.S.), and K24 CA80916 (P.D.E.).

K.S. designed research, generated primary data and performed analyses in her laboratory, and wrote the paper; M.W. performed genotyping experiments in K.S.'s lab; K.A.L. generated and analyzed primary cytogenetic data; K.M. developed gene dosage assay and performed experiments in K.S.'s lab; P.D.E. contributed well-characterized patient samples; M.M.L.B. helped to design research, generated primary data on interphase FISH, and performed analysis in her laboratory; K.M.S. helped to design research, identified LOH in NF1-associated leukemias, and assisted in writing the paper.

The online version of this article contains a data supplement.

Reprints: Karen Stephens, University of Washington, Medical Genetics 357720, Seattle, WA 98195; e-mail: millie@u.washington.edu.

The publication costs of this article were defrayed in part by page charge payment. Therefore, and solely to indicate this fact, this article is hereby marked "advertisement" in accordance with 18 U.S.C. section 1734.

familial cancer genes, tumors from individuals with familial NF1 invariably show loss of the allele inherited from the unaffected parent (reviewed in Side and Shannon[11]). Somatic intragenic *NF1* mutations have been identified in primary neoplasms, (reviewed in Stephens[14]), providing compelling evidence that functional inactivation of *NF1* is central to tumorigenesis. Deregulated Ras signaling has been reported in tumors from NF1 patients and *Nf1* mutant mice. These data are consistent with the idea that the tumor suppressor function of *NF1* is related to the ability of neurofibromin to negatively regulate Ras output (reviewed in Side and Shannon,[11] Cichowski and Jacks,[15] and Dasgupta and Gutmann[16]).

In the course of investigating the extent and mechanism of LOH at the *NF1* locus in myeloid malignancies, we unexpectedly identified interstitial isodisomy for a large segment of chromosome 17 as a frequent underlying genetic mechanism. Remarkably, the LOH breakpoints clustered within centromeric and telomeric marker intervals in these leukemias. To our knowledge, this is the first report of interstitial isodisomy as a frequent mechanism of somatic TSG inactivation. These data have implications for uncovering novel TSGs and for understanding pathogenic mechanisms that contribute to the development of hematopoietic malignancies as well as solid tumors.

Patients, materials, and methods

Patients

Clinical descriptions, LOH, and mutation analyses of the *NF1* gene have been reported for most of the patients.[17-19] Selected demographic and laboratory data are summarized in Table 1. Additional patient characteristics from previous reports are in Table S1, available on the *Blood* website (see the Supplemental Materials link at the top of the online article). Study procedures involving human subjects were approved by the University of California at San Francisco (UCSF) Committee for Human Research. Informed consent was provided according to the Declaration of Helsinki.

NF1 gene dosage assay

This assay measures the copy number of *NF1* exon 32 by quantitating polymerase chain reaction (PCR) amplicons relative to those of a competitively amplified disomic control locus. Validation of the assay on nontumor DNA demonstrated that *NF1* disomy gave dosage values of 0.98 ± 0.08 SD, while monosomy gave values of 0.45 ± 0.04 SD (SD indicates 1 standard deviation). A range involving 2 SD was used to predict gene copy number (Table 1, ‡ footnote). Briefly, the assay is a quantitative, competitive PCR adapted from the method of Celi et al.[20] Assay conditions are available upon request.

FISH

Metaphase chromosome preparations of immortalized lymphoblastoid cells from patient 1 were prepared and hybridized as described previously.[21] The bacteriophage P1 probe P1-12 contains approximately 55 kb of sequence from *NF1* intron 27b.[21] Bacterial artificial chromosome (BAC) clone 1000G21 (17q25) was identified by hybridization of D17S928 amplicons to filter arrays of the RPCI-11 human male BAC library, segment 4 (Roswell Park Cancer Institute, Buffalo, NY). Hybridization signals were detected using a commercial system (Vector Laboratories, Burlingame, CA). Chromosomes were banded using Hoechst 33258–actinomycin D staining, counterstained with propidium iodide, and signals visualized by fluorescence microscopy using a dual-band pass filter (Omega, Brattleboro, VT). Images in Figure 2A-B were visualized using a Zeiss Axioskop 2 plus microscope (Carl Zeiss, Thornwood, NY) equipped with a 100×/1.2 numeric aperture (NA) oil objective. Images were acquired using Spot software version 3.5.9 (Diagnostic Instruments, Sterling Heights, MI) and were processed using Adobe Photoshop software (Adobe Systems, San Jose, CA).

Cryopreserved bone marrow samples were thawed and cultured at 1×10^6 cells/mL for 24 hours (90% RPMI 1640/10% fetal bovine serum, 100 U/mL penicillin, 100 μg/mL streptomycin, and 10 mM HEPES) at 37°C in 95% air/5% CO_2. Following incubation, the cells were exposed to hypotonic KCl (0.75 M for 8 minutes at 37°C), fixed in absolute methanol-glacial acetic acid (3:1), and air-dried on slides. *NF1* probes were P1 bacteriophage clone P1-9, which spans approximately 65 kb of the *NF1* gene, including exons 2-11, and clone P1-12.[21] Centromere-specific probes for chromosomes 7 and 17 (CEP7-Spectrum Green and CEP17-Spectrum Green; Abbott Molecular, Abbott Park, IL), and the P1-derived artificial chromosome (PAC) clone P263P1 (Genome Systems, St Louis, MO), were hybridized as controls. P263P1 was isolated by screening the PAC library using primers for *D5S479*, and contains an insert of 70 kb derived from 5q31. Labeled probes were prepared by nick-translation using Bio-11-dUTP (Enzo Diagnostics, New York, NY) or digoxigenin-11-dUTP (Boehringer Mannheim, Indianapolis, IN). Interphase fluorescence in situ hybridization (FISH) was performed as described previously.[22] Hybridization of

Table 1. *NF1* gene dosage in bone marrows of children with NF1 and malignant myeloid disorders

Patient no.	Sex	Age at onset, mo	Diagnosis	Parental origin		*NF1* gene dosage value*†	Predicted *NF1* gene copy no.‡
				NF1 mutation	LOH at *NF1* locus		
1	M	9	MPS	Paternal	Maternal	0.99	Disomy
2	M	10	AML	Paternal	Maternal	0.93	Disomy
3	M	24	Monosomy 7	Unknown	Maternal	0.96	Disomy
4	M	14	JMML	Maternal	Paternal	0.86	Disomy
5	F	30	JMML	Maternal	Paternal	0.94	Disomy
6	M	10	JMML	Maternal	Paternal	0.87	Disomy
7	M	5	Monosomy 7	Maternal	Paternal	0.90	Disomy
8	F	18	MPS	Paternal	Maternal*	0.85	Disomy
9	M	60	JMML	Maternal	Paternal	0.57	Monosomy
10	M	19	Monosomy 7	De novo	Maternal*	0.48	Monosomy

Clinical descriptions, LOH, and NF1 mutation analyses have been reported previously for most of the patients.[17-19]

*Data from this study employing quantitative PCR at *NF1* gene segment.

†Measured in unfractionated bone marrow cells except in patients 3 and 9, for whom leukemic cells in peripheral blood were used.

‡Predicted gene copy number based on *NF1* gene dosage values. Validation of the assay on nontumor DNA demonstrated that *NF1* disomy gave dosage values of 0.98 ± 0.08 SD, while monosomy gave values of 0.45 ± 0.04 SD. A range of 2 SD was used to approximate a 95% confidence interval. Therefore, values from 0.82 to 1.14 predicted disomy, and values from 0.37 to 0.53 predicted monosomy.

probes labeled with either biotin or digoxigenin was detected with fluorescein-conjugated avidin (Vector Laboratories) and rhodamine-conjugated antidigoxigenin antibodies (Boehringer Mannheim), respectively. Nuclei were counterstained with DAPI. The slides were randomized and examined by 2 observers in a blinded fashion, with 500 cells scored by each observer for each probe. We established control values by hydridizing the probes to cryopreserved bone marrow cells from patients in remission (C1, AML-M4) or with myeloid leukemias that retained heterozygosity at *NF1* (C2-C5 in Table S2). The cutoff value was set as the mean ± 3 SD.

The distribution of hybridization signals per nucleus for the CEP17 probe was determined in bone marrow cells from healthy control individuals (n = 10; Table S2).

Mapping the LOH region

Polymorphic loci were genotyped by PCR. LOH at the *NF1* locus was evaluated by PCR analysis of at least 1 informative intragenic site including exon 5, intron 27B *Alu*I/*Alu*II, and intron 38. LOH was determined by comparing the genotype of the patient's tumor DNA to that of peripheral blood DNA of the patient's parents. For patients 1, 4, 5, 9, and 10, normal tissue or an Epstein-Barr virus (EBV)–transformed cell line was available to confirm a constitutional genotype with biparental inheritance of *NF1* alleles.[18,23] Segregation of alleles from parents to child for multiple informative loci on autosomes other than 17 was consistent with parentage as stated for each case (data not shown). Physical distances between chromosome 17 loci are based on the May 2004 assembly of the human genome (http://genome.ucsc.edu).

Results

Delineation of a large region of isodisomy in an NF1-associated MPD

Previous molecular analysis of bone marrow cells from children with NF1 revealed LOH at *NF1* in $CD34^+$ cells in 3 informative cases, whereas lymphoblasts immortalized by EBV retained heterozygosity in 2 of these patients.[18] The remaining child with LOH at *NF1* in EBV-transformed lymphoblasts was a 9-month-old boy with an unusual MPD and loss of the maternal *NF1* allele (Table 1, patient 1).[18] The retained paternal allele carried a de novo R1276X mutation (Table S1) that encoded a truncated protein lacking the GTPase-activating protein (GAP) domain.[19] We performed extended LOH analyses of chromosome 17, which demonstrated loss of maternally derived alleles from *D17S975* at 17q11.2 to *D17S1830* at 17q25.3, a segment of 50.3 Mb (Figure 1). Although a deletion of this size is readily detected by cytogenetic techniques, the bone marrow and lymphoblastoid cells of patient 1 had a normal 46, XY karyotype. These data suggested that the 50.3-Mb LOH region was not deleted, but present on both chromosome 17 homologs. To address this possibility, the lymphoblastoid cells were analyzed by FISH with an *NF1* intron 27b probe.[21] Hybridization signals were detected on both chromosome 17 homologs (Figure 2A). Together, these data suggest that a 50.3-Mb interstitial interval of the maternal chromosome had been replaced with a homologous paternal DNA segment, resulting in homozygosity for the mutant R1276X *NF1* allele (Figure 1). FISH with a BAC harboring the *D17S928* locus confirmed that the heterozygous 17qter segment had not translocated elsewhere in the genome of the leukemic clone (Figure 2B). Taken together, these data confirmed interstitial isodisomy.

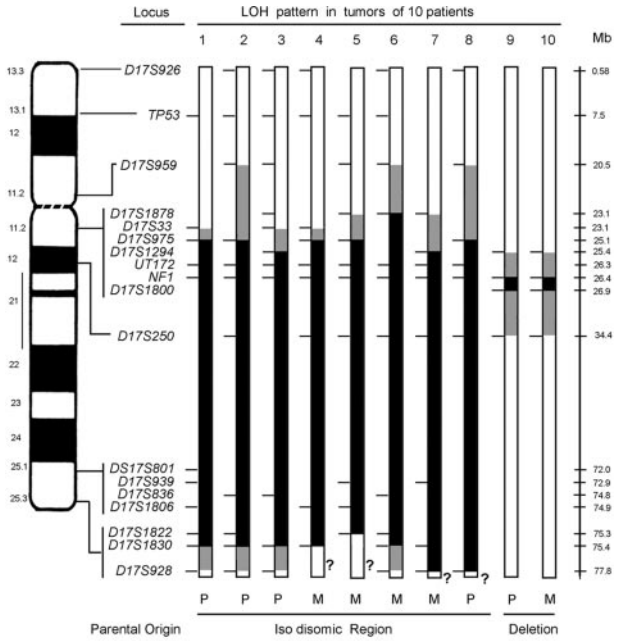

Figure 1. LOH at chromosome 17 loci in NF1-associated myeloid malignancies. Ideogram and schematic of chromosome 17 showing the loci that were screened for LOH. For each tumor, a bar shows the single chromosome 17 that underwent LOH with informative loci (tick marks), segments showing biparental inheritance (□), segments that underwent LOH (■), segments where a recombination event occurred (▤), and qter segments that lacked informative loci (?). Below the schematic, the parental origin is given for the isodisomic and deleted regions for each tumor. For patients 1, 2, 3, and 8, the maternal homolog is shown with the region of paternal isodisomy indicated in black. For patients 4 through 7, the paternal homolog is shown with the region of maternal isodisomy indicated in black. LOH in patients 9 and 10 occurred by intrachromosomal deletion indicated in black. Additional chromosome 17 loci that were tested, but not informative, are not shown. Physical distances (rounded to the nearest tenth of a megabase) are based on the May 2004 assembly of the human genome (http://genome.uscs.edu), in which the length of chromosome 17 is given as 78 774 742 bp.

Uniparental isodisomy is a frequent mechanism of LOH in NF1-associated leukemias

The unexpected findings in patient 1 prompted us to use a quantitative *NF1* gene dosage PCR assay to assess *NF1* copy numbers in 9 additional NF1-associated leukemia specimens with LOH at *NF1*.[17-19] Bone marrow DNA from patient 1 (Table 1) and from the normal tissues of his parents (data not shown) gave *NF1* gene dosage values ranging from 0.91 to 1.08, which are consistent with disomy. Surprisingly, the *NF1* dosage values for 7 of the 9 remaining NF1-associated myeloid malignancies were also consistent with disomy, whereas 2 cases had values consistent with monosomy (Table 1). Cryopreserved bone marrow specimens were available from 5 of these patients for copy number confirmation. FISH analyses using a chromosome 17 centromere-specific probe (Cep17) and 2 *NF1* probes (P1-9 and P1-12) provided physical confirmation that the leukemias of all 4 cases in which the dosage assay predicted disomy contained 2 *NF1* alleles (Figure 2D; patients 3-6 in Table S2). By contrast, the bone marrow of patient 10 demonstrated monosomy for *NF1* with 2 signals in 67% and 1 signal in 29% of cells (Figure 2D and Table S2), which was also consistent with the gene dosage assay (Table 1). To confirm that the cells being examined were from the malignant clone with LOH at *NF1*, a chromosome 7–specific probe (Cep7) was hybridized to bone marrow cells of patient 3, who had monosomy 7 and was disomic at *NF1* as measured by both gene dosage and FISH (Table 1, Figure 2D, Table S2). As expected, dual-color FISH

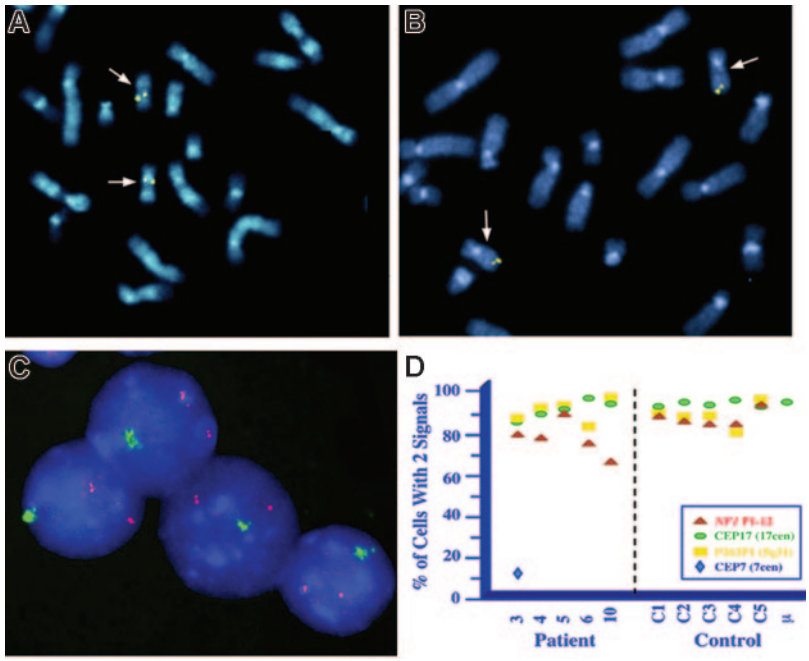

Figure 2. FISH analysis of NF1-associated myeloid malignancies. (A-B) Metaphase spreads of EBV-transformed cells from patient 1 that were hybridized with *NF1* probe P1-12 (A) and BAC clone 1000G21, which contains the *D17S928* locus at 17q25 (B). Each of 20 metaphase cells examined showed signals on both chromosome 17 homologs, consistent with disomy. The chromosome 17 homologs were identified by Hoechst–actinomycin D staining, which reveals a Q-banding–like pattern. (C) Dual-color FISH performed by cohybridizing a digoxigenin-labeled probe P1-12 (rhodamine signal) and an α-satellite probe specific for the centromere of chromosome 7 (CEP7, SpectrumGreen), which showed monosomy 7 and *NF1* disomy in bone marrow cells from patient 3. Interphase nuclei were counterstained with DAPI, and the slides mounted with PDD antifade solution. Images were visualized using a Zeiss Axioplan microscope equipped with a 63×/1.25 NA oil Plan Neofluar lens, Optivar setting 1.6. Images were acquired using a Photometrics cooled charge-coupled device (CCD) camera (Photometrics, Tucson, AZ) and NIH Image software (National Institutes of Health, Bethesda, MD), and were processed using Adobe Photoshop. (D) Graphic summary of interphase FISH analyses of myeloid leukemia cells with *NF1* (red triangle) and control probes. Probe 263P1 is a 70-kb PAC clone containing *D5S479* (chromosome band 5q31; yellow squares). CEP17 is a centromere-specific probe for chromosome 17 (green circles), and CEP7 is a centromere-specific probe for chromosome 7 (blue diamond). C1 is a cryopreserved bone marrow sample from a patient with AML-M4 in complete remission. Control samples C2 through C5 are cryopreserved bone marrow samples from 4 children with myeloid leukemias that retained heterozygosity at the *NF1* locus. The mean distribution of signals for the chromosome 17 centromere-specific probe was determined by the interphase analysis of bone marrow cells from 10 healthy individuals. This graph is a summary of data given in Table S2.

revealed monosomy 7 in cells that also had 2 structural *NF1* alleles (Figure 2C-D and Table S2). Together these studies demonstrate that LOH at *NF1* in myeloid malignancies is preferentially associated with isodisomy of a chromosomal segment carrying the mutant *NF1* allele.

Clustering and parental origin of chromosome 17 LOH breakpoints

Each of the 8 leukemias with isodisomy at *NF1* showed a large segment of LOH that minimally ranged from 50 to 52.7 Mb (Figure 1). Among these cases, both the proximal and distal LOH breakpoints were clustered. In all 8, the centromeric breakpoints mapped to a maximum interval of 4.9 Mb (6% of the chromosome 17 length of 78.77 Mb) between *D17S959* and *D17S1294*. In some leukemias, additional informative markers narrowed the breakpoint interval, as in patient 5 with a 2-Mb interval between *D17S1878* and *D17S975*. With the exception of case 6, the minimum common breakpoint region is 2 Mb and is delineated by *D17S33* and *D17S975*. The distal breakpoints in patients 1, 2, 3, and 6 were clustered between *D17S1830* and *D17S928*, an interval of 2.4 Mb (Figure 1). Lack of informativeness at *D17S928* and other 17qter loci tested precluded determining whether the large LOH segments in the tumors of patients 4, 5, 7, and 8 were isodisomic.

The bone marrows of patients 9 and 10 had LOH at loci flanking the *NF1* region. The leukemias of these 2 patients showed structural deletions that included the *NF1* locus as determined by gene dosage (Table 1) and FISH data (Figure 2D; Table S2). The centromeric breakpoints mapped to a 1.2-Mb interval between *D17S1294* and *NF1* intron 38 and the telomeric breakpoints were in a 7.5-Mb interval between *D17S1800* and *D17S250*. These data are consistent with an interstitial deletion ranging from 268 kb *(NF1* ex38 to *D17S1800)* to 9 Mb *(D17S1294* to *D17S250)*.

The bone marrows of patients 1, 2, 3, and 8 lost chromosome 17 maternal alleles and were isodisomic for a paternally derived DNA segment, whereas the cells of patients 4 through 7 lost paternal alleles and were isodisomic for a maternally derived interval of comparable length (Figure 1). In each patient with familial NF1, the isodisomic segment was derived from the parent with NF1 (Tables 1, S1). The bone marrow of patient 10, who had de novo NF1, showed loss of the maternal *NF1* allele (Table 1; Figure 1B). These data infer that patient 10 carried a germline mutation of the paternal *NF1* allele and underwent somatic deletion of the normal maternal *NF1* allele, which is consistent with the reported parental predisposition for *NF1* germline mutations.[24,25]

Discussion

Our analyses of myeloid malignancies from children with NF1 uncovered 2 distinct mechanisms underlying inactivation of the normal *NF1* allele: interstitial isodisomy and interstitial deletion (Figure 3A). The somatic interstitial deletions involving *NF1* are of interest as they may occur by a mechanism similar to that identified in constitutional and somatic mosaic *NF1* microdeletions in normal (nontumor) tissues. In these cases, the deletions are 1.2 to 1.4 Mb and occur by nonallelic homologous recombination between pairs of high-identity, low copy number repeat (LCR) elements that flank the *NF1* gene (reviewed in Stephens[26]). Microdeletions mediated by germline or somatic recombination between different LCR pairs[27,28] both involve the entire *NF1* gene and the D17S1800 locus, which are deleted in the tumors of patients 9 and 10. A mechanism of LCR-mediated recombination could be tested by precise mapping of the deletion breakpoints by single nucleotide polymorphism (SNP) mapping in the myeloid malignancies. Alternatively, the length of these somatic microdeletions in myeloid malignancies may be constrained if a 50% reduction in the expression of a critical flanking gene(s) inhibited outgrowth of the leukemic clone.

While segmental or interstitial uniparental isodisomy has been reported in constitutional rearrangements (reviewed in Vianna-Morgante[29]), we were surprised to find that interstitial isodisomy for 50 to 52.7 Mb of chromosome 17 is a common mechanism underlying LOH in NF1-associated myeloid malignancies. The leukemias of each of the 4 patients (1, 2, 3, and 6 in Figure 1) in whom *D17S928* was

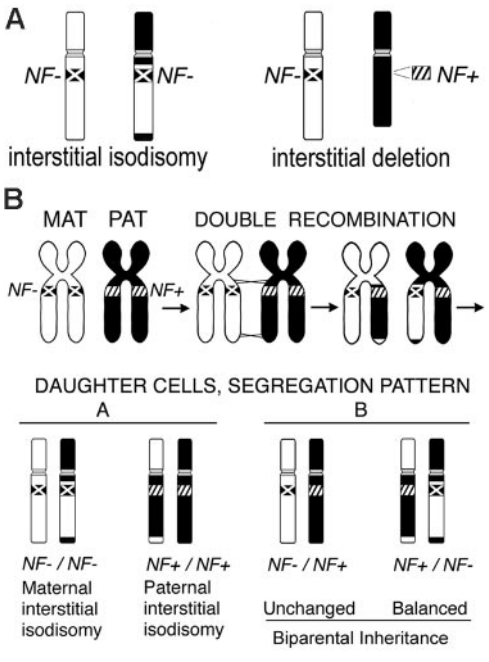

Figure 3. LOH in NF1-associated myeloid malignancies and proposed mechanism of interstitial isodisomy. (A) The schematic depicts the 2 different patterns of LOH observed in the tumors. The inactivated *NF1* allele (NF−) is marked with an X on the chromosome, while the normal *NF1* allele (NF+) is indicated by diagonal hashmarks (////). The interstitial isodisomic and deleted regions can be of maternal or paternal origin. (B) Proposed mechanism for double mitotic recombination during the S/G_2 phase of the cell cycle leading to interstitial uniparental isodisomy in a leukemic-initiating cell. The 4 possible daughter cells are depicted, along with their *NF1* genotypes and disomy patterns. Although this example depicts a cell with maternal interstitial isodisomy and *NF1* inactivation, paternal interstitial isodisomy was also observed in our study (Figure 1).

informative had interstitial isodisomy. The remaining 4 tumors (4, 5, 7, and 8 in Figure 1) may also be interstitial, but D17S928 or other regional markers were not informative. We propose that interstitial isodisomy results from a double mitotic recombination event between chromatids of the 2 chromosome 17 homologs during the S/G_2 phase of the cell cycle of a leukemia-initiating cell (Figure 3B). Depending upon the segregation pattern during mitosis, the daughter cells would have biparental inheritance at all chromosome 17 loci, or alternatively, would show interstitial isodisomy (Figure 3B). Only 1 of 4 possible daughter cells would have interstitial isodisomy along with homozygous inactivation of *NF1*, the latter of which is presumably essential for leukemic outgrowth.[30,31] The low frequency of double-mitotic recombination events, estimated at about 10^{-10} in normal lymphocytes,[32] infers that *NF1* inactivation confers a strong proliferative advantage in the leukemia-initiating cell. A possible mechanism may involve nonallelic mitotic homologous recombination between LCRs or Alu elements, which has been implicated in recurring translocations, isochromosomes, deletions, and amplifications in tumor tissues.[33-35] Other mechanisms that could give rise to 17q interstitial isodisomy are less likely. For example, 2 sequential single recombination events in different precursor cells are also possible, but would imply that each independent event conferred a proliferative advantage. A gene conversion–like event of a 50-Mb segment would be unprecedented as estimated conversion tracts in humans are typically less than 2 kb.[36,37] The clustered breakpoint intervals of the isodisomic segments suggest that mitotic recombination may be favored in these regions.

Our data are intriguing in light of recent reports showing *JAK2* point mutations in most patients with polycythemia vera (PV) and in some cases of essential thrombocythemia (ET) and chronic idiopathic myelofibrosis (CIMF).[38-41] An unexpected and intriguing result of these studies was the finding of biallelic mutations in approximately 30% of the PV specimens. The underlying genetic mechanism in these cases was a mitotic recombination that led to loss of the normal *JAK2* allele and resulted in isodisomy for a segment of the short arm of chromosome 9 estimated to span approximately 40 cM.[42] The most telomeric marker studied showed LOH in many cases, which is consistent with a single recombination event. We did not prove that the isodisomic regions were interstitial in patients 4, 5, 7, and 8 due to a lack of informative polymorphic markers near 17qter (Figure 1), and it is therefore possible that isodisomy resulted from a single recombination event in 1 or more of our cases. Similarly, it is possible that studies with additional markers near 9pter would uncover double-mitotic recombination events in some PV samples. Whereas biallelic *NF1* inactivation deregulates Ras signaling in response to hematopoietic growth factors, it is less obvious why loss of the normal *JAK2* allele and isodisomy of the mutant homolog would confer a growth advantage beyond that of a dominant heterozygous mutation. Since JAK2 molecules that are recruited to activated growth factor receptors transphosphorylate each other, it is possible that the normal protein has a dominant interfering activity that impairs the ability of mutant JAK2 to deregulate downstream effectors. Consistent with this idea, James et al[38] found that coexpressing wild-type and mutant JAK2 proteins restored erythropoietin-dependence in the Ba/F3 pro–B-cell line.

A broad implication of our work and of the recent studies of *JAK2* mutations in MPD is that segmental uniparental isodisomy may be a frequent but unrecognized mechanism in human cancers. Although isodisomy of a 25-cM interval was first described in children with Down syndrome who developed acute lymphoblastic leukemia by Rogan et al,[43] this genetic mechanism has received limited attention in hematologic malignancies until recently. The availability of automated allelotyping and the use of SNP and high-density arrays have been developed for high-resolution analysis of allelic losses and gains in tumors.[44-46] Interestingly, a number of investigators are now identifying regions of isodisomy in acute myeloid leukemia.[47-49] Our data extend these studies by showing that inactivation of a known myeloid TSG is frequently associated with acquired uniparental disomy. Importantly, DNA segments that are associated with partial or interstitial isodisomy will appear normal when examined by conventional cytogenetic analysis, FISH, or comparative genomic hybridization, making these approaches of limited use for cancers where LOH results in isodisomy. Together, LOH and copy-number analyses provide the opportunity to define new genetic mechanisms of somatic mutation, mitotic recombination sites, putative modifying or imprinted genes, and/or correlations between tumor genotype and neoplastic transformation. In addition, mono- or biallelic expression from a locus (loci), other than the TSG itself, could affect the efficacy of putative therapeutic agents.

Acknowledgments

We thank Virginia P. Sybert and Eric Sievers for referring patient 1, Melvin H. Freedman for bone marrow samples, Michael Dorschner for BAC1000G21, and Elizabeth M. Davis and Rafael Espinosa III for technical assistance.

References

1. Fearon ER. Human cancer syndromes: clues to the origin and nature of cancer. Science. 1997; 278:1043-1050.
2. Tischfield JA. Loss of heterozygosity or: how I learned to stop worrying and love mitotic recombination. Am J Hum Genet. 1997;61:995-999.
3. Qian F, Germino GG. "Mistakes happen": somatic mutation and disease. Am J Hum Genet. 1997; 61:1000-1005.
4. Cavenee WK, Dryja TP, Phillips RA, Benedict WF, et al. Expression of recessive alleles by chromosomal mechanisms in retinoblastoma. Nature. 1983;305:779-784.
5. Boguski MS, McCormick F. Proteins regulating Ras and its relatives. Nature. 1993;366:643-654.
6. Donovan S, Shannon KM, Bollag G. GTPase activating proteins: critical regulators of intracellular signaling. Biochim Biophys Acta. 2002;1602:23-45.
7. Friedman J, Riccardi VM. Clinical and epidemiological features. In: Friedman JM, Butmann DH, MacCollin M, Riccardi VM, eds. Neurofibromatosis Phenotype, Natural History, and Pathogenesis. 3rd ed. Baltimore, MD: The Johns Hopkins University Press; 1999:29-86.
8. Stiller CA, Chessells JM, Fitchett M. Neurofibromatosis and childhood leukemia/lymphoma: a population-based UKCCSG study. Br J Cancer. 1994;70:969-972.
9. Arico M, Biondi A, Pui CH. Juvenile myelomonocytic leukemia. Blood. 1997;90:479-488.
10. Emanuel PD, Shannon KM, Castleberry RP. Juvenile myelomonocytic leukemia: molecular understanding and prospects for therapy. Mol Med Today. 1996;2:468-475.
11. Side LD, Shannon KM. The NF1 gene as a tumor suppressor. In: Upadhyaya M, Cooper DN, eds. Neurofibromatosis type 1. Oxford, United Kingdom: Bios Scientific; 1998:133-152.
12. Mahgoub N, Taylor BR, Le Beau MM, et al. Myeloid malignancies induced by alkylating agents in Nf1 mice. Blood. 1999;93:3617-3623.
13. Jacks T, Shih TS, Schmitt EM, Bronson RT, Bernards A, Weinberg RA. Tumour predisposition in mice heterozygous for a targeted mutation in Nf1. Nat Genet. 1994;7:353-361.
14. Stephens K. Genetics of neurofibromatosis 1-associated peripheral nerve sheath tumors. Cancer Invest. 2003;21:901-918.
15. Cichowski K, Jacks T. NF1 tumor suppressor gene function: narrowing the GAP. Cell. 2001; 104:593-604.
16. Dasgupta B, Gutmann DH. Neurofibromatosis 1: closing the GAP between mice and men. Curr Opin Genet Dev. 2003;13:20-27.
17. Shannon KM, O'Connell P, Martin GA, et al. Loss of the normal NF1 allele from the bone marrow of children with type 1 neurofibromatosis and malignant myeloid disorders. N Engl J Med. 1994;330: 597-601.
18. Miles DK, Freedman MH, Stephens K, et al. Patterns of hematopoietic lineage involvement in children with neurofibromatosis type 1 and malignant myeloid disorders. Blood. 1996;88:4314-4320.
19. Side L, Taylor B, Cayouette M, et al. Homozygous inactivation of the NF1 gene in bone marrow cells from children with neurofibromatosis type 1 and malignant myeloid disorders. N Engl J Med. 1997;336:1713-1720.
20. Celi F, Cohen M, Antonarakis S, Wertheimer E, Roth J, Shuldiner A. Determination of gene dosage by a quantitative adaptation of the polymerase chain reaction (gd-PCR): rapid detection of deletions and duplications of gene sequences. Genomics. 1994;21:304-310.
21. Leppig KA, Viskochil D, Neil S, et al. The detection of contiguous gene deletions at the neurofibromatosis 1 locus with fluorescence in situ hybridization. Cytogenet Cell Genet. 1996;72:95-98.
22. Le Beau MM, Espinosa R III, Davis EM, Eisenbart JD, Larson RA, Green ED. Cytogenetic and molecular delineation of a region of chromosome 7 commonly deleted in malignant myeloid diseases. Blood. 1996;88:1930-1935.
23. Luna-Fineman S, Shannon KM, Lange BJ. Childhood monosomy 7: epidemiology, biology, and mechanistic implications. Blood. 1995;85: 1985-1999.
24. Jadayel D, Fain P, Upadhyaya M, et al. Paternal origin of new mutations in von Recklinghausen neurofibromatosis. Nature. 1990;343:558-559.
25. Stephens K, Kayes L, Riccardi VM, Rising M, Sybert VP, Pagon RA. Preferential mutation of the neurofibromatosis type 1 gene in paternally derived chromosomes. Hum Genet. 1992;88:279-282.
26. Stephens K. Neurofibromatosis 1. In: Lupski JR, Stankiewicz P, eds. Genomic Disorders: The Genomic Basis of Disease. 1st ed. Totowa, NJ: Humana Press; 2006:207-219.
27. Dorschner MO, Sybert VP, Weaver M, Pletcher BA, Stephens K. NF1 microdeletion breakpoints are clustered at flanking repetitive sequences. Hum Mol Genet. 2000;9:35-46.
28. Kehrer-Sawatzki H, Kluwe L, Sandig C, et al. High frequency of mosaicism among patients with neurofibromatosis type 1 (NF1) with microdeletions caused by somatic recombination of the JJAZ1 gene. Am J Hum Genet. 2004;75:410-423.
29. Vianna-Morgante AM. The ratio of maternal to paternal UPD associated with recessive diseases. Hum Genet. 2005;117:288-290.
30. Kalra R, Paderanga DC, Olson K, Shannon KM. Genetic analysis is consistent with the hypothesis that NF1 limits myeloid cell growth through p21ras. Blood. 1994;84:3435-3439.
31. Largaespada DA, Brannan CI, Shaughnessy JD, Jenkins NA, Copeland NG. The neurofibromatosis type 1 (NF1) tumor suppressor gene and myeloid leukemia. Curr Top Microbiol Immunol. 1996;211:233-239.
32. Morley AA, Grist SA, Turner DR, Kutlaca A, Bennett G. Molecular nature of in vivo mutations in human cells at the autosomal HLA-A locus. Cancer Res. 1990;50:4584-4587.
33. Bien-Willner GA, Stankiewicz P, Lupski JR, Northup JK, Velagaleti GV. Interphase FISH screening for the LCR-mediated common rearrangement of isochromosome 17q in primary myelofibrosis. Am J Hematol. 2005;79:309-313.
34. Saglio G, Storlazzi CT, Giugliano E, et al. A 76-kb duplicon maps close to the BCR gene on chromosome 22 and the ABL gene on chromosome 9: possible involvement in the genesis of the Philadelphia chromosome translocation. Proc Natl Acad Sci U S A. 2002;99:9882-9887.
35. van Dartel M, Hulsebos TJ. Amplification and overexpression of genes in 17p11.2 ~ p12 in osteosarcoma. Cancer Genet Cytogenet. 2004;153: 77-80.
36. Jeffreys AJ, May CA. Intense and highly localized gene conversion activity in human meiotic crossover hot spots. Nat Genet. 2004;36:151-156.
37. Padhukasahasram B, Marjoram P, Nordborg M. Estimating the rate of gene conversion on human chromosome 21. Am J Hum Genet. 2004;75: 386-397.
38. James C, Ugo V, Le Couedic JP, et al. A unique clonal JAK2 mutation leading to constitutive signalling causes polycythaemia vera. Nature. 2005; 434:1144-1148.
39. Levine RL, Wadleigh M, Cools J, et al. Activating mutation in the tyrosine kinase JAK2 in polycythemia vera, essential thrombocythemia, and myeloid metaplasia with myelofibrosis. Cancer Cell. 2005;7:387-397.
40. Baxter EJ, Scott LM, Campbell PJ, et al. Acquired mutation of the tyrosine kinase JAK2 in human myeloproliferative disorders. Lancet. 2005;365: 1054-1061.
41. Kralovics R, Passamonti F, Buser AS, et al. A gain-of-function mutation of JAK2 in myeloproliferative disorders. N Engl J Med. 2005;352: 1779-1790.
42. Kralovics R, Guan Y, Prchal JT. Acquired uniparental disomy of chromosome 9p is a frequent stem cell defect in polycythemia vera. Exp Hematol. 2002;30:229-236.
43. Rogan PK, Close P, Blouin JL, et al. Duplication and loss of chromosome 21 in two children with Down syndrome and acute leukemia. Am J Med Genet. 1995;59:174-181.
44. Huang J, Wei W, Zhang J, et al. Whole genome DNA copy number changes identified by high density oligonucleotide arrays. Hum Genomics. 2004;1:287-299.
45. Zhou X, Mok SC, Chen Z, Li Y, Wong DT. Concurrent analysis of loss of heterozygosity (LOH) and copy number abnormality (CNA) for oral premalignancy progression using the Affymetrix 10K SNP mapping array. Hum Genet. 2004;115: 327-330.
46. Zhou X, Rao NP, Cole SW, Mok SC, Chen Z, Wong DT. Progress in concurrent analysis of loss of heterozygosity and comparative genomic hybridization utilizing high density single nucleotide polymorphism arrays. Cancer Genet Cytogenet. 2005;159:53-57.
47. Fitzgibbon J, Smith LL, Raghavan M, et al. Association between acquired uniparental disomy and homozygous gene mutation in acute myeloid leukemias. Cancer Res. 2005;65:9152-9154.
48. Gorletta TA, Gasparini P, D'Elios MM, Trubia M, Pelicci PG, Di Fiore PP. Frequent loss of heterozygosity without loss of genetic material in acute myeloid leukemia with a normal karyotype. Genes Chromosomes Cancer. 2005;44:334-337.
49. Raghavan M, Lillington DM, Skoulakis S, et al. Genome-wide single nucleotide polymorphism analysis reveals frequent partial uniparental disomy due to somatic recombination in acute myeloid leukemias. Cancer Res. 2005;65:375-378.

Neurocutaneous syndromes, P. Curatolo and D. Riva (eds.)

Chapter 17

Clinical molecular genetics of the neurofibromatoses

Karen Stephens

Departments of Medicine and of Laboratory Medicine, University of Washington, Seattle, WA 98195, USA
millie@u.washington.edu

Summary

The neurofibromatoses are a heterogeneous group of genetic disorders that share a predisposition to the development of tumours of the nerve sheath. There are three major types – neurofibromatosis type 1 (NF1), neurofibromatosis type 2 (NF2), and schwannomatosis. Each of these disorders is genetically distinct and is caused by defects in different genes. This chapter focuses on the clinical value of, and issues related to, DNA based testing for NF1 and NF2. In the past 5 years, significant advances have been made in understanding the types of mutation that inactivate the *NF1* and *NF2* genes and their clinical consequences. This has led to the development and availability of sensitive and specific DNA-based tests. These tests have already altered the clinical diagnosis, management, and outcome for at least a subset of affected patients.

Introduction

The neurofibromatoses are a heterogeneous group of genetic disorders that share a predisposition to the development of tumours of the nerve sheath. There are three major types, known as neurofibromatosis type 1 (NF1), neurofibromatosis type 2 (NF2), and schwannomatosis. Each of these disorders is genetically distinct and caused by defects in different genes (Table 1). In this chapter, I will focus on the clinical value of, and issues related to, DNA-based testing for NF1 and NF2. Currently, there is no molecular test available for schwannomatosis, as the gene is yet to be identified. An excellent review of this form of neurofibromatosis has recently been published (MacCollin *et al.*, 2005).

Molecular basis of NF1 and NF2

NF1 is a progressive disorder with an unpredictable course, even among family members carrying the same mutation. The common features of NF1 are café au lait macules, intertriginous freckling, Lisch nodules, and multiple neurofibromas, although learning disabilities, bony abnormalities, and numerous other features and complications are not uncommon (reviewed in Friedman *et al.*, 1999; Friedman, 2002; Friedman, 2004). The clinical criteria for a diagnosis

of NF1 are well established and widely used (Debella *et al.*, 2000). Patients can develop several different forms of neurofibroma (Woodruff, 1999), which are benign tumours of the peripheral nerve sheath. Virtually all patients develop cutaneous neurofibromas, which typically appear in the second decade of life, grow slowly, increase in number with age, and are considered to carry a low risk of transformation into malignant peripheral nerve sheath tumours (MPNST; formerly known as neurofibrosarcomas). The types of neurofibroma known as 'diffuse plexiform' and 'deep nodular' are considered to carry an increased risk of giving rise to MPNST. Individuals with NF1 have an 8 to 13 per cent lifetime risk of MPNST (Evans *et al.*, 2002), which is a significant cause of the decreased life expectancy in the NF1 patient population (Rasmussen *et al.*, 2001). NF1 subjects are also at increased risk of non-nerve-sheath tumours (Mulvihill, 1994) and children in particular are at increased risk for brain stem gliomas, rhabdomyosarcomas, and malignant myeloid leukaemias (Friedman *et al.*, 1999).

The hallmark of NF2 is the development of bilateral vestibular schwannomas. Other commonly associated tumours include schwannomas of other central, spinal, and peripheral nerves, and meningiomas (reviewed in Friedman *et al.*, 1999; Evans *et al.*, 2000; Baser *et al.*, 2003; Evans, 2004; Ruggieri *et al.*, 2005). The majority of patients become completely deaf and can have poor balance, vision, and weakness. Juvenile posterior subcapsular cataract is common. Although NF2 patients are not at increased risk for malignancy, this is a life threatening disorder

Table 1. Features of the neurofibromatoses

Feature	**Neurofibromatosis 1 (NF1)**	**Neurofibromatosis 2 (NF2)**	**Schwannomatosis**[1]
Alternative name:	Peripheral neurofibromatosis; von Recklinghausen neurofibromatosis	Central neurofibromatosis; bilateral acoustic neuroma	Neurilemmomatosis
OMIM accession number[2]:	162200	101000	162091
Mode of inheritance:	Autosomal dominant	Autosomal dominant	Autosomal dominant
Penetrance:	Very high	Very high	Unknown, but reduced compared with NF1 and NF2
Frequency of disorder:	1/3000–1/4000[3]	1/25,000[4]	Unknown, but may be as high as NF2
% Sporadic cases:	30–50%	~50%	Unknown, probably > 50%
% Cases with mosaicism:	> 4%[5]	17–28%[6]	Unknown
Gene:	*NF1*	*NF2*	Gene not yet identified
Chromosomal location:	17q11.2	22q12.2	22q[7]
Commonly associated tumours:	Neurofibroma, MPNST, optic pathway and brain stem gliomas	Bilateral vestibular schwannomas, schwannomas (without schwannomas of other central and peripheral nerves), meningiomas	Bilateral vestibular schwannomas

1 Information from recent review MacCollin *et al.*, 2005; 2 Online Mendelian Inheritance in Man (http://www.ncbi.nlm.nih.gov:80/entrez/query.fcgi?db=OMIM); 3 Friedman *et al.*, 1999; 4 Evans *et al.*, 2005b; 5 About 40 per cent of the estimated 5 to 10 per cent of NF1 contiguous gene deletions are mosaic (Kehrer-Sawatzki *et al.*, 2004); 6 Kluwe *et al.*, 2003; 7 Schwannomatosis locus is not mapped precisely, but is distinct from, and proximal to, the *NF2* gene.
MPNST, malignant peripheral nerve sheath tumour.

because of the tumour location and the tendency to develop multiple tumours. The mean age of onset is between 18 and 24 years and the mean age of death is 36 years. The age of onset of symptoms and the age at diagnosis are both predictors of vestibular schwannoma growth rate and risk of death (Baser *et al.*, 2004 and references therein). Diagnostic criteria and a consensus statement on management of the NF2 patient and family were published recently (Baser *et al.*, 2002; Evans *et al.*, 2005a).

Clinical utility and testing issues

Diagnostic, presymptomatic, prenatal, and preimplantation testing are available for both NF1 and NF2 (consult www.genetest.org and www.gendia.net for information on laboratories that offer testing). The clinical utility of diagnostic testing and presymptomatic testing of at-risk individuals is different for the two disorders. Because a diagnosis of NF1 can be established with high certainty, particularly after 8 years of age, diagnostic and presymptomatic testing is of limited use. However, DNA-based testing is useful to confirm a diagnosis or to identify a mutation in an affected parent, permitting prenatal or preimplantation diagnosis. Furthermore, there has been a recommendation for routine testing to identify carriers of an NF1 contiguous gene deletion (~5 per cent of the patient population; Table 2) for purposes of increased surveillance, as this type of mutation doubles the lifetime risk of MPNST (De Raedt *et al.*, 2003).

Table 2. *NF1* and *NF2* genes and mutations

Feature	NF1 gene	NF2 gene
Gene size; transcript size:	~350 kb; ~11–13 kb[1]	~110 kb; 2 kb[1]
Genbank accession No. (gene; cDNA):	NT_010799; NM_000267	Y18000; NM_000268
Number of exons:	60	17
Protein product (size (kDa); No. of amino acid residues):	Neurofibromin (> 220 kDa; 2818)	Merlin, also known as schwannomin (65 kDa; 595)
Normal protein function:	Tumour suppressor; negative regulator of Ras oncogene[2]	Tumour suppressor; cytoskeletal protein that associates with proteins important in adhesion, signalling, and the cytoskeleton[3]
Types of constitutional mutations (familial and *de novo*):	85–90% nonsense, splicing defects, missense; ~5% contiguous gene deletions[4]	Nonsense, splicing defects, multi-exonic deletion, whole gene deletion, 5% missense[5]
Types of mutation in cases of generalized or localized somatic mosaicism:	Contiguous gene deletions[6]; one case of multiexonic deletion	nonsense, frameshift, splice site[7]
Types of somatic mutation in tumour tissues:	Neurofibroma: splicing defects, LOH[8]	
MPNST: LOH[8], deletion	Bilateral vestibular schwannomas: nonsense, frameshift, splice site, LOH[8]	

1 Alternative splicing produces transcripts of varying lengths; 2 Reviewed in Dasgupta & Gutman, 2003 ; 3 Reviewed in McClatchey & Giovannini, 2005; 4 For example, Mattocks *et al.*, 2004; 5 Wallace *et al.*, 2004; Kluwe *et al.*, 2005; 6 Kehrer-Sawatzki *et al.*, 2004; technical difficulties have discouraged he search for subtle intragenic mutations; 7 Kluwe *et al.*, 2005; Moyhuddin *et al.*, 2003; 8 LOH, loss of heterozygosity by mitotic recombination or deletion.
MPNST, malignant peripheral nerve sheath tumour.

Less rigorous studies suggest that this subset of patients may be predisposed to childhood overgrowth, early age of onset, and excessive numbers of cutaneous and internal neurofibromas, learning disabilities, vascular anomalies, and astrocytomas (Dorschner *et al.*, 2000; Gutmann *et al.*, 2003; Venturin *et al.*, 2004; Kehrer-Sawatzki *et al.*, 2005;

NF1 contiguous gene deletions are recurring 1.4 Mb or 1.2 Mb deletions that span the entire *NF1* gene along with neighbouring genes (Dorschner *et al.*, 2000; Lopez-Correa *et al.*, 2001; Kehrer-Sawatzki *et al.*, 2004; 2006a). These recurring deletions arise by recombination between high identity sequence elements that flank the *NF1* gene.

While testing a patient with equivocal findings can be done, it is important to realize that the frequency of positive test results is expected to be quite low. DNA-based clinical testing for NF2 is primarily used for presymptomatic testing of at-risk individuals, typically young children of an affected parent, in conjunction with genetic counselling. An early diagnosis of NF2 improves management, which is primarily surgical and radiological and may improve outcome. For at-risk children who test negative, they and their families will be spared the worry and the expense of periodic diagnostic screening. Correlations between NF2 mutations and phenotype have been described, although they cannot predict the age of onset or the course of disease for an individual patient. Typically constitutional frameshift and nonsense mutations are associated with more severe NF2, defined by earlier age at onset and higher frequency and mean numbers of tumours (Parry *et al.*, 1996; Evans *et al.*, 1998). Constitutional missense and small in-frame mutations are considered to be associated with mild disease, and mutations in splice donor/acceptor sites result in variable clinical outcomes (Evans *et al.*, 1998; Kluwe *et al.*, 1998); although slice site mutations in certain exons are more severe mutations (Baser *et al.*, 2005). Interestingly, certain mutation types are associated with increased non-vestibular nervous system tumours (Baser *et al.*, 2004).

Diagnostic testing to confirm a clinical diagnosis may also be helpful in sporadic NF2 cases in children or adults with equivocal findings or mild disease. Couples seeking prenatal or preimplantation diagnosis for either NF1 or NF2 are advised to seek genetic counselling before pregnancy, as identification of the mutation carried by the affected parent can take weeks or months. A confounding factor in diagnostic testing of either NF1 or NF2 is somatic mosaicism for a post-zygotic mutation (see Table 1 for estimated frequency). Mosaic individuals are always sporadic cases (that is, the first person in their family to have the disease) and carry the mutated gene in only a fraction of their cells, depending upon the developmental interval and cell type in which the mutation occurred (Fig. 1). Therefore, individuals with mosaicism can have localized disease or mild to severe generalized disease; this is likely to be the cause of the clinical entity known as segmental NF1 (Ruggieri & Huson, 2001). Individuals mosaic for an *NF1* or *NF2* mutation have a (50 per cent risk of have an affected child, depending upon the proportion of gametes that carry the mutation. Offspring that do inherit the mutation will have it in every cell of the body and may have more severe disease than the parent. Genetic counselling regarding the clinical and reproductive implications of mosaicism is important (Ruggieri & Huson, 2001).

The profile of constitutional mutations in NF1 and NF2 is similar. Both disorders are both caused by a mutation that inactivates one allele (or copy) of the gene resulting in haploinsufficiency for the protein product of the gene, neurofibromin or merlin, respectively (Table 2). Many types of mutations have been identified that affect the normal gene structure and function at all levels (Table 2, Fig. 2). Thus DNA-based testing for either NF1 or NF2 disease, typically undertaken on peripheral leucocytes, often employs a multipronged approach using molecular techniques that can detect different types of mutation at high frequency. In general, the testing

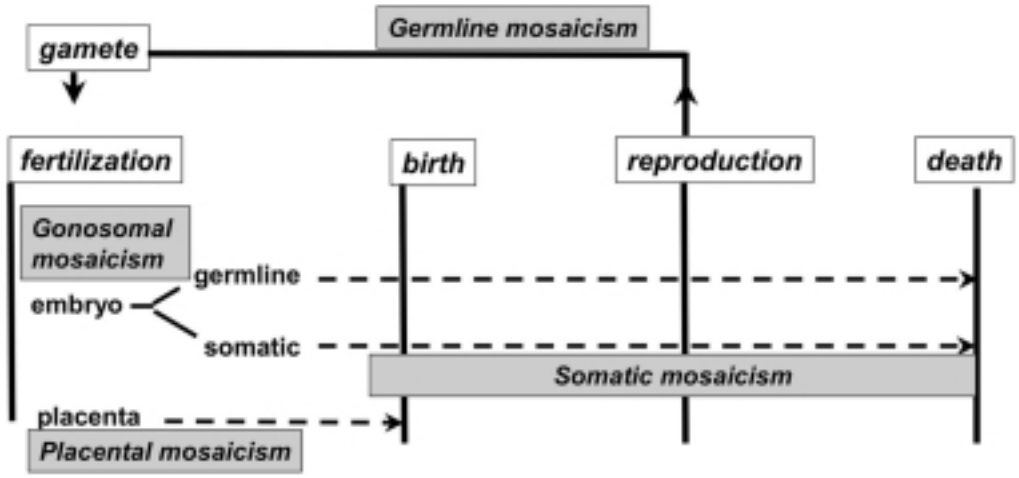

Fig. 1. The types of mosaicism that can occur during the human life cycle. Mutation in NF1 and NF2 (and other genes) can occur throughout the life cycle from fertilization to death. Gonosomal mosaicism refers to a mutation that occurs in the early embryo before the split of the germline and somatic progenitors; such individuals are at risk for having the disease and for having an affected offspring. Individuals with only somatic mosaicism may have no, mild, or severe disease depending upon the developmental interval and the somatic cell type; they are not at risk for having affected offspring. In practice, it is impractical or impossible to distinguish between gonosomal and somatic mosaicism unless the patient has an affected child, which would indicate involvement of the germline. Placental and germline mosaicism have no impact on the patient's phenotype but, depending upon the gene involved, may affect fetal development; the consequences of NF1 or NF2 placental mosaicism on the fetus are unknown. Germline mosaicism results from a new mutation in a germ cell or progenitor germ cell; the carrier will not develop the disease, but their offspring are at risk of inheriting a gamete carrying a mutation and being affected.

methodologies employ either direct sequence analysis of amplified products of each exon and the associated intronic regions or mutation scanning methodology (for example, denaturing high performance liquid chromatography, premature protein termination, heteroduplex analysis) that detects putative mutations in amplified products from genomic or cDNA templates. These are subsequently confirmed by direct DNA sequence analysis or other appropriate method. The detection of *NF1* contiguous gene deletions typically involves fluorescence *in situ* hybridization, while smaller multiexonic deletions, typical of NF2, are often detected by a type of quantitative gene dosage assay. Routine cytogenetic analysis has a very low sensitivity for detecting NF1 or NF2 mutations. A recent review of available assays used in NF1 and NF2 testing has been published (2006b). The choice of assay and testing laboratory depends upon the reason for referral and the detection rates for different mutation types and mutation. Although published reports may give high detection rates for a specific protocol, it is important to realize that detection rates – particularly for mutation scanning protocols – will be laboratory-specific owing to the degree of optimization of a specific technique. The clinician is advised to survey testing laboratories before submitting samples.

DNA-based diagnosis of NF2, but not NF1, can often be facilitated by analysis of unused pathology tissue after surgical removal of a bilateral vestibular schwannoma. These tumours develop from a progenitor Schwann cell that carries a somatic inactivating mutation in the single remaining NF2 gene. Thus these cells have no functional merlin. Because these tumours are clonal with minimal cellular admixture, *NF2* mutations can be detected at high frequency.

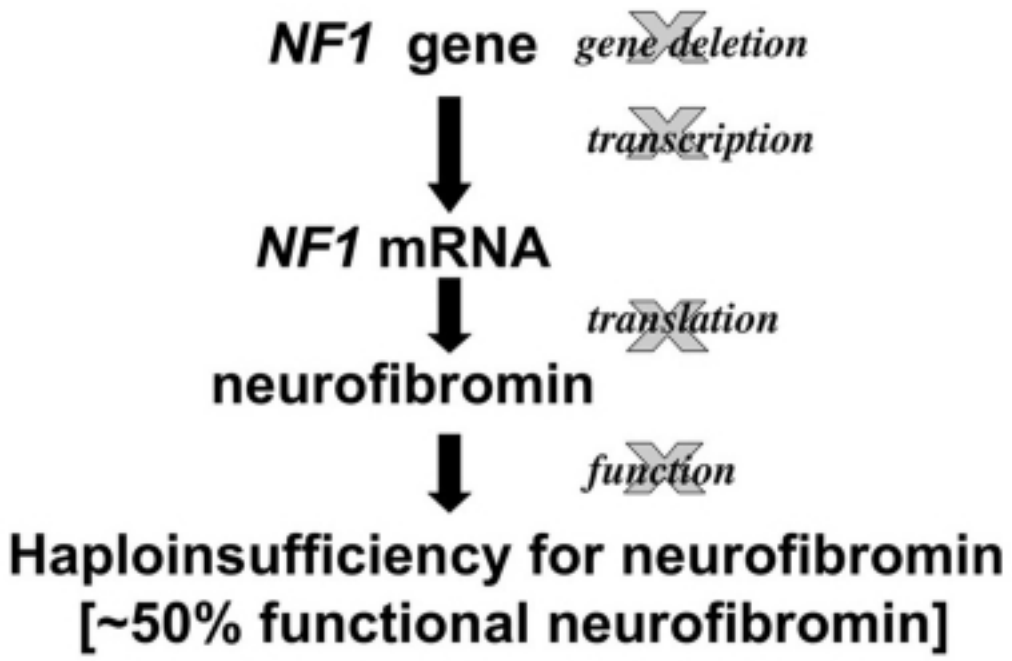

Fig. 2. The consequences of NF1 gene mutation. Different types of NF1 mutation affect the gene structure and function at all levels from deletion of the entire gene to inhibiting transcription or transcript stability, affecting translation or inactivating, or altering the normal function of the protein. The result of all these mutations is haploinsufficiency for neurofibromin. Although this schematic is for NF1, the same is true for the NF2 gene and its protein product merlin.

This is most useful in cases where a mutation is not detected in primary leucocytes of a patient in whom the clinical manifestations suggest somatic mosaicism, or where normal tissue is unavailable (Kluwe *et al.*, 2003; Moyhuddin *et al.*, 2003; Wallace *et al.*, 2004). For NF2 patients undergoing surgery, it is advisable to arrange to have a portion of the tumour frozen and saved, as it may be valuable for future mutational analysis for the benefit of the patient or their relatives. Although neurofibromas and MPNST of NF1 patients also arise from progenitor cells with both copies of the *NF1* gene inactivated, these tumours are typically not useful tissue for mutational analyses because the tumour is composed of numerous other cell types that compromise mutation detection.

Linkage testing for NF1 and NF2 may be the quickest, most economical test for at-risk individuals and fetuses of families that fulfil the testing criteria. This is an indirect form of testing that does not identify the specific mutation in the gene but tracks the inheritance of the mutant *NF1* or *NF2* allele in members of a family (Fig. 3). Multiple family members whose NF1 (or NF2) disease status is unambiguous must participate in the testing process. Prenatal testing of the example in Fig. 3 would determine if the fetus inherited the at-risk haplotype R. Linkage testing is compromised by somatic mosaicism and this possibility must be evaluated carefully before embarking on this form of testing (Fig. 3). Additional issues related to test interpretation and laboratory issues related to clinical testing for NF1 and NF2 have been reviewed recently (

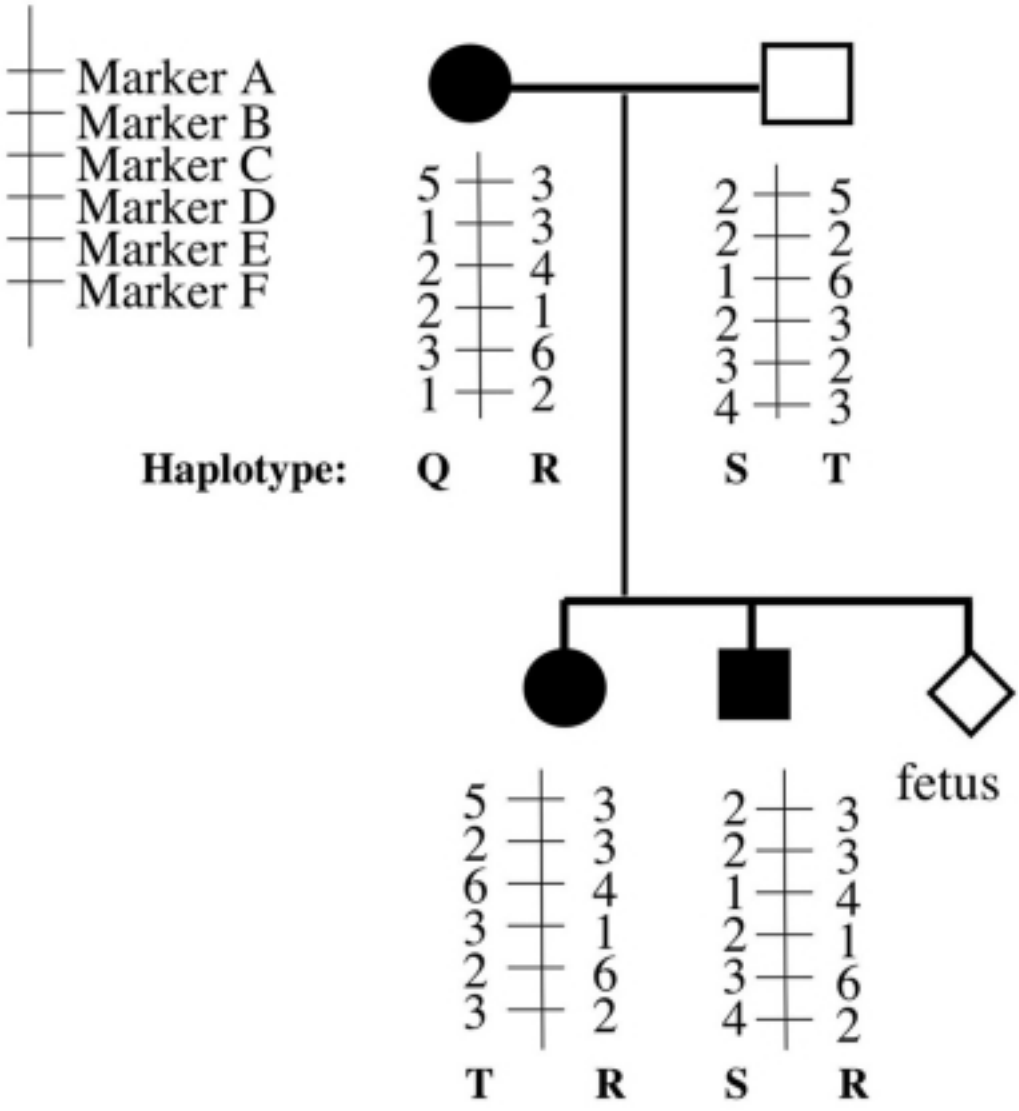

Fig. 3. Example of linkage testing for prenatal diagnosis. The schematic shows a generic example of linkage testing in which markers A-F are polymorphic sites at known positions in, or very close to, the gene of interest. The genotypes at each marker are determined in multiple family members of known disease status. The arrangement of genotypes in this segment of the chromosome is known as a haplotype. In this example, the at-risk haplotype carrying the mutated gene is R; testing the fetus will determine if it has inherited the R haplotype and therefore the disease. Gonosomal mosaicism may compromise linkage testing: if the mother is a gonosomal mosaic, then a fraction of her R chromosomes would carry a mutant gene and a fraction would have a normal gene. Therefore, if the fetus inherited the R haplotype, one could not predict the disease status. Circles, female; squares, male; filled symbols, affected; empty symbols, unaffected; diamond, foetus.

Conclusions

In the past 5 years, significant advances have been made in understanding the types of mutation that inactivate the *NF1* and *NF2* genes and their clinical consequences. This has led to the development and availability of sensitive and specific DNA-based tests for diagnostic, presymptomatic, prenatal, and preimplantation diagnosis of the NF1 and NF2 disorders. Already these tests have altered clinical diagnosis, management, and outcome for at least a subset of affected patients. Future advances are expected to provide new correlations between genotype and management, and possibly therapeutic, decisions for clinicians caring for individuals affected with these disorders.

Acknowledgments: This work was supported by a grant DAMD17-03-1-0203 from the U.S. Army Materiel and Medical Command awarded to K.S.

References

Baser, M.E., Friedman, J.M., Wallace, A.J., Ramsden, R.T., Joe, H. & Evans, D.G. (2002): Evaluation of clinical diagnostic criteria for neurofibromatosis 2. *Neurology* **59**, 1759–1765.

Baser, M.E., Dg, R.E. & Gutmann, D.H. (2003): Neurofibromatosis 2. *Curr. Opin. Neurol.* **16**, 27–33.

Baser, M.E., Kuramoto, L., Joe, H., Friedman, J.M., Wallace, A.J., Gillespie, J.E., Ramsden, R.T. & Evans, D.G. (2004): Genotype-phenotype correlations for nervous system tumors in neurofibromatosis 2: a population-based study. *Am. J. Hum. Genet.* **75**, 231–239.

Baser, M.E., Kuramoto, L., Woods, R., Joe, H., Friedman, J.M., Wallace, A.J., Ramsden, R.T., Olschwang, S., Bijlsma, E., Kalamarides, M., Papi, L., Kato, R., Carroll, J., Lazaro, C., Joncourt, F., Parry, D.M., Rouleau, G.A. & Evans, D.G. (2005): The location of constitutional neurofibromatosis 2 (NF2) splice site mutations is associated with the severity of NF2. *J. Med. Genet.* **42**, 540–546.

Dasgupta, B. & Gutmann, D.H. (2003): Neurofibromatosis 1: closing the GAP between mice and men. *Curr. Opin. Genet. Dev.* **13**, 20–27.

Debella, K., Szudek, J. & Friedman, J.M. (2000): Use of the national institutes of health criteria for diagnosis of neurofibromatosis 1 in children. *Pediatrics* **105**, 608–614.

De Raedt, T., Brems, H., Wolkenstein, P., Vidaud, D., Pilotti, S., Perrone, F., Mautner, V., Frahm, S., Sciot, R. & Legius, E. (2003): Elevated risk for MPNST in NF1 microdeletion patients. *Am. J. Hum. Genet.* **72**, 1288–1292.

Dorschner, M.O., Sybert, V.P., Weaver, M., Pletcher, B.A. & Stephens, K. (2000): NF1 microdeletion breakpoints are clustered at flanking repetitive sequences. *Hum. Mol. Genet.* **9**, 35–46.

Evans, D.G. (2004): Updated 4/6/2004. Neurofibromatosis 2. In: GeneReviews at GeneTests: Medical Genetics Information Resource (database online). Copyright, University of Washington, Seattle. 1997–2005. Available at http://www.genetests.org. Accessed [11/07/2005].

Evans, D.G., Trueman, L., Wallace, A., Collins, S. & Strachan, T. (1998): Genotype/phenotype correlations in type 2 neurofibromatosis (NF2): evidence for more severe disease associated with truncating mutations. *J. Med. Genet.* **35**, 450–455.

Evans, D.G., Sainio, M. & Baser, M.E. (2000): Neurofibromatosis type 2. *J. Med. Genet.* **37**, 897–904.

Evans, D.G., Baser, M.E., Mcgaughran, J., Sharif, S., Howard, E. & Moran, A. (2002): Malignant peripheral nerve sheath tumours in neurofibromatosis 1. *J. Med. Genet.* **39**, 311–314.

Evans, D.G., Baser, M.E., O'Reilly, B., Rowe, J., Gleeson, M., Saeed, S., King, A., Huson, S.M., Kerr, R., Thomas, N., Irving, R., Macfarlane, R., Ferner, R., Mcleod, R., Moffat, D. & Ramsden, R. (2005a): Management of the patient and family with neurofibromatosis 2: a consensus conference statement. *Br. J. Neurosurg.* **19**, 5–12.

Evans, D.G., Moran, A., King, A., Saeed, S., Gurusinghe, N. & Ramsden, R. (2005b): Incidence of vestibular schwannoma and neurofibromatosis 2 in the North West of England over a 10-year period: higher incidence than previously thought. *Otol. Neurotol.* **26**, 93–97.

Friedman, J.M. (2002): Neurofibromatosis 1: clinical manifestations and diagnostic criteria. *J. Child Neurol.* **17**, 548–554.

Friedman J. Updated 10/5/2004. Neurofibromatosis 1. In: GeneReviews at GeneTests: Medical Genetics Information Resource (database online). Copyright, University of Washington, Seattle. 1997–2005. Available at http://www.genetests.org. Accessed [11/10/2005].

Friedman, J.M., Butmann, D.H., Maccollin, M. & Riccardi, V.M., eds. (1999): *Neurofibromatosis. Phenotype, natural history, and pathogenesis*, 3rd ed. Baltimore, The Johns Hopkins University Press.

Gutmann, D.H., James, C.D., Poyhonen, M., Louis, D.N., Ferner, R., Guha, A., Hariharan, S., Viskochil, D. & Perry, A. (2003): Molecular analysis of astrocytomas presenting after age 10 in individuals with NF1. *Neurology* **61**, 1397–1400.

Kehrer-Sawatzki, H., Kluwe, L., Sandig, C., Kohn, M., Wimmer, K., Krammer, U., Peyrl, A., Jenne, D.E., Hansmann, I. & Mautner, V.F. (2004): High frequency of mosaicism among patients with neurofibromatosis type 1 (NF1) with microdeletions caused by somatic recombination of the JJAZ1 gene. *Am. J. Hum. Genet.* **75**, 410–423.

Kehrer-Sawatzki, H., Kluwe, L., Funsterer, C. & Mautner, V.F. (2005): Extensively high load of internal tumors determined by whole body MRI scanning in a patient with neurofibromatosis type 1 and a non-LCR-mediated 2-Mb deletion in 17q11.2. *Hum. Genet.* **116**, 466–475.

Kluwe, L., MacCollin, M., Tatagiba, M., Thomas, S., Hazim, W., Haase, W. & Mautner, V.F. (1998): Phenotypic variability associated with 14 splice-site mutations in the NF2 gene. *Am. J. Med. Genet.* **77**, 228–233.

Kluwe, L., Mautner, V., Heinrich, B., Dezube, R., Jacoby, L.B., Friedrich, R.E. & Maccollin, M. (2003): Molecular study of frequency of mosaicism in neurofibromatosis 2 patients with bilateral vestibular schwannomas. *J. Med. Genet.* **40**, 109–114.

Kluwe, L., Nygren, A. O., Errami, A., Heinrich, B., Matthies, C., Tatagiba, M. & Mautner, V. (2005): Screening for large mutations of the NF2 gene. *Genes Chromosomes Cancer* **42**, 384–391.

Lopez-Correa, C., Dorschner, M., Brems, H., Lazaro, C., Clementi, M., Upadhyaya, M., Dooijes, D., Moog, U., Kehrer-Sawatzki, H., Rutkowski, J.L., Fryns, J.P., Marynen, P., Stephens, K. & Legius, E. (2001): Recombination hotspot in NF1 microdeletion patients. *Hum. Mol. Genet.* **10**, 1387–1392.

MacCollin, M., Chiocca, E.A., Evans, D.G., Friedman, J.M., Horvitz, R., Jaramillo, D., Lev, M., Mautner, V.F., Niimura, M., Plotkin, S.R., Sang, C.N., Stemmer-Rachamimov, A. & Roach, E.S. (2005): Diagnostic criteria for schwannomatosis. *Neurology* **64**, 1838–1845.

Mattocks, C., Baralle, D., Tarpey, P., Ffrench-Constant, C., Bobrow, M. & Whittaker, J. (2004): Automated comparative sequence analysis identifies mutations in 89% of NF1 patients and confirms a mutation cluster in exons 11–17 distinct from the GAP related domain. *J. Med. Genet.* **41**, e48.

McClatchey, A.I. & Giovannini, M. (2005): Membrane organization and tumorigenesis – the NF2 tumor suppressor, Merlin. *Genes Dev.* **19**, 2265–2277.

Moyhuddin, A., Baser, M.E., Watson, C., Purcell, S., Ramsden, R.T., Heiberg, A., Wallace, A.J. & Evans, D.G. (2003): Somatic mosaicism in neurofibromatosis 2: prevalence and risk of disease transmission to offspring. *J. Med. Genet.* **40**, 459–463.

Mulvihill, J.J. (1994): Malignancy: epidemiologically associated cancers. In: *The neurofibromatoses: a pathogenetic and clinical overview*, 1st edition., ed. S.M. Huson & R.A.C. Hughes, pp. 487. London: Chapman & Hall Medical.

Parry, D.M., Maccollin, M.M., Kaiser-Kupfer, M.I., Pulaski, K., Nicholson, H.S., Bolesta, M., Eldridge, R. & Gusella, J.F. (1996): Germ-line mutations in the neurofibromatosis 2 gene: correlations with disease severity and retinal abnormalities. *Am. J. Hum. Genet.* **59**, 529–539.

Rasmussen, S.A., Yang, Q. & Friedman, J.M. (2001): Mortality in neurofibromatosis 1: an analysis using U.S. death certificates. *Am. J. Hum. Genet.* **68**, 1110–1118.

Ruggieri, M. & Huson, S.M. (2001): The clinical and diagnostic implications of mosaicism in the neurofibromatoses. *Neurology* **56**, 1433–1443.

Ruggieri, M., Iannetti, P., Polizzi, A., La Mantia, I., Spalice, A., Giliberto, O., Platania, N., Gabriele, A.L., Albanese, V. & Pavone, L. (2005): Earliest clinical manifestations and natural history of neurofibromatosis type 2 (NF2) in childhood: a study of 24 patients. *Neuropediatrics* **36**, 21–34.

Stephens, K. (2006a): The neurofibromatoses. In: *Molecular pathology in clinical practice*, ed. D.G.B. Leonard, A. Bagg, A. Caliendo, K. Kaul, K. Snow-Bailey, & V. Van Deerlin. New York: Springer-Verlag.

Stephens, K. (2006b) Neurofibromatosis 1. In: *Genomic disorders: the genomic basis of genetic disease*, ed. J.R. Lupski & P.T. Stankiewicz. Trenton: Humana Press.

Venturin, M., Guarnieri, P., Natacci, F., Stabile, M., Tenconi, R., Clementi, M., Hernandez, C., Thompson, P., Upadhyaya, M., Larizza, L. & Riva, P. (2004): Mental retardation and cardiovascular malformations in NF1 microdeleted patients point to candidate genes in 17q11.2. *J. Med. Genet.* **41**, 35–41.

Wallace, A.J., Watson, C.J., Oward, E., Evans, D.G. & Elles, R.G. (2004): Mutation scanning of the NF2 gene: an improved service based on meta-PCR/sequencing, dosage analysis, and loss of heterozygosity analysis. *Genet. Test.* **8**, 368–380.

Woodruff, J.M. (1999): Pathology of tumors of the peripheral nerve sheath in type 1 neurofibromatosis. *Am. J. Med. Genet. (Semin. Med. Genet.)* **89**, 23–30.

14 Neurofibromatosis 1

Karen Stephens, PhD

CONTENTS

INTRODUCTION

Among genomic disorders, submicroscopic deletions underlying neurofibromatosis 1 (NF1) are unusual because they involve the deletion of a tumor suppressor gene (*NF1*), they show a different preference for low-copy repeats (LCR) as substrates for meiotic vs mitotic recombination events, and they account for only a small fraction of mutations that cause the disorder. The *NF1* gene at chromosome 17q11.2 is flanked by two sets of LCRs in direct orientation that undergo paralogous recombination. A pair of NF1-REPs mediate the recurrent constitutional 1.4-Mb microdeletion that occurs preferentially during maternal meiosis, whereas a pair of *JJAZ1* pseudogene and functional gene mediate the recurrent 1.2-Mb microdeletion that occurs preferentially during postzygotic mitosis in females. Breakpoints have been mapped at the nucleotide level for both deletions and sequence features that may contribute to the choice of discrete sites for strand exchange have been identified. NF1-REP-mediated *NF1* microdeletions involve 13 additional genes, whereas *JJAZ1*-mediated microdeletions involve the same genes but one. *NF1* microdeletions are of great interest because they predispose to a heavy tumor burden, malignancy, and possibly other severe manifestations.

In 1992, the first report of a NF1 patient with a submicroscopic contiguous gene deletion spanning the *NF1* tumor suppressor gene provided direct evidence that this common autosomal dominant disorder was caused by haploinsufficiency of the *NF1* protein product, neurofibromin *(1)*. Here, subsequent molecular, genetic, and clinical studies of *NF1* microdeletions are reviewed, which have made significant contributions to our understanding of the mutational mechanisms and pathogenesis of this common multisystemic, progressive, tumor predisposition disorder, and to genomic disorders in general.

From: *Genomic Disorders: The Genomic Basis of Disease*
Edited by: J. R. Lupski and P. Stankiewicz © Humana Press, Totowa, NJ

MOLECULAR BASIS OF NEUROFIBROMATOSIS 1

Virtually all subjects affected with NF1 develop multiple benign neurofibromas, which are tumors of superficial and deep peripheral nerves that increase in number with age, along with pigmentation changes of café au lait macules, axillary/inguinal freckling, and hamartomas of the iris of the eye *(2)*. Neurofibromas are unpredictable with regards to number, location, rate of growth, and potential for malignant transformation. Additional complications unrelated to neurofibroma development are legion, and include learning disabilities, scoliosis and other bone abnormalities, optic glioma, and malignancies of various organ systems, such as malignant peripheral nerve sheath tumors (MPNST), rhabdomyosarcoma, and myeloid leukemias *(3)*. Although a deletion or other constitutional inactivating mutation of one *NF1* allele predisposes to benign or malignant tumorigenesis, a somatic inactivating mutation of the remaining *NF1* allele in a tumor progenitor cell is an early, if not initiating, event in most, if not all, NF1-associated tumors. The tumor progenitor cell of the cellularly heterogeneous neurofibroma and the MPNST is the Schwann cell *(4)*. A second requirement for neurofibroma development in a mouse model is the presence of heterozygous $Nf1^{+/-}$ murine cells in the micro-tumor environment *(4)*. The requirement of different neurofibromin levels in target cells vs supportive cells results in modulation of the RAS signaling pathway, as neurofibromin is a guanosine-5'-triphosphatase (GTPase)-activating protein that catalyzes the conversion of active RAS-GTP to inactive RAS-GDP *(5)*. The requirement for *Nf1* heterozygosity in the mouse brain for the development of optic nerve glioma by *Nf1* ablated astrocytes *(6)* extends the emerging paradigm that neurofibromin haploinsufficiency in cells of the micro-tumor environment is critical.

The NF1 Mutational Profile

The mutational profile of the *NF1* gene at chromosome 17q11.2 is complex, as both constitutional and somatic mutations occur that result in generalized or segmental (localized) NF1 disease and tumor development (Table 1). NF1 is inherited as an autosomal dominant trait, but also occurs sporadically in approx 30–50% of cases. In 80–90% of cases owing to intragenic *NF1* inactivating mutations, no correlation has been detected between mutation type and/or location and the development of specific manifestations *(7–9)*. Approximately 5% of NF1 cases are because of submicroscopic, contiguous gene deletions *(10–12)*. Most *NF1* microdeletions are *de novo* and are predominantly of maternal origin, although familial cases do occur *(13–17)*. Subjects with *NF1* microdeletions tend to have a high tumor burden and may have facial anomalies, early age at onset of dermal neurofibromas, vascular anomalies, learning disabilities, astrocytomas, and malignancy *(12–14,18,19)*. Formal studies regarding *NF1* microdeletion genotype/phenotype correlations await a comprehensive clinical and molecular evaluation of a cohort of *NF1* microdeletion subjects ascertained in an unbiased manner. One such study has shown that *NF1* microdeletion doubles the lifetime risk of MPNST relative to nondeletional genotypes *(20)*. One confounding factor in such studies is that approx 25% of *NF1* microdeletions occur as postzygotic mutations and different levels of mosaicism in patient tissues can result in generalized or localized NF1 (*see* LCR-Mediated Somatic *NF1* Microdeletions) *(21)*. A major area of research is focused on identifying genes in the deleted region that modify NF1-related tumorigenesis or other manifestations of the disorder. As summarized in Table 1, somatic second hit inactivating mutations of *NF1* are typically owing to loss of heterozygosity by recombination, chromosomal deletion that is not known to be LCR-mediated or intragenic inactivating mutations (Table 1).

Table 1
Mutational Profile of the *NF1* Gene

NF1 *mutation category*	*Patient phenotype/ tissue*	*Mode of inheritance*	NF1 *mutation type*	*Selected references*
Constitutional	NF1	familial or *de novo*	LCR-mediated contiguous gene deletion (approx 5%)	*10*
			Nonsense, splicing defects, missense (85–90%)	*39–41*
Somatic mosaicism	NF1	*de novo*	LCR-mediated contiguous gene deletion	*21,38,42–44*
	Localized NF1	*de novo*	LCR-mediated contiguous gene deletion, multi-exonic deletion	*21,38,45*
Germline mosaicism	Unaffected	*de novo*	Intragenic deletion	*46*
Somatic 2nd hits in tumor tissue[a]	Neurofibroma	*de novo*	Splicing defects, LOH[b]	*47–49*
	MPNST	*de novo*	LOH[b], deletion	*48–52*
	Myeloid leukemia	*de novo*	Nonsense, others that predict premature truncation	*7*

[a]Reviewed in ref. *52*.
[b]Loss of heterozygosity via recombination or deletion.

RECURRENT NF-REP-MEDIATED *NF1* MICRODELETIONS

An estimated (50–60%) of constitutional *NF1* microdeletions have a common recurrent 1.4-Mb deletion that includes *NF1* and at least 13 other genes (Fig. 1; Table 2) (11). Both centromeric and telomeric deletion breakpoints cluster within two LCR sequences, or paralogs, termed NF1-REP-P1 and NF1-REP-M (Fig. 1). The direct orientation of these two NF1-REPs suggested a mechanism consistent with the existing paradigm whereby deletions occur by nonallelic homologous recombination, or paralogous recombination, between misaligned paralogs on the interchromosomal, intrachromosomal, or intrachromatidal level *(22)*. For *NF1*, this mechanism was confirmed by mapping NF1-REP-mediated deletion breakpoints at the nucleotide level *(17,23)* and by haplotype analyses *(16)*.

NF1-REPs are complex assemblies of paralogs from different sequence families consisting of expressed genes, pseudogenes, gene fragments, and non-coding sequence (Fig. 2) *(24)*. NF1-REP-P1 and NF1-REP-M share a 51-kb segment of 97.5% sequence identity, termed NF1-REP-51, which serves as the substrate for paralogous recombination events. Two other components of the NF1-REP family include NF1-REP-P2, which is centromeric to *NF1*, and NF1-REP-E19 located on chromosome 19p13.13 (Fig. 2) *(24,25)*. *NF1* microdeletions owing to apparent paralogous recombination between NF1-REP-P2 and -M have been reported, but their breakpoints have not been mapped at the nucleotide level *(26)*. Large kilobase-sized polymorphisms have not been observed in the NF1-REPs, although certain structural features, such as the inverted repeats in *KIAA0563rel*-ψ of NF1-REP-P1 that could mediate an inversion event, may generate such polymorphisms in the general population. There is no evidence of constitutional or somatic chromosomal translocations that could be attributable to recombina-

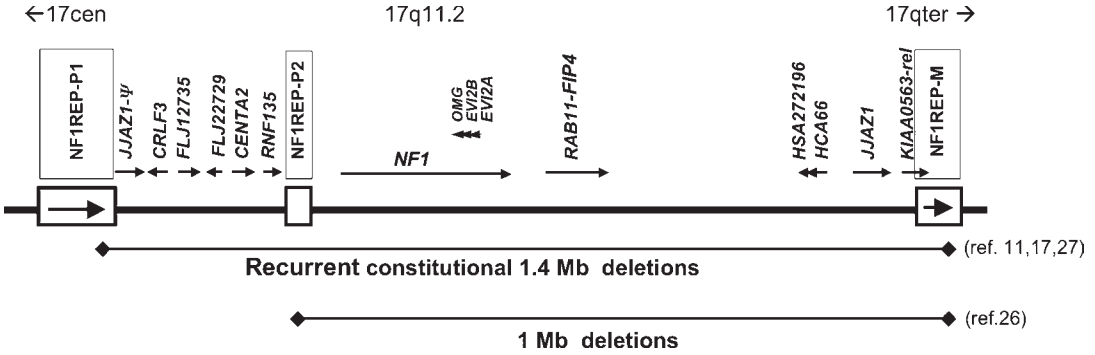

Fig. 1. Genomic structure of the *NF1* microdeletion region in chromosome 17q11.2 and the recurrent constitutional 1.4-Mb deletion. The 350-kb *NF1* gene, and other regional genes, are indicated by arrows showing their direction of transcription. *OMG*, *EVI2A*, and *EVI2B* are within an *NF1* intron and are transcribed on the alternate strand. Table 2 details the genes in this region. Boxes designate the 3 NF1-REPs, with arrows indicating direct repeat orientation of NF1-REP-P1 and -M. Genomic length from NF1-REP-P1 through NF1-REP-M is 1.5 Mb and the most frequent constitutional deletions are 1.4 Mb. Two approx 1-Mb deletions have been reported apparently because of recombination between NF1-REP-P2 and -M (*see* Recurrent NF-REP-Mediated *NF1* Microdeletions; *26*). NF1-REP-P1, -P2, -M are 131, 43, and 75 kb in length, respectively (*see* Fig. 2 for details). Gene names are from May 2004 assembly of the human genome (http://genome.ucsc.edu/) and may differ from names on previously published maps of the region *(23,25,26)*.

Table 2
Functional Genes Within the Recurrent 1.4-Mb *NF1* Microdeletion Region

Gene/marker[a]	*Description*	*REFSEQ mRNA accession number*
CRLF3	Cytokine receptor-like factor 3	NM_015986.2
FLJ12735	Putative ATP(GTP)-binding protein[b]	NM_024857.3
FLJ2279	Hypothetical protein, unknown function	NM_024683.1
CENTA2	Centaurin alpha 2, binds phosphatidylinositol 3,4,5-triphosphate and inositol 1,3,4,5,-tetrakisphophate	NM_018404.1
RFN135	Ring finger protein 135	NM_032322.3 NM_197939.1
NF1	Ras GTPase stimulating protein	NM_000267.1
OMG	Oligodendrocyte myelin glycoprotein; cell adhesion molecule contributing to myelination in the central nervous system	NM_002544.2
EVI2B	Ecotropic viral integration site 2B, membrane protein	NM_006495.2
EVI2A	Ecotropic viral integration site 2A, membrane protein	NM_014210.1
RAB11-FIP4	Putative Rab11 family interacting protein 3	NM_032932.2
HSA272196	Hypothetical protein, unknown function	NM_018405.2
HCA66	Hepatocellular carcinoma-associated antigen 66	NM_018428.2
JJAZ1	Protein with zinc finger domain and homology to Drosophia Polycomb protein SUZ12	NM_015355.1
KIAA0563-rel	KIAA0563-related, unknown function	NM_014834.2

[a]From the May 2004 genome assembly (http://genome.ucsc.edu/).
[b]ATP, adenosine-5'-triphosphate; GTP, guanosine-5'-triphosphate.

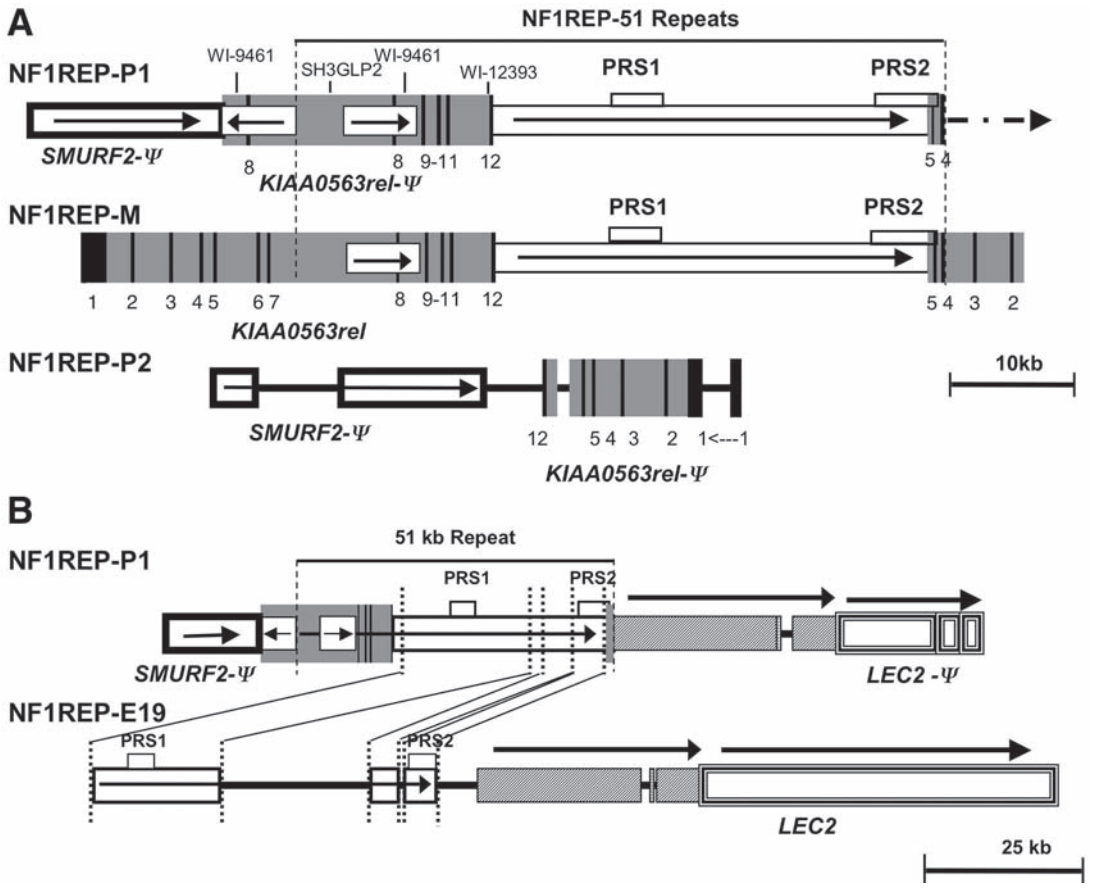

Fig. 2. The structure of the NF1-REP paralogs. (A) The structure of NF1-REP-P1 (131 kb) and a partial structure of NF1-REP-M (*see* B for complete structure) are shown. These serve as paralogous recombination substrates for the common 1.4-Mb *NF1* microdeletion. The 51-kb high sequence identity region, designated NF1-REP-51 harbors the recombination hotpots PRS1 and PRS2. Gray blocks indicate the *KIAA0563rel* functional gene and related pseudogene (ψ) fragments with numbered black bars designating exons or exon-derived sequences. White boxes with arrows inside *KIAA0563rel* sequences designate the orientation of a 5.9-kb inverted repeats with two copies in NF1-REP-P1 and one in NF1-REP-M. STS in KIAA0563rel are shown as landmarks. Open blocks with bold margins are *SMURF2*-derived pseudogene (ψ) fragments. The arrow at the telomeric end of NF1-REP-P1 indicates that it is truncated; see panel B for full-length structure. NF1-REP-P2 is a partial NF1-REP with fragments derived from *SMURF2* and *KIAA0563* pseudogenes. Figures are oriented from centromere (left) to telomere. BAC identities and accession numbers for each NF1-REP are given in Forbes et al. *(24)*. (B) Comparison of NF1-REP-P1 and NF1-REP-E19, at chromosome 19p13.13. Boxes are labeled as in (A), in addition to *LEC2* and its pseudogene (open blocks with borders of multiple lines) and non-coding sequences between PRS2 and *LEC2* (blocks filled with diagonal lines); sequence orientations are shown with arrows. The *SMURF2*, non-coding, and *LEC2* sequences flanking the 51-kb repeat are considered part of NF1-REP-P1 based on paralogy with NF1-REP-P2 and NF1-REP–E19. BAC identities and accession numbers for each NF1-REP are given in Forbes et al. *(24)*. Note difference in scales between panels A and B. (Adapted with permission from ref. *24*.)

tion between chromosome 17 NF1-REPs and NF1-REP-E19, although NF1-REP-P1-51 and NF1-REP-E19 share 94–95% sequence identity that includes the recombination hotspots PRS1 and PRS2 (*see* next section) (Fig. 2) *(24)*. Additional NF1-REP-like elements with KIAA0563 fragments are at chromosome 17q12 and 17q24, but they do not share any other sequences with NF1-REP-P1, -P2, or –M *(11,24,25)*. Whether these LCRs mediate chromosomal rearrangements is unknown. Similar to those of other LCRs that mediate genomic disorders on chromosome 17, the segmental duplications giving rise to NF1-REPs originated in recent hominoid evolution about 25 million years ago before the separation of orangutan from the human lineage *(25)*. Fluorescent *in situ* hybridization (FISH) studies showed the presence of NF1-REP-P1 and NF1-REP-M orthologs flanking the *NF1* gene in the Great Apes *(27)*.

Discrete Paralogous Recombination Sites

Despite 51 kb of 97.5% sequence identity between NF1-REP-P1-51 and NF1-REP-M-51, paralogous recombination occurred preferentially at two discrete sites. *NF1* microdeletion breakpoints were mapped at the nucleotide level to intervals defined by paralogous sequence variants (PSV; also known as NF1-REP-specific variants). The product of paralogous recombination is a chimeric NF1-REP-P1/NF1-REP-M and shows a pattern of PSVs with transition from NF1-REP-P1 PSVs to NF1-REP-M PSVs at the breakpoint interval. Breakpoint mapping was facilitated by use of human/rodent somatic hybrid cell lines that carried only the deleted homolog 17 of the patient *(17,23)*. Sixty-nine percent ($N = 78$) of *NF1* microdeletion cases had breakpoints that clustered at paralogous recombination sites 1 and 2 (PRS1 and PRS2) (Fig. 3) *(17,23,24) (23)*. PRS2 harbored 51% of breakpoints, whereas PRS1 harbored 18%. A single case UWA160-1 had a distinct breakpoint centromeric to PRS sites (Fig. 3). The PRS1 and PRS2 regions are 4.1 and 6.3 kb in length, respectively, and are 14.5 kb apart. Each PRS has a hotspot where the majority of breakpoints mapped; PRS2 has a 2.3-kb hotspot that accounts for 93% of breakpoints, whereas PRS1 has a 0.5-kb hotspot accounting for 60% of breakpoints. During sequence analysis of recombinant PRS in several cases, instead of a perfect transition of PSVs from NF1-REP-P1 to -M, the PSVs were in "patches" with a complex transition from NF1-REP-P1 to -M to -P1 to -M *(17,23)*, indicating apparent gene conversion events. These regions were relatively short (<627 bp) and, like similar events of REP-mediated rearrangements in CMT1A and *AZFa* and *IDS (28–31)*, are considered consistent with a mechanism of double-strand break repair.

There was no significant difference between PRS1- and PRS2-mediated microdeletions for the parent of origin or for *de novo* vs familial cases *(17,23)*. In a series of 59 *NF1* microdeletion cases for which clinical evaluation of the parents was available, 10% inherited the disease, and presumably the microdeletion, from an affected parent. Among 45 *de novo* cases where parental origin could be determined, 80% were of maternal origin. The recent development of deletion-specific amplification assays that detect the recurrent *NF1* microdeletions at PRS1 and PRS2 will facilitate the assembly of patient cohorts of the same genotype for clinical evaluation and will quickly identify those patients with variant deletions, which will be important to narrow the critical region of the deletion responsible for the increased tumor load and malignancy risk of microdeletion patients *(17,23)*.

Genomic Context and Sequence Analysis of Paralogous Recombination Sites

Detailed analysis of the PRS and the NF1-REP-51 paralogs at the nucleotide level identified interesting features, but lacked compelling evidence for why breakpoints preferentially occur at these sites *(24)*. There were no obligate local sequence features shared by PRS1 and PRS2.

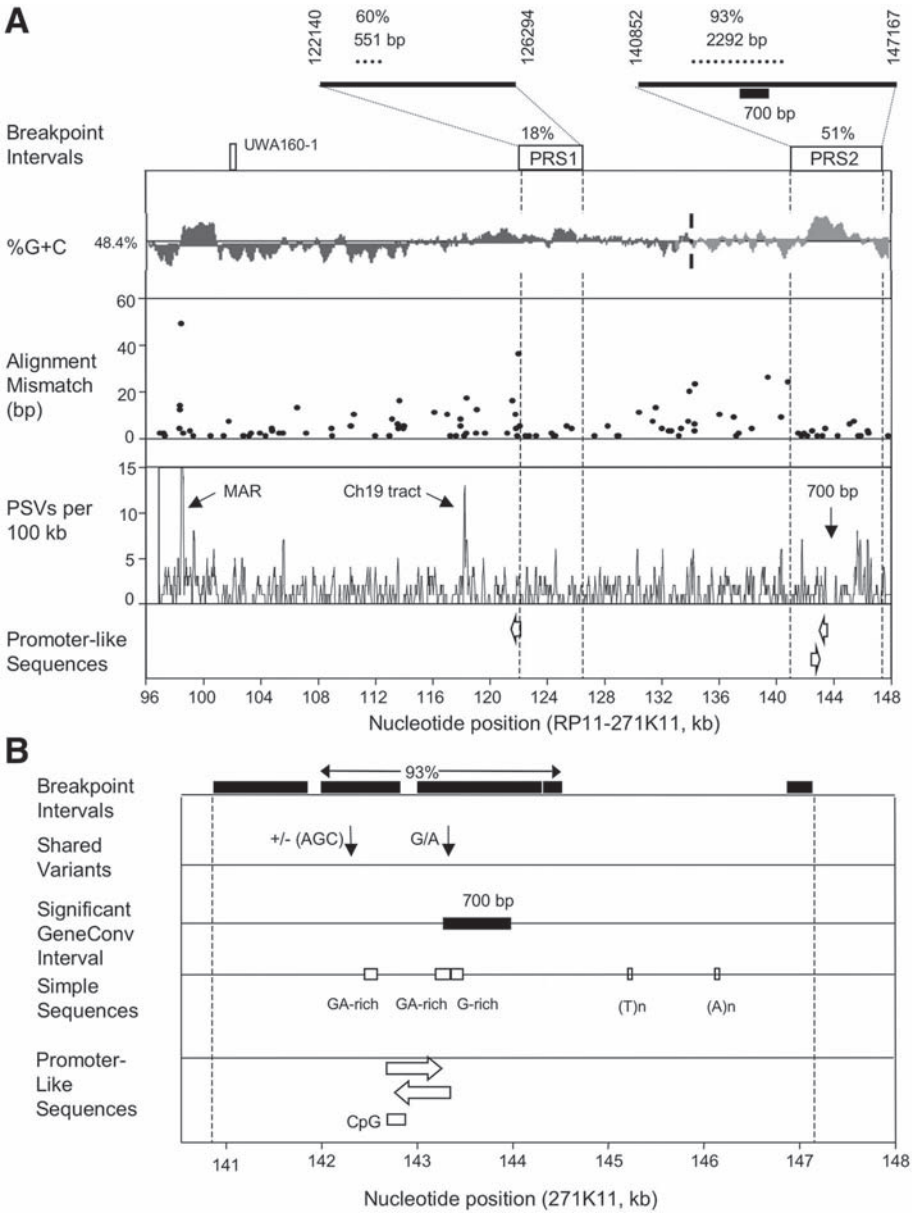

Fig. 3. Genomic context of the paralogous recombination hotspots for *NF1* microdeletion. (A) Alignment, identity, and sequence features of the 51-kb high identity NF1-REP-P1-51 and NF1-REP-M-51 paralogs. Alignment mismatch panel shows gap alignments ranging from 1 to 50 bp between NF1-REP-P1-51 and NF1-REP-M-51 in BACs RP11-271K11 and RP11-640N20, respectively. PSVs for each REP, indels excluded, with a sliding 100-bp window are shown, including a matrix attachment site (MAR), an apparent gene conversion tract with variants matching NF1-REP-E19, and a 700-bp segment of perfect match with statistical evidence of gene conversion. The positions of promoter like sequences not associated with known genes are indicated in the lower panel. (B) Detailed structure of the PRS2 region. Breakpoint intervals are shown along with the 2.3-kb hotspot, which harbors 93% of breakpoint intervals in PRS2 region. Finer localization of the 700-bp gene conversion tract and the promoter like sequences from (A) are shown. Nucleotide positions for both panels refer to the NF1-REP-P1-51 in BAC RP11-271K11. (Adapted from ref. *24* with permission.)

Basic Local Alignment Search Tool (BLAST; www.ncbi.nlm.nib.gov/blast) comparison of PRS1 and PRS showed no significant sequence identity with the exception of *Alu* elements, LINES and other high-copy repeats, which typically shared less than 80% identity in short segments *(24)*. PRS1 and 2 regions have quite different patterns of G+C content; the PRS2 hotspot is very G+C rich, while the PRS1 hotspot is not (Fig. 3). Both PRS hotspots are 1–2 kb distal to relative large alignment gaps (Fig. 3A), yet these did not suppress pairing as recombination in at least a few cases occurred within less than 1 kb from the gaps. The PRS regions are not of greater or lesser paralogous sequence identity as shown by the spatial distribution of PSVs, which are relatively evenly distributed across the NF1-REP-51 segment (Fig. 3) *(24)*. Numerous tests for the presence of motifs with demonstrated or suspected roles in recombination, transcription, or translation were performed. A *Chi* element within PRS2 was identified *(17)*, but this association is not preferential, as it is one of four evenly spaced *Chi* elements in NF1-REP-51 *(24)*. Figure 3B shows the location of a CpG island and two promoter-like sequences, which although not associated with any known gene, may function to provide chromatin accessibility. Statistical tests for gene conversion identified the 700-bp perfect match between NF1-REP-P1-51 and NF1-REP-M-51 that coincided with PRS2 (Fig. 3B). Although perfect sequence match may contribute to breakpoint localization, these results suggest that perfect tracts at paralogous recombination hotspots may be a result of gene conversion at sites at which preferential pairing occurs for other unknown reasons *(24)*. A search for palindromes, which are associated with other genomic rearrangements *(32–35)*, found no palindromes larger than 18 bp and separated by 63 bp. The palindromes within the KIAA0563-ψ of NF1-REP-P1 are considered too distant to influence recombination at the PRS regions (Fig. 2A).

UNIQUE, NON-LCR-MEDIATED *NF1* MICRODELETIONS

A subset of submicroscopic *NF1* microdeletions have breakpoints outside of the NF1-REP paralogs (Fig. 4) and appear to arise by a mechanism other than paralogous recombination. Among the five larger deletions, all except the BUD case (patient B in Fig. 4) have a telomeric breakpoint within the *ACCN1* gene. BUD has a telomeric breakpoint in the *SLFN* gene cluster. At least four of these deletions also have different centromeric breakpoint intervals. Only breakpoints in case six have been mapped at the nucleotide level with the centromeric breakpoint between *BLMH* and *CPD* and the telomeric breakpoint in *ACCN1* intron 1. The breakpoints were not located within LCR elements. However, there were stretches of 20–21 bp of *Alu*-like elements at the two breakpoints and LINE and short interspersed nuclear element (SINE) elements within several hundred bp from the breakpoints. Together, these data provide support for a mechanism of nonhomologous end-joining (NHEJ) (36). Because LCRs are not known to be located in/near the breakpoints of the other *NF1* microdeletions shown in Fig. 4, they may well arise by NHEJ also. As more such deletions are identified, it will be of interest to determine if there is a preferential parent of origin effect. In these examples, UWA106-3, BUD, and 96-2 have paternally derived deletions, whereas 372A was maternally derived. In general, larger deletions tend to occur in NF1 patients with severe or additional complications, but phenotypic information is limited and the extent of an *NF1* deletion has no predictive value to date.

The smaller deletions depicted on Fig. 4 are of interest because precise breakpoint mapping and full clinical evaluation of such patients may serve to narrow the critical region between NF1-REP-P1 and NF1-REP-M that confers the phenotype of heavy tumor load and increased

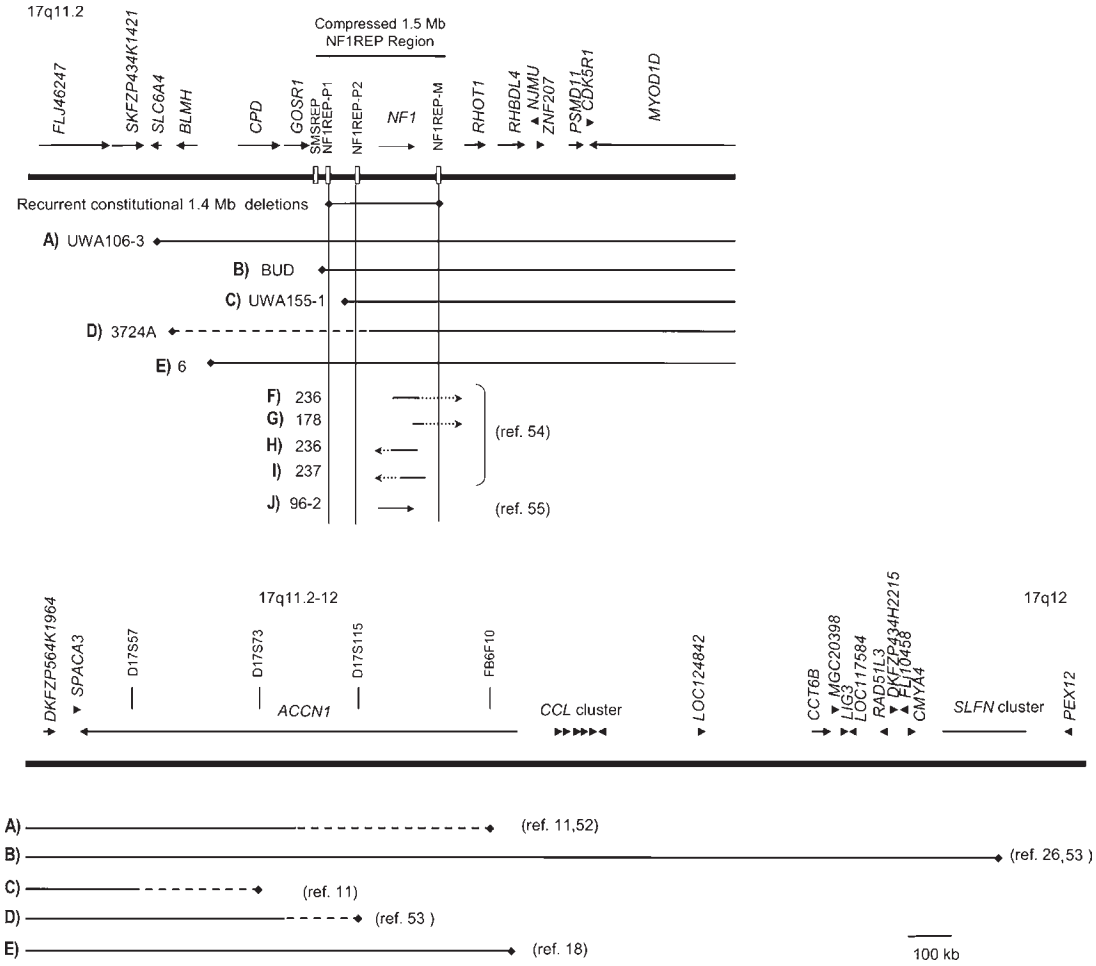

Fig. 4. Nonrecurrent *NF1* microdeletions. A schematic of the 5.6-Mb region from *FLJ46247* to *PEX12* is diagrammed in two panels. Figures are drawn to scale with the exception of the 1.5-Mb NF1-REP region, which is compressed for space considerations. Gene names and gene clusters are written above arrows indicating their direction of transcription. The three NF1-REP (open boxes) and an adjacent SMS REP (gray box) are indicated. Four markers within *ACCN1* are shown that serve to differentiate the extent of deletions with breakpoints within this large gene. Below the map, the recurrent 1.4-Mb deletion is shown compared to that of 10 cases (A–J) with unique breakpoints. Solid lines indicated deleted region and dashed lines indicate uncertainty in the precise endpoint (*see* text for details). Gene names in this figure are from a May, 2004 assembly of the human genome (http://genome.ucsc.edu/) and may differ from names on previously published maps of the region*(23,25,26,36)*.

malignancy risk to deletion patients. Patients 236, 178, 236, and 237 have at least one breakpoint within the *NF1* gene, but the extent of the deletion and position of the other breakpoints are not known. Patient 96-2 is deleted for much of the *NF1* gene, but whether other genes are involved in this deletion is not known.

LCR-MEDIATED SOMATIC *NF1* MICRODELETIONS

An estimated 25% of *NF1* microdeletions occur as postzygotic mutations during mitosis resulting in tissue mosaicism *(21)* and a phenotype that can vary from the classical generalized

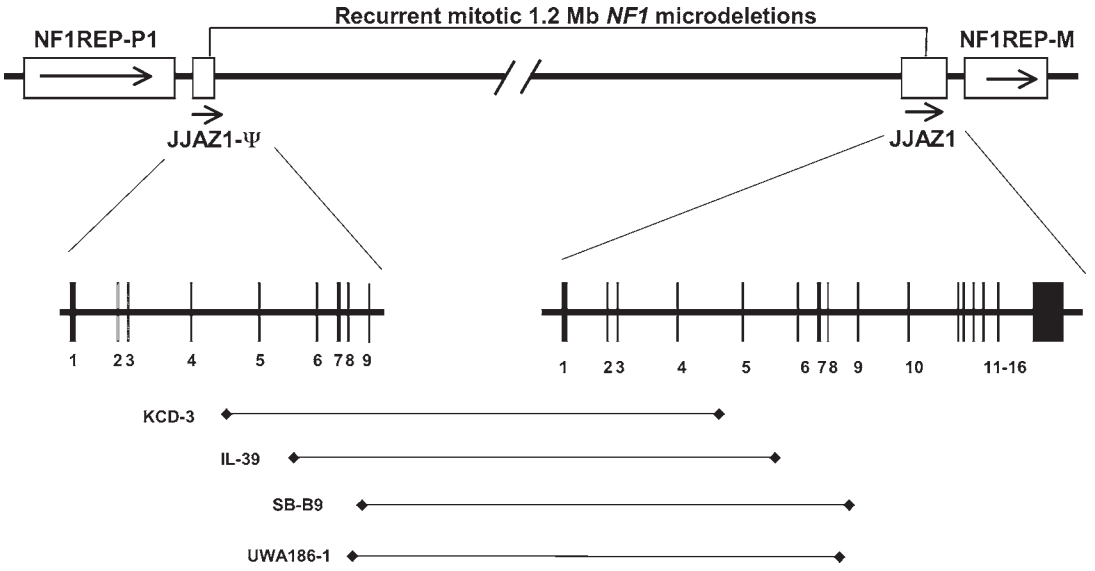

Fig. 5. Recurrent mitotic *NF1* microdeletions. The schematic shows the pair of *JJAZ1* low-copy repeats (LCRs) that mediate recurrent mitotic microdeletions of the *NF1* region (refer to Fig. 1 for genomic context of the region). These LCRs share 46 kb of homology with 97% sequence identity and are located just "internal" to the NF1-REP-P1 and –M *(26)*. Breakpoints are drawn for four cases of 1.2-Mb deletions mediated by paralogous recombination between the *JJAZ1*-ψ pseudogene and the *JAZZ1* functional gene. (Three from ref. *21* and UWA186-1 as an additional unpublished case from my laboratory.)

NF1 to localized or segmental NF1 *(37,38)*. Like the common recurrent meiotic *NF1* microdeletions, somatic rearrangements occur by paralogous recombination; however, the site of preferential exchange was different. Seven of eight mitotic *NF1* microdeletions had breakpoints that clustered at the *JJAZ1*-ψ pseudogene and the *JJAZ1* functional gene, which are direct repeats located adjacent and NF1-REP-P1 and NF1-REP-M (Fig. 1) *(21)*. The *JJAZ1*-ψ has 9 exons that share 46-kb homology at 97% identity with the functional *JJAZ1* gene (Fig.5) *(26)*. In three cases, breakpoint intervals were mapped at the nucleotide level by use of PSVs and the microdeletions occurred at different sites (Fig. 5). Consistent with this observation is the breakpoint of a somatic mosaic female patient in my laboratory, UWA186-1, whose breakpoint in intron 8 is approx 2 kb proximal to that of SB-B9 (Stephens, unpublished observations). The *JJAZ1*-ψ/*JJAZ1* fusion product of the recombination is expressed in human-rodent somatic cell lines, but unlikely to be translated owing to stop codons in the pseudogene *(21)*.

The level of somatic mosaicism for *JJAZ1*-mediated *NF1* microdeletions varied significantly in different patient tissues. The percentage of deleted cells as determined by FISH was quite high in peripheral blood (91–100%) and significantly lower in buccal cells or skin fibroblasts (51–59%) *(21)*. These data suggest that a selective growth advantage of hematopoetic stem cells carrying *NF1* microdeletions. Different levels of mosaicism significantly compound both the diagnosis and counseling of patients with *JJAZ1*-mediated mosaic *NF1* microdeletions.

JJAZ1- and NF1-REP-mediated *NF1* microdeletions have striking differences and parallels. First, paralogous recombination at *JJAZ1* LCRs is preferentially mitotic, whereas that at NF1-REP LCRs is meiotic. Second, *JJAZ1* paralogous recombination is intrachromosomal in

two cases examined *(21)*, whereas NF1-REP paralogous recombination is primarily interchromosomal *(16)*. Third, small inverted repeats of 75–127 bp flank the intronic *JJAZ1* breakpoints in two cases and may cause double strand breaks by forming hairpins *(21)*. Parallels between the two types of microdeletions include paralogous recombination, and deletion of the same set of contiguous genes, except for the functional *KIAA0563-rel* gene near NF1-REP-M, which is not deleted in *JJAZ1*-mediated rearrangements (Fig. 1). Furthermore, both paralogous recombination events occur preferentially in females for reasons that are not known *(15,17,21)*.

FUTURE DIRECTIONS

It will be important to determine the molecular basis for the different preferences for LCR substrates during meiotic vs mitotic recombination. Furthermore, does *JJAZ1*-mediated recombination contribute to somatic *NF1* second hit mutations at NF1-associated tumors? Does this site represent a mitotic recombination hotspot in the genome, perhaps in the female genome? And why is maternal recombination more prevalent for both LCR-mediated microdeletions? Clinical studies to identify the putative modifying gene that confers the increased risk for tumorigenesis and malignancy remain a priority. These studies will be facilitated by new assays and approaches to identify patient cohorts of the same deletion genotype and exclude mosaic cases that would confound the analyses.

SUMMARY

Submicroscopic deletions at chromosome 17q11.2 underlying the common genetic disorder NF1 are of great interest because they predispose to a heavy neurofibroma burden, malignancy, and possibly other severe manifestations. The NF1 microdeletion phenotype, which remains to be defined in detail, is thought to be owing to the deletion of the *NF1* tumor suppressor gene and an additional unidentified flanking gene(s). Surprisingly, there is a different preference for LCR recombination substrates for recurrent meiotic versus recurrent mitotic *NF1* microdeletion events. Paralogous recombination between a pair of 51-kb NF1-REPs mediate the recurrent common constitutional 1.4-Mb microdeletion that occurs preferentially during maternal meiosis. Recombination between the *JJAZ1* pseudogene and functional gene mediate the recurrent 1.2-Mb microdeletion, which occurs preferentially during postzygotic mitosis in females. NF1-REP-mediated *NF1* microdeletions involve 13 additional genes, whereas *JJAZ1*-mediated microdeletions involve the same genes but one. Breakpoints of both deletions mapped at the nucleotide level identify several potential sequence features that may contribute to the choice of discrete sites for strand exchange.

REFERENCES

1. Kayes LM, Riccardi VM, Burke W, Bennett RL, Stephens K. Large de novo DNA deletion in a patient with sporadic neurofibromatosis 1, mental retardation, and dysmorphism. J Med Genet 1992;29:686–690.
2. Friedman JM. Neurofibromatosis 1: clinical manifestations and diagnostic criteria. J Child Neurol 2002;17: 548–554.
3. Friedman JM, Gutmann DH, MacCollin M, Riccardi VM, (eds.) *Neurofibromatosis. Phenotype, Natural History, and Pathogenesis, 3rd edition.* Baltimore: The Johns Hopkins University Press, 1999.
4. Zhu Y, Ghosh P, Charnay P, Burns DK, and Parada LF. Neurofibromas in NF1: Schwann cell origin and role of tumor environment. Science 2002;296:920–922.
5. Dasgupta B, Gutmann DH. Neurofibromatosis 1: closing the GAP between mice and men. Curr Opin Genet Dev 2003;13:20–27.

6. Bajenaru ML, Hernandez MR, Perry A, et al. Optic nerve glioma in mice requires astrocyte Nf1 gene inactivation and Nf1 brain heterozygosity. Cancer Res 2003;63:8573–8577.
7. Side L, Taylor B, Cayouette M, et al. Homozygous inactivation of the NF1 gene in bone marrow cells from children with neurofibromatosis type 1 and malignant myeloid disorders. N Engl J Med 1997;336:1713–1720.
8. Kluwe L, Friedrich RE, Mautner VF. Allelic loss of the NF1 gene in NF1-associated plexiform neurofibromas. Cancer Genet Cytogenet 1999;113:65–69.
9. Messiaen L, Riccardi, V, Peltonen, J, et al. Independent NF1 mutations in two large families with spinal neurofibromatosis. J Med Genet 2003;40:122–126.
10. Kluwe L, Siebert R, Gesk S,et al. Screening 500 unselected neurofibromatosis 1 patients for deletions of the NF1 gene. Hum Mutat 2004;23:111–116.
11. Dorschner MO, Sybert VP, Weaver M, Pletcher BA, Stephens K. NF1 microdeletion breakpoints are clustered at flanking repetitive sequences. Hum Mol Genet 2000;9:35–46.
12. Kayes LM, Burke W, Riccardi VM, et al. Deletions spanning the neurofibromatosis 1 gene: identification and phenotype of five patients. Am J Hum Genet 1994;54:424–436.
13. Leppig K, Kaplan P, Viskochil D, Weaver M, Orterberg J, Stephens K. Familial neurofibromatosis 1 gene deletions: cosegregation with distinctive facial features and early onset of cutaneous neurofibromas. Am J Med Genet 1997;73:197–204.
14. Wu BL, Schneider GH, Korf BR. Deletion of the entire NF1 gene causing distinct manifestations in a family. Am J Med Genet 1997;69:98–101.
15. Upadhyaya M, Ruggieri M, Maynard J, et al. Gross deletions of the neurofibromatosis type 1 (NF1) gene are predominantly of maternal origin and commonly associated with a learning disability, dysmorphic features and developmental delay. Hum Genet 1998;102:591–597.
16. Lopez-Correa C, Brems H, Lazaro C, Marynen P, Legius E. Unequal Meiotic Crossover: A Frequent Cause of NF1 Microdeletions. Am J Hum Genet 2000;66:1969–1974.
17. Lopez-Correa C, Dorschner M, Brems H, et al. Recombination hotspot in NF1 microdeletion patients. Hum Mol Genet 2001;10:1387–1392.
18. Venturin M, Guarnieri P, Natacci F, et al. Mental retardation and cardiovascular malformations in NF1 microdeleted patients point to candidate genes in 17q11.2. J Med Genet 2004;41:35–41.
19. Gutmann DH, James CD, Poyhonen M, et al. Molecular analysis of astrocytomas presenting after age 10 in individuals with NF1. Neurology 2003;61:1397–1400.
20. De Raedt T, Brems H, Wolkenstein P, et al. Elevated risk for MPNST in NF1 microdeletion patients. Am J Hum Genet 2003;72:1288–1292.
21. Kehrer-Sawatzki H, Kluwe L, Sandig C, et al. High frequency of mosaicism among patients with neurofibromatosis type 1 (NF1) with microdeletions caused by somatic recombination of the JJAZ1 gene. Am J Hum Genet 2004;75:410–423.
22. Stankiewicz P, Lupski JR. Genome architecture, rearrangements and genomic disorders. Trends Genet 2002;18:74–82.
23. Dorschner MO, Brems H, Le R, et al. Tightly clustered breakpoints permit detection of the recurrent 1.4 Mb NF1 microdeletion by deletion-specific amplification. 2005; submitted.
24. Forbes SH, Dorschner MO, Le R Stephens K. Genomic context of paralogous recombination hotspots mediating recurrent NF1 region microdeletion. Genes Chromosomes Cancer 2004;41:12–25.
25. De Raedt T, Brems H, Lopez-Correa C, Vermeesch JR, Marynen P, Legius, E. Genomic organization and evolution of the NF1 microdeletion region. Genomics 2004;84:346–360.
26. Jenne DE, Tinschert S, Dorschner MO, et al. Complete physical map and gene content of the human NF1 tumor suppressor region in human and mouse. Genes Chromosomes Cancer 2003;37:111–120.
27. Jenne DE, Tinschert S, Reimann H, et al. Molecular Characterization and Gene Content of Breakpoint Boundaries in Patients with Neurofibromatosis Type 1 with 17q11.2 Microdeletions. Am J Hum Genet 2001;69:3.
28. Lagerstedt K, Karsten SL, Carlberg BM, et al. Double-strand breaks may initiate the inversion mutation causing the Hunter syndrome. Hum Mol Genet 1997;6:627–633.
29. Lopes J, Ravise N, Vandenberghe A, et al. Fine mapping of de novo CMT1A and HNPP rearrangements within CMT1A-REPs evidences two distinct sex-dependent mechanisms and candidate sequences involved in recombination. Hum Mol Genet 1998;7:141–148.
30. Reiter LT, Hastings PJ, Nelis E, De Jonghe P, Van Broeckhoven C, Lupski JR. Human meiotic recombination products revealed by sequencing a hotspot for homologous strand exchange in multiple HNPP deletion patients. Am J Hum Genet 1998;62:1023–1033.

31. Sun C, Skaletsky H, Rozen S, et al. Deletion of azoospermia factor a (AZFa) region of human Y chromosome caused by recombination between HERV15 proviruses. Hum Mol Genet 2000;9:2291–2296.
32. Repping S, Skaletsky H, Lange J, et al. Recombination between palindromes P5 and P1 on the human Y chromosome causes massive deletions and spermatogenic failure. Am J Hum Genet 2002;71:906–922.
33. Kurahashi H, Emanuel BS. Long AT-rich palindromes and the constitutional t(11;22) breakpoint. Hum Mol Genet 2001;10:2605–2617.
34. Kurahashi H, Inagaki H, Yamada K, et al. Cruciform DNA structure underlies the etiology for palindrome-mediated human chromosomal translocations. J Biol Chem 2004;279:35,377–35,383.
35. Nag DK, Kurst A. A 140-bp-long palindromic sequence induces double-strand breaks during meiosis in the yeast Saccharomyces cerevisiae. Genetics 1997;146:835–847.
36. Venturin M, Gervasini C, Orzan F, et al. Evidence for non-homologous end joining and non-allelic homologous recombination in atypical NF1 microdeletions. Hum Genet 2004;115:69–80.
37. Ruggieri M, Huson SM. The clinical and diagnostic implications of mosaicism in the neurofibromatoses. Neurology 2001;56:1433–1443.
38. Petek E, Jenne DE, Smolle J, et al. Mitotic recombination mediated by the JJAZF1 (KIAA0160) gene causing somatic mosaicism and a new type of constitutional NF1 microdeletion in two children of a mosaic female with only few manifestations. J Med Genet 2003;40:520–525.
39. Mattocks C, Baralle D, Tarpey P, French-Constant C, Bobrow M, Whittaker J. Automated comparative sequence analysis identifies mutations in 89% of NF1 patients and confirms a mutation cluster in exons 11-17 distinct from the GAP related domain. J Med Genet 2004;41:e48.
40. Messiaen LM, Callens T, Mortier G, et al. Exhaustive mutation analysis of the NF1 gene allows identification of 95% of mutations and reveals a high frequency of unusual splicing defects. Hum Mutat 2000;15:541–555.
41. Ars E, Kruyer H, Morell M, et al. Recurrent mutations in the NF1 gene are common among neurofibromatosis type 1 patients. J Med Genet 2003;40:e82.
42. Streubel B, Latta E, Kehrer-Sawatzki H, Hoffmann GF, Fonatsch C, Rehder H. Somatic mosaicism of a greater than 1.7-Mb deletion of genomic DNA involving the entire NF1 gene as verified by FISH: further evidence for a contiguous gene syndrome in 17q11.2. Am J Med Genet 1999;87:12–16.
43. Tinschert S, Naumann I, Stegmann E, et al. Segmental neurofibromatosis is caused by somatic mutation of the neurofibromatosis type 1 (NF1) gene. Eur J Hum Genet 2000;8:455–459.
44. Colman SD, Rasmussen SA, Ho VT, Abernathy CR, Wallace MR. Somatic mosaicism in a patient with neurofibromatosis type 1. Am J Hum Genet 1996;58:484–490.
45. van den Brink HJ, van Zeijl CM, Brons JF, van den Hondel CA, van Gorcom RF. Cloning and characterization of the NADPH cytochrome P450 oxidoreductase gene from the filamentous fungus Aspergillus niger. DNA Cell Biol 1995;14:719–729.
46. Lazaro C, Gaona A, Lynch M, Kruyer H, Ravella A, Estivill X. Molecular characterization of the breakpoints of a 12-kb deletion in the NF1 gene in a family showing germ-line mosaicism. Am J Hum Genet 1995;57: 1044–1049.
47. Serra E, Ars E, Ravella A, et al. Somatic NF1 mutational spectrum in benign neurofibromas: mRNA splice defects are common among point mutations. Hum Genet 2001;108:416–429.
48. Rasmussen SA, Overman J, Thomson SA, et al. Chromosome 17 loss-of-heterozygosity studies in benign and malignant tumors in neurofibromatosis type 1. Genes Chromosomes Cancer 2000;28:425–431.
49. Serra E, Rosenbaum T, Nadal M, et al. Mitotic recombination effects homozygosity for NF1 germline mutations in neurofibromas. Nat Genet 2001;28:294–296.
50. Legius E, Marchuk DA, Collins FS, Glover TW. Somatic deletion of the neurofibromatosis type 1 gene in a neurofibrosarcoma supports a tumour suppressor gene hypothesis. Nature Genet 1993;3:122–126.
51. Frahm S, Mautner VF, Brems H,et al. Genetic and phenotypic characterization of tumor cells derived from malignant peripheral nerve sheath tumors of neurofibromatosis type 1 patients. Neurobiol Dis 2004;16:85–91.
52. Stephens K. Genetics of neurofibromatosis 1- associated peripheral nerve sheath tumors. Cancer Invest 2003;21:901–918.
53. Kehrer-Sawatzki H, Tinschert S, Jenne DE. Heterogeneity of breakpoints in non-LCR-mediated large constitutional deletions of the 17q11.2 NF1 tumor suppressor region. J Med Genet 2003;10:e116.
54. Fang LJ, Vidaud D, Vidaud M, Thirion JP. Identification and characterization of four novel large deletions in the human neurofibromatosis type 1 (NF1) gene. Hum Mutat 2001;18:549–550.
55. Lopez Correa C, Brems H, Lazaro C, et al. Molecular studies in 20 submicroscopic neurofibromatosis type 2 gene deletions. Hum Mutat 1999;14:387–393.

Journal of Neuroscience Research 85:1347–1357 (2007)

Plexiform-Like Neurofibromas Develop in the Mouse by Intraneural Xenograft of an NF1 Tumor-Derived Schwann Cell Line

George Q. Perrin,[1,2]* Lauren Fishbein,[3] Susanne A. Thomson,[3] Stacey L. Thomas,[7,8] Karen Stephens,[9] James Y. Garbern,[10] George H. DeVries,[8,11] Anthony T. Yachnis,[4] Margaret R. Wallace,[3,5] and David Muir[1,2,6]

[1]Department of Neuroscience, College of Medicine, University of Florida, Gainesville, Florida
[2]Shands Cancer Center, College of Medicine, University of Florida, Gainesville, Florida
[3]Department of Molecular Genetics and Microbiology, College of Medicine, University of Florida, Gainesville, Florida
[4]Department of Pathology and Laboratory Medicine, College of Medicine, University of Florida, Gainesville, Florida
[5]Department of Pediatrics, Genetics Division, College of Medicine, University of Florida, Gainesville, Florida
[6]Department of Pediatrics, Neurology Division, College of Medicine, University of Florida, Gainesville, Florida
[7]Neuroscience Program, Loyola University Medical Center, Maywood, Illinois
[8]Hines VA Hospital, Hines, Illinois
[9]Department of Medicine, University of Washington, Seattle, Washington
[10]Department of Neurology; Wayne State University, Detroit, Michigan
[11]Department of Anatomy and Cell Biology, University of Illinois, Chicago, Illinois

Plexiform neurofibromas are peripheral nerve sheath tumors that arise frequently in neurofibromatosis type 1 (NF1) and have a risk of malignant progression. Past efforts to establish xenograft models for neurofibroma involved the implantation of tumor fragments or heterogeneous primary cultures, which rarely achieved significant tumor growth. We report a practical and reproducible animal model of plexiform-like neurofibroma by xenograft of an immortal human NF1 tumor-derived Schwann cell line into the peripheral nerve of *scid* mice. The S100 and p75 positive sNF94.3 cell line was shown to possess a normal karyotype and have apparent full-length neurofibromin by Western blot. These cells were shown to have a constitutional *NF1* microdeletion and elevated Ras-GTP activity, however, suggesting loss of normal neurofibromin function. Localized intraneural injection of the cell line sNF94.3 produced consistent and slow growing tumors that infiltrated and disrupted the host nerve. The xenograft tumors resembled plexiform neurofibromas with a low rate of proliferation, abundant extracellular matrix (hypocellularity), basal laminae, high vascularity, and mast cell infiltration. The histologic features of the developed tumors were particularly consistent with those of human plexiform neurofibroma as well. Intraneural xenograft of sNF94.3 cells enables the precise initiation of intraneural, plexiform-like tumors and provides a highly reproducible model for the study of plexiform neurofibroma tumorigenesis. This model facilitates testing of potential therapeutic interventions, including angiogenesis inhibitors, in a relevant cellular environment.

Key words: neurofibromatosis; neurofibroma; angiogenesis; plexiform; xenograft

Neurofibromatosis type 1 (NF1) is a common autosomal dominant condition caused by disruptive mutations in the *NF1* gene, which encodes the GAP-related protein neurofibromin. These mutations result in absent or abnormal neurofibromin, which is associated with a high frequency of peripheral nerve sheath tumors called neurofibromas (Gutmann et al., 1991). Plexiform neurofibromas are often congenital, typically involve large nerves, can become very large, and when large, may cause serious functional impairment. Because they often occur on critical nerves and are not discrete masses, surgical removal is rarely complete. Recurrence is associated with increased morbidity and fatality, with progression to malignancy occurring in about 6% of NF1 patients. Although neurofibromas show marked cellular heterogeneity, Schwann cells (SCs) are the major

Contract grant sponsor: National Institutes of Health Training; Contract grant number: T32-CA09126-27; Contract grant sponsor: U.S. Department of Defense; Contract grant number: DAMD 17-01-10707, DAMD 17-03-1-0224.

*Correspondence to: George Q. Perrin, PhD, Dept. of Neuroscience, Box 100244, University of Florida College of Medicine, Gainesville, FL 32610-0244. E-mail: gperrin@ufl.edu

Received 13 July 2006; Revised 17 October 2006; Accepted 5 December 2006

Published online 4 March 2007 in Wiley InterScience (www.interscience.wiley.com). DOI: 10.1002/jnr.21226

cell type amplified and typically comprise 40–80% of the tumor cells (Hirose et al., 1986; Krone et al., 1986). Moreover, cumulative evidence indicates that neurofibromas contain a clonal population of Schwann cells that have disruptive mutations on the remaining *NF1* allele (Colman et al., 1995). Human plexiform neurofibromas have distinct characteristics (Scheithauer et al., 1997). They are hypocellular and composed of widely spaced, spindle-shaped cells with ovoid nuclei that variably stain positive for S-100. Most exhibit a low proliferative index (1–13% Ki67 positive cells), as compared to the high proliferative index (5–38% Ki67 positive cells) exhibited by malignant peripheral nerve sheath tumors (MPNST). They feature a prominent endoneurial mucopolysaccharide deposition, a variously collagenous matrix and basal laminae. Plexiform neurofibromas diffusely infiltrate the affected nerve and spread longitudinally as a fusiform enlargement rather than a globular mass. As with many other types of tumors, they can promote angiogenesis, are highly vascular and are infiltrated by numerous mast cells.

Several mouse models of NF1 engineered genetically have been developed to study tumorigenesis by neurofibromin-deficient mouse Schwann cells (Stemmer-Rachamimov et al., 2004). Past efforts to establish xenograft models of neurofibroma, however, have achieved limited success. Despite tumorigenic properties shown in vitro, neurofibroma cultures fail to form subcutaneous tumors in immunodeficient mice (Sheela et al., 1990; Muir et al., 2001). Inceptive studies showed limited growth by implanted human neurofibroma tissue or mixed cell preparations into the sciatic nerves of immunodeficient mice and advanced the potential of xenograft models for studying the tumorigenesis in NF1 (Appenzeller et al., 1986; Lee et al., 1992). Early xenografts of human neurofibromas relied on tissue explants and primary cultures of limited cell number with marked cellular heterogeneity and never were established as effective working models of NF1 tumors. Previously, we established highly enriched SC cultures from numerous benign and malignant NF1 peripheral nerve sheath tumors (Muir et al., 2001; Li et al., 2004). These cell lines were enriched for the somatically mutated SCs and most show no full-length neurofibromin. Schwann cell lines derived from benign NF1 tumors had low tumorigenic potential in classical in vitro assays yet several unique preneoplastic properties were observed frequently. In addition, several neurofibroma SC cultures when engrafted into the peripheral nerves of *scid* mice produced infiltrative and very slow-growing neurofibroma-like tumors. Although these xenografts provide an informative and useful model of neurofibroma, considerable time is required to achieve tumor growth representative of that seen in a clinical setting. Therefore, we developed more practical xenograft models of NF1 tumorigenesis by implantation of rapidly growing NF1 MPNST cell lines into the mouse nerve.

MATERIALS AND METHODS

Originative Tumor and NF1 Cell Line

The NF1 tumor cell line, sNF94.3, was derived from tumor tissue resected from a 43-year-old, female patient who met NF1 diagnostic criteria (Gutmann et al., 1997). Although there was no positive family history, the patient had definite features of NF1 including a mild learning disability, scoliosis, café-au-lait spots, Lisch nodules, hundreds of dermal neurofibromas, a congenital plexiform in the ankle and foot, and a MPNST in the thigh. The originative tumor tissue for the sNF94.3 cell line was obtained from a lung metastasis diagnosed by histopathology as an MPNST. The portion of the tumor specimen used for tissue culture was characterized independently by immuno histopathology as an MPNST. The tissue was acquired with patient consent and used according to IRB approved protocols.

DNA was extracted from blood leukocytes and tumor specimens as described previously by Colman et al. (1995). The sNF94.3 tumor cell line was established by methods described previously (Wallace et al., 2000; Muir et al., 2001). Briefly, tumor pieces were minced and dissociated for 3–5 hr with dispase (1.25 U/ml; Collaborative Research, Bedford, MA) and collagenase (300 U/ml; Type XI; Sigma, St. Louis, MO) in L15 medium containing 10% calf serum and antibiotics. The digested tissue was dispersed by trituration and strained through a 30-mesh nylon screen. Collected cells were seeded on laminin-coated dishes and grown in DMEM containing 10% fetal bovine serum, 5% calf serum, glial growth factor-2 (25 ng/ml), and antibiotics. Cultures were subsequently grown and expanded rapidly without laminin and glial growth factor-2. The sNF94.3 cell line showed a homogenous Schwann cell-like population and a clonal morphology, which was retained through protracted passages (19 thus far). The apparently immortal cell line has spindle-shape morphology and is immunopositive for S-100 and faintly for p75 (low-affinity neurotrophin receptor), indicating Schwann cell lineage. Nuclear S100 staining might indicate a dedifferentiated tumor cell line (Mirsky and Jessen, 1999). The sNF94.3 cell line was deposited in the American Type Culture Collection.

Clonality Analysis

Tumor clonality was analyzed by an X-chromosome inactivation assay. This PCR polymorphism-based assay allows for differential detection of the maternal and paternal chromosomes by methylation-sensitive enzymes (Singer-Sam et al., 1990). Both the androgen receptor gene locus (Allen et al., 1992) and the phosphoglycerate kinase gene (*PGK*) (Lee et al., 1994) were analyzed. On digestion of genomic DNA with HpaII followed by PCR amplification using primers flanking the HpaII sites, a clonal sample only shows amplification of one allele whereas a polyclonal sample shows amplification of both alleles (that can be distinguished in heterozygotes). For this study, 10 ng of genomic DNA was digested with 20 U of HpaII and 10 U of RsaI (New England Biolabs, Ipswich, MA) in a 20-μL reaction. Two microliters of the digest was used for PCR amplification. The following primers were used for the androgen receptor repeat polymorphism; A-Receptor 5′: 5′-GCT GTG AAG GTT GCT GTT CCT

CAT-3′, A-Receptor 3′: 5′-TCC AGA ATC TGT TCC AGA GCG TGC-3′ under the following standard PCR conditions: 94°C for 1 min, 65°C for 1 min, 72°C for 1 min for 35 cycles with a 30-min 72°C final extension step. The samples were electrophoretically separated on a 10% native polyacrylamide gel and stained with ethidium bromide for visualization. The *PGK* gene single nucleotide polymorphism was amplified under similar conditions, except with an annealing temperature of 58°C, with the following primers; PGK-5′: 5′-CTG TTC CTG CCC GCG CGG TGT TCC GCA TTC-3′, PGK-3′: 5′-ACG CCT GTT ACG TAA GCT CTG CAG GCC TCC-3′. In addition, 8 μL of amplified product was digested with 20 U of BstXI to detect the RFLP before separating fragments on a 10% PAGE. Densitometric analysis was carried out on all samples using NIH Image (freeware; National Institute of Health) and values were statistically analyzed by a *t*-test using Microsoft Excel.

NF1 Mutation Analysis

NF1 exons from tumor DNAs were analyzed by heteroduplex and SSCP analysis, as well as by direct sequencing (Abernathy et al., 1997). Samples were analyzed for loss of heterozygosity (LOH) using standard methods for genotyping *NF1* polymorphisms as described previously by Colman et al. (1995) and Rasmussen et al. (1998). Blood and tumor DNA results were compared when constitutional heterozygosity was seen at a given marker. In addition, standard cytogenetic analysis was carried out on the tumor derived Schwann cell cultures. Analysis for *NF1* region microdeletion used specific PCR assays.

Western Blot Analysis

Cell cultures were scraped from dishes and cell pellets were homogenized in ice-cold extraction buffer consisting of 50 mM Tris-HCl (pH 7.4), 250 mM NaCl, 1% Nonidet P-40, 0.25% sodium deoxycholate, and Complete protease inhibitor cocktail (Boehringer-Mannheim, Indianapolis, IN). The soluble fraction was collected by centrifugation (10,000 × *g*, 20 min) and reconstituted to be 2 M in urea. The extract was concentrated and fractionated by ultrafiltration using a 100-kDa cut-off membrane. Total protein content of the high molecular mass retentate was determined using Bradford Reagent (Bio-Rad, Hercules, CA). Samples were mixed with sodium dodecyl sulfate electrophoresis sample buffer containing 2 M urea and 5% 2-mercaptoethanol, normalized for total protein content and then heated at 80°C for 2 hr. Samples (50 μg of total protein) were electrophoresed into 4–15% polyacrylamide gradient gels and electroblotted to nitrocellulose sheets in transfer buffer containing 0.1% sodium dodecyl sulfate. Blots were rinsed in water and fixed in 25% isopropanol/10% acetic acid. Nitrocellulose sheets were washed with 50 mM Tris-HCl (pH 7.4) containing 1.5% NaCl and 0.1% Triton X-100 and then blocked in the same buffer with the addition of 5% dry milk (blocking buffer). The blots were incubated for 2 hr with anti-NF1GRP(N) antibody (1 μg/ml) (Santa Cruz Biotechnology, Inc., Santa Cruz, CA) in blocking buffer. Bound antibody was detected by peroxidase-conjugated swine anti-rabbit IgG (affinity purified; DAKO, Carpinteria, CA) diluted 1/2,000 in blocking buffer. Immunoreactive bands were developed by chemiluminescent methods (Pierce Chemical, Rockford, IL) according to the manufacturer's instructions. Relative molecular mass was determined using prestained markers including myosin (233 kDa) (Bio-Rad). Control samples were similarly processed from cell pellets obtained from normal human nerve Schwann cell cultures and Schwann cell cultures derived from embryonic homozygous *Nf1* knockout mice. In these studies, neurofibromin was detected using a number of antibodies. We used the antibody available from Santa Cruz Biotechnology raised against a peptide corresponding to residues 509–528 of the predicted *NF1* gene product. To further investigate the possible effects of truncated *NF1* gene products, we have developed monoclonal antibodies (McNFn27a, McNFn27b) raised against a peptide corresponding to the N-terminal residues 27–41 of the predicted *NF1* gene product. Similar results were obtained with all antibodies. Next, the blot was stripped with Restore Western Blot Stripping Buffer (Pierce Chemical), per manufacturers instructions, and blocked as described above. The blot was then re-immunoblotted with polyclonal anti-huGST (DAKO) (1/200) (that binds only human glutathione s-transferase) to check sample loading. This immunoblot was developed as described above.

Ras Activation Assay

Ras activation assay kit (Upstate Biotech, Lake Placid, NY) was used according to the manufacturer's protocol. The assay uses affinity precipitation to isolate Ras-GTP from cell lysate. Cells were lysed using RIPA buffer (1% Igepal, 0.5% NaDOC, 0.1% SDS in PBS) and the DC protein assay (Bio-Rad) was used to determine the protein concentration of the cell lysates. Cell lysate (500 μg) was incubated with an agarose-bound Raf-1 RBD fusion protein. Agarose beads were collected by pulsing with a microcentrifuge (5 sec at 14,000 × *g*), washed with lysis buffer, and resuspended in Laemmli sample buffer. The samples were then boiled for 5 min after which the supernatants were loaded onto a 4–20% gradient Novex Tris-Glycine gel (Invitrogen, Carlsbad, CA) along with SeeBlue Plus2 molecular weight standards (5 ul) (Invitrogen). The samples were electrophoresed (20 mA/gel) and then transferred (100 V) to a PVDF membrane (NEN, Boston, MA). The membrane was blocked with 5% nonfat dry milk and then incubated with primary antibody overnight at 4°C as follows: 1 μg/ml Anti-Ras clone RAS10 (Upstate Biotechnology, Lake Placid, NY); 1/250 Anti-N-Ras (F155), and Anti-K-Ras (F234) (Santa Cruz Biotechnology). This was followed by incubation with HRP-conjugated secondary antibody at room temperature for 1 hr. The blot was developed using Western Lightning Chemiluminescence Reagent (NEN).

Mouse Strains

Immunodeficient B6 *scid* mice were used as hosts to minimize immunologic rejection of the xenografted human cell line. The *scid* nonsense mutation in the DNA-PKCS gene, was described by Blunt et al. (1996). Based on genomic DNA sequence (GenBank AB005213) PCR primers were

designed flanking the mutation site in exon 85: scid 5 (GAGTTTTGAGCAGACAATGCTGA), and scid 3 (CTTTTGAACACACACTGATTCTGC). The resulting 180 bp PCR product was digested with Alu I to distinguish wild-type allele from mutant allele extra cut site via agarose gel electrophoresis, to genotype animals at the *scid* locus.

Intraneural Tumor Xenografting

Intraneural xenografts were initiated by injecting human NF1 tumor-derived, sNF94.3 cells (passage 5–8) into the sciatic nerves of adult *scid* mice. sNF94.3 cultures from cryopreserved stocks were grown in DMEM containing 10% FBS and antibiotics. Dissociated cells were collected, rinsed thoroughly, and resuspended at 1×10^8 cells/ml in calcium- and magnesium-free Hank's Balanced Salt Solution (HBSS). Young adult mouse hosts were anesthetized with isoflurane and the sciatic nerves exposed bilaterally at mid-thigh. A cell suspension (5×10^5 cells in 5 μl) was injected gradually into the sciatic nerve through a FlexiFil (0.2-mm OD) titanium needle syringe (World Precision Instruments, Sarasota, FL) driven by a UMII microinjector mounted on a motorized micromanipulator (World Precision Instruments). These techniques are for optimized tumor cell injection but successful xenografts can be accomplished by hand and with simple equipment, as they were in our initial studies. The surgical site was closed in layers. Muscles were sutured with 4-0 nylon monofilament. The skin opening was stapled with 9-mm stainless steel wound clips that were removed 7–10 days after surgery. The revived mouse was returned to specific pathogen-free housing. At 2–8 weeks after implantation, the animals were sacrificed under anesthesia and the nerves were removed and fixed by immersion in 4% paraformaldehyde. Xenograft success rate, based on the appearance of human glutathione s-transferase (huGST) immunopositive tumors, was approximately 95% (including initial studies). Nerve segments were embedded in paraffin and sectioned for staining. All animal use was carried out in accordance to the guidelines of the University of Florida Animal Care and Use Committee.

Immunohistochemistry

Cell Cultures. sNF94.3 monolayer cultures were examined for immunoreactivity with antibodies to the SC antigens S-100 (DAKO) (1/300) and the low-affinity neurotrophin receptor (p75) (4 μg/ml, hybridoma 200-3-G6-4; American Type Culture Collection, Rockville, MD). Cultures grown on laminin-coated chamber slides were fixed with 2% paraformaldehyde in 0.1 mM phosphate buffer (pH 7.2) for 20 min, then washed with PBS containing 0.5% Triton X-100. Nonspecific antibody binding was blocked with PBS containing 0.1% Triton X-100 and 10% normal swine serum (blocking buffer) for 1 hr. Primary antibodies were diluted in blocking buffer and applied to wells and allowed to incubate overnight at 4°C. Bound primary antibodies were labeled with swine anti-rabbit Igs (DAKO) (1/200) conjugated with fluorescein for 1 hr at 37°C diluted in blocking buffer in darkness and post-fixed with 2% paraformaldehyde in PBS for 10 min. After washing with PBS, slides were cover slipped and kept in the dark at 4°C until imaging. Imaging was carried out using an excitation wavelength of 450–490 nm and an emission wavelength of 515–565 nm.

Tissue Specimens. Portions of the primary human tumor specimen used for cell culture and xenografted mouse nerves were fixed by immersion in 4% paraformaldehyde in 0.1 mM phosphate buffer (pH 7.2) overnight at 4°C, embedded in paraffin, sectioned on the longitudinal nerve axis, and stained with hematoxylin and eosin (H&E) for routine light microscopic examination. Deparaffinized sections were pretreated with methanol containing 1% hydrogen peroxide for 30 min to quench endogenous peroxidase activity. Nonspecific antibody binding was blocked with 10% normal serum in PBS for 60 min at 37°C. Primary antibodies were diluted in blocking buffer and applied to sections overnight at 4°C. Bound antibody was labeled with a biotinylated secondary antibody for 4 hr at 37°C followed by the avidin-biotin-peroxidase reagent (DAKO) for 2 hr. Chromogenic development was accomplished with diaminobenzidine-$(HC1)_4$ (0.05%) and hydrogen peroxide (0.03%) in PBS. Immunostained sections were lightly counter-stained with hematoxylin. Primary tumor tissue sections were immunolabeled for neurofibromin using polyclonal NF1GRP(N) antibody (1 μg/ml) (Santa Cruz Biotechnology) and monoclonal NFn27b (5 μg/ml) (Novus Biologicals, Littleton, CO). Human sNF94.3 tumor cells were identified in mouse nerve xenografts by immunostaining with polyclonal anti-huGST (DAKO) (1/100). sNF94.3 xenografts were examined for immunoreactivity with antibodies to the SC antigens S100 (DAKO) (1/300) and the low-affinity neurotrophin receptor (p75) (5 μg/ml, Promega, Madison, WI). Cellular proliferation in vivo was assessed by immunostaining with a monoclonal antibody to Ki67 (DAKO) (1/100) (a nuclear antigen present in proliferating human cells). Blood vessels were immunolabeled with polyclonal anti-von Willebrand Factor (DAKO) (1/500) (that binds endothelial cells). Basal laminae produced by the xenografted sNF94.3 cells was immunolabeled with monoclonal anti-laminin (3 μg/ml) (2E8) with pepsin antigen retrieval (Engvall et al., 1986; Graham et al., 2007). This antibody recognizes only human laminin and not laminin of mouse origin. Negative controls used no primary antibody. Mast cells were visualized using acidic toluidine blue as described by Enerback et al. (1986) on sections immunostained for huGST previously. Mucopolysaccharide was stained with 1% Alcian blue (Scott and Mowry, 1970) in combination with H&E staining.

RESULTS

Phenotypic and Genetic Characterization of the sNF94.3 Cell Line

Samples of the sNF94.3 tumor showed ultrastructural features and focal S100 immunopositivity indicative of a neurofibrosarcoma (data not shown). The Schwann cell cultures derived from the originative sNF94.3 sample immunostained for the Schwann cell marker S-100 (Fig. 1A) and the low-affinity nerve growth factor receptor p75 (Fig. 1B), indicating a Schwann cell-like phenotype.

The spindle-shaped monolayer cultures of sNF94.3 cells showed apparent full-length neurofibromin (Mr

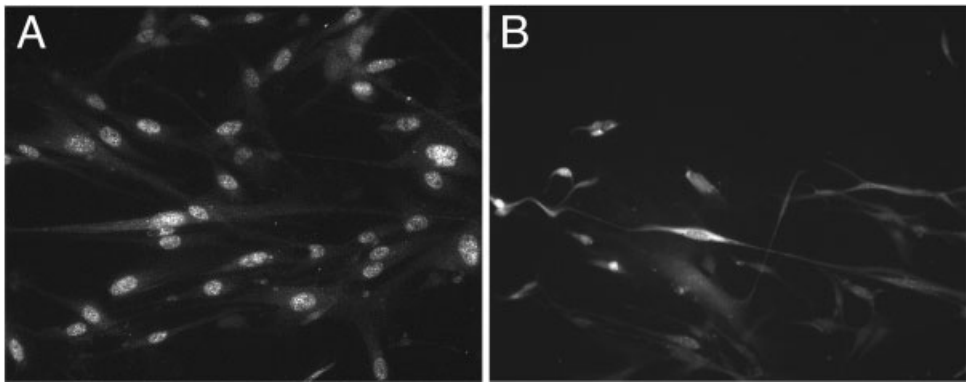

Fig. 1. sNF94.3 cells have a Schwann-like phenotype. sNF94.3 cultures were examined for the immuno expression of two Schwann cell markers, S-100 (**A**) and p75 (**B**) by fluorescent immunocytochemistry. p75 was easily detected on the surface of sNF94.3 cells and cytoplasmic labeling for S-100 was observed. Original magnifications: 400×.

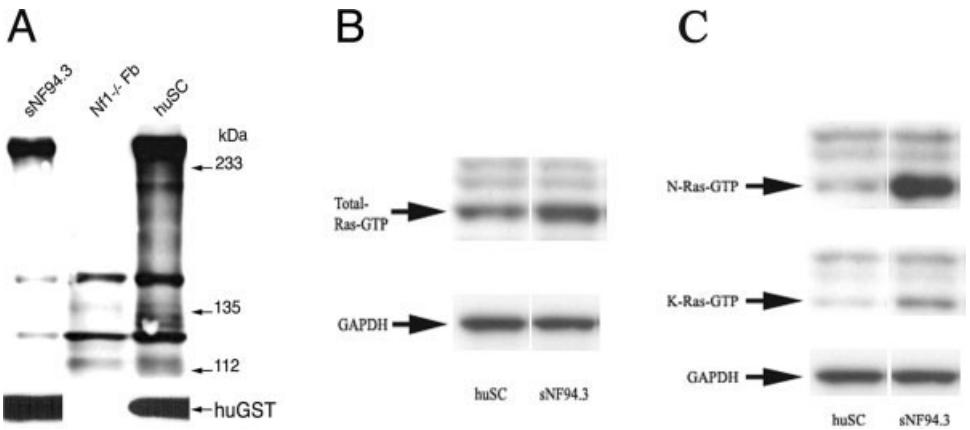

Fig. 2. sNF94.3 cells express apparently full-length but non-functional neurofibromin. **A:** Extracts from sNF94.3 cultures, fibroblast cultures derived from embryonic *Nf1−/−* knockout mice, and normal human Schwann cell cultures were analyzed for neurofibromin expression by Western immunoblotting. Full-length neurofibromin appeared as a ≈250 kDa band in the normal human Schwann cell sample. An equal amount of total protein was loaded for each sample. **B:** Increased activated Ras is seen in serum-starved sNF94.3 cells, as are increased levels of activated N-Ras and K-Ras isoforms (**C**).

≈250 kDa) by Western immunoblotting using several anti-neurofibromin antibodies (Fig. 2A). Full-length neurofibromin was not detected in extracts of fibroblast cultures derived from embryonic *Nf1−/−* knockout mice. As a positive control, normal human Schwann cell cultures showed a substantial band-pair corresponding to full-length neurofibromin. A secondary immunolabeling of the blot for huGST showed consistent loading for all of the human samples. Next, sNF94.3 cells and normal human Schwann cells were serum-starved and Ras activation was determined by Western immunoblotting. Total activated Ras-GTP was elevated in sNF94.3 cells when compared to normal human Schwann cell cultures (Fig. 2B). In addition, both of the specific N-Ras and K-Ras isoforms were activated in sNF94.3 cells (Fig. 2C). Similar results have been reported for other NF1-derived Schwann cells (Thomas, et al., 2006). Consistent with Ras activation, sNF94.3 cells proliferate rapidly and display vigorous growth in culture, on par with other human NF1 MPNST cell lines established in our lab.

sNF94.3 leukocyte DNA (from a polyclonal population of cells) was analyzed first for heterozygosity at the androgen receptor and *PGK* gene polymorphisms. This sample was heterozygous at the androgen receptor gene, warranting additional DNA analysis. The X-chromosome inactivation pattern for sNF94.3 at the androgen receptor locus was consistent with that of a clonally derived tumor sample ($P = 0.008$, data not shown).

The cytogenetic analysis showed a normal 46, xx karyotype, which is unusual for MPNSTs (Mertens et al., 2000). Sample sNF94.3 cells do not have p53 loss of heterozygosity but showed a constitutional *NF1* mutation, which is a microdeletion of the common 1.4 Mb type with breakpoints in the NFREPs and was detected using PCR (Dorschner et al., 2000; Lopez-

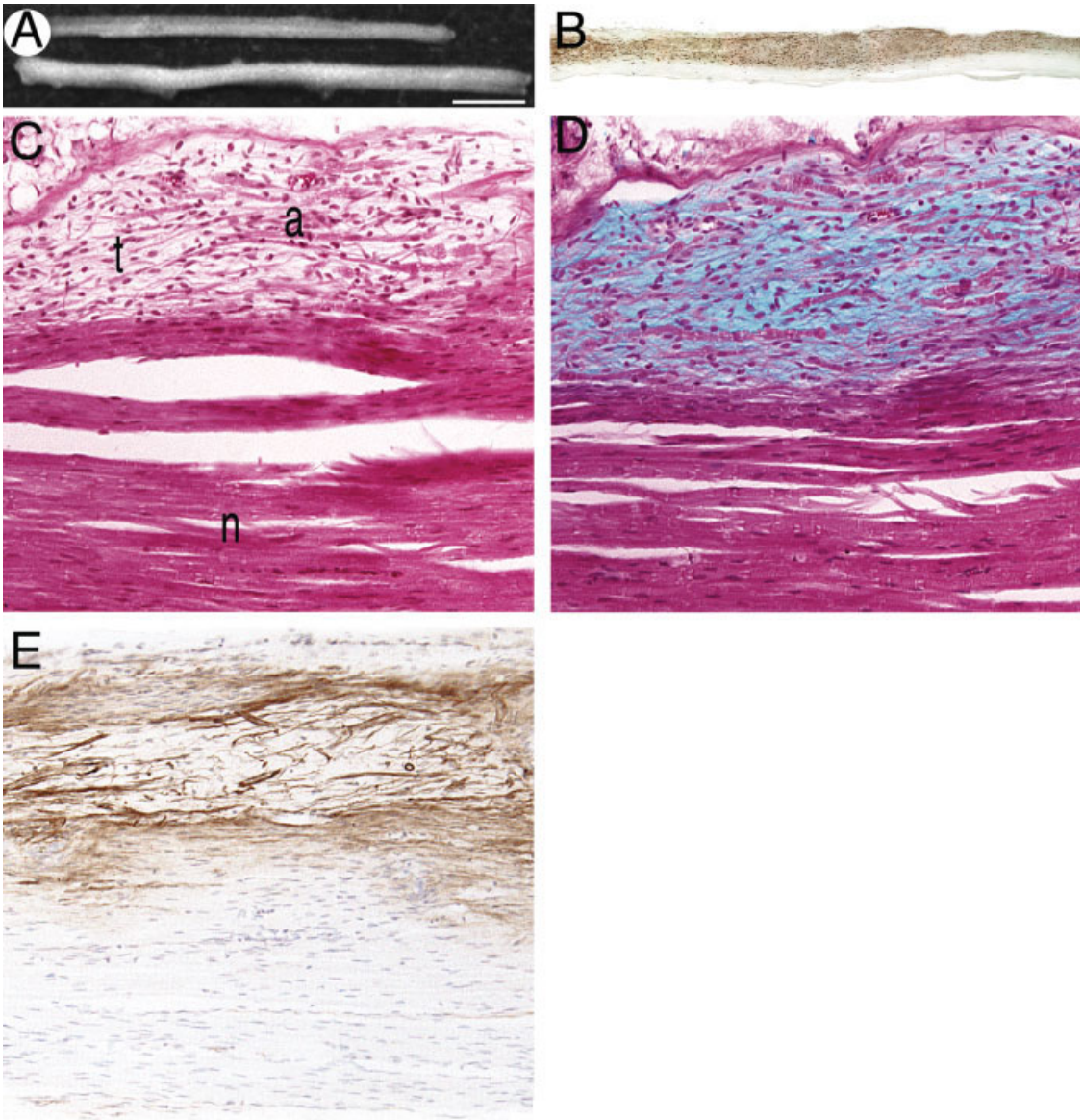

Fig. 3. sNF94.3 xenografts form hypocellular plexiform-like tumors. **A:** The normal mouse sciatic nerve (**upper**) is slender and symmetric whereas 8 weeks after implantation with sNF94.3 the nerve appears swollen and mildly deformed (**lower**) (scale bar = 2 mm). **B:** HuGST immunostaining readily identifies and traces the infiltration of human sNF94.3 cells throughout the xenografted host sciatic nerve. C: H&E stain shows tumor hypocellularity and nerve remodeling. Developing tumor (t), axons (a) displaced by infiltrating tumor and a small region with relatively normal nerve structure (n) are visible. **D:** A serial section stained with Alcian blue highlights the abundant deposition of extracellular mucopolysaccharide matrix associated with the hypocellular tumor. Immunostaining for human laminin (**E**) showed the presence of basal laminae. Original magnification: 100× (B); 200× (C–F).

Correa et al., 2001). The somatic mutation is not a large deletion and remains unknown despite analysis of numerous exons. This is consistent with the patient's heavy dermal tumor burden and occurrence of the MPNST (De Raedt et al., 2003). The NF1 mRNA is of the Type II isoform, which is due to inclusion of exon 23a (encoding 21 amino acids). This isoform is known to have reduced GAP activity, and is the predominant type expressed in normal peripheral nerve, brain tumors, and neurofibromas (Suzuki et al., 1991; Teinturier et al., 1992; Andersen et al., 1993). All exon and immediate flanking intron bases have been sequenced and are normal. There is no evidence for aberrant splicing at the RNA level, via reverse transcriptase (RT)-PCR polyacrylamide gel analysis, and sequencing. It is possible, however, that a mutation lies in an untranslated region or promoter region, affecting RNA transcription level or stability, or hemizygosity for the Type II isoform results in Ras-GAP activity reduced sufficiently to allow tumor progression.

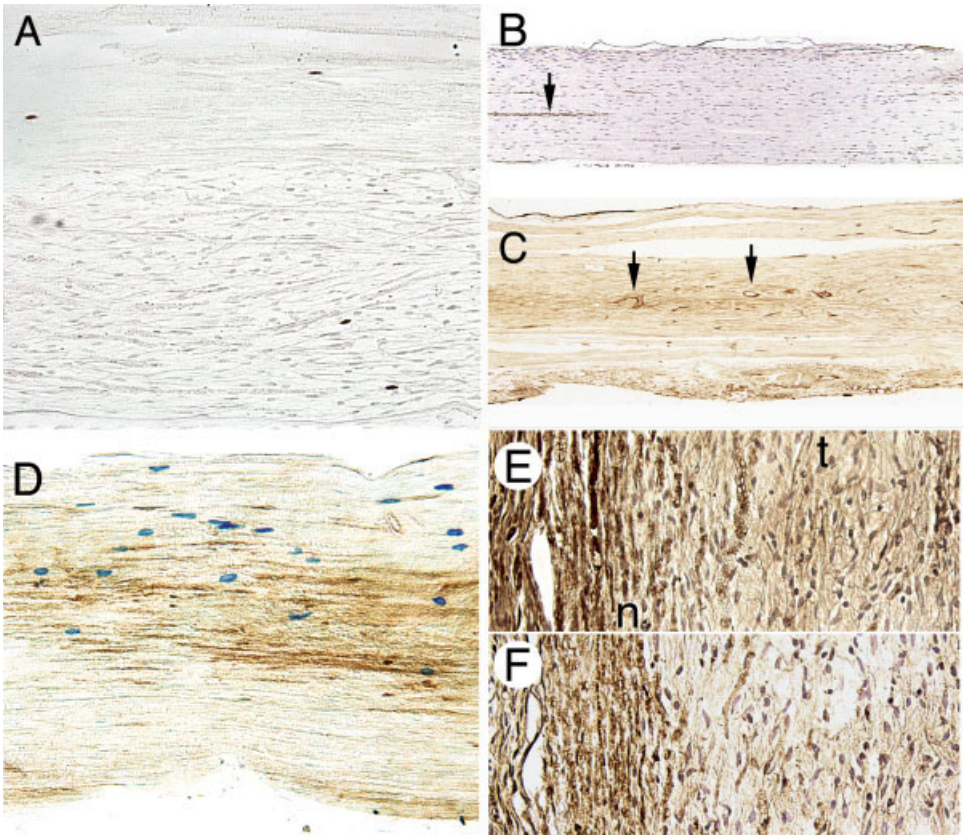

Fig. 4. sNF94.3 tumors proliferate slowly, are highly vascular, are infiltrated by mast cells and display Schwann cell markers. **A:** Eight weeks after xenograft, Ki67 immunostaining of an sNF94.3 tumor indicates a low rate of proliferation. **B:** Immunostaining for von Willebrand's Factor shows normal mouse nerve has scant and slender vasculature (arrow) aligned with the longitudinal axis. **C:** Increased vascularity (arrows) was associated with sNF94.3 xenograft tumors as early as two weeks. The blood vessels splay into the developing tumor indicative of angiogenic activity. **D:** Xenografted nerves were immunostained for huGST (brown) and counterstained for mast cells using acidic toluidine blue. Compared to normal nerve, there was an apparent increase in mast cell infiltration in the xenografted nerves closely associated with the expanding tumor. Nerves were also immunostained for two Schwann cell markers, S-100 (**E**) and p75 (**F**). Faint and variable immuno expression of these Schwann cell markers by sNF94.3 xenograft tumors was observed by immunoperoxidase methods (n, normal nerve; t, xenograft tumor). Original magnification: 200× (A,D–F); 100× (B,C).

Intraneural sNF94.3 Xenograft Tumors Resemble Plexiform Neurofibroma

Like cultures from neurofibromas, sNF94.3 failed to form subcutaneous tumors in *scid* mice. Nevertheless, sNF94.3 xenografts consistently formed slow growing, infiltrative tumors in the mouse nerve. Figure 3A shows the gross morphology of a normal mouse sciatic nerve and a representative sNF94.3 nerve xenograft 8 weeks after intraneural implantation. Thirty-nine sNF94.3 engraftments were carried out and examined at time points from 8 days to 1 year after initiation. Overall, 94.9% of the sNF94.3 xenografts were successful and resulted in established foci of huGST-immunopositive cells. Most sNF94.3 tumors caused a moderate enlargement of the host nerve. Eight weeks after implantation with sNF94.3, nerve diameters were on average 55% larger (0.472 mm ± 0.1469, n = 6) than normal, age-matched mouse sciatic nerves (0.304 mm ± 0.0392, n = 4). Vehicle injected mouse sciatic nerves were not increased in size compared to normal nerves (0.293 mm ± 0.0645, n = 2 vs. 0.304 mm ± 0.0392, n = 4, respectively), indicating the increase in nerve diameter did not result from surgically induced inflammation. In addition, xenograft of normal human Schwann cells resulted in only a slight, 9.7% increase in nerve diameter (0.334 mm ± 0.0643, n = 6 vs. 0.304 mm ± 0.0392, n = 4) after 8 weeks. This occurred despite only transient occupancy and limited survival as the normal Schwann cells were most often undetectable after 8 weeks in vivo. Xenografts of sNF94.3 grew slowly and were histopathologically similar to human NF1 plexiform neurofibromas. Immunostaining for the marker protein huGST identified the xenografted human tumor cells and their propensity to diffusely involve the nerve, mimicking the hypocellular growth pattern often found in plexiform neurofibromas (Fig. 3B). The engrafted tumor cells increased in number over time and eventually infiltrated the nerve far from the site of initial implantation.

Regardless of the extent of tumor growth, no overt signs indicating loss of nerve function were observed in any of the xenografted mice, also commonly the case with human NF1 plexiform neurofibromas. Growth of the sNF94.3 cell line in sciatic nerves of adult *scid* mice caused intraneural disruption and nerve remodeling (Fig. 3C). The hypocellular tumors were composed of diffusely distributed, spindle-shaped cells and were associated with deposition of a mucopolysaccharide-rich, collagenous extracellular matrix (Fig. 3D) and basal laminae (Fig. 3E), hallmarks of NF1 plexiform neurofibroma (Scheithauer et al., 1997). The basal laminae found in sNF94.3 xenografts was produced by the sNF94.3 cells themselves, not the host mouse cells, because the monoclonal antibody used for laminin immunolabeling is specific for human laminin only and does not immunostain mouse laminin (Engvall et al., 1986; Graham et al., 2007). This specificity for human laminin is further shown by the lack of laminin immunostaining in the unaffected portion of the mouse nerve (Fig. 3E). Mucopolysaccharide deposition, shown by Alcian blue staining, was observed as early as 2 weeks after sNF94.3 xenograft and increased over time, as did hypocellularity observed with H&E staining. Neither Alcian blue staining nor H&E hypocellularity was observed in xenografts of normal human Schwann cells after 8 weeks ($n = 6$) nor nerves injected with vehicle alone ($n = 4$). Furthermore, xenografts of another human NF1 cell line using the exact same procedures results in large hypercellular tumors with little mucopolysaccharide and laminin deposition (data not shown).

sNF94.3 xenografts were immunostained for Ki67 (a nuclear antigen found in proliferating cells) and von Willebrand Factor (vWF), an endothelial cell marker. Ki67-positive nuclei were found only within the tumor xenografts (huGST-immunopositive cells) and not in adjacent normal host nerve tissue. A low percentage of tumor cells labeled for Ki67 (Fig. 4A). Similar observations were made in xenografts after 8 days and 1 year, indicating slow but sustained proliferation by the sNF94.3 tumor cells, mimicking that of plexiform neurofibromas. Immunostaining for vWF showed scant blood vessels in normal mouse nerves arranged almost exclusively along the longitudinal nerve axis (Fig. 4B). Increased vascularity was evident in sNF94.3 xenografts as early as 2 weeks (Fig. 4C) and 8-week tumors showed a high degree of vascularity. A more centripetal pattern of blood vessels was observed indicating an angiogenic response to the developing neoplasm. Nearly identical results were obtained by labeling xenograft tumor tissue with antibodies to Flk-1, a high affinity receptor for vascular endothelial growth factor (VEGF) also found on blood vessels (not shown). These results indicate the induction of new blood vessels by the tumor xenograft and provide the opportunity to examine angiogenesis in this NF1 tumor model. Sections of sNF94.3 xenografts immunostained for huGST were counterstained with acidic toluidine blue to visualize mast cells. Although a few mast cells were found in normal mouse sciatic nerves, there was a conspicuous increase in mast cell number in the xenografted nerves (Fig. 4D). Given the fact that mast cells are known to release factors that influence tumor formation, these results may indicate a potential mast cell influence on intraneural sNF94.3 xenograft tumorigenicity. S-100 and p75 immunostaining of sNF94.3 xenograft tumors was faint and variable (Fig. 4E,F, respectively), similar to that of the originative tumor specimen.

TABLE I. Characteristics of sNF94.3 Xenograft Tumor and NF1 Benign Plexiform Neurofibroma

	sNF94.3 xenograft tumors[a]	NF1 plexiform neurofibroma[b]
Hypocellularity	+	+
Low proliferation	+	+
Spindle-shaped cells	+	+
S-100 immunoexpression	+	+
p75 immunoexpression	+	+
Diffusely infiltrative	+	+
Longitudinal spread	+	+
Invade basement membranes	+	+
Cells align along nerve axis	+	+
Abundant ECM	+	+
Possess basal laminae	+	+
Unencapsulated	+	+
Highly vascular	+	+
Intact nerve function	+	+
"Bag of worms" appearance	–	+
Severely deform tissue	–	+

[a]Eight week xenografts.
[b]Described by Scheithauer et al. (1997).

Table I summarizes the histologic observations and indicates similarities and differences between the sNF94.3 xenograft tumors and human NF1 plexiform neurofibroma. Based on these criteria and the findings presented we conclude that intraneural sNF94.3 xenografts show tumorigenic growth in the nerves of *scid* mice highly consistent with that of naturally-occurring human plexiform neurofibroma. Classifications for peripheral nerve sheath tumors arising in genetically engineered mouse (GEM) models have been devised because of some important differences between human and murine lesions (Stemmer-Rachamimov et al., 2004). In the same way it is difficult to apply the GEM classifications to tumors arising in xenografting models. Clearly, sNF94.3 xenograft tumors result from the proliferation of NF1-deficient Schwann cells and the admixture of various cell types from the mouse nerve including endothelial and mast cells. For the most part, sNF94.3 xenografts fit the Grade I GEM tumor classification because of low cellularity and no necrosis. They exceed that classification, however, due to their low to moderate proliferation (Ki67 positivity) and infiltration.

DISCUSSION

A variety of genetic strategies have been tested to determine the role of *Nf1*-deficiency in tumorigenesis and to induce peripheral nerve sheath tumors in animal

models. Genetic manipulations to generate *Nf1−/−* chimera and conditional knockout mice have provided valuable insights into the role of the *Nf1* gene in tumor pathogenesis (Cichowski et al., 1999; Zhu et al., 2002; Stemmer-Rachamimov et al., 2004). On the other hand, tumor xenografting is a time-tested approach with numerous advantages for testing anti-cancer therapies. Despite tumorigenic properties shown in vitro, neurofibroma cultures fail to form subcutaneous tumors in immunodeficient mice (Sheela et al., 1990; Muir et al., 2001). Early studies achieved limited growth by transplantation of human neurofibroma tissue or mixed cell preparations into mice (Appenzeller et al., 1986; Lee et al., 1992), yet reliable working xenograft models for NF1 tumors have been difficult to establish. In previous work we found that a subset of neurofibromin-negative Schwann cell cultures derived from neurofibromas did form slow growing tumors as intraneural xenografts (Muir et al., 2001). Although these xenografts provide a useful model of neurofibroma, several months are required to develop histologically detectable tumors for experimental therapeutics. In addition, cell lines derived from benign neurofibromas are not immortal and thus are a limited resource. Therefore, we investigated more advantageous xenograft models of NF1 tumorigenesis by implantation of rapidly growing NF1 MPNST cell lines into the mouse nerve.

We report a practical and reproducible NF1 tumor xenograft model by transplantation of an immortal human NF1 tumor-derived Schwann cell line, sNF94.3, into the peripheral nerve of *scid* mice. sNF94.3 is a stable and homogeneous cell line that provides a permanent and consistent cell source for xenograft initiation. sNF94.3 are Schwann-like cells that express S-100 and p75, as do the clonal element of most human NF1 plexiform neurofibromas. sNF94.3 cells have an apparently normal karyotype. The manifestation and severity of the originative patient's NF1 symptoms (including abundant dermal and plexiform neurofibromas and MPNST) are consistent with a germline $\sim$1.4 megabase microdeletion of the *NF1* gene (De Raedt et al., 2003). The germline mutation completely deletes the *NF1* and surrounding genes, whereas the somatic *NF1* mutation(s) remain unknown. It is likely the somatic *NF1* mutation in sNF94.3 is subtle, such as a missense mutation, because this cell line produces apparently full-length neurofibromin protein as seen by Western blotting. Our studies show that these cells, however, have constitutively activated Ras indicating that the neurofibromin in sNF94.3 cells is not functional. This functional deficit is consistent with the phenotype of sNF94.3 cells in vitro and in vivo.

Although no animal model system can recapitulate every aspect of a complex human disease such as NF1, we conclude the sNF94.3 xenograft is a valid model of plexiform-like neurofibroma and provides a valuable tool in the study of NF1 tumorigenesis. Like human NF1 plexiform neurofibroma, intraneural sNF94.3 xenografts displayed hypocellularity with widely-spaced spindle-shaped cells, a low proliferative index, an extracellular matrix-rich stroma and basal laminae. Neurofibromas and MPNST have been shown previously to produce laminin (Chanoki et al., 1991). Schwann cells require the presence of other cell types, such as axons and fibroblasts, to produce basal laminae (Obremski et al., 1993). The fact that basal laminae are formed by sNF94.3 tumors suggests that these tumor cells interact with the surrounding host cells to form highly differentiated Schwann cell neoplasms (Leivo et al. 1989). Additionally, the tumors spread longitudinally in the nerve fascicles, intermingling with host axons while causing little or no impairment of nerve function, similar to human plexiform neurofibromas.

The increase of blood vessels observed in benign sNF94.3 xenograft tumors recapitulates another important feature of NF1 plexiform neurofibroma, which are angiogenic and highly vascularized (Arbiser et al., 1998). Angiogenesis has been suggested as a potentially important target for therapeutic treatment of many types of cancers (Folkman, 2003). As in human NF1 plexiform neurofibromas, the induction of angiogenesis points to the possible effectiveness of anti-angiogenic therapies to limit and control tumor growth. Therefore, the sNF94.3 xenograft model facilitates testing anti-angiogenic therapies for NF1 tumors. In addition, we have established *scid* mice with a heterozygous *Nf1* genotype, providing the opportunity to examine the interactions of xenografts with haplo-insufficient host cells. This may be particular interesting for further studies of angiogenesis given our recent observations of exaggerated neovascular responses in *Nf1* haplo-insufficient mice (Wu et al., 2006).

Xenografting requires the use of immunodeficient mice that can complicate the interpretation of host–implant cell interactions. *Scid* mice lack a functional adaptive immune system, yet they do possess a completely intact innate immune system, including mast cells (Dorshkind et al., 1984). Additionally, NF1 tumorigenic Schwann cells are known to produce stem cell factor, a potent mast cell mitogen (Ryan et al., 1994). It has been shown that murine innate immune cells can contribute to the inhibition of human tumor-cell engraftment in some human tumor-*scid* mouse models (Lozupone et al., 2000). Alternatively, this innate immune response may also contribute to tumor engraftment and growth. Previous studies have suggested that mast cells may induce or contribute to tumor formation in *Nf1* mutant mouse models (Zhu et al., 2002; Yang et al., 2003). It is interesting to speculate whether this mast cell infiltration and activation may be a relevant feature of slow-growing plexiform tumors, as suggested by our xenograft model and by others (Viskochil, 2003).

Although a number of NF1 mouse models have been developed in recent years (Gutmann and Giovannini, 2002; Stemmer-Rachamimov et al., 2004), ours is the first xenograft model allowing the properties of human NF1 tumor-derived cells to be examined in a relevant cellular environment. The sNF94.3 xenograft model closely recapitulates the natural history, pathobiol-

ogy, and biochemistry of human NF1 plexiform neurofibroma (Table I). This model is reproducible and consistent with a xenograft success rate of nearly 95%. Because the tumor cell injection is fully controlled by the investigator, a low tumor burden can be established precluding premature death from tumor overload. Also, tumors develop with a relatively short latency.

In summary, the plexiform-like sNF94.3 xenograft model offers several advantages. First, the sNF94.3 xenografts can be compared to the originative tumor specimen as well as other xenografts and cognate tumor specimens. Second, before implantation, sNF94.3 cultures can be examined for in vitro neoplastic properties, karyotype, and genetic abnormalities. Third, the investigator can precisely define the initiation of tumor xenografts by cell number, time, and location in a relevant cellular environment. Fourth, xenografts can be initiated in hosts with various genetic and phenotypic alterations and at various developmental stages. In addition, for future studies, we have also developed a strain of *scid* mice with an *Nf1+/−* background (Brannan et al., 1994; Jacks et al., 1994) to enhance the validity and relevance of tumor-host cell interactions. The plexiform-like sNF94.3 xenograft model recapitulates the main aspects of plexiform neurofibroma. These features, combined with high reproducibility and technical simplicity, will greatly facilitate preclinical testing of new therapeutic approaches for NF1 tumors.

ACKNOWLEDGMENTS

The authors thank D. Neubauer, E. Baldwin, and T. Lewis for their assistance in performing experiments, Dr. L. Zhang, Dr. H. Li, and F. Kweh for mouse breeding and colony maintenance and the University of Florida Cytogenetics Lab for cytogenetic analysis. This study was supported by the National Institutes of Health Training Grant T32-CA09126-27 (G.Q.P.), the U.S. Department of Defense grants DAMD 17-01-10707 (M.R.W.), and DAMD 17-03-1-0224 (D.M.).

REFERENCES

Abernathy CR, Rasmussen SA, Stalker HJ, Zori R, Driscoll DJ, Williams CA, Kousseff BG, Wallace MR. 1997. NF1 mutation analysis using a combined heteroduplex/SSCP approach. Hum Mutat 9:548–554.

Allen RC, Zoghbi HY, Moseley AB, Rosenblatt HM, Belmont JW. 1992. Methylation of HpaII and HhaI sites near the polymorphic CAG repeat in the human androgen-receptor gene correlates with X chromosome inactivation. Am J Hum Genet 51:1229–1239.

Andersen LB, Ballester R, Marchuk DA, Chang E, Gutmann DH, Saulino AM, Camonis J, Wigler M, Collins FS. 1993. A conserved alternative splice in the von Recklinghausen neurofibromatosis (NF1) gene produces two neurofibromin isoforms, both of which have GTPase-activating protein activity. Mol Cell Biol 13:487–495.

Appenzeller O, Kornfeld M, Atkinson R, Snyder RD. 1986. Neurofibromatosis xenografts. Contribution to pathogenesis. J Neurol Sci 74: 69–77.

Arbiser JL, Flynn E, Barnhill RL. 1998. Analysis of vascularity of human neurofibromas. J Am Acad Dermatol 38:950–954.

Blunt T, Gell D, Fox M, Taccioli GE, Lehmann AR, Jackson SP, Jeggo PA. 1996. Identification of a nonsense mutation in the carboxyl-terminal region of DNA-dependent protein kinase catalytic subunit in the scid mouse. Proc Natl Acad Sci U S A 93:10285–10290.

Brannan CI, Perkins AS, Vogel KS, Ratner N, Nordlund ML, Reid SW, Buchberg AM, Jenkins NA, Parada LF andCopeland NG. 1994. Targeted disruption of the neurofibromatosis type-1 gene leads to developmental abnormalities in heart and various neural crest-derived tissues. Genes Dev Rev 8:1019–1029.

Chanoki M, Ishii M, Fukai K, Kobayashi H, Hamada T, Muragaki Y, Ooshima A. 1991. Immunohistochemical localization of type I, III, IV, V, and VI collagens and laminin in neurofibroma and neurofibrosarcoma. Am J Dermatopathol 13:365–373.

Cichowski K, Shih TS, Schmitt E, Santiago S, Reilly K, McLaughlin ME, Bronson RT, Jacks T. 1999. Mouse models of tumor development in neurofibromatosis type 1. Science 286:2172–2176.

Colman SD, Williams CA, Wallace MR. 1995. Benign neurofibromas in type 1 neurofibromatosis (NF1) show somatic deletions of the NF1 gene. Nat Genet 11:90–92.

De Raedt T, Brems H, Wolkenstein P, Vidaud D, Pilotti S, Perrone F, Mautner V, Frahm S, Sciot R, Legius E. 2003. Elevated risk for MPNST in NF1 microdeletion patients. Am J Hum Genet 72:1288–1292.

Dorschner MO, Sybert VP, Weaver M, Pletcher BA, Stephens K. 2000. NF1 microdeletion breakpoints are clustered at flanking repetitive sequences. Hum Mol Genet 9:35–46.

Dorshkind K, Keller GM, Phillips RA, Miller RG, Bosma GC, O'Toole M, Bosma MJ. 1984. Functional status of cells from lymphoid and myeloid tissues in mice with severe combined immunodeficiency disease. J Immunol 132:1804–1808.

Enerback L, Miller HRP, Mayrhofer G. 1986. Methods for the identification and characterization of mast cells by light microscopy. In: Befus AD, Bienenstock J, Denburg JA, editors. Mast cell differentiation and heterogeneity. New York, NY: Raven Press. p 405–417.

Engvall E, Davis GE, Dickerson K, Ruoslahti E, Varon S andManthorpe M. 1986. Mapping of domains in human laminin using monoclonal antibodies: localization of the neurite-promoting site. J Cell Biol 103: 2457–2465.

Folkman J. 2003. Angiogenesis and apoptosis. Semin Cancer Biol 13: 159–167.

Graham JB, Neubauer D, Xue QS, Muir D. 2007. Chondroitinase applied to peripheral nerve repair averts retrograde axonal regeneration. Exp Neurol Jan; 203:185–195.

Gutmann DH, Wood DL, Collins FS. 1991. Identification of the neurofibromatosis type 1 gene product. Proc Natl Acad Sci USA 88:9658–9662.

Gutmann DH, Aynsworth A, Carey JC, Korf B, Marks J, Pyeritz RE, Rubenstein A, Viskochil D. 1997. The diagnostic evaluation and multidisciplinary management of neurofibromatosis 1 and neurofibromatosis 2. JAMA 278:51–57.

Gutmann DH, Giovannini M. 2002. Mouse models of Neurofibromatosis 1 and 2. Neoplasia 4:279–290.

Hirose T, Sano T, Hizawa K. 1986. Ultrastructural localization of S-100 protein in neurofibroma. Acta Neuropathol 69:103–110.

Jacks T, Shih TS, Schmitt EM, Bronson RT, Bernards A, Weinberg RA. 1994. Tumour predisposition in mice heterozygous for a targeted mutation in Nf1. Nat Genet 7:353–361.

Krone W, Mao R, Muhleck OS, Kling H, Fink T. 1986. Cell culture studies on neurofibromatosis (von Recklinghausen). Characterization of cells growing from neurofibromas. Ann NY Acad Sci 486:354–370.

Lee JK, Sobel RA, Chiocca EA, Kim TS, Martuza RL. 1992. Growth of human acoustic neuromas, neurofibromas and schwannomas in the sub renal capsule and sciatic nerve of the nude mouse. J Neurooncol 14:101–112.

Lee ST, McGlennen RC, Litz CE. 1994. Clonal determination by the fragile X (FMR1) and phosphoglycerate kinase (PGK) genes in hematological malignancies. Cancer Res 54:5212–5216.

Leivo I, Engvall E, Laurila P, Miettinen M. 1989. Distribution of myrosin, a laminin-related tissue-specific basement membrane protein, in human Schwann cell neoplasms. Lab Invest 61:426–432.

Li Y, Rao PK, Wen R, Song Y, Muir D, Wallace P, Van Horne SJ, Tennekoon GI, Kadesch T. 2004. Notch and Schwann cell transformation. Oncogene 23:1146–1152.

Lopez-Correa C, Dorschner M, Brems H, Lazaro C, Clementi M, Upadhyaya M, Dooijes D, Moog U, Kehrer-Sawatzki H, Rutkowski JL, Fryns JP, Marynen P, Stephens K, Legius E. 2001. Recombination hotspot in NF1 microdeletion patients. Hum Mol Genet 10:1387–1392.

Lozupone F, Luciani F, Venditti M, Rivoltini L, Pupa S, Parmiani G, Belardelli F, Fais S. 2000. Murine granulocytes control human tumor growth in SCID mice. Int J Cancer 87:569–573.

Mertens F, Dal Cin P, De Wever I, Fletcher CD, Mandahl N, Mitelman F, Rosai J, Rydholm A, Sciot R, Tallini G, van Den Berghe H, Vanni R, Willen H. 2000. Cytogenetic characterization of peripheral nerve sheath tumours: a report of the CHAMP study group. J Pathol 190:31–38.

Mirsky R, Jessen KR. 1999. The neurobiology of Schwann cells. Brain Pathol 9:293–311.

Muir D, Neubauer D, Lim IT, Yachnis AT, Wallace MR. 2001. Tumorigenic properties of neurofibromin-deficient neurofibroma Schwann cells. Am J Pathol 158:501–513.

Obremski VJ, Johnson MI, Bunge MB. 1993. Fibroblasts are required for Schwann cell basal lamina deposition and ensheathment of unmyelinated sympathetic neurites in culture. J Neurocytol 22:102–117.

Perrin GQ, Fishbien L, Thompson S, Wallace M, Hwang MS, Mareci T, Yachnis AT, Muir D. 2006. Malignant peripheral nerve sheath tumors developed in the mouse by xenograft of an NF1 tumor-derived Schwann cell line. Oncogene. Submitted.

Rasmussen SA, Colman SD, Ho VT, Abernathy CR, Arn PH, Weiss L, Schwartz C, Saul RA, Wallace MR. 1998. Constitutional and mosaic large NF1 gene deletions in neurofibromatosis type 1. J Med Genet 35: 468–471.

Ryan JJ, Klein KA, Neuberger TJ, Leftwich JA, Westin EH, Kauma S, Fletcher JA, DeVries GH, Huff TF. 1994. Role for the stem cell factor/KIT complex in Schwann cell neoplasia and mast cell proliferation associated with neurofibromatosis. J Neurosci Res 37:415–432.

Scheithauer BW, Woodruff JM, Erlandson RA. 1997. Tumors of the peripheral nervous system. In: Rosai J, Sobin LH, editors. Atlas of tumor pathology. Series 3. Fascicle 24. Washington, DC: Armed Forces Institute of Pathology. p 385–405.

Scott JE, Mowry RW. 1970. Alcian blue—a consumer's guide. J Histochem Cytochem 18:842.

Sheela S, Riccardi VM, Ratner N. 1990. Angiogenic and invasive properties of neurofibroma Schwann cells. J Cell Biol 111:645–653.

Singer-Sam J, LeBon JM, Tanguay RL, Riggs AD. 1990. A quantitative HpaII-PCR assay to measure methylation of DNA from a small number of cells. Nucleic Acids Res 18:687.

Stemmer-Rachamimov AO, Louis DN, Nielsen GP, Antonescu CR, Borowsky AD, Bronson RT, Burns DK, Cervera P, McLaughlin ME, Reifenberger G, Schmale MC, MacCollin M, Chao RC, Cichowski K, Kalamarides M, Messerli SM, McClatchey AI, Niwa-Kawakita M, Ratner N, Reilly KM, Zhu Y, Giovannini M. 2004. Comparative pathology of nerve sheath tumors in mouse models and humans. Cancer Res 64:3718–3724.

Suzuki Y, Suzuki H, Takamasa K, Yoshimoto T, Shibahara S. 1991. Brain tumors predominantly express the neurofibromatosis type 1 gene transcripts containing the 63 base insert in the region coding for GTPase activating protein-related domain. Biochem Biophys Res Commun 181:955–961.

Teinturier C, Danglot G, Slim R, Pruliere D, Launay JM, Bernhiem A. 1992. The neurofibromatosis 1 gene transcripts expressed in peripheral nerve and neurofibromas bear the additional exon located in the GAP domain. Biochem Biophys Res Commun 188:851–857.

Thomas SL, Deadwyler GD, Tang J, Stubbs EB, Muir D, Hiatt KK, Clapp DW, DeVries GH. 2006. Reconstitution of the *NF1 GAP*-related domain in NF1-deficient human Schwann cells. Biochem Biophys Res Comm 348:971–980.

Viskochil DH. 2003. It takes two to tango: mast cell and Schwann cell interactions in neurofibromas. J Clin Invest 112:1791–1793.

Wallace MR, Rasmussen SA, Lim IT, Gray BA, Zori RT, Muir D. 2000. Culture of cytogenetically abnormal Schwann cells from benign and malignant NF1 tumors. Genes Chromosomes Cancer 27:117–123.

Wu M, Wallace MR, Muir D. 2006. Nf1 haploinsufficiency augments angiogenesis. Oncogene 25:2297–2303.

Yang F-C, Ingram DA, Chen S, Hingtgen CM, Ratner N, Monk KR, Clegg T, White H, Mead L, Wenning MJ, Williams DA, Kapur R, Atkinson SJ, Clapp DW. 2003. Neurofibromin-deficient Schwann cells secrete potent migratory stimulus for Nf1 +/− mast cells. J Clin Invest 112:1851–1861.

Zhu Y, Ghosh P, Charnay P, Burns D, Parada LF. 2002. Neurofibromas in NF1: Schwann cell origin and role of tumor environment. Science 296:920–922.